The University Of Sheffield.

Analysis of Corticosteroid Drug Delivery using Tissue Engineered Oral Mucosa for the Treatment of Inflammatory Mucosal Diseases

Zulfahmi Said

A thesis submitted in partial fulfilment of the requirements for the degree of Doctor of Philosophy

The University of Sheffield
Faculty of Medicine, Dentistry and Health
Department of Oral & Maxillofacial Pathology
School of Clinical Dentistry

September 2018

LIST OF PUBLICATION

Colley, H*., **Said, Z***., Santocildes-Romero, M., Baker, S., D'Apice, K., Hansen, J., Madsen, L., Thornhill, M., Hatton, P. and Murdoch, C. (2018). Pre-Clinical Evaluation of Novel Mucoadhesive Bilayer Patches for Local Delivery of Clobetasol-17-Propionate to The Oral Mucosa. *Biomaterials*, 178, pp.134-146.

**These authors contributed equally to the study and are joint first authors.*

LIST OF PRESENTATIONS

1. Characterisation of A Three-Dimensional Tissue-Engineered *In Vitro* Model of The Oral Mucosa Using TERT-2 Immortalised Oral Keratinocytes. Cell Culture 2016, London. (February 2016) – Poster

2. Use of Immortalised Oral Keratinocytes for The Generation of Oral Mucosal Equivalents to Study Drug Delivery. Biomaterials & Tissue Engineering Group (BiTEG), 18th Annual White Rose Work in Progress Meeting, Durham University. (December 2016). – Poster and Flash presentation (90 seconds)

   Won Best Poster Award – First Place

3. Use of Tissue-Engineered Oral Mucosa (TEOM) Based on Immortalised Keratinocytes for Oral Drug Delivery Studies. Future Investigators of Regenerative Medicine (FIRM) Symposium, Spain. (September 2017) - Poster

TABLE OF CONTENTS

LIST OF FIGURES

LIST OF TABLES

LIST OF ABBREVIATIONS

2D	Two-dimensional
3D	Three-dimensional
3R	Reduction, replacement and refinement
ACN	Acetonitrile
ALI	Air-to-liquid
ANOVA	Analysis of variance
AP-1	Activator protein 1
APC	Antigen-presenting cells
API	Active pharmaceutical ingredient
BD	Betamethasone 17, 21-dipropionate
BL	Basal layer
BM	Basement membrane
BNF	British National Formulary
BU	Budesonide
BV	Betamethasone 17-valerate
C	Carbon
CF	Collagen fibrils
CK	Cytokeratin
COX	Cyclooxygenase
CP	Clobetasol 17-propionate
CS	Corticosteroids
CT	Connective tissue
CTE	Connective tissue equivalent
CYP	Cytochrome
De	Desmosome
DED	De-epidermalised dermis
DMEM	Dulbecco's modified Eagle medium
DMSO	Dimethyl sulfoxide
DPX	Dibutylphthalate polystyrene xylene
EC	Epithelial cells
ECM	Extracellular matrix
EDTA	Ethylenediaminetetraacetic acid
EGF	Epidermal growth factors
ELISA	Enzyme-linked immunosorbent assay
Epi	Epithelium
EVOM	Epithelial Volt Ohm Meter
FBS	Foetal bovine serum
FDA	Food and Drug Administration
FITC	Fluorescein isothiocyanate
FNB6	Immortalized human normal oral keratinocyte cell derived from buccal
GIT	Gastrointestinal tract
GL	Granular layer
GM-CSF	Granulocyte-macrophage colony-stimulating
GR	Glucocorticoid receptor
GRE	Glucocorticoid responsive element

H&E	Hematoxylin and eosin
H_2O_2	Hydrogen peroxide
HB	Hydrocortisone 17-butyrate
HBSS	Hank's Balanced Salts solution
HCL	Hydrochloric acid
He	Hemidesmosome
HPLC	High Performance Liquid Chromatography
HRP	Horseradish peroxidase
HV	Hydrocortisone 17-valerate
i3T3	Irradiated 3T3
IC_{50}	Inhibitory concentration (Concentration of a drug that is required for 50% inhibition)
IFN- γ	Interferon-gamma
IHC	Immunohistochemistry
IL	Interleukin
IMS	Industrial methylated spirits
KL	Keratinised layer
MCG	Membrane coating granules
MHC	Major histocompatibility complex
MTT	3-(4,5-dimethylthiazol-2-yl)-2,5 diphenyl tetrazolium bromide
$NaHCO_3$	Sodium bicarbonate
NaOH	Sodium hydroxide
NFAT	Nuclear factor of activated T-cells
NF-kB	Nuclear factor kappa-light-chain-enhancer of activated B cells
NOF	Primary normal oral fibroblasts
OD	Optical density
OECD	Organisation for Economic Co-operation and Development
OH	Hydroxyl group
OKF6	Immortalised human oral keratinocyte cell derived from floor of the mouth
OLP	Oral lichen planus
OSCC	Oral squamous cell carcinoma
PAS	Periodic Acid-Schif stain
PBS	Phosphate-buffered saline
PCNA	Proliferating cell nuclear antigen
PEO	Polyethylene oxide
PET	Polyethylene terephthalate
PHA	Phytohaemagglutinin
PLA2	Phospholipase A2
PLC	Polycaprolactone (PCL)
PLGA-PCL	Poly (lactic-co-glycolic acid-poly (caprolactone)
PMA	Phorbol-12-myristate-13-acetate
PS-iPSCs	Patient-specific induced pluripotent stem
PVP	Polyvinylpyrrolidone
RAS	Recurrent aphthous stomatitis
RDEB	Recessive dystrophic epidermolysis bullosa
RHOE	Reconstituted human oral epithelial

RPMI	Roswell Park Memorial Institute
SD	Standard deviation
SDS	Sodium dodecyl sulphate
SEM	Scanning electron microscope
SL	Superficial layer
SPL	Spinous/prickle layer
SPSS	Statistical Package of Social Science
T_3	Triiodothyronine
TA	Triamcinolone acetonide
TE	Tissue engineering
TEER	Transepithelial electrical resistance
TEM	Transmission electron microscope
TEOM	Tissue engineered oral mucosa
TERT	Telomerase reverse transcriptase
TNF-α	Tumor necrosis factor alpha
TR146	Metastasis buccal carcinoma cell line
UV	Ultraviolet
WHO	World Health Organization
α	Alpha
β	Beta

ACKNOWLEDGMENTS

I would like to take this opportunity to thank all the individuals who gave great support to me throughout my Ph.D studies. First and foremost, I would like to express my deepest gratitude to my supervisor, Dr. Craig Murdoch, for his tremendous advice, guidance, patience and endless support that have been important in all the time of research and writing of this thesis. My sincere gratitude is also dedicated to my co-supervisor, Dr. Helen Colley for her priceless advice and invaluable comments throughout the entire course of this research. Their immense knowledge, reviews and constructive comments are incredibly precious in completing this study and for my future career development.

I wish to convey my appreciation to the staff who provided technical support and their kind assistance throughout this study, especially to Mrs. Brenka McCabe, Ms. Kirsty Franklin, Mr. Jason Heath, Mr. Dave Thompson, Mr. Robert J Hanson and Mr. Christopher J Hill.

My sincere thanks are also devoted to everyone in iBio Science group and my research group members who directly or indirectly involved in 4 years of my study, especially to my colleagues, Amir Zaki, Zulaiha and Siti Amalina. Without their valuable support and cooperation, it would not have been possible to conduct this research.

Not to forget, I wish to express my appreciation to the Government of Malaysia under the Ministry of Education and Universiti Sains Islam Malaysia (USIM) for the financial support, giving me the opportunity to pursue this Ph.D.

Last but not least, I would like to express my heartiest appreciation to all my family members for their understanding and encouragement throughout my studies.

ABSTRACT

Introduction: Tissue-engineered oral mucosa (TEOM) is increasingly being used to assess drug delivery and toxicity, as well as for modeling oral diseases. Current TEOM models are constructed using primary oral fibroblasts and keratinocytes that display donor-to-donor variability and whose widespread use is restricted by availability and ethic limitations. To address these issues, an attractive approach is the development of TEOM using immortalised cells.

Aim: This study aimed to construct and characterise TEOM based on TERT2-immortalised oral keratinocytes (FNB6) cells and use these TEOM to assess the toxicity and delivery of corticosteroids using a novel electrospun-based oral patch.

Methods: TEOM were constructed by culturing immortalised FNB6 oral keratinocytes on top of a normal oral fibroblast (NOF)-populated collagen type 1 hydrogel in tissue culture transwell inserts at an air-to-liquid interface (ALI) for up to 14 days. The TEOM were characterised using histological, immunohistological, ultrastructural (TEM), tissue viability (AlamarBlue), trans-electrical resistance (TEER), and permeability (FITC-dextran) analysis. Cytotoxicity assessment of seven corticosteroids was performed using MTT assay on monolayer cultures (FNB6 and NOF cells) and TEOM. Novel mucoadhesive bilayer patches containing clobetasol 17-propionate (CP) were subjected to morphological, physicochemical, drug release, swelling and cytotoxicity analysis. *In vitro* permeation studies of the corticosteroids against TEOM was measured using HPLC. The immunosuppressive effect of delivered CP against activated Jurkat T-cells was assessed by measuring changes in interleukin-2 (IL-2) release.

Results: Histologically, TEOM mimicked native oral mucosa displaying a stratified epithelium, fibroblast-containing connective tissue and basement membrane. IHC revealed the expression markers for differentiation (cytokeratin 4,13,14), proliferation (Ki-67), cell adhesion (E-cadherin, claudin-4). Furthermore, TEM confirmed the presence of desmosomes and hemidesmosomes in the epithelium. Maximal TEOM

viability was found up to day 25 and maximal TEER value was exhibited at day 20 (155.8 $\Omega.cm^2$). Permeability analysis showed that only small molecules (3 kDa) could pass through the epithelium. Differential drug sensitivity of corticosteroids against monolayer cultures was ranked as follow; CP > BU > BD > BV > TA > HV > HB by IC_{50} value, and this was similar for TEOM although IC_{50} values were higher for 3D models. Novel mucoadhesive bilayer patches containing CP exhibited good physicochemical characteristics and drug release profiles. Toxicity testing to the OECD standard revealed that patch delivered CP was considered a non-irritant. Oral mucosal delivered CP using liquid or patch formulation into the TEOM tissue or receptive medium was both dose and time-dependent. In addition, both liquid and patch delivered CP significantly reduced the secretion of IL-2 by activated Jurkat T cells in a TEOM model replicating an oral inflammatory disease.

Conclusion: FNB6 TEOM models are able to mimic the native oral mucosa and have the potential to be used for drug delivery and toxicity evaluation. Oral patch-delivered CP was able to cross the TEOM and inhibit the IL-2 secretion of activated T cells, suggesting that this mode of drug delivery could be used to treat oral inflammatory diseases.

CHAPTER 1

LITERATURE REVIEW

1.1 Overview

The development of tissue engineered oral mucosa (TEOM) has become an option available in pre-clinical studies (Moharamzadeh et al., 2007). The resemblance of TEOM structurally and physiologically to native oral mucosa has been valuable for various applications including drug toxicity and delivery evaluation (Edmondson et al., 2014). Most TEOM models available have been developed using primary human cells, but the access to these cells is limited and differences of genetic background cause batch-to-batch variability (Dongari-Bagtzoglou and Kashleva, 2006; Southgate et al., 1987). Recent research has moved to use immortalised human cells for tissue engineering as these cells can propagate almost indefinitely whilst retaining the morphology of normal cells, but very a few studies have conducted research on TEOM reconstruction using immortalised cells (Buskermolen et al., 2016; Jennings et al., 2016; Dongari-Bagtzoglou and Kashleva, 2006).

The administration of pharmaceutical agents through oral mucosal is an alternative route of both injectable/parenteral and enteral delivery (Zhang et al., 2002). The oral mucosal route offers localised delivery that may be preferential to other administration routes (Anoop, 2015; Sankar et al., 2011). Oral mucosal diseases are often treated using topical therapy approaches such as creams, ointments, sprays, gels etc. (Mehta et al., 2016; González-Moles, 2010). However, these formulations are affected by oral cavity conditions such as saliva flow and mechanical factors, causing short residence time of the drugs, and leading to unpredictable absorption and distribution, and thus low therapeutic efficacy (Paderni et al., 2012; Chinna Reddy et al., 2011). The possibility of local delivery through the oral mucosa has led to the development of new drug delivery formulations such as oral films or patches (Santocildes-Romero et al., 2017) that can increase the retention time of the drug at the affected area, increasing its absorption. These new delivery systems may be ideal for the treatment of mucosal diseases such as oral lichen planus (OLP) and recurrent aphthous stomatitis (RAS).

The further development of disease models of TEOM is an attractive strategy in evaluating the effectiveness of a novel formulation of the therapeutic agent. Instead of using animals, tissue engineered disease models may be suitable to study the clinical as well as mechanistic aspects of the disease (Van De Worp et al., 2010; Yamada and Cukierman, 2007) whilst also contributing to the ethos of reduction, replacement and refinement (3Rs) of the use of animals in research. The data presented in this thesis aims to contribute to the field of oral mucosal tissue engineering and its usefulness in evaluating novel modes of drug delivery.

1.2 The oral mucosa

The oral cavity encompasses a number of soft tissue structures including the gingiva, vermillion, buccal, hard and soft palate, floor of the mouth and tongue (Nguyen and Hiorth, 2015: Zhang et al., 2002). These areas are lined by epithelial mucosa that differs structurally and demonstrates differences in barrier properties (Gandhi and Robinson, 1994) depending on its location within the oral cavity. This oral mucosa has a variety of functions, including protection, sensation, secretion and thermal regulation (Çelebi and Yörükan, 1999; Squier, 1991).

1.2.1 Organisation of the oral mucosa

There are three types of the oral mucosa lining the oral cavity. These have been categorised according to their functions and characteristics into lining, masticatory and specialised mucosa (Smart, 2004; Rathbone and Hadgraft, 1991) and cover around 60%, 25% and 15% of the total surface area of mucosal, respectively (Squier, 1991; Collins and Dawes, 1987).

Lining mucosa is covered by a non-keratinised stratified squamous epithelium providing an elastic, deformable surface capable of stretching with movements during, for example, mastication and speech. It covers regions of the buccal and labial mucosa, vestibular, floor of mouth, ventral tongue and soft palate. Lining mucosa is attached by a loose, elastic connective tissue to underlying structures (Bhati and Nagrajan, 2012; Lesch et al., 1989). Masticatory mucosa covers the gingiva and hard palate areas. Mechanical forces of mastication at these areas causes abrasion and

shearing and therefore to withstand these forces the mucosa is comprised of a keratinised stratified squamous epithelium which is tightly attached to the underlying structures by a collagenous connective tissue (Sohi et al., 2010). Specialised mucosa has characteristics of both masticatory and lining mucosa and covers the filiform, fungiform and circumvallate papillae of the dorsal tongue. It has a surface comprised of areas of both keratinised and non-keratinised epithelium that are tightly bound to the underlying muscle of the tongue (Bhati and Nagrajan, 2012; Patel et al., 2011).

1.2.2 Structure of the normal oral mucosa

Morphologically, the normal oral mucosa is comprised of three distinct layers; namely the epithelium, connective tissue (lamina propia) and submucosa that are located as an outermost, intermediate and innermost layer, respectively. The epithelial and connective tissue layer is separated by a basement membrane (Dodla and Velmurugan, 2013; Winning and Townsend, 2000; Sudhakar et al., 2006) (Figure 1.1).

The oral epithelium acts as a protective layer that provides protection against potentially harmful agents such as mechanical, microbial and chemicals (Squier et al., 1975). The epithelium of the oral mucosa is classified as stratified squamous epithelium that is either keratinised and non-keratinised (Sankar et al., 2011; Sangeetha et al., 2010). Histologically, the oral epithelium is comprised as four distinct layers of keratinocytes: basal, spinous, granular (keratinised epithelium) or intermediate (non-keratinised epithelium) and superficial layers (Hand and Frank, 2014; Squier and Kremer, 2001; Winning and Townsend, 2000). The superficial layer can be keratinised or non-keratinised, based on the area of the mouth. Structurally, the keratinocytes increase in size and become flatter as they move upward to the superficial layers undergoing differentiation before being shed from the surface of the epithelium (Sangeetha et al., 2010; Squier and Kremer, 2001) (Figure 1.1).

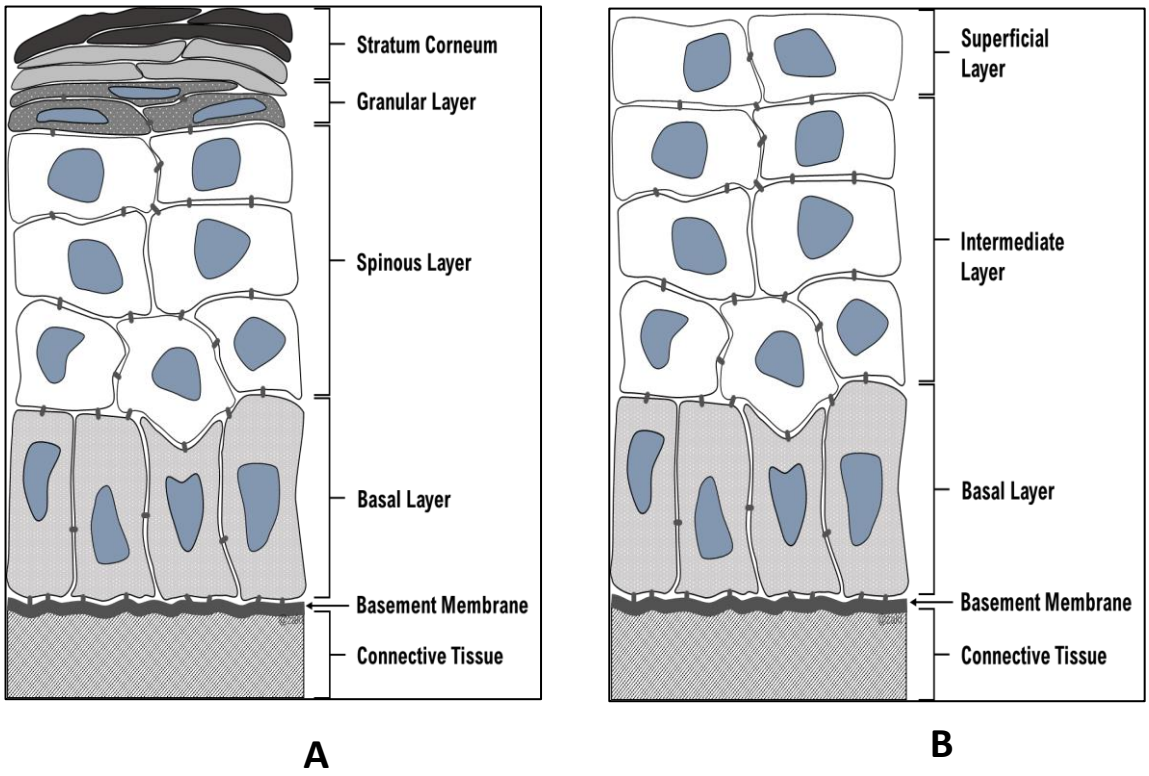

Figure 1.1: Composition of layers of mucosal epithelium: (A) keratinised tissue and (B) non-keratinised tissue.

Other cell types including melanocytes, Langerhans cells, lymphocytes and Merkel cells are also found, representing approximately 10% of the cell population within oral epithelium in both keratinised and non-keratinised forms (Hand and Frank, 2014; Squier and Kremer, 2001; Winning and Townsend, 2000; Squier and Finkalstein, 1998). All these cells lack desmosomal attachments to the neighbouring cells, except Merkel cells and these cells do not participate in the process of maturation seen in epithelial keratinocytes. Histologically, these cells exhibited as a small rounded cell with a clear halo around their nuclei and are classified as non-keratinocytes. The distribution and density of these cells are varied and dependent on the different oral regions (Squier and Kremer, 2001; Barrett et al., 1996; Ramieri et al., 1992; Barrett and Beynon, 1991).

Desmosomes are junctional complexes that adhere epithelial cells together and so play an important role in tissue integrity. These complexes are mainly comprised of proteins from three major gene families: desmosomal cadherins (e.g. desmogleins and desmocollins), armadillo family proteins (e.g. plakoglobin and plakophilin) and the plakin family of cytolinkers (e.g. desmoplakin) (Kottke et al., 2006; Yin and Green, 2004). There are two regions in the desmosome including a core region and plaque region, which mediates tight cell-cell adhesion and attachment to the intermediate filament cytoskeleton, respectively. The core region comprises the extracellular domains of the desmosomal cadherins members that are desmocollins and desmogleins. While the plaque region contains the C-terminal tails of the desmosomal cadherins, which associate directly and indirectly with various cytoplasmic proteins. The armadillo family proteins such as plakoglobin and plakophilins mediate the interactions between desmosomal cadherin tails and desmoplakin that binds directly to the intermediate filaments (Kottke et al., 2006). E-cadherin mediates cell-cell adhesion in a calcium-dependent manner (Kowalczyk et al., 1999). Intracellularly, E-cadherin interacts with either β-catenin or plakoglobin that then combines with actin cytoskeleton filaments through α-catenin (actin-binding protein). E-cadherin also interacts with p120-catenin (Aktary and Pasdar, 2012) allowing tethering of the intermediate filaments to the plasma membrane (Bastos et al., 2014), to provide structural integrity and epithelial barrier function to tissue (Bardag-Gorce et al., 2016; Kottke et al., 2006) (Figure 1.2).

The basement membrane (approximately 1 μm in thickness) is a continuous layer of extracellular material that forms a distinguishing layer between the connective tissues and the epithelium (Winning and Townsend, 2000; Schroeder, 1981). It acts to anchor the underlying connective tissue to the epithelium and functions as a mechanical support (Dodla and Velmurugan, 2013; Shinkar et al., 2012). The basement membrane region has been implicated as the rate-limiting barrier to the passage of some molecules such as chlorhexidine and beta-blocking agents (Rathbone and Tucker, 1993). The basement membrane is attached to the basal keratinocytes through protein complexes called hemidesmosomes (Garrod, 1993), to provide the stable cohesion of these cells to the underlying connective tissue, ensuring resistance to mechanical stresses (Walko et al., 2015; Litjens et al., 2006). The hemidesmosome is composed of anchoring fibrils (collagen VII) that attach to collagen fibres of the underlying connective tissue (Moll and Moll, 1998; Jones et al., 1993; Schroeder, 1981). The core of the complex consists of integrin α6β4 that bind to the extracellular matrix protein laminin-332 (laminin 5) and plectin isoform 1a (P1a), forming a bridge to the cytoplasmic keratin intermediate filament network. Other important components of this complex include BPAG1e (the epithelial isoform of bullous pemphigoid antigen 1 also called BP230), BPAG2 (a collagen-type transmembrane protein also called BP180 or type XVII collagen), and the tetraspanin protein CD151 that is often found associated with integrins (Walko et al., 2015; Owaribe et al., 1990) (Figure 1.2).

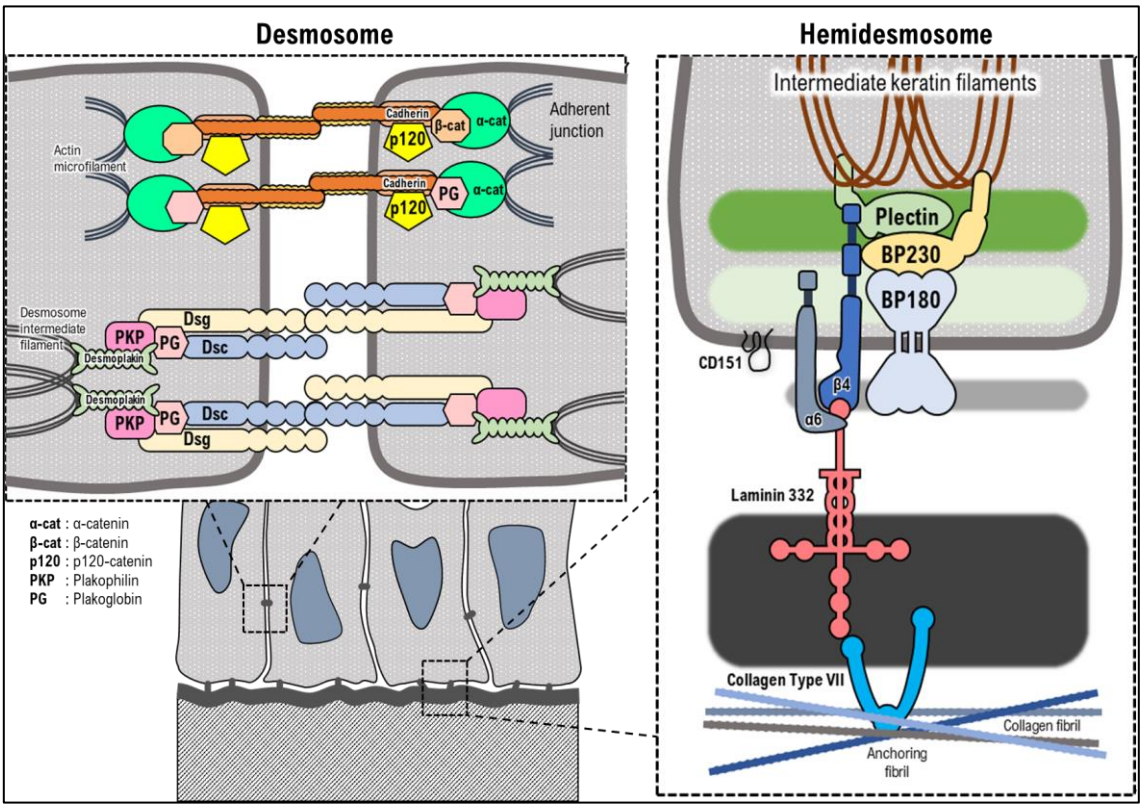

Figure 1.2: The schematic diagram of a desmosome and hemidesmosome and their components illustrating the molecular interactions involved in its assembly.

The connective tissue, also known as the lamina propria, provides mechanical support for the mucosa (Schroeder, 1991) and is the tissue where the blood vessels and nerves reside (Shinkar et al., 2012). It consists mainly of several types of collagen (Sattar et al., 2014) and although it depends upon the location, collagen type I is the most abundantly found in the connective tissue along with collagen type III and elastic fibres (elastin) that is found in the deeper layers. Fibroblasts are the most common cells found in the connective tissue and are involved in producing and maintaining the collagen fibres (type I, III, V and VI) (Becker et al., 1986), proteoglycans (e.g. hyaluronan, heparan sulphate) (Oksala et al., 1995) and also glycoproteins (e.g. fibronectin) (Luomanen et al., 1997). Structurally, the collagen fibres appear thin and loose in the lining mucosa but arrange in bundles in masticatory mucosa (Winning and Townsend, 2000). The fibroblasts that synthesise collagen and promote cross-linking are therefore responsible for extracellular matrix (ECM) production can also differentiate into a myofibroblastic phenotype to facilitate wound closure (Wojtowicz et al., 2014; Schultz et al., 2011; Martin, 1997). Fibroblasts also secrete growth factors and interact with the epithelium via paracrine signaling that enables the keratinocytes to proliferate (Fusenig, 1994) while the differentiation of the epithelium continues (Smola et al., 1998). Macrophages, plasma cells, mast cells, lymphocytes, blood vessels, lymphatic vessels, and nerves are also found in the connective tissue in varying numbers depending on the site (Atkinson et al., 2000; Hilliges et al., 1996; Ramieri et al., 1990).

The submucosa occurs in many regions (cheeks, vermillion) and comprises a layer of loose fatty or glandular connective tissue containing the major blood vessels and nerves supplying the mucosa that separates the oral mucosa from underlying bone or muscle (Squier and Kremer, 2001).

1.2.3 Permeability of the oral mucosa

The permeability barrier of the oral mucosa acts to prevent exogenous and endogenous materials from entering the body and prevents loss of fluid from the underlying tissues to the environment (Hearnden et al., 2012). There are significant differences in the permeability across different areas of the oral cavity, for example,

the epithelium of the floor of the mouth is much more permeable than that of the hard palate (Squier, 1991). The relative impermeability of the oral mucosa is predominantly due to the presence of lipid membrane coating granules (MCG) that are spherical or oval intracellular organelles (100-300 nm in diameter) that are located in the apical layers of the epithelium particularly in the prickle cell layer (Squier, 1977). As the mucosal cells move upward from the basal layer, the cells are differentiated and flattened. The accumulation of lipids occurs and concentrates in the MCG. The number of MCG within cells increases as the cells differentiate and move apically within the epithelium (Squier and Kremer, 2001; Matoltsy, 1976; Elias and Friend, 1975). At the apical cell surfaces, the MCG fuse with the plasma membrane, emptying its lipid content via exocytosis into the intercellular spaces that are lined with lipid lamellae at the upper one-third of the epithelium (Sattar et al., 2014; Sankar et al., 2011; Manganaro, 1997). Subsequently, the plasma membranes become thickened and coated by lipid lamellae that also play a role in the development of a protective layer (Matoltsy and Parakkal, 1965). In addition to the presence of MCG's, the variation in permeability across different regions of the oral mucosa is also due to the relative thickness and pattern of keratinisation of the epithelium (Satheesh Madhav et al., 2009). Whereas sublingual mucosa is relatively thin (100 – 200 μm) and non-keratinised, the buccal mucosa is thicker (500 – 600 μm) and non- or para-keratinised, and the palatal mucosa is intermediate in thickness (250 μm) but keratinised (Satheesh Madhav et al., 2012; Patel et al., 2011), these tissues also differ in permeability levels.

The distinctive feature between keratinised and non-keratinised oral epithelium is its lipid composition in MCG and the presence of keratin (Sankar et al., 2011). Although keratinisation is primarily concerned with increased resistance to abrasion, keratinised tissues also exhibit a lower permeability compared to non-keratinised tissues. Keratinised epithelium contains predominantly neutral lipids (e.g., ceramides and acylceramides) that have been associated with barrier function and decreased permeability to water. In contrast, non-keratinised epithelium has few polar lipids, particularly cholesterol sulphate and glucosylceramides and thus is considerably more permeable to water than keratinised epithelia (Hooda et al., 2012; Satheesh Madhav

et al., 2009). Therefore, it is suggested that the epithelium acts as a greater barrier to the permeation of hydrophilic compounds than to the relatively more lipophilic compounds (Kulkarni et al., 2009).

1.2.4 Protein biomarker expression in the oral mucosa

Immunohistochemistry (IHC) is a common method used to determine the expression of proteins in tissue sections. For the oral mucosa, there are a number of common biomarkers whose expression is used to classify the tissue.

Cytokeratins are the most basic markers of epithelial differentiation and are found in all types of epithelia (Moharamzadeh et al., 2007). Cytokeratin (CK) 4 and 13 are expressed in the suprabasal cells in non-keratinised stratified epithelium (Moll et al., 2008; Izumi et al., 2000), while CK1 and CK10 are expressed in the suprabasal cells in keratinised stratified epithelium (Yuspa et al., 1991). CK5 and CK14 are typically expressed in the basal cell layer and their expression is reduced in the differentiating, suprabasal cell layers (Alam et al., 2011; Fuchs and Green, 1980). CK19 is expressed in the basal keratinocytes of non-keratinising stratified squamous epithelia (Moll et al., 2008). Another differentiation marker is filaggrin that has been suggested to define a premature keratinised state (Izumi et al., 2000).

The expression of proliferation markers such as PCNA and Ki-67 can be found in the basal and in some instances, parabasal layers of the epithelium (Izumi et al., 2004). Protein laminin 5 and collagen IV are classical markers for the basement membrane of the oral mucosa (Kinikoglu et al., 2009; Tunggal et al., 2002; Sahuc et al., 1996). These proteins play a significant role in anchoring basal epithelial cells to the underlying extracellular matrix by contributing to the formation of hemidesmosomes (Kinikoglu et al., 2009; El-Ghannam et al., 1998).

1.3 Tissue engineering

Tissue engineering is a multi-disciplinary field that applies the principles of biology and engineering toward the development of biological equivalents that could restore, maintain, or improve tissue function following damage either by disease or traumatic

processes (Knight and Evans, 2004; Kaihara and Vacanti, 1999). Tissue engineering involves a number of disciplines including clinical medicine, mechanical engineering, materials science, genetics, and related disciplines from both engineering and the life sciences (O'Brien, 2011). According to Izumi et al., tissue engineering is defined as '*the reconstitution of tissues and organs, in vitro, for use as model systems in basic and applied research or for use as grafts to replace damaged or diseased body parts or body functions*' (Izumi et al., 2004).

Fundamentally, tissue engineering involves combining cells, signals and scaffold (Payne et al., 2014; Izumi et al., 2004) in order to fabricate biological substitutes that are similar in terms of function, structure and mechanical properties of the native tissue (Bhat et al., 2011; Knight and Evans, 2004). The fabrication of a tissue-engineered three-dimensional (3D) model requires biomaterials such as cells, scaffold, growth factors and ECM (Knight and Evans, 2004). Typically, cells are seeded in a porous scaffold that acts as a template for tissue formation and to provide the appropriate environment for the regeneration of tissues and organs. Occasionally, the cells seeded in the scaffolds are stimulated chemically by growth factors and physically by culture in a bioreactor (O'Brien, 2011).

1.3.1 Tissue engineering of the oral mucosa

Clinically, TEOM has been utilised for the replacement of tissues damaged or removed as a result of disease or surgery (Rameez et al., 2008; Ohki et al., 2006). It also has been utilised to investigate disease phenomena, pathogenesis, and treatment aspects of oral epithelium (Moharamzadeh et al., 2012; Costea et al., 2003; Duong et al., 2005) and as a substitute to animal models to examine the safety and efficacy profiles of pharmaceuticals and other consumer products (Klausner et al., 2007; Schmalz et al., 2002). The selection of biomaterials for TEOM is essential to ensure a good fabrication of oral mucosa tissue. Attempts to improve the oral mucosa equivalent fabrication have been conducted by investigators and different strategies have been undertaken to develop, optimise and characterise the cell types, scaffolds and cell culture media used in their construction (Moharamzadeh et al., 2007).

1.3.2 Biomaterials used for tissue engineered oral mucosa

1.3.2.1 Scaffolds

The choice of scaffold materials is essential since the success of tissue engineered 3D model fabrication mostly depends on it. Ideally, the scaffold should demonstrate properties including, biocompatibility, biostability and biodegradability (Moharamzadeh et al., 2007). Furthermore, it should be readily available and capable of being prepared and stored for a long shelf-life (MacNeil, 2007). Porosity is also a key element of the scaffold because a connective tissue equivalent should possess an optimum pore size and distribution to allow cell attachment and migration, delivery of biochemical factors and nutrients as well as cell-cell communication (Will et al., 2008; Muschler et al., 2004).

Many types of scaffold have been studied in fabricating tissue engineered 3D models such as fibroblast-populated skin substitutes (e.g. Dermagraft) (Purdue, 1997), natural derived connective tissue (e.g. De-epidermalised dermis (DED)) (Nakamura et al., 2003; Izumi et al., 1999), animal (rat or bovine) type 1 collagen-based (Moriyama et al., 2001; Masuda, 1996), fibrin-based (Ruszymah, 2004), gelatin-based (Mao et al., 2003), synthetic (e.g. poly (lactic-co-glycolic acid-poly (caprolactone) (PLGA-PCL))(Ng et al., 2004) and hybrid scaffolds (e.g. poly (lactic-co-glycolic acid) (Ng et al., 2005).

1.3.2.2 Cell types and sources

The selection of the appropriate cell types or sources is another essential element in ensuring the successful development of oral mucosa equivalents. Fibroblasts and keratinocytes are two main cell types used in constructing 3D oral mucosal models. Fibroblasts and keratinocytes are commonly isolated from the gingiva, buccal, tongue or hard palate regions of oral mucosal biopsies from patients. These two cell types may be primary cells or immortalised cell lines (Moharamzadeh et al., 2007; Dongari-Bagtzoglou and Kashleva, 2006).

The interaction between epithelium and connective tissue are essential factors where the underlying fibroblasts in the connective tissue play a substantial role in epithelial proliferation and differentiation (Kriegebaum et al., 2012; Marionnet et al., 2006;

Costea et al., 2003; Mackenzie and Fusenig, 1983), formation of a basement membrane (Dongari-Bagtzoglou and Kashleva, 2006; Gallico and O'Conner, 1995), keratinocyte adhesion and formation of complex dermal-epithelial junction by synthesising ECM (Moharamzadeh et al., 2008b). In addition, culturing the mucosal models at an air-to-liquid interface (ALI) is another factor that influences epithelial morphogenesis in which the ALI condition encourages the stratification of epithelial cells and enhances the expression of differentiation markers (Bhargava et al., 2004; Feinberg et al., 2005). Typically, normal human cells can only divide a limited number of times, after which point they enter an irreversible state of growth arrest (Kassem et al., 2004). The keratinocyte and fibroblast cultures are employed in early passage and commonly cannot be propagated more than passage four for keratinocytes and up to 10 for fibroblasts (Moharamzadeh et al., 2007; Dongari-Bagtzoglou and Kashleva, 2006).

The reconstituted human oral epithelial (RHOE) model is an example of tissue-engineered oral mucosa that has been commercialised. This model is fabricated using a metastatic buccal carcinoma cell line (TR146) (Jayatilake et al., 2006; Rupniak et al., 1985). It has been reported that carcinoma cell lines do not form a fully differentiated oral epithelium (Yadev et al., 2011) and therefore do not accurately represent normal epithelium due to its abnormal structures and functions. Furthermore, cancerous cells are abnormal and inappropriate for a clinical setting (Moharamzadeh et al., 2012; Dongari-Bagtzoglou and Kashleva, 2006). In contrast, the 3D model of the oral mucosa that has been fabricated using primary cells mimicks the human mucosa (Dongari-Bagtzoglou and Kashleva, 2006). However, construction of oral mucosa equivalents using primary cells requires large quantities of resected tissues in order to ensure adequate numbers of keratinocytes for seeding onto scaffolds. Primary cells have a short lifespan and display variable numbers of epithelium layers because cells from different donors vary in their proliferation rates and longevity (Dongari-Bagtzoglou and Kashleva, 2006).

An immortalised oral keratinocyte cell line is another type of cell that has been developed to overcome the limitation of carcinoma and primary cells in fabricating

the oral mucosa models. Overexpression of telomerase reverse transcriptase-2 (TERT-2) allows cells to continually lengthen their telomeres during cell division, thereby avoiding cellular senescence and death via apoptosis, and enabling prolonged cell replication often termed immortalisation (Irfan Maqsood et al., 2013; Morales et al., 1999). Examples of immortalised human oral keratinocyte cell line are OKF6 derived from floor of the mouth (Dickson et al., 2000) cells that have been developed to enhance the reproducibility of the 3D model of oral mucosa and to avoid dyskeratotic changes in oral mucosa equivalents (Moharamzadeh et al., 2007). Alternatively, 3D models of oral mucosa have also been recently developed using immortalised cells derived from the buccal mucosa of a female donor called FNB6 cells (Jennings et al., 2016).

The production of patient-specific induced pluripotent stem cells (PS-iPSCs) derived from patients is another type of cell that has been utilised to construct 3D skin equivalents. Thus far, this type of cells has not been utilised in developing the oral mucosal equivalents. The autologous PS-iPSCs have the potential to provide an unlimited source of cells and it is believed that this type of cells has the unlimited proliferative capacity and extensive differentiation capability into a wide range of cell types (Onder and Daley, 2012). A study conducted by Itoh et al., have succeeded in developing the full-thickness of skin model using iPSCs-derived keratinocytes and fibroblasts, enabling the development of iPSC-based cell and gene therapy for skin diseases such as recessive dystrophic epidermolysis bullosa (RDEB). In addition, they have proven that the differentiating human iPSCs into fully functional dermal fibroblasts, which can synthesize mature type VII collagen to treat RDEB (Itoh et al., 2013).

1.3.2.3 Cell culture medium

Rheinwald and Green (1975) established a method for the isolation and cultivation of primary keratinocytes cells. They co-cultured keratinocytes with lethally irradiated 3T3 (i3T3) cells as feeder layers that enhance proliferation of the epidermal cells (Kriegebaum et al., 2012). Rheinwald and Green also proposed the use of epidermal growth factors (EGF) as a medium supplement that delays cellular senescence

(Rheinwald and Green, 1977). Several investigators have developed and characterised the 3D model of oral mucosa using a serum-free culture medium where they remove the use of i3T3 feeder layers, in order to reduce the exposure of human graft recipients to xenogenetic DNA or viruses that might be present in serum (Khmaladze et al., 2013; Yoshizawa et al., 2004; Izumi et al., 2000).

Currently, the contents of the medium have been modified by supplementing a few growth factors in Dulbecco's modified Eagle medium (DMEM)-Ham's F-12 medium (3:1), including fetal bovine serum (FBS), glutamine, EGF, hydrocortisone, adenine, insulin, transferrin, tri-iodothyronine, fungizone, penicillin, and streptomycin for oral mucosa reconstruction (Moharamzadeh et al., 2007).

1.3.3 Applications of the tissue engineered oral mucosa

1.3.3.1 Pre-clinical studies

Under the Food and Drug Administration (FDA) regulations, it is necessary for investigators to perform thorough pre-clinical works either *in vitro* or *in vivo* before any substance can be introduced to humans. A Recent study was conducted on measuring the secretion of growth factors and chemokines of healthy tissue-engineered oral mucosa prior to graft implantation into severely combined immunodeficiency mice (Kuo et al., 2015). Moharamzadeh and co-workers used tissue engineered oral mucosa to determine the safety of mouthwashes (Moharamzadeh et al., 2009) and dental materials (Moharamzadeh et al., 2008a). Moharamzadeh et al., have extended their study by assessing and comparing the cytotoxicity of ethanol-containing solutions against tissue engineered oral mucosa with fresh oral mucosal biopsies and monolayer keratinocytes culture (Moharamzadeh et al., 2015). Chai and colleagues have also conducted a study on the dental implant treatment where they have worked on the implant-soft tissue interactions (Chai et al., 2010).

Several investigators have developed an oral cancer model (Marsh et al., 2011; Colley et al., 2011; Gaballah et al., 2008; Gaggioli et al., 2007) that allows research on the pathogenesis, new treatment strategies, diagnostic tests and drug delivery for oral cancer. Oral infection models such as oral candidiasis have also been developed

(Yadev et al., 2011; Mostefaoui et al., 2004) that facilitate identifying the mechanisms of fungal pathogenesis and examine the interaction of oral microbes with the oral epithelium (Gursoy et al., 2010). Meanwhile, drug delivery mechanisms are another area which has the potential to be studied using TEOM (Hearnden et al., 2012). Hearnden and colleagues have shown that fluorescently labelled polymersomes which have been exposed to the TEOM can be traced using laser scanning confocal microscopy (Hearnden et al., 2009). Their findings have created opportunities for other investigators to explore the mechanism of drug delivery, screening drug toxicity, assessing novel dosage as well as to examine the therapeutic and adverse effects of drugs.

The effectiveness of TEOM has also been assessed using animals (*in vivo*). Studies have used TEOM against athymic mice to examine the potential usefulness for repairing mucosal defects (Peña et al., 2011; Rouabhia et al., 2010; Garzón et al., 2009; Izumi et al., 2003). Several investigators have compared wound healing and tissue response after grafting TEOM with different cellular components using different types of animal such as athymic/nude mice, dogs, and rabbits, (Yoshizawa et al., 2012; Bornstein et al., 2011; Ophof et al., 2008; Imaizumi et al., 2004).

The efforts to develop improved oral mucosal models have been performed by incorporating other types of cells, including endothelial cells, which can promote the angiogenesis and revascularisation process (Sahota et al., 2004). In addition, the incorporation of immune cells in the oral mucosal models such as monocytes, Langerhans cells and lymphocytes would benefit in assessing the immune responses (Moharamzadeh et al., 2007). Therefore, these strategies provide a higher degree of complexity of oral mucosal models that could simulate as close as possible to native oral mucosa and broaden their applications.

1.3.3.2 Clinical applications

A few studies have utilised the TEOM for intra- and extra-oral clinical applications. In intraoral applications, engineered human oral mucosa has been applied in maxillofacial reconstructive surgery such as maxillary alveolar cleft (Chin et al., 2005),

mandibular defects (Herford et al., 2010; Chao et al., 2006; Warnke et al., 2004; Orringer et al., 1999) and maxillary sinus augmentation (Voss et al., 2010). In addition, a number of investigators have demonstrated that TEOM can be applied in periodontal therapy (Köseoğlu et al., 2013; Dominiak et al., 2012; Jhaveri et al., 2010; Murata et al., 2008; Mohammadi et al., 2007). GINTUIT® is the first product of oral mucosa tissue which has been approved by FDA. This tissue is an allogeneic cellularised scaffold product, where a thin cellular sheet composed of human fibroblasts, keratinocytes, human ECM proteins and bovine collagen. It is indicated for topical application to a surgically created wound bed in the treatment of mucogingival conditions in adults, but not intended for root coverage (Gupta et al., 2015; Schmidt et al., 2012). For extra-oral application, TEOM has been utilised for substitution urethroplasty (Bhargava et al., 2004), ocular reconstruction (Nakamura et al., 2003), eyelid reconstruction (Yoshizawa et al., 2004), burn wound (Iida et al., 2005), corneal (Nishida et al., 2004) and oesophageal repair (Takagi et al., 2012).

1.4 Oral lichen planus

Oral lichen planus (OLP) is a chronic autoimmune, mucocutaneous disease that affects various parts of the body including the oral mucosa, skin, genital mucosa, scalp and nails (Ismail et al., 2007). Commonly, OLP affects the stratified squamous epithelium in which auto-cytotoxic T lymphocytes trigger apoptosis of oral epithelial cells leading to chronic inflammation (Schlosser, 2010; Scully and Carrozzo, 2008).

1.4.1 Epidemiology of oral lichen planus

The onset of the disease usually occurs between 30 and 60 years of age (mean at 50 years) and, in general, this disease affects approximately 0.5-2% of the adult population (Sonthalia and Singal, 2012). OLP occurs predominantly in adults over 40, however, it may occasionally affect younger adults and children (Scully and Carrozzo, 2008; Sugerman and Savage, 2002). Based on gender, women have a slightly higher tendency than men to be affected with OLP with a ratio of 1.4:1 (Scully and Carrozzo, 2008; Sugerman and Savage, 2002). According to the World Health Organization (WHO), OLP has been classified as a disease that has potential to cause malignant transformation, with reports suggesting that approximately 1–2% of OLP patients go

on to develop oral squamous cell carcinoma (OSCC) (Georgakopoulou et al., 2012; Warnakulasuriya et al., 2007).

1.4.2 Clinical features

OLP characteristically presents as symmetrical and bilateral lesions or multiple lesions that clinically present as white striations, plaques or papules, erosion, erythema or blisters (Figure 1.3). OLP may present as painless or painful lesions with features such as erythema, erosions and ulceration being the most painful OLP manifestations (Georgakopoulou et al., 2012; Ismail et al., 2007). The condition typically affects the buccal mucosa (90%), tongue (mainly the dorsum), gingiva, labial mucosa and lower lip (Schlosser, 2010; Eisen, 2002). Less common sites include the palate, upper lip and floor of the mouth (Schlosser, 2010; Bagan-Sebastian et al., 1992). Simultaneous association of extraoral sites (i.e., scalp, skin, nails, conjunctiva, esophagus, larynx, urethra, vulva and vagina, and perianal area) is common and results in severe morbidity (Schlosser, 2010; Eisen, 1999) (Figure 1.3).

The classic histopathological features of OLP are characterised by a dense inflammatory infiltrate in the upper lamina propria, predominantly containing T-cells, degeneration of basal keratinocytes and basal membrane hyperkeratosis or atrophy of the keratin layer (Georgakopoulou et al., 2012; Thongprasom and Dhanuthai, 2008; Dorrego et al., 2002) and rare areas of atrophic epithelium where the rete pegs may be shortened and pointed (a characteristic known as ‘sawtooth’ rete pegs). In addition, eosinophilic colloid bodies (Civatte bodies), that demonstrate degenerating keratinocytes, are commonly visible in the lower half of the epithelium (Carozzo, 2014; Edwards and Kelsch, 2002; Helander and Rogers, 1994) (Figure 1. 4).

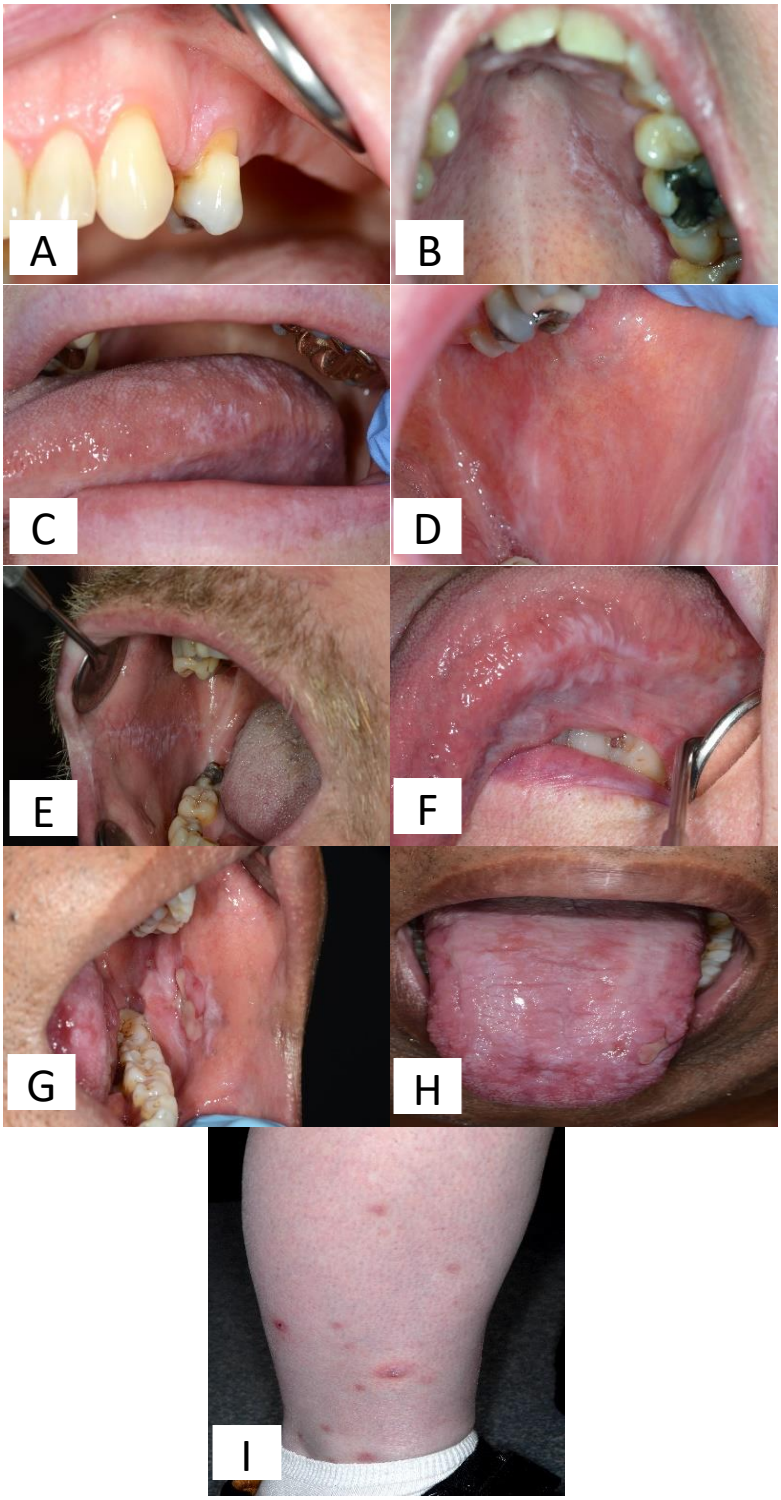

Figure 1.3: Clinical presentations of oral lichen planus with different forms: (A) gingival, (B) reticular palatal, (C) reticular tongue, (D) reticular buccal, (E) papular, (F) ulcerative tongue, (G) ulcerative erosive buccal, (H) ulcerative erosive tongue and (I) cutaneous. Images were kindly supplied by Dr. Sabine Jurge, Consultant in Oral Medicine, Sheffield Teaching Hospitals NHS Foundation Trust. (Images were taken with written, informed consent under NHS ethical approval).

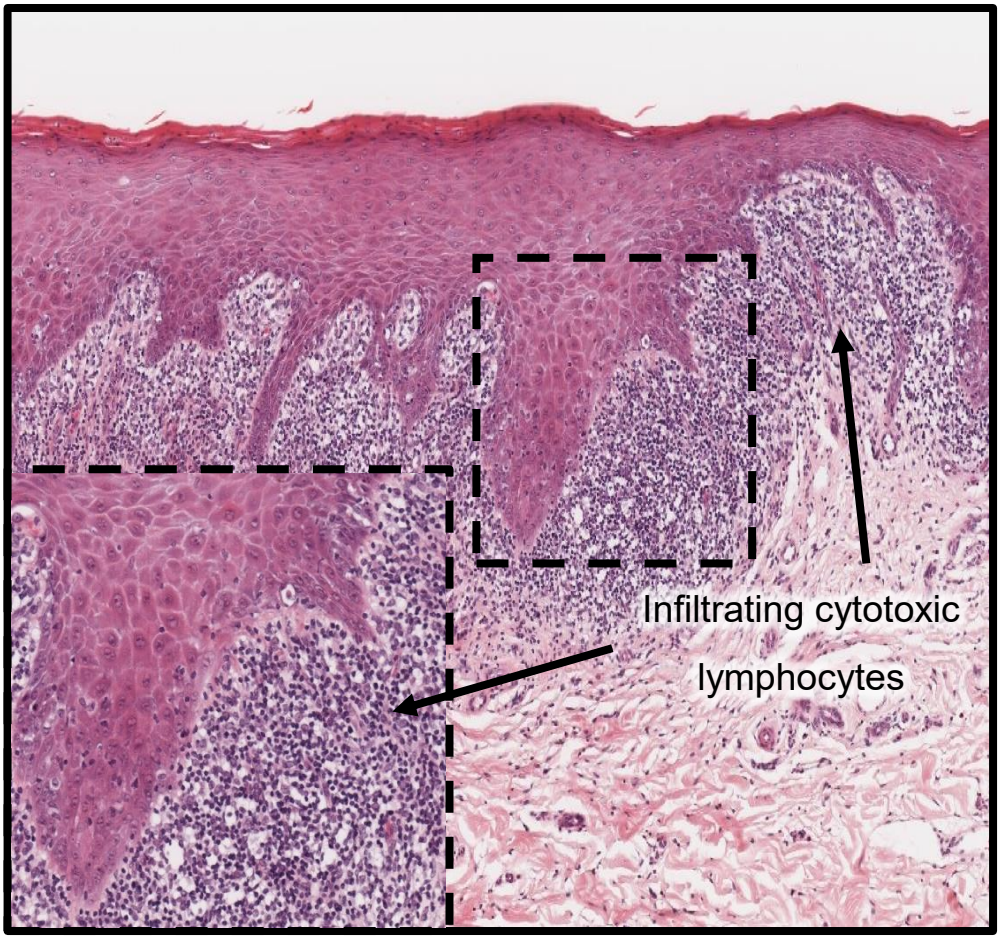

Figure 1.4: Histopathological features of oral lichen planus. (Image supplied by Oral Medicine, Charles Clifford Dental Hospital, Sheffield Teaching Hospitals NHS Foundation Trust).

1.4.3 Aetiology and Pathogenesis

The exact aetiology of OLP is idiopathic. It is suggested that cell-mediated immunity plays a major role in the pathogenesis of OLP (Farhi and Dupin, 2010; Lodi et al., 2005). An immunological process is believed to be triggered by activation of antigen-presenting cells (APC), most likely Langerhans or stromal dendritic cells (Sugerman et al., 2002) by viral infection (e.g. Hepatitis C virus) (Lodi et al., 2005), contact allergen (e.g. dental amalgam) (Carrozzo and Thorpe, 2009) or systemic drugs (e.g. NSAIDs) (Figure 1.5-1) (Thompson and Skaehill, 1994). The secretion of chemokines such as CCL5/CCL20/CCL19 by activated APCs and keratinocytes (Ichimura et al., 2006) attracts T lymphocytes into the developing OLP lesion. Both the activated APCs and keratinocytes present antigen associated with MHC class II to $CD4^+$ T cells (Figure 1.5-2a) and MHC class I to $CD8^+$ T cells (Figure 1.5-2b), respectively (Carrozzo, 2014; Sugerman et al., 2002). The activated helper $CD4^+$ T lymphocytes secrete IL-2, IL-12 and IFN-gamma that bind to their respective receptors on $CD8^+$ T cells promoting the cytotoxicity of CD8+ T lymphocytes (Figure 1.5-3a) (Shirasuna, 2014; Farhi and Dupin, 2010). Activated $CD8^+$ T cells then express cytotoxic and pro-apoptotic mediators (TNF-α, granzyme B, FasL or perforin), that mediate apoptosis of basal keratinocytes causing pathology (Figure 1.5-3b) (Carrozzo, 2014; Iijima et al., 2003). In addition, degranulation by mast cells releases chymase, causing degradation of the basement membrane aiding the migration of lymphocytes to basal keratinocytes (Figure 1.5-4) (Zhao et al., 2001; Zhou et al., 2001; Farthing et al., 1990).

The precise mechanism of OLP develops to OSCC remains poorly understood. However, investigators hypothesise that the chronic inflammation due to inflammatory cells, cytokines and other stromal cells provide signals that result in epithelial cells to derange their growth control and in combination with oxidative stress, which subsequently provokes DNA damage that may initiate neoplastic changes, hence the link to development of oral cancer (Ergun et al., 2011; Battino et al., 2008; Gonzalez-Moles et al., 2008; Mignogna et al., 2004).

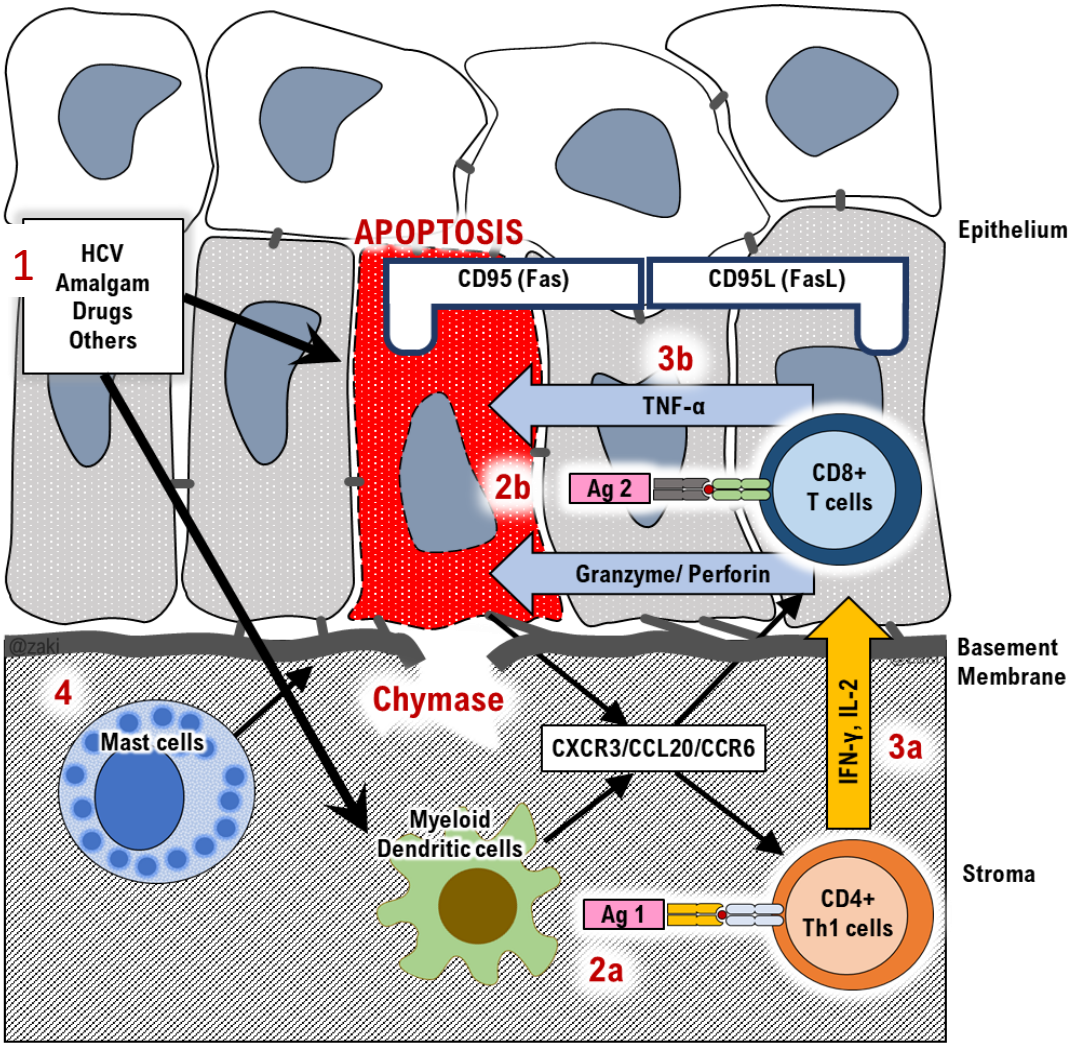

Figure 1.5: Immunopathogenesis mechanism of oral lichen planus.

1.4.4 Management

Although many alternatives for the treatment of OLP are available, no therapy is curative (Sonthalia and Singal, 2012). Current treatments are palliative and vary in efficacy (Schlosser et al., 2010; Sugerman and Savage, 2002). The aims of OLP treatment include diminishing symptoms, curing erosive lesions and reducing the functional impact of OLP (Schlosser, 2010). Treatment of OLP relies on symptoms, the extent of oral and extra-oral clinical involvement, medical history and other factors. Patients with reticular and other asymptomatic OLP lesions usually require no active treatment (Schlosser, 2010; Scully and Carrozzo, 2008). Good oral hygiene, together with the use of mouthwashes and plaque decrease, may have valuable effects on lesions (Córdova et al., 2014; Boorghani et al., 2010). Patients with symptomatic lesions may also need treatment, usually with steroids (Scully and Carrozzo, 2008).

1.4.4.1 Drug Treatment for OLP

Corticosteroids are also known as glucocorticosteroids or glucocorticoids (Barnes, 2006; Gibson and Ferguson, 2004). Corticosteroids are the first-line treatments of OLP since their topical form has better benefits and less adverse effects (Córdova et al., 2014; Sonthalia and Singal, 2012). Drug treatments for OLP are topical and systemic agents that are immunosuppressive (Scully et al., 2000). Treatment with topical corticosteroids is preferred more than systemic corticosteroids because these have fewer side effects. However, systemic corticosteroids may be applied if lesions are widespread and there is a recalcitrant disease (Scully and Carrozzo, 2008; Scully et al., 2000).

Currently, topical corticosteroids are the agents that are being used for localised OLP treatment. The most effective topical corticosteroids in treating the OLP patients include triamcinolone (mid potency), fluocinolone acetonide and fluocinonide (potent fluorinated steroids) and clobetasol-17-propionate (CP) (superpotent halogenated steroids) (Carbone et al., 2009; Al-Hashimi et al., 2007; Lavanya et al., 2011). Patients with localised OLP are usually treated with potent steroids. Particularly, CP seems to be the most effective topical steroid, showing a high remission rate (56-75%) of OLP signs and symptoms. Furthermore, CP has shown to be more effective than

triamcinolone acetate and fluocinolone in comparative studies (Córdova et al., 2014; Carrozzo and Gandolfo, 1999).

The topical corticosteroids have been formulated into a few types of dosage forms such as elixir, ointment, spray, mouthwash and adhesive bases (Thongprasom and Dhanuthai, 2008). Commonly, patients are instructed to apply the topical corticosteroids a few times daily and they should not eat or drink for 1 hour in order to maintain drug contact with the mucosal surface. Based on previous studies, the intake of topical corticosteroids is safe when applied to the mucosa membrane for short intervals and they can be applied for long time periods (up to 6 months) (Carbone et al., 2003). OLP patients are examined carefully and monitored regularly if they use the steroids for prolonged periods because this has the potential to lead to adrenal suppression (adrenal atrophy) (Scully and Carrozzo, 2008), which causes inadequate production of cortisol (adrenal insufficiency) (Younes and Younes, 2017; Broersen et al., 2015; Chrousos et al., 2000), leading to complications such as inhibition of growth, hypogonadism or osteoporosis (Uva et al., 2012; Schacke et al., 2002). OLP patients are also at risk of developing mucocutaneous candidiasis, thought to be due to the weakened or undeveloped immune system (local immunosuppression) at the mucosal surfaces (Buhl, 2006; Hanania et al., 1995), which can be prevented by using antifungals such as miconazole gel or chlorhexidine rinses (Córdova et al., 2014; Van Boven et al., 2013; Thongprasom and Dhanuthai, 2008).

Systemic corticosteroids are used to treat patients with generalised OLP where the lesions are recalcitrant, erosive, erythematous and also in the condition when the lesions are widespread to another area such as skin, genitals, oesophagus or scalp (Carbone et al., 2009; Scully and Carrozzo, 2008; Scully et al., 2000). Likewise, this type of corticosteroid treatment is reserved for cases when topical corticosteroid treatments have failed (Scully and Carrozzo, 2008). Prednisolone is an example of systemic corticosteroids that are used at 40 to 80 mg daily (Córdova et al., 2014; Scully and Carrozzo, 2008). This range of dose is commonly adequate to achieve a response and its toxicity requires to be used only when necessary, at the lowest dose, and for the shortest time possible (Scully and Carrozzo, 2008). Systemic steroids should be

taken either for brief periods of time (5–7 days) and then withdrawn abruptly, or the dose should be reduced by 5–10 mg/day gradually over 2–4 weeks (Carbone et al., 2009; Scully and Carrozzo, 2008; Thongprasom and Dhanuthai, 2008; Scully et al., 2000).

Additionally, a range of other treatments also have been used, including oral steroids, topical and systemic retinoids, topical cyclosporine, oral dapsone, tetracycline, levamisole, antimalarials, azathioprine, enoxaparin, thalidomide, photochemotherapy, laser treatments, and surgery, all with variable outcomes (Schlosser, 2010; Lodi et al., 2005).

1.4.4.1.1 Corticosteroids - mechanism of action

Corticosteroids have various effects including anti-inflammatory, anti-proliferative, immunosuppressive and vasoconstrictive effects that are mediated by intracellular glucocorticoid-specific receptors (GR) expressed by immune cells as well as fibroblasts and keratinocytes (Van Der Velden, 1998; Marks et al., 1982; Ponec et al., 1981).

Corticosteroids are lipophilic molecules that enter cells through the cell membrane by passive diffusion into the cytoplasm. Within the cell cytoplasm, GR bind with steroid ligands to form GR complexes that eventually translocate to the cell nucleus. Within the nucleus, these complexes bind to a region of DNA called the glucocorticoid responsive element (GRE) (Wiedersberg et al., 2008; Van Der Velden, 1998; Hughes and Rustin, 1997) and this interaction either up-regulates or down-regulates specific gene expression such as lipocortin and inflammatory cytokines (Burkholder, 2000).

Corticosteroids act by suppressing the inflammatory process through several pathways (Burkholder, 2000). These include mediators of inflammation that are involved in phospholipid-arachidonic acid cascades such as phospholipase A2 (PLA2) and cyclooxygenase (COX). Expression of both enzymes is suppressed, causing the reduced formation of prostaglandins and thromboxanes (Mitchell et al., 1994; Schalkwijk et al., 1991). GR complex suppresses the expression of PLA2 by inducing the activity of a protein called lipocortin 1. This protein binds to the membrane

phospholipid, which is a substrate for PLA2, thus, reducing substrate availability to generate mediators like prostaglandins and leukotrienes (Uva et al., 2012; Rhen and Cidlowski, 2005; Burkholder, 2000; Ahluwalia, 1998). The GR complex is also suggested to suppress cytokine activity by blocking the effects of certain transcription factors such as nuclear factor kB (NF-kB) and activator protein 1 (AP-1), resulting in the reduction of IL-2, IL-6 and CXCL8 levels (Burkholder, 2000; Ray et al., 1995) (Figure 1.6).

Furthermore, the use of corticosteroids exhibits apoptotic and anti-apoptotic properties. Corticosteroids markedly reduce the number of inflammatory cells such as eosinophils and lymphocytes. The survival of eosinophils is dependent on the presence of cytokines such as IL-5 and granulocyte-macrophage colony-stimulating factor (GM-CSF). The blockade of IL-5 and GM-CSF by corticosteorids leads to eosinophil apoptosis (Barnes, 1998; Owens et al., 1991). In contrast, it has been suggested that the corticosteroid therapy enhances neutrophil survival by inhibition of apoptosis through various pathways including the upregulation of the anti-apoptotic Bcl-2 family members and activation of NF-κB (Saffar et al., 2011; Liles et al., 1995).

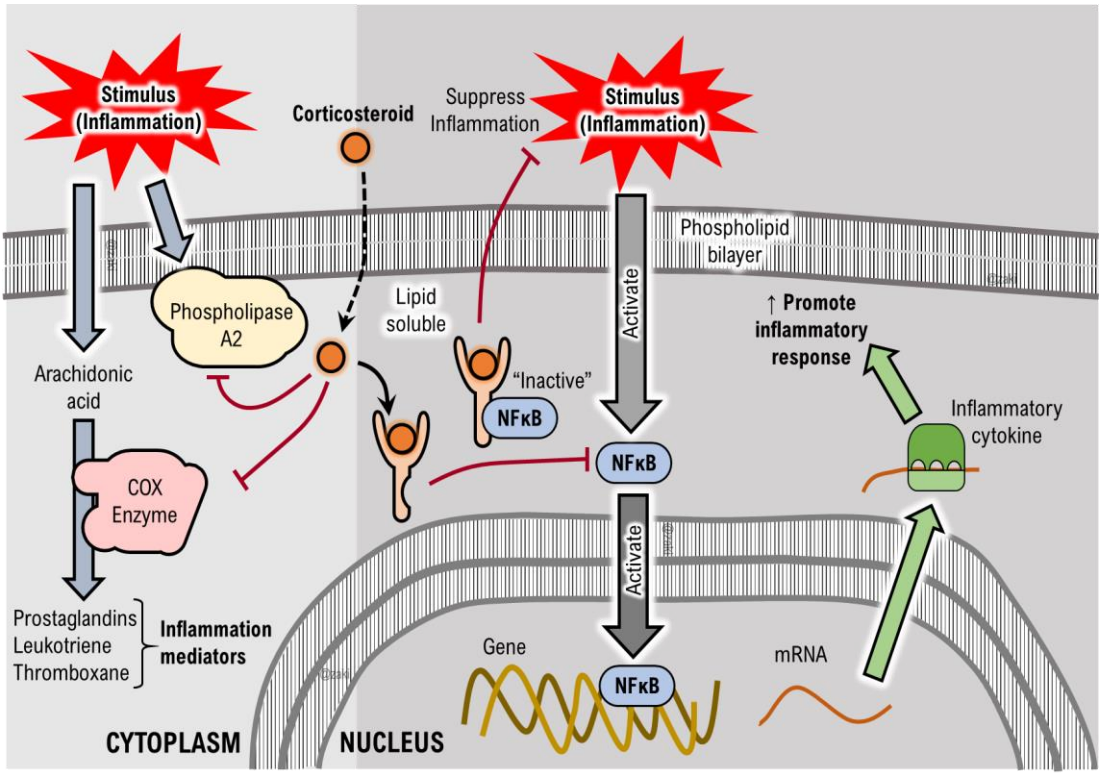

Figure 1.6: Mechanism of actions for corticosteroids.

1.4.4.1.2 Structure-activity relationship of corticosteroids

The efficacy of corticosteroids is related to its level of potency and capability of the drug to reach its target site (Wiedersbeg et al., 2008; Federman et al., 1999). The potency of corticosteroids is influenced by several factors including chemical structure, concentration and its carrier vehicle (Wiedersbeg et al., 2008; Hengge et al., 2006; Kansky et al., 2000; Pershing et al., 1994; Stoughton, 1987).

Corticosteroids are comprised of a 21-carbon (C) structure that includes a 4-ring cyclo-pentane-perhydro-phenanthrene nucleus and a 17, 21-dihydroxy (OH)-20-keto (O) side chain. The rings are designated as A – D, with 3 six-membered rings and one five-membered ring. Also, these structures have a double bond between C4 and C5, hydroxyl (OH) group at C11, and ketone group at C3 that provide the glucocorticoid and mineralocorticoid properties (Kwatra and Mukhopadhyay, 2018; Mehta et al., 2016). The hydroxyl (OH) group at C17 also increases the glucocorticoid effects (Burkholder, 2000) (Figure 1.7).

The alteration or substitution of basic cyclo-pentane-perhydro-phenanthrene ring structures produces corticosteroids with varying potency (Gual et al., 2015; Hengge et al., 2006; Thorburn and Ferguson, 1994). In general, the potency of corticosteroids is dramatically augmented by introducing an unsaturated double bond between the C1 and C2 position, removing the hydroxyl groups, introducing long carbon side chains especially at the C21 position or adding a halogen group at the C9 position (Gual et al., 2015; Kansky et al., 2000; Burkholder, 2000). Modification of the corticosteroid chemical structure can be achieved by dehydrogenation, alkylation (e.g. methylation), halogenation and esterification reaction (Kerscher et al., 2006). It has been reported that halogenation increases the potency and adverse effects of corticosteroids (Gual et al., 2015) and also attributes to higher mineralocorticoid activity and greater cytotoxicity (Mehta et al., 2016). While the esterification reaction enhances the lipophilicity by adding lipophilic components such as acetonide, valerate or propionate (Gual et al., 2015; Kansky et al., 2000; Thorburn and Ferguson, 1994), improving the absorption of the corticosteroid (Kwatra and Mukhopadhyay, 2018). Esterification also improves the safety profile of corticosteroids (Gual et al., 2015).

Addition of an unsaturated double bond between C1 – C2 position in ring A enhances the glucocorticoids activity and anti-inflammatory effect, whilst simultaneously decreasing the cell metabolism rate and salt-retaining activities (Burkholder, 2000; Thorburn and Ferguson, 1994). All corticosteroids used in this study contain an unsaturated double bond between the C1 – C2 position except hydrocortisone valerate (HV) and hydrocortisone butyrate (HB). Hydrocortisone contains the basic corticosteroid structure with the addition of an ester group such as valerate and butyrate at the C17 position through esterification, forming HV and HB, respectively (Kansky et al., 2000; Bodor et al., 1983). The enhancement of glucocorticoid and mineralocorticoid activities is due to increased affinity of the molecules to the glucocorticoid receptors that can be achieved by halogenation at position 6 and/or 9 (Kwatra and Mukhopadhyay, 2018; Thorburn and Ferguson, 1994). The modification of corticosteroid chemical structure by halogenation at the C9 position is present in most of corticosteroids used in this study except HV, HB and Budesonide (BU). Substitution of 16, 17-acetal molecule with butyraldehyde to non-halogenated corticosteroid forms BU (Szefler, 1999; Boobis, 1998).

The combination of the unsaturated double bond between C1 and C2 and substitution at C16 to the halogenated corticosteroids can reduce the mineralocorticoid activity whilst simultaneously elevating the anti-inflammatory effects (Kwatra and Mukhopadhyay, 2018; Kerscher et al., 2006). These effects can be observed when the methyl group is inserted through methylation at C16 to the halogenated corticosteroids that forms betamethasone. The esterification of the hydroxyl group in betamethasone with valerate and propionate at C17 and, C17 and C21 forms betamethasone valerate (BV) and betamethasone dipropionate (BD), respectively (Kwatra and Mukhopadhyay, 2018; Burkholder, 2000). While, the combination of the unsaturated bond (C1 – C2) and the addition of acetonide at hydroxyl group on C16 and C17 position to the halogenated corticosteroid forms Triamcinolone acetonide (TA) (Kwatra and Mukhopadhyay, 2018). Clobetasol-17-propionate (CP) has been classified as a di-halogenated corticosteroid (Zampetti et al., 2010) that contains a fluoride group in ring B at the C9 position. An additional augmentation potency of CP has been performed by adding the chloride group as a second halogenation that

distinguishes CP apart from other corticosteroids used in this study (Katz and Gans, 2008; Burkholder, 2000). CP comprises a double bond between C1 and C2 position and substitution of the hydroxyl group with a propionate at the C17 position through esterification, which increases its cell absorption (Gual et al., 2015; Wiedersberg et al., 2008). The combination of all these modifications has made CP a superpotent corticosteroid (Zampetti et al, 2010; Kerscher et al., 2006). CP has been described as 1800 times more potent as compared to hydrocortisone (least potent) and is associated with a higher risk for adverse effects (Bassuoni et al., 2016; Zampetti et al., 2010). Principally, non-halogenated corticosteroids (e.g. HV and HB) often result in fewer adverse effects than halogenated corticosteroids (e.g. CP) (Allenby and Saprkes, 1981) and consequently less potent and safer to use (Kansky et al., 2000).

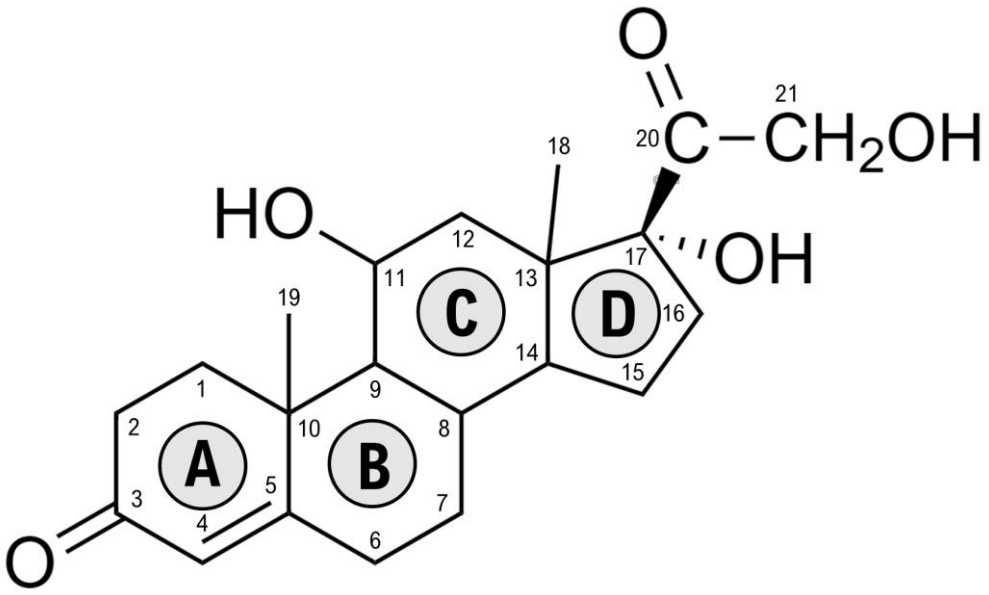

Figure 1.7: Basic molecular structures of corticosteroids.

1.4.4.1.3 Adverse effects

Systemic side effects occur because the drug is being absorbed into the bloodstream and distributed to and affect other parts of the body, such as the adrenal gland (Mehdipour and Zenouz, 2012; Hengge et al., 2006). Systemic side effects can be serious and may include a hypothalamic-pituitary-adrenal axis, weight gain, osteoporosis, avascular necrosis, diabetes, Cushing's syndrome and hypertension (Mason et a., 2002; Bircher et al., 1996; Lozada-Nur 1991). The long-term use of topical corticosteroids may have substantial local side effects although it demonstrates remarkable benefit in reducing inflammation. However, some side effects may be noticed within days of starting therapy. Local side effects may include tachyphylaxis, hypogeusia, burning mouth, skin atrophy, hypersensitive reactions and oral hairy leukoplakia (Baid and Nieman, 2006; Key et al., 2003).

1.5 Drug delivery systems

Drug delivery systems can be defined as the process of an active pharmaceutical ingredient (API) administration (Meehta et al., 2012) to the body in order to attain a therapeutic effect and also increases its effectiveness and safety by controlling the rate, time and place of release of drugs in the body (Tiwari et al., 2012). Once the API is inside the body the drug will cross the biological barrier such as ECM cells and intracellular compartments before it can reach target organs or tissues. Before it reaches the desired site, the API could be inactivated or become trapped at non-target sites and at the same time can produce undesirable effects on non-target organs or tissues. Therefore, efficient delivery of API to target tissues is critical to reduce unintended off-target toxicity to other organs, while delivering the drug in a cost-effective manner (Mehta et al., 2012).

1.5.1 Oral mucosal drug delivery

The oral cavity is a potential route to deliver therapeutic agents either locally or systemically (Rathbone et al., 2015). Local administration of therapeutic agents may provide a more targeted and efficient drug-delivery option as well as reducing the side effects of systemic delivery for diseases of the oral mucosa (Nguyen and Hiorth, 2015; Sankar et al., 2011). However, drug absorption to the mucosa is often disrupted due

to several factors including saliva, mucus, membrane coating granules (apical layers), variable thickness and pattern of keratinisation of the epithelium and basement membrane. As a result, sometimes only small quantities of drug are able to penetrate through the oral mucosa epithelium (Hooda et al., 2012; Satheesh Madhav et al., 2012; Verma and Chattopadhay, 2011; Sankar et al., 2011; Sudhakar et al., 2006) and therefore several challenges need to be addressed by researches for mucosal delivery to become the choice route of administration. The development of modern formulations is not only focussed on attaining the therapeutic aims of drug delivery but also to overcome unfavourable environmental conditions found in the oral cavity (Satheesh Madhav et al., 2012; Sudhakar et al., 2006). An ideal oral transmucosal drug delivery system should quickly attach to the mucosal surface and maintain a strong interaction to prevent displacement. In addition, the bioadhesive performance should not be impacted by the surrounding environmental pH (Shakya et al., 2011). Other desirable characteristics of an oral transmucosal drug delivery system include high drug loading, complete drug release and convenient administration (Satheesh Madhav et al., 2012; Sudhakar et al., 2006).

1.5.2 Advantages and disadvantages of oral mucosal drug delivery

Generally, the oral route (tablet formulation) is the first choice of patients and clinicians for drug administration as it is considered the most convenient route for drug delivery and therefore has the highest compliance rates. However, this route has several potential drawbacks, such as extensive hepatic first-pass metabolism and pre-systemic drug degradation in the gastrointestinal tract, which results in compromised dosing accuracy, low drug availability at the site of action and the necessity for frequent administration (Singh et al., 2011; Scholz et al., 2008; Sudhakar et al., 2006).

These restrictions have driven the development of alternative administration routes with the absorptive mucosae attracting extensive research. The oral mucosa has a number of advances as a drug delivery route such as a rich blood supply, being relatively permeable, robust, short recovery times after stress or damage and tolerant to potential allergens (Singh et al., 2011; Scholz et al., 2008). Delivering drugs across the oral mucosa shows rapid onset of effect, good bioavailability, bypasses the hepatic

first-pass metabolism**,** reduced amount of administered drug and low-dose related side effects (Sangeetha et al., 2010; Scholz et al., 2008). Likewise, it is non-invasive and less intimidating for many patients compared with other routes of administration particularly drug delivery by injection such as via intravenous, intramuscular or intraperitoneal routes. Therefore, this route could increase patient compliance and it is greatly acceptable by patients (Troung-Le et al., 2015; Satheesh Madhav et al., 2012).

1.5.3 Oral mucosa formulations

The oral mucosal dosage form can be broadly classified into three major categories including liquid, semisolid and solid or spray dosage forms (Patel et al., 2011; Sudhakar et al., 2006). Liquid dosage forms can be formulated as solutions or suspensions in which the drug is solubilised or suspended into an appropriate aqueous vehicle. Application of such types of dosage can produce local action into the oral cavity and several antibacterial mouthwashes and mouth-freshener are commercially available for this purpose. The drawback associated with these types of dosage forms is that they are not readily retained or targeted to oral mucosa and can deliver relatively uncontrolled amounts of drug throughout the oral cavity. The absorption of the drug formulated into these types of dosage forms is enhanced by using polymers (Patel et al., 1999) or iontophoretic techniques (Jacobson, 2001; Campisis et al., 2010). Previous studies have shown that a novel bioadhesive liquid, the sodium alginate suspension has exhibited the capability to protect the oesophageal surface against reflux and delivering the drug at the affected mucosal area (Avinash et al., 2008; Santos et al., 1999).

Gels, creams, hydrogel, emulgels and ointments are examples of semisolid solid preparation that can be used topically on mucosal areas either to produce local or systemic effects. The advantages of semisolid dosage forms include ease of drug administration to the periodontal pockets (Needleman, 1991) and facilitating the dispersion of drug throughout the mucosal surface of the oral cavity (Squier and Kremer, 2001). Meanwhile, the disadvantage of semi-solid dosage forms is poor retention at the site of application. However, this disadvantage can be solved by the

integration of a bioadhesive polymer into the drug formulation (Jones et al., 1996). A study has recommended emulgels (gellified emulsion) form of flurbiprofen for buccal delivery. Perioli et al., have reported that the release of drug ranged from 50–80% within 100 minutes of administration. Moreover, it has also been reported that the application of emulgels on human buccal mucosa can be retained for approximately one hour (Perioli et al., 2008).

Solid dosage forms are formulated into tablets, lozenges, patches, films and wafers. Drawbacks of tablets can include discomfort feeling to children and elderly, as they cannot be retained for long periods at the lesion site (Patel et al., 2011), patient acceptability and the non-ubiquitous distribution of the drug within saliva for local therapy (Squier and Kremer, 2001). Examples of tablets on the market are nitroglycerin (sublingual) and prochlorperazine (buccal) (Patel et al., 2011). The dissolution or disintegration of lozenges is usually controlled by the patient. Commonly increased sucking and saliva production causes uncontrolled swallowing and loss of drug down the GI tract. Therefore, solid dosage forms generally have a much higher inter- and intra-individual variation in absorption and bioavailability. Also, such systems are not able to provide unidirectional release of the drug. Continuous secretion of saliva is another major impediment to the performance of such dosage forms (Patel et al., 2011).

Patches, films and wafers can be prepared with multidirectional or unidirectional release. The relative thinness of the films, however, means that they are more susceptible to over hydration and loss of adhesive properties (Squier and Kremer, 2001). Patch form is an ideal formulation for a retentive delivery system as these types of formulations can be administered to the mucosal areas as it contains a large expanse of smooth and immobile tissue (Bruschi and Freitas, 2005).

An aerosol spray is an alternative to the solid dosage form. This type of dosage form can deliver the drug in fine particulates or droplets onto the mucosal area. Therefore, it is readily available for the absorption and the lag time for the drug to be available for the site of the absorption is reduced. Previously, it has been reported that the

administration of insulin in spray form to the buccal mucosa has an effective therapeutic effect for diabetes. Generex's Oral-lyn™ is an example of an oral spray of insulin for treating the type I and II diabetes (Xu et al., 2002). In addition, another form of spray based on RapidMist™ technology by Generex also in clinical development which intended for buccal delivery of fentanyl citrate, morphine and low molecular weight heparin (Patel et al., 2011).

1.5.4 Technologies for improving drug delivery

In spite of obstacles in the oral mucosa drug delivery system, there are many emerging technologies that could enhance delivery of drugs across the oral mucosa. The various strategies for improvements have been carried out to increase the bioavailability of the drugs including the incorporation of permeation enhancers and enzyme inhibitors in the formulation as well as novel formulation strategies (Muheem et al., 2016; Sudhakar et al., 2006).

Permeation enhancers are components that are incorporated in the formulation of the drug that could increase the permeability of normally impermeable drug molecules (e.g. proteins and peptides) through epithelia either transported via paracellular and/or the transcellular pathway (Mahato et al., 2003). Permeation enhancers are categorised into surfactants, bile salts, chelators, fatty acids, cyclodextrins, azone, ethanol, chitosans and lecithin (Troung-Le et al., 2015; Jani et al., 2012; Sohi et al., 2010). The mechanism of permeation enhancer action is different between the category of enhancers. For example, the proposed mechanism of action for fatty acids is by disturbing the intracellular lipid packing through the interaction with either lipid or protein components which lead to increased fluidity of cell membranes (Reddy et al., 2011; Sohi et al., 2010). Bile salts decrease the viscosity and rheology properties of the mucus to help drug absorption whilst also increasing drug solubilisation by formation the micelles (creation of aqueous channels) leading to the permeation enhancement of hydrophilic molecules (Sohi et al., 2010; Lee, 1999; Ganem-Quintanar et al., 1997).

Enzyme inhibitors are other excipients that could be incorporated in drugs to protect against proteolytic inactivation in the GI tract. In the oral cavity, the enzymatic activity is relatively low than the GIT with enzymes such as aminopeptidase and carboxypeptidase being found in the buccal mucosa (Veuillez et al., 2001; Walker et al., 2002). Enzyme inhibitors include the aminopeptidase inhibitors (puromycin, aprotinin, bestatin, soybean trypsin inhibitor, and amastatin), sodium glycholate, camostat mesilate, 4-(4-isopropylpiperadinocarbonyl) phenyl 1,2,3,4-tetrahydro- 1-naphthoate methanesulphonate (FK-448), camostatmesilate, and ovalbumin (Ueno et al., 2007; Yamamoto, 2001). For example, the soybean trypsin inhibitors act by inhibiting the serine protease chymotrypsi (Bruno et al., 2013), acting in the digestive system and enhancing the absorption of insulin (Fujii et al., 1985).

Enteric coating can also be incorporated with tablets or capsules to prevent breakdown of the dosage presentation in the acidic compartment of the stomach and has been shown to have good results (Hussan et al., 2012). Common enteric coatings that have been used include methyl acrylatemethacrylic acid copolymers, sodium alginate, cellulose acetate succinate, polyvinyl acetate phthalate (PVAP), hydroxy propyl methyl cellulose phthalate, Shellac, cellulose acetate trimellitate, etc (Felton and Porter, 2013). In addition, plasticisers (e.g. glycerol, sorbitol, DMSO, etc.) are another group of excipients that can be added to special oral dosage forms to improve tensile strength, improve dissolution time, or change water vapour permeability and play a role in protein stabilisation (Leerahawong et al., 2012).

1.5.5 Drug absorption mechanisms through the oral mucosa

Drug absorption through a mucosal surface is more efficient when the stratum corneum, the major barrier to absorption across the skin, is absent (Satheesh Madhav et al., 2012; Motlekar and Youan, 2006; Lu and Low, 2002). The principle of drug absorption via the oral mucosa is a passive diffusion process (Shinkar et al., 2012) and includes transcellular (or intracellular) and paracellular (or intercellular) routes (Figure 1.8). The transcellular route is where a drug permeates directly through a cell. While, paracellular transport is the transport of molecules around or between cells. Some researchers have suggested that hydrophilic molecules will permeate via the

paracellular route while lipophilic molecules will be absorbed preferentially via the transcellular route (Sattar et al., 2014; Deneer et al., 2002; Zhang and Robinson, 1996).

The buccal, sublingual, palatal and gingival mucosae are regions in the oral cavity that can used to deliver the drug effectively (Shakya et al., 2011). Buccal and sublingual regions may be used as the most suitable areas to administer the drug for treating either local or systemic diseases (Satheesh Madhav et al., 2009; Scholz et al., 2008). The buccal mucosa is relatively permeable, robust and tolerant to potential allergens (Satheesh Madhav et al., 2012; Singh et al., 2011), and therefore a useful route for either local or systemic treatment (Shinkar et al., 2012; Satheesh Madhav et al., 2009). Also, the buccal mucosa has smooth and relatively immobile surface that is appropriate for the administration of a retentive sustained- or controlled-release system (Satheesh Madhav et al., 2009; Scholz et al., 2008).

In comparison with the buccal mucosa, the sublingual mucosa is even more permeable, with a thinner epithelium and high blood flow. Therefore, the sublingual mucosa is a possible site for rapid onset of drug action. The sublingual route has been employed to administer drugs for acute disorders treatment such as angina pectoris and hypertension (Khan et al., 2017; John et al., 1992). However, it is difficult to place the dosage form for an extended period of time at the mucosa surface as it is affected by the condition of the oral cavity that is continuously washed by saliva and tongue activity (Satheesh Madhav et al., 2012; Scholz et al., 2008).

The soft palatal mucosa is non-keratinised and has an intermediate thickness thus reducing its permeability. It offers numerous advantages over the buccal and sublingual route such as the performance of drug administered through soft palatal does not affected by salivary secretion and tongue activity (Satheesh Madhav et al., 2012). However, this area is difficult to reach area for application.

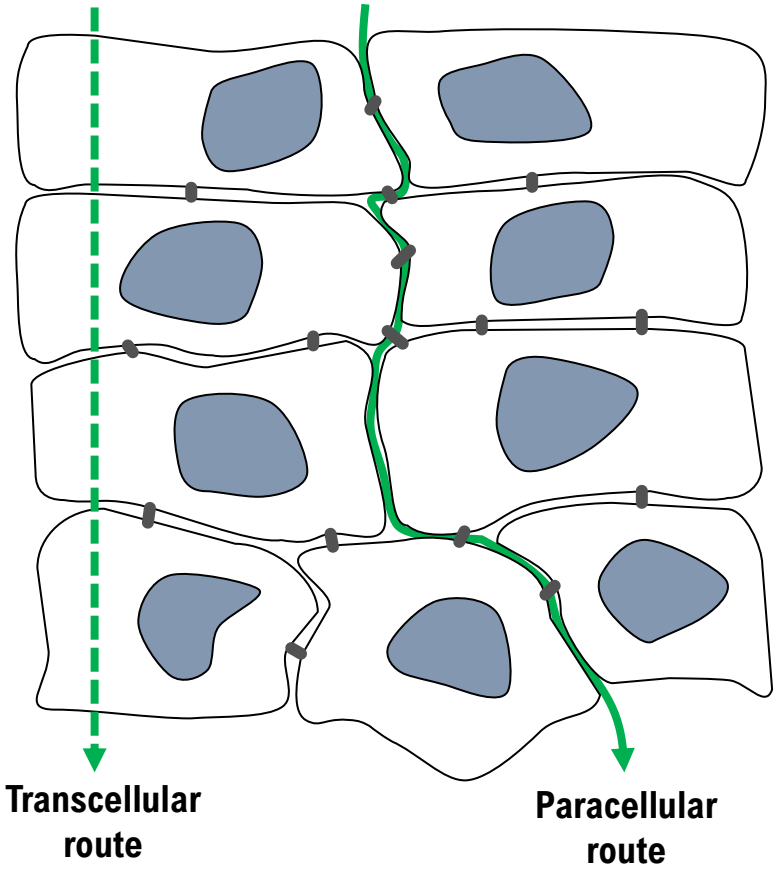

Figure 1.8: A schematic diagram of drug permeation routes.

1.5.6 Permeation studies

Permeation studies are required in order to determine the feasibility of the oral mucosa route for the candidate drug. These studies involve methods that examine *in vitro*, *ex vivo* and/or *in vivo* buccal permeation profile and absorption kinetics of the drug (Patel et al., 2011).

Identification and isolation of tissue from animals is an essential process because different species of animal have different patterns of keratinisation (Shojaei et al., 1996; Squier and Wertz, 1993). Porcine mucosa is the most commonly employed tissue due to its relative resemblance to human tissue, ethical considerations and low cost (Patel et al., 2012). Kulkarni and colleagues have reported that the permeability

of model diffusants (e.g. antipyrine, buspirone, bupivacaine and caffeine) on porcine mucosa was significantly higher in the region behind the lip when compared to the cheek region as the cheek has a thicker epithelium (Kulkarni et al., 2010). A comparative study was conducted to examine the effects of compounds with a different level of lipophilicity using caffeine (hydrophilic molecule) and oestradiol (lipophilic molecule) on the porcine buccal tissue. They found that permeability via the buccal epithelium was 1.8-fold greater for caffeine and 16.7-fold greater for oestradiol as compared to full thickness buccal tissue (Nicolazzo et al., 2003).

Buccal cell culture has been utilised as the *in vitro* model to investigate drug permeation. A few studies have used the human buccal cancer cell line (TR146), which has been grown on transwell filters as a model to study the buccal experiments (Nielsen and Rassing, 1999; Nielsen et al., 1999; Jacobsen et al., 1995). For example, a study was carried out to investigate and compare the effect of pH and drug concentration on nicotine permeability across the TR146 cell culture model and porcine buccal mucosa *in vitro*. The investigators found that permeability of nicotine increased significantly with increasing pH in both models (Nielsen and Rassing, 2002). Another tumour cell line derived from sublingual squamous cell carcinoma (HO-1-u-1) (Miyauchi et al., 1985) seeded on cell culture inserts was evaluated as an *in vitro* model of the sublingual mucosa. This preliminary study demonstrated that this model differentiated into stratified epithelial-like morphology, resembling to the native sublingual epithelium. The permeation studies also confirmed that this model provides a permeability barrier to both hydrophilic and lipophilic molecules and beta-blockers (Wang et al., 2007). Wang and co-workers also found that pH change appeared to be an efficient strategy to improve beta-blocker permeation (Wang et al., 2009).

1.6 Metabolising enzymes in the oral epithelium

The liver is a primary site for drug metabolism, however, it can occur in extra-hepatic sites of the body including skin, intestinal walls, kidneys, lung and oral mucosa (McDonnell and Dang, 2013; Smith et al., 2006). Drug delivery through the oral mucosa may also encounter xenobiotic metabolising enzymes within the oral

epithelium that could affect the concentration of the drug. Metabolising enzymes called cytochrome P450 (CYP450) are family enzymes responsible for oxidative metabolism of endogenous and xenobiotic compounds (Benedetti et al., 2009; Gonzales and Tukey, 2005; Vondracek et al., 2001). CYP450 enzymes belonging to the CYP1, CYP2 and CYP3 families are responsible for metabolising most of the foreign compounds including approximately 70 – 80% of drugs in clinical use (Zanger and Schwab, 2013).

The CYP3A sub-family contains three members; CYP3A4, CYP3A5 and CYP3A7 (Nelson et al., 1996) that have been associated with metabolism of corticosteroids (e.g. budesonide, dexamethasone) (Mortimer et al., 2006). Among the CY3A sub-family, CYP3A4 is the most abundant enzyme that can be found in human liver, accounting about 30% of CYP content and it metabolises the greatest number of drugs and other xenobiotics (Pelkonen et al., 2008; Aoyama et al., 1998). CYP3A enzymes show a great clinical importance as it metabolises approximately 60% of drugs (El-Sankary et al., 2002; Cholerton et al., 1992) and it has been considered central in many clinically important drug interactions (Michalets, 1998).

Vondracek et al., reported that the human buccal tissues from 13 individuals exhibited expression of CYP450 enzymes particularly CYPs 1A1, 1A2, 2C, 2E1, 3A4/7 and 3A5, whereas only 6 of the cases demonstrated CYP2D6 expression. The immortalised (SVpgC2a) and carcinoma (SqCC/Y1) buccal keratinocyte cell line expressed the same CYPs as seen in human tissues except for 3A4/7 and 3A5 (SVpgC2a) and 2C, 2D6 and 3A4/7 (SqCC/Y1) (Vondracek et al., 2001). In addition, a few studies have demonstrated the expression of CYP3A4/5 in both human skin and tissue-engineered skin equivalents (TESE) (Smith et al., 2018; Wiegand et al., 2014; Luu-The et al., 2009).

The family of CYP450 enzymes can be considered as the starting point for studying drug-drug interactions (Wilk-Zasadna et al., 2015). In general, drugs can be either inhibitor or inducer to one or more CYP450 enzymes during their interactions, which therefore markedly influence their metabolism and clearance leading to altered effectiveness of the drug or unanticipated adverse reactions due to increased

production of toxic metabolites (Wilk-Zasadna et al., 2015; Lynch and Price, 2007; Chang and Kam, 1999).

The inhibition of CYP450 enzymes by certain particular drugs can lead to decreased metabolism of other drugs metabolised by the same enzyme, resulting in higher drug levels and drug toxicity or altered the effectiveness of the drug (Rainone et al., 2015; Pelkonen et al., 2008). For example, the administration of budesonide with cimetidine (a known inhibitor of CYP3A4) resulted in a 51% elevation of budesonide plasma concentration (US Food and Drug Administration, 2009). Therefore, the co-administration of budesonide with cimetidine needs to be considered carefully by lowering the dose of budesonide (Chen et al., 2018). While the induction of CYP450 enzymes by drugs caused an increased clearance and concurrent decrease in the pharmacologic effects of other drugs metabolised by the same enzyme (Rainone et al., 2015; Pelkonen et al., 2008). For example, rifampicin (an inducer of CYP3A4) accelerated the clearance of hydrocortisone that is a substrate for CYP3A4 (Chen and Raymond, 2006; Rendic, 2002).

1.7 Hypothesis, aims and objectives

1.7.1 Hypothesis:

3D oral mucosal models based on immortalised keratinocytes (FNB6) can be used to examine novel mechanisms of corticosteroid drug delivery across the oral mucosa.

1.7.2 Aims:

Tissue engineered oral mucosa can be used as a model system to examine novel topical corticosteroids drug delivery strategies.

1.7.3 Specific objectives:

- To develop and characterise tissue engineered oral mucosa using human immortalised oral keratinocyte (FNB6) and primary normal oral fibroblasts (NOF).
- To determine the cytotoxic effects of corticosteroids on monolayer cultures of epithelial cells (keratinocytes and fibroblasts) and TEOM.

- To assess novel drug delivery methods for mucosal delivery of corticosteroids.
- To investigate the distribution and penetration capacity of a number of corticosteroids using TEOM models.
- To develop a simple tissue-engineered model of OLP.
- To assess the effects of clobetasol-17-propionate (CP) on interleukin–2 (IL-2) secretions using an *in vitro* model of OLP.

CHAPTER 2

MATERIALS AND METHODS

2.1 Materials

The following are the materials used in this study.

Table 2.1: Chemicals and reagents.

Chemicals/reagents	Company/Source
3-(4,5-dimethylthiazol-2-yl)-2,5 diphenyl tetrazolium bromide (MTT)	Sigma-Aldrich, UK
3, 3, 5- Tri-iodothyronine (T3)	Sigma-Aldrich, UK
4-(2-hydroxyethyl)-1-piperazineethanesulfonic acid)	Sigma-Aldrich, UK
Acetic acid	ThermoFisher scientific, UK
Adenine	Sigma-Aldrich, UK
Alamar Blue (AB)	ThermoFisher Scientific, UK
Aluminum	Agar Scientific, UK
Amphotericin B	Sigma-Aldrich, UK
Apo-transferrin	Sigma-Aldrich, UK
Cholera toxin	Sigma-Aldrich, UK
Collagenase IV	ThermoFisher Scientific, UK
Copper	Sigma-Aldrich, UK
Dextrans (3, 10 and 70 kDa)	ThermoFisher Scientific, UK
Diastase	Sigma-Aldrich, UK
Dibutyl phthalate polystyrene xylene (DPX)	ThermoFisher Scientific, UK
Dimethylsulfoxide (DMSO)	Sigma-Aldrich, UK
Dulbecco's modified Eagle's medium (DMEM) (1x and 10X)	Sigma-Aldrich, UK
Eosin	ThermoFisher Scientific, UK
Epidermal growth factor (EGF)	Sigma-Aldrich, UK
Ethanol	ThermoFisher Scientific, UK
Eudragit RS100®	Evonik Industries AG, Germany
Foetal bovine serum (FBS)	Sigma-Aldrich, UK
Gold	Denton Vaccum, Desk II, USA
Glutaraldehyde	ThermoFisher Scientific, UK
Hank's Balanced Salts solution (HBSS)	Sigma-Aldrich, UK
Haematoxylin	ThermoFisher Scientific, UK
Horse serum	Sigma-Aldrich, UK
Horseradish peroxidase (HRP)-streptavidin	Vector Laboratories Ltd, UK
Hydrochloric acid (HCL)	ThermoFisher Scientific, UK
Hydrocortisone	Sigma-Aldrich, UK

Hydrogen peroxide (H_2O_2)	ThermoFisher Scientific, UK
Industrial methylated spirits (IMS)	ThermoFisher Scientific, UK
Insulin	Sigma-Aldrich, UK
Isopropanol	ThermoFisher Scientific, UK
L-glutamine	Sigma-Aldrich, UK
Lead citrate	Sigma-Aldrich, UK
Methanol	ThermoFisher Scientific, UK
Neutral buffered formalin	ThermoFisher Scientific, UK
Nutrient mixture F12 (Ham's F12)	Biosera, UK
Osmium tetroxide	Sigma-Aldrich, UK
Paraffin wax	ThermoFisher Scientific, UK
Paraformaldehyde	Sigma-Aldrich, UK
Penicillin and streptomycin	Sigma-Aldrich, UK
Periodic acid	ThermoFisher Scientific, UK
Phorbol-12-myristate-13-acetate (PMA)	Sigma-Aldrich, UK
Phosphate buffer saline (PBS)	Oxoid Ltd, UK
Phytohaemagglutinin (PHA)	Sigma-Aldrich, UK
Platinum	Sigma-Aldrich, UK
Polycaprolactone (PLC)	Sigma-Aldrich, UK
Polyethylene oxide (PEO)	Sigma-Aldrich, UK
Polyvinylpyrrolidone (PVP)	BASF, UK
Propylene oxide	Agar Scientific, UK
Rat tail collagen	In-house
Resin	Agar Scientific, UK
Roswell Park Memorial Institute (RPMI)-1640	Sigma-Aldrich, UK
Schiff's solution	ThermoFisher Scientific, UK
Sodium bicarbonate ($NaHCO_3$)	Sigma-Aldrich, UK
Sodium citrate	Sigma-Aldrich, UK
Sodium dodecyl sulfate (SDS)	ThermoFisher Scientific, UK
Sodium cacodylate buffer	VWR, UK
Sodium hydroxide (NaOH)	ThermoFisher Scientific, UK
Trypan blue	Sigma-Aldrich, UK
Trypsin/ Ethylenediaminetetraacetic acid (EDTA)	Sigma-Aldrich, UK
Uranyl citrate	Agar Scientific, UK
Xylene	ThermoFisher Scientific, UK

Table 2.2: Drugs.

Drugs	Company/Source
Betamethasone-17,21-dipropionate	Sigma-Aldrich, UK
Betamethasone-17-valerate	Sigma-Aldrich, UK
Budesonide	Sigma-Aldrich, UK
Clobetasol-17-propionate	Sigma-Aldrich, UK
Clobetasol-17-propionate (patch)	DermTreat Aps, Denmark.
Hydrocortisone-17-butyrate	Sigma-Aldrich, UK
Hydrocortisone-17-valerate	Sigma-Aldrich, UK
Triamcinolone acetonide	Sigma-Aldrich, UK

Table 2.3: Cells.

Cell	Company/Source
Human normal oral keratinocyte (FNB6) cell line	Professor Dr. Keith Hunter
Jurkat (T) cells	American Type Culture Collection (ATCC), USA
Primary normal oral fibroblasts (NOF)	Human Biopsy (reference number 09/H1308/66)

Table 2.4: Kits.

Kit	Company/Source
3,3'-Diaminobenzidine (DAB)Peroxidase (HRP) Substrate	Vector Laboratories Ltd, UK
Human IL-2 (DuoSet ELISA)	R&D Systems, UK
Vecstastain® Elite ABC	Vector Laboratories Ltd, UK

Table 2.5: Consumables.

Consumables	Company/Source
Centrifuge tubes	Greiner Bio-One GmbH, Germany
Centrifuge tubes (15 and 50 mL)	Becton Dickinson, UK
Cryovials	Greiner Bio-One GmbH, Germany
Flasks (T25, T75 cm^2)	Greiner Bio-One GmbH, Germany

Glass microscope slides (SuperFrost® Plus)	VWR International, UK
Histology cassettes	Wheaton, UK
Microscope coverslips	VWR International, UK
Polyethylene terephthalate (PET) hanging cell culture inserts	Millipore, Switzerland
Serological pipette (5, 10 and 25 mL)	ThermoFisher Scientific, UK
Tissue-culture plates (6, 12, and 24 and 96 well)	Greiner Bio-One GmbH, Germany

Table 2.6: Equipment.

Equipment	Company/Source
Agilent Zorbax RX - C18 250 mm x 4.6 mm column	Agilent Technologies, US
CO_2 incubator	Scientific-Lab Supplies, U
Digital micrometre	Digital Micrometers Ltd, UK
Dissolution apparatus (Erweka DT80)	ERWEKA GmbH, Germany
Electronic balance	Fisher Scientific, UK
Embedding machine (Leica EG1160)	Leica Microsystems, UK
Epithelial Volt Ohm Meter (EVOM)	World Precision Instrument, Inc. US
Freeze dryer	VirTis Benchtop, BioSurplus, US
Freezer/Fridge	Proline, UK
High-performance liquid chromatography (HPLC) (Waters 2690)	Agilent Technologies, US
Microcentrifuge	Fisher Scientific, UK
Microplate reader (TECAN Infinite M200 Pro)	LabX, Canada
Microscope (Eclipse TS100-F)	Nikon, Japan
Microscope (Olympus BX51 microscope and Colour view IIIu camera with associated Cell^D software)	Olympus soft imaging solutions, GmbH, Germany
Microtome blade (S35 type)	Feather, Japan
Microtome machine (Leica RM2235)	Leica Microsystems, UK
Mount water bath	Grant Instruments Ltd, UK
Neubauer haemocytometer	Weber Scientific International, UK
pH meter	Fisher Scientific, UK
Processing machine (Leica TP1020 benchtop tissue processor)	Leica Microsystems, UK
Scanning electron microscope (SEM) (Philips XL-20)	Electron Microscopy Unit, Department of Biomedical Science, University of Sheffield, UK

Staining machine (Shandon linear UK)	Department of Pathology, School of Clinical Dentistry, University of Sheffield
Transmission electron microscope (TEM) (FEI Tecnai G2 Spirit)	Electron Microscopy Unit, Department of Biomedical Science, University of Sheffield, UK

2.2 Methodology

2.2.1 Cell culture

2.2.1.1 Preparation of reagents

2.2.1.1.1 Phosphate buffer saline

Phosphate buffer saline (PBS) was prepared by dissolving one tablet in 100 mL of distilled water in an autoclaving bottle to give a final concentration of 0.1 M. The PBS solutions stored at the room temperature.

2.2.1.1.2 Trypsin/EDTA solution

Trypsin/EDTA (0.05% trypsin/0.02% EDTA w/v) solutions was purchased as ready-to-use and aliquoted in 5 mL tubes before storage at -20 °C.

2.2.1.1.3 Foetal bovine serum

Foetal bovine serum (FBS) was purchased as ready-to-use, aliquoted in 50 mL tubes and stored at -20 °C.

2.2.1.1.4 Penicillin/streptomycin solution

Antibiotic solutions contained penicillin (10,000 IU/mL) and streptomycin (10 mg/mL) were bought as ready-to-use, aliquoted in 5 mL tubes and stored at -20 °C.

2.2.1.1.5 Cryopreservation medium

Cryopreservation medium was prepared using FBS containing 10% dimethyl sulfoxide (DMSO), (v/v) and stored at -20 °C before use.

2.2.1.1.6 Trypan blue solution

Trypan blue dye was purchased as ready-to-use and diluted with a cell suspension (1:1) before counting cells.

2.2.1.2 Preparation of cell culture growth medium

2.2.1.2.1 Green's medium

Oral keratinocytes (FNB6) were cultured in an adenine-enriched medium as previously described (Allen-Hoffmann and Rheinwald, 1984) and will be referred to as Green's medium. Green's medium was prepared by mixing DMEM and Nutrient mixture F12 (3:1, v/v), 50 ml FBS, 5 mL penicillin (10,000 IU/mL) and streptomycin (10 mg/mL), 1.25 mL amphotericin B (250 µg/mL), 2 mL adenine (6.25 µg/ml), 2.5 mL insulin (1 mg/mL), 0.5 ml 3, 3, 5- Tri-iodothyronine (1.36 µg/mL) and apo-transferrin (5 mg/mL), 80 µL hydrocortisone (2.5 mg/mL), 25 µL EGF (100 µg/mL) and 500 µL cholera toxin (8.47 µg/mL).

2.2.1.2.2 DMEM

NOF and 3t3 fibroblasts were cultured in DMEM supplemented with 10% FBS, penicillin (10,000 IU/mL and streptomycin (10 mg/mL).

2.2.1.2.3 RPMI

Jurkat T cells were cultured in RPMI supplemented with 10% FBS, penicillin (10,000 IU/mL) and streptomycin (10 mg/mL).

2.2.1.3 Cells used in the study

2.2.1.3.1 Adherent cells

The human normal oral keratinocyte cell line (FNB6) was a gift from Professor Keith Hunter. The cells, originally isolated from the buccal region of a healthy volunteer, were immortalised by ectopic expression of human telomerase reverse transcriptase (hTERT) (McGregor et al., 2002).

Primary normal oral fibroblasts (NOF) were isolated from buccal or gingival biopsies collected with written, informed consent from patients undergoing routine dental procedures under ethical approval (reference number 09/H1308/66) and isolated as previously described (Colley et al., 2011).

2.2.1.3.2 Suspension cell line

Jurkat T cells are an immortalised T lymphocyte cell line. The cells were originally isolated from the peripheral blood of a 14 years old male suffering from acute T cell leukaemia (Schneider et al., 1977).

2.2.1.4 Maintenance and passaging of cells

FNB6 cells were cultured on previously prepared irradiated 3T3 (i3T3) cell feeder layers in Green's medium and NOF cultured in DMEM. The cells were cultured in a T75 cm^2 flask at a density of 2.0 x 10^6 cells/mL in a humidified atmosphere (95% air, 5% CO_2) at 37^oC. The medium was replenished every 2 days until the monolayer cultures reached 80-90% confluency.

After the cells reached 80-90% confluency, they were sub-cultured to maintain cells in exponential growth. For passaging, the medium was discarded and washed with 10 mL of PBS to remove all dead cells and debris. The cells were then detached using 5 mL of trypsin/EDTA and incubated for 5 minutes at 37^oC. The flask was tapped gently until the cells detached as single cells, at which point 5 mL of medium was added to stop the trypsin activity. Cells were centrifuged for 5 minutes at 250 xg to pellet the cells, the resulting supernatant was discarded and the cells resuspended in a known volume of media and counted.

Jurkat T cells were cultured in a T75 cm^2 at a cell density of 0.5 to 1.5 x 10^6 cells/mL in Green's or RPMI medium depending on the experiment performed. For continuous passage, cells were diluted every 2 to 3 days.

2.2.1.5 Counting cells

Ten microlitres of cell suspension were used to determine cell numbers using a haemocytometer and inverted light microscope. The cells located in four 1 mm^2 areas were counted and the average is taken. The cell number was calculated as follows:

$$\text{Cell number}\left({}^{\text{cells}}/_{\text{mL}}\right) = \left(\frac{\text{Total number of cell per 1 mm}^2\text{ square}}{4^{(4)}}\right)^{(1)} \times 10{,}000^{(2)} \times 10^{(3)}\ \text{mL}$$

(1) = Average number of cells
(2) = Number of cell per 1 mm^2 square
(3) = Amount of medium in the tube
(4) = Number of 1 mm^2 square counted

2.2.1.6 Cryopreservation and thawing of cells

Following trypsinisation, the cells were transferred into a 20 mL centrifuge tube and centrifuged for 5 minutes at 250 xg. The supernatant was discarded, and the cell pellet resuspended in cryopreservation medium. The mixture was transferred to a cryovial and placed on ice before storage in a -80°C freezer overnight. The cryovial was then transferred to a liquid nitrogen dewar for long-term storage.

To resurrect cells, a cryovial was thawed, added to 10 mL of medium and centrifuged for 5 minutes at 250 xg to obtain a cell pellet. The cell pellet was resuspended in fresh medium and transferred to a T75 cm^2 flask.

2.2.2 Preparation of tissue engineered oral mucosa

2.2.2.1 Collagen extraction

Rat tails were collected following Home Office guidelines and stored at -20 °C until use. Frozen rat tails were thawed overnight prior to use. The base of the tails was held firmly and manipulated backwards and forwards in order to break the bone and expose the tendons. The skin of the tail was removed and the tendons (string-like white fibres) collected (Figure 2.1). All tendons were washed in sterile PBS and placed in sterile 0.1 M acetic acid on a stirrer at 4°C until dissolved (approximately 7 days). Once dissolved, the collagen was freeze-dried. The resultant collagen was weighed

and stored at -20°C. Before use, the collagen was dissolved in 0.1 M acetic acid to a final concentration of 5 mg/mL.

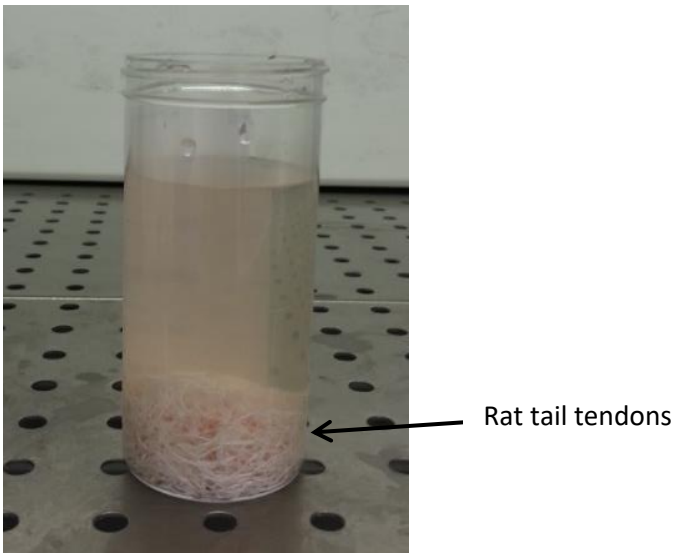

Figure 2.1: String-like white fibres (tendons) are extracted from rat tails.

2.2.2.2 Construction of tissue engineered oral mucosa in PET hanging cell culture inserts

2.2.2.2.1 Addition of NOF cells to the collagen hydrogels

Following trypsinisation, NOF cells were counted and transferred to a centrifuge tube and centrifuged at 250 xg for 5 minutes. The resulting supernatant was removed, and the cell pellet resuspended in DMEM medium to give a final cell count of 6.25 x 10^6 cells per mL. The cells were kept on ice until use.

The collagen hydrogel was composed of DMEM (10X), reconstitution buffer (10X), FBS, L-glutamine and collagen. The pH of the gel was adjusted to 7.4 using 1 M NaOH. The details of the collagen gel composition are described in Table 2.7.

Forty µL of the NOF cell suspension were added to the collagen gel to give a final concentration of 2.5 x 10^5 cells per model and the tube inverted gently to evenly disperse the cells within the hydrogel. Nine hundred µL of the resultant collagen

solution was then added to the well of a hanging cell culture insert (Filter: PET, pore size: 0.4 µm and diameter: 12 mm) and incubated at 37°C for 2 hours to allow the hydrogel to set. Once the hydrogel had solidified, the medium was added on top (500 µL) and underneath (1 mL) of the models and incubated at 37°C for 48 hours.

Table 2.7: Hydrogel components.

Items	Volume (µL) (per model)
DMEM (10X)	100
Reconstitution Buffer (10X): $NaHCO_3$ (2.2 g), Hepes (4.8 g), NaOH (0.248 g), 100 mL H_20	100
Foetal Bovine Serum	83
L-Glutamine	10
Collagen	673

2.2.2.2.2 Addition of FNB6 cells to the collagen models

After 48 hours, FNB6 cells (2.5 x 10^5/model) were added to the surface of each model in 200 µL Green's medium and incubated for a further 5 days. At which point all media was removed and replenished with fresh Green's media and models brought to an air-to-liquid interface (ALI) where the basement of the models was in contact with Green's media and any excess of media on the top of the models was removed to expose the keratinocytes to the air. The models were cultured for a further 10 days at ALI with the media being replaced every 2 days. All experiments using TEOM were performed on day 10 at ALI. The summary of TEOM preparation is described in Figure 2.2.

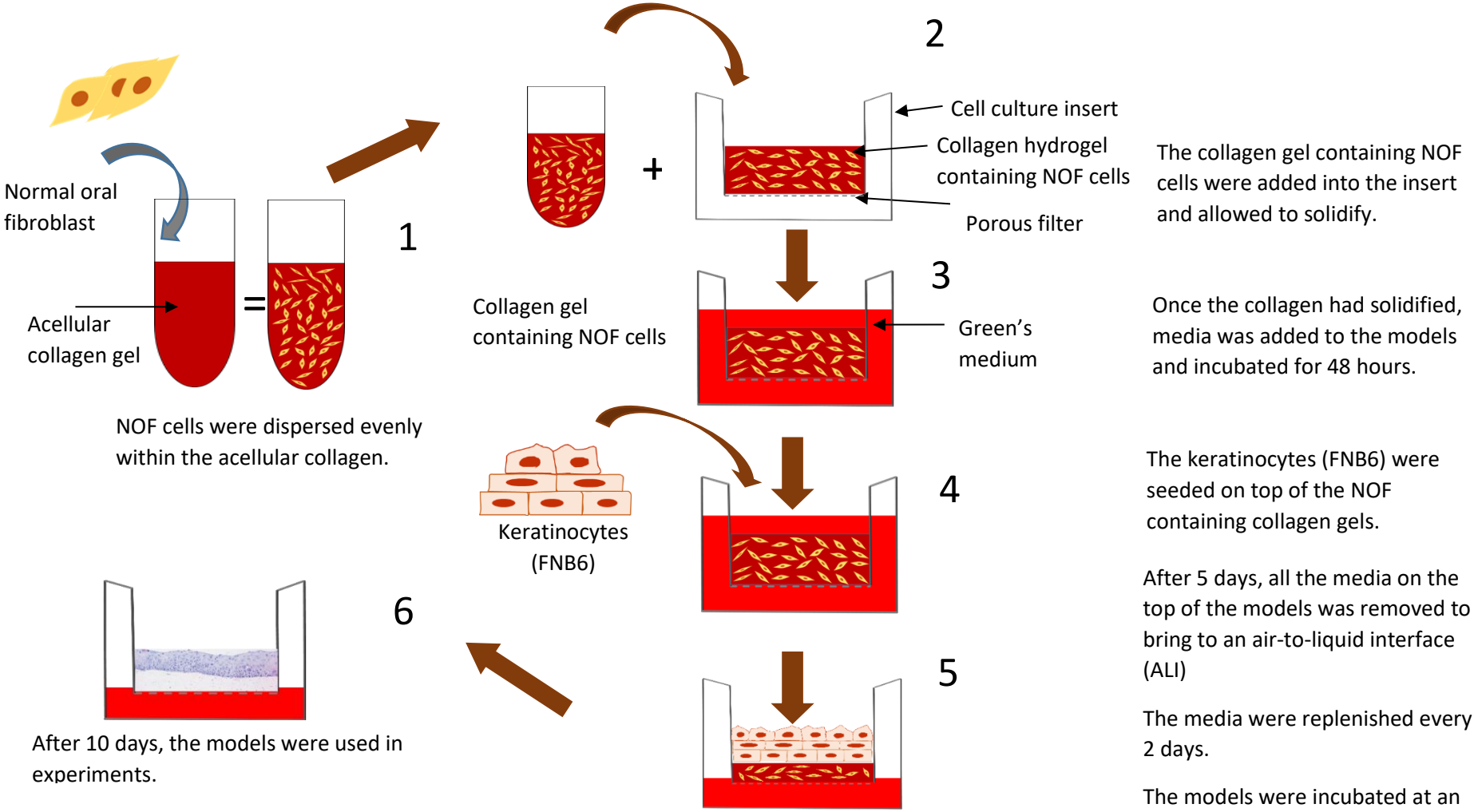

Figure 2.2: Schematic diagram to show the methodology to generate the TEOM.

2.2.3 Morphological analysis

2.2.3.1 Histological processing and haematoxylin and eosin staining

The microscopic structures of TEOM incubated for 5, 10 and 14 days at ALI were analysed using haematoxylin and eosin (H&E) staining. TEOM were fixed in paraformaldehyde (4%) solution for at least 24 hours at room temperature prior to histological processing (Table 2.8). The TEOM were processed using a benchtop tissue processor. Tissue samples were embedded in molten paraffin wax using an embedding machine. The blocks of tissues were sectioned with microtome blades using a microtome, 5 µm thick sections were mounted onto glass slides and stained using H&E staining (Table 2.9) in a Shandon linear staining machine. After staining, all slides were mounted with dibutyl phthalate polystyrene xylene (DPX) and a coverslip placed on the top of the sample. Images were captured using the microscope (Olympus BX51) and Colour view IIIu camera with associated Cell^D software.

Table 2.8: Histological processing schedule.

Solution	Duration (min.)
10% neutral buffered formalin	60
70% alcohol	60
70% alcohol	60
90% alcohol	60
90% alcohol	60
Absolute alcohol	60
Absolute alcohol	60
Absolute alcohol	60
Xylene	90
Xylene	90
Paraffin wax I	120
Paraffin wax II	120

Table 2.9: H&E staining procedure.

Solution	Duration (second)
Xylene I	45
Xylene II	
Xylene III	
Absolute alcohol I	
Absolute alcohol II	
70% alcohol	
Running tap water	
Harris's Haematoxylin I	
Harris's Haematoxylin II	
Harris's Haematoxylin III	
Harris's Haematoxylin IV	
Harris's Haematoxylin V	
Running tap water I	
Running tap water II	
0.1% HCl in 70 % alcohol	
Running tap water	
Eosin I	
Eosin II	
Running tap water	
95% alcohol	
Absolute alcohol I	
Absolute alcohol II	
Absolute alcohol III	
Absolute alcohol IV	
50:50 absolute alcohol: xylene	
Xylene I	
Xylene II	

2.2.3.2 Periodic acid-Schiff (PAS) staining

Periodic acid-Schiff is a staining method used to detect polysaccharides such as glycogen and glycoproteins, and is often used to detect basement membranes within tissue sections. Paraffin-embedded TEOM sections were brought onto a Shandon Automated Stainer and passed through the following solutions for 15 seconds each incubation: xylene (3X), absolute alcohol (2X), 70% alcohol and running tap water. TEOM sections were removed from the stainer and placed in a coplin jar containing 0.5% diastase solution diluted in distilled water and transferred into a waterbath for 20 minutes. Afterward, the sections were rinsed in running tap water. The sections were stained with periodic acid for 5 minutes and then rinsed thoroughly in distilled water. The sections were then stained with Schiff's Reagent for 10 minutes and washed in running tap water for 5 minutes. The sections were counter-stained with haematoxylin for 1 minute, rinsed in running tap water and passed through with the following solutions: acid alcohol (1%), running tap water, Scott's tap water, 95% alcohol, absolute alcohol (4X) and xylene (2X) for 45 seconds each incubation. Finally, the sections were mounted with DPX and a coverslip placed on the top of the sample. The images of the section were viewed and captured under a light microscope (Olympus BX51) and Colour view IIIu camera with associated Cell^D software.

2.2.3.3 Transmission electron microscope analysis

The ultrastructures of TEOM incubated for 14 days at ALI were evaluated using transmission electron microscope (TEM). TEOM were cut into 2 mm sections and fixed in 3% glutaraldehyde diluted in 0.1 M cacodylate buffer at pH 7.4 for 2 hours at $4^{O}C$ before rinsing twice in 0.1 M phosphate buffer (pH 7.4) with a 30-minute interval at $4^{O}C$. TEOM were then post-fixed in 2% osmium tetroxide for 2 hours at room temperature and rinsed in 0.1 M phosphate buffer. Afterward, the TEOM were dehydrated in an ethanol gradient from 75% (1X), 95% (1X) and 100% (2X), dried 100% ethanol (2X) and propylene oxide (2X) for 15 minutes at room temperature. The TEOM were then incubated in a 50/50 mixture of propylene oxide/Araldite resin (v,v) overnight at room temperature. Following overnight incubation, excess resin mixture was removed by evaporation for 1 hour at room temperature. TEOM were next

incubated in 100% Araldite resin for 6 hours at room temperature and then finally embedded in fresh Araldite resin for 48 – 72 hours. The block was cut approximately 70 – 90 nm thick using a diamond knife and the sections transferred to a copper circle. The section was then stained with 3% uranyl acetate (25 minutes) and Reynold's lead citrate (5 minutes) and dried for 10 minutes. The sections were examined using TEM at an accelerating voltage of 80 kV.

2.2.4 Protein expression analysis

Expression of proteins within paraffin-embedded TEOM sections was determined by immunohistochemistry staining. Five micrometres sections were cut and mounted onto Superfrost glass slides. The slides were incubated in a warming oven at $60^{O}C$ for 30 minutes before being dewaxed in two changes of xylene for 5 minutes each. The tissue sections were then hydrated with graded ethanol (100%, 95%, and 70%) for 3 minutes each and rehydrated in distilled water. Tissue sections were incubated in methanol that contained 3% hydrogen peroxide (H_2O_2) for 20 minutes in order to quench endogenous peroxidases that could affect the results of the hybridisation. After rinsing 3 times in PBS for 5 minutes each, all tissue sections were subject to heat-mediated antigen retrieval in citrate buffer (pH 6). After cooling, the tissue sections were rinsed again in PBS for 10 minutes and any unspecific binding sites blocked with horse serum for 30 minutes at room temperature. Primary antibodies (Table 2.10) diluted in horse serum were then applied and incubated overnight at $4^{0}C$. After 3 rinses (5 minutes each) in PBS, the slides were incubated with biotinylated second antibody for 30 minutes at room temperature, followed by 2 rinses in PBS for 5 minutes each. HRP-streptavidin reagent was applied for 30 minutes at room temperature and subsequently, 3 rinses in PBS (5 minutes each). Colour was developed by incubating the slides with DAB solutions for up to 10 minutes and transferred to distilled water. Finally, the slides were counterstained with haematoxylin and mounted in DPX and a coverslip applied. For a negative control, the primary antibody was emitted. Tissue sections were viewed and captured using the microscope (Olympus BX51) and Colour view IIIu camera with associated Cell^D software

Table 2.10: Primary antibody details.

Primary antibody	Clone	Species	Dilution	Final concentration (mg/mL)
Anti-cytokeratin 13	AE8	Mouse	1:300	0.4
Anti-cytokeratin 4	6B10	Mouse	1:40	Not provided
Anti-cytokeratin 14	LL002	Mouse	1: 1000	0.1
Anti-Ki67	SP6	Rabbit	1: 100	Not provided
Anti-claudin 4	EPRR17575	Rabbit	1:4000	Not provided
Anti-E-cadherin	HECD-1	Mouse	1:200	Not provided

2.2.5 Viability of TEOM analysis

Measuring the reducing environment within the cytosol of living cells can assess cell viability. AlamarBlue® contains resazurin, a non-toxic, cell permeable compound that is blue in colour and non-fluorescent. Upon entering viable cells, resazurin is reduced to resorufin, to produce a compound that is red in color and highly fluorescent. alamarBlue® was used to determine the viability of the TEOM. Briefly, TEOM were rinsed with PBS and 1 mL alamarBlue® solution (10% v/v prepared in Green's medium) was added to each TEOM in the insert and incubated for 5 hours. After the incubation, a triplicate 200 μL solution from the apical compartment of the insert was removed and placed into the well of a 96-well plate. The fluorescence intensity was measured at an excitation wavelength of 550 nm and an emission wavelength of 590 nm using a microplate spectrophotometer. Transwell inserts without TEOM containing only alamarBlue® solution was also prepared and incubated for 5 hours and set as a background fluorescence. The background fluorescence was subtracted from the fluorescence intensity of each sample to obtain the fluorescence intensity of each TEOM.

2.2.6 Barrier functional analysis

2.2.6.1 Transepithelial electrical resistance analysis

Transepithelial electrical resistance (TEER) is the measurement of electrical resistance across an epithelium and is a widely used quantitative technique to measure the integrity of epithelial tight junctions to confirm the integrity and permeability of the tissue. The barrier of TEOM was assessed using an Epithelial Volt Ohm Meter (EVOM) and electrode set at the room temperature. TEOM cultured in the insert was placed in a laminar flow hood for at least 15 minutes before the measurements were recorded to allow the cells to adjust from incubator to room temperature. Simultaneously, the EVOM electrodes were sterilised by immersing in ethanol (70%) for 15 minutes to ensure the sterility and left to air dry before rinsing in sterile medium prior to use (Buchert al., 2012). To measure the TEER of TEOM, 300 µL and 500 µL of PBS were added in the apical and basolateral compartment of the inserts, respectively. The setup for the TEER is shown in figure 2.3. The shorter electrode was placed in the insert while the longer electrode was placed between the insert and the outer wall of the plate. As a precaution, tips of the electrode should completely be covered in solutions and the shorter electrode should not touch the models in the inserts. The TEER value of a naked insert was measured and set as the blank and TEOM treated with SDS (5%) for 5 minutes to disrupt barrier function were used as a positive control.

The unit of TEER is $\Omega.cm^2$. The following equations were used to measure the resistance of the models:

$$\text{Resistance (Tissue)} = \text{Resistance (Total)} - \text{Resistance (Blank)}$$

$$\text{TEER (reported)} = \text{Resistance}(\ (\Omega)\ \times\ \text{Effective membrane}\ (\text{cm}^2)$$

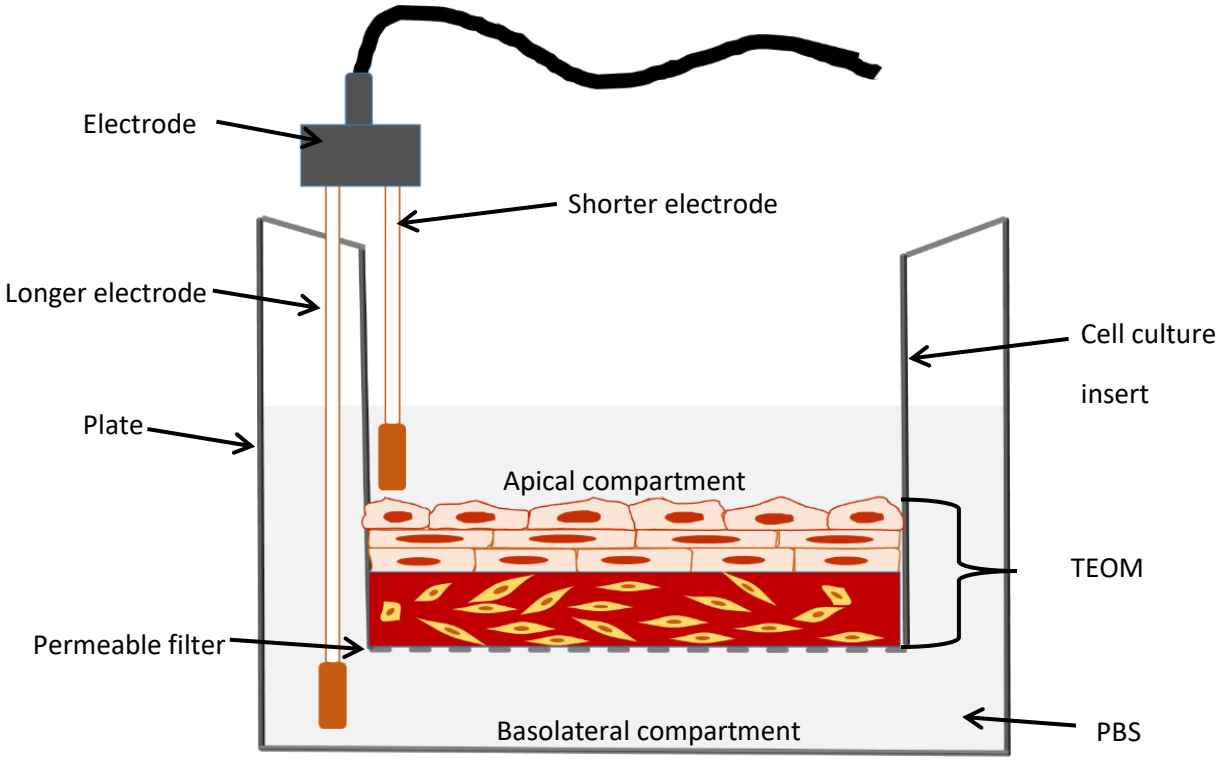

Figure 2.3: Classical setup to measure transepithelial electrical resistance measurement using a Epithelial Volt Ohm Meter.

2.2.6.2 TEOM permeability analysis

Three different fluorescently-labelled dextrans all with different molecular weights (MW: 3, 10 and 70 kDa respectively) were used to evaluate the permeability of the TEOM at day 10 ALI culture. The dextran solution was prepared by mixing the three fluorescently labelled dextrans in Hank's Balanced Salts solution (HBSS) to give a final concentration of 62.5 µg/mL for each dextran. The media in the apical and basolateral compartment of the inserts were removed and the TEOM washed with PBS. All TEOM were transferred to a new plate and refreshed with 500 µL of HBSS in the apical and basolateral compartment. All models were left to equilibrate in the incubator at 37^0C for 15 minutes on a shaker. After equilibration, the solutions in the apical compartment were replaced with 300 µL of HBSS solution containing 250 µg/mL of each fluorescently labelled dextran and incubated at 37^0C on a shaker (Figure 2.4A). The permeability of the TEOM was determined over time. Two hundred fifty µL of the solution from the basolateral compartment of the inserts with or without TEOM were

collected at different time point (30, 60, 90, 120, 180, 240 and 300 minutes) (Figure 2.4B) and 250 µL HBSS added to replace the removed solution. Solutions were transferred to microcentrifuge tubes and stored at -80^{o}C before being analysed. The solutions taken from inserts without TEOM acted as controls. The permeability of TEOM was also determined after the models had been treated with SDS (5%) for one hour to disrupt barrier function and act as a positive control.

The amount of dextran was measured using a microplate spectrometer with excitation and emission wavelengths: 3 kDa (excitation: 590 nm, emission: 620 nm), 10 kDa (excitation: 548 nm, emission: 578 nm) and 70 kDa (excitation: 495 nm, emission: 525 nm). The value obtained from inserts without TEOM used as controls. The percentage of dextran was calculated as follows:

$$\text{Percentage of dextran } (\%) = \frac{\text{Fluorescence (TEOM)}}{\text{Fluorescence (Control)}} \times 100\%$$

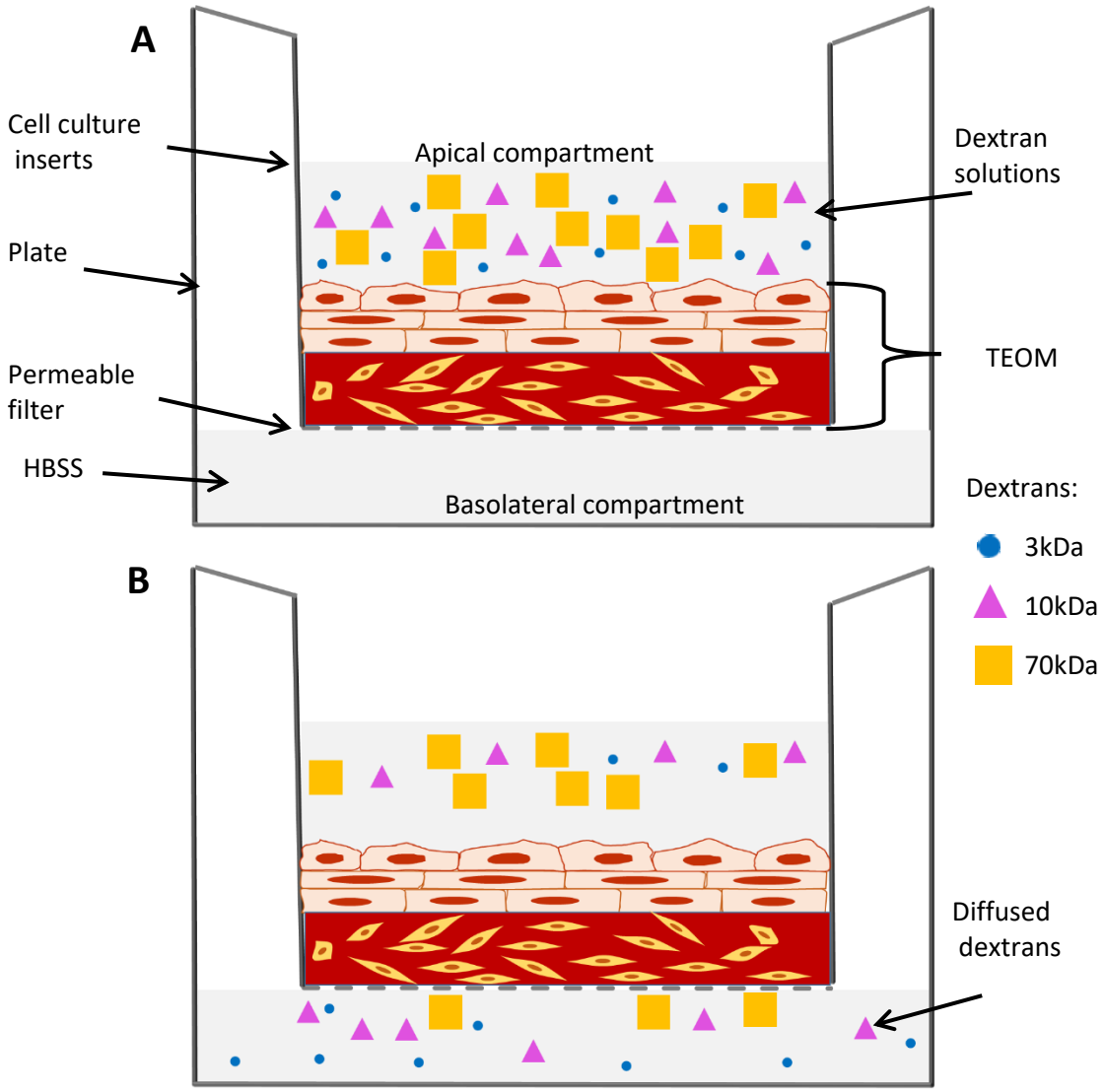

Figure 2.4: Permeability analysis of dextrans (3, 10 and 70 kDa) across TEOM. A**:** Dextran solutions were added to the apical surface of TEOM. B**:** Dextran diffusion through the TEOM was determined by molecular weight. Accumulated of the dextrans in the basolateral compartment over time was measured using a spectrometer.

2.2.7 Cytotoxic effects of corticosteroids solution on oral keratinocyte and fibroblasts in 2D and 3D

2.2.7.1 Cytotoxic effects of corticosteroids solution on oral keratinocyte and fibroblast monolayers

The corticosteroids (CS); betamethasone-17,21-dipropionate (BD), betamethasone-17-valerate (BV), budesonide (BU), clobetasol-17-propionate (CP), hydrocortisone-17-butyrate (HB), hydrocortisone-17-valerate (HV) and triamcinolone acetonide (TA), were used in this study to determine the cytotoxic effects on FNB6 and NOF cells.

Stock solutions of CS were prepared by dissolving in DMSO to give a final concentration of 100 mM. The stock solutions were mixed with medium to prepare working solutions at various concentrations ranging from 0.01 µM to 500 µM. DMSO in medium acted as a vehicle control in all experiments. Cells were seeded into a 96-well plate at a density of 5 x 10^4 cells/well and incubated for 24 hours to allow the cells to adhere. After incubation, the cells were treated with 100 µL of drug solutions in gradient concentrations. DMSO was used as a vehicle control. The cells were incubated in the presence of the CS for 24, 48 and 72 hours.

The effect of CS against FNB6 and NOF cells was determined using a metabolic MTT assay according to Mosmann et al, (1983). This is a colourimetric assay for assessing cell metabolic activity and by extension cell viability. Cellular NAD(P)H-dependent oxidoreductases reduce the tetrazolium MTT substrate to an insoluble formazan product that is purple in colour and so can be measured spectrophotometrically. Following treatment, media was aspirated and the adhering cells in each well washed once with 100 µL of PBS. After washing, 100 µL of MTT solution (0.5 mg/mL in PBS) was added to each well and incubated for 2 hours at 37°C in 5% CO_2. The MTT solution was removed and acidified isopropanol (50 µL/well) added to solubilise the formazon-blue. Gentle shaking of the plates was applied for 15 seconds to completely dissolve the formazans. A microplate spectrometer was used to measure the optical density (OD) of the solution at 570 nm with a reference at 630 nm. Data were processed using Microsoft Excel, expressed as a percentage of cell viability relative to vehicle control

(DMSO only), and plotted in the dose-response curve using GraphPad Prism 6 (GraphPad Software, Inc.), allowing derivation of IC_{50} values by non-linear regression.

2.2.7.2 Cytotoxic effects of corticosteroids solution on TEOM

The cytotoxic effects of CP, BV, and HV were selected and further analysed based on their relative potency ranking, highest, medium and lowest, respectively, obtained from the analysis in section 2.2.7.1. The working solutions of CP, BV, and HV were prepared from stock solutions (100 mM) at various concentrations ranging from 5 – 400 µM. TEOM were topically exposed to various concentrations of CP, BV, and HV for 60 minutes. After exposure to the test substances, TEOM were thoroughly rinsed using PBS and blotted with the absorbent tissue to remove the test substances. TEOM were transferred to a new 12-well plate and cultured with fresh medium for a further 42 hours. TEOM treated with DMSO and SDS (5%) were used as a negative control (NC) and positive control (PC), respectively.

Based on OECD Test Guideline 431 (OECD, 2004), 1 mL of MTT solution (1 mg/mL) was added on the TEOM and incubated for 3 hours. After the MTT incubation, TEOM were blotted on the absorbent tissue to remove the excess liquid. The cultures were extracted in 2 mL of isopropanol for 2 hours while shaking at room temperature. A triplicate of 200 µL aliquots of blue formazan solution was then transferred to a flat bottom 96-well plate. The absorbance was recorded at OD 570 nm and the isopropanol was used as a blank correction. The relative percentage of TEOM viability was determined using the following formulas:

Blank corrected at an OD 570 nm (OD_{570}) of the individual TEOM was determined as follows:

$$\text{Correction OD}_{570} = \text{Individual model (OD}_{570}) - \text{Blank mean (OD}_{570})$$

The individual relative TEOM viability was determined as follows:

$$\text{Relative viability of PC } (\%) = \frac{\text{OD}_{570}\ (\text{PC})}{\text{Mean OD}_{570}\ (\text{NC})} \times 100\%$$

$$\text{Relative viability of CS } (\%) = \frac{\text{OD}_{570}\ (\text{CS})}{\text{Mean OD}_{570}\ (\text{NC})} \times 100\%$$

Based on the OECD guidelines, data was interpreted as follows:

Mean relative tissue viability ≤ 50% = irritant
Mean relative tissue viability ≥ 50% = non-irritant

2.2.8 Mucoadhesive clobetasol-17- propionate patch formulations

Mucoadhesive CP patches were a kind gift from Dermtreat Aps, Denmark. The patches had been fabricated by electrospinning as previously described (Santocildes-Romero et al., 2017). Briefly, the CP-loaded patches were loaded with CP, formulated into three concentrations 1, 5 and 20 µg/patch and a no drug, placebo patches. The surface area of the patches was 25.4 mm (length) x 12.7 mm (width). Structurally, the patches comprised of a dual-layer mucoadhesive system: an outer hydrophobic polycaprolactone (PCL) (backing layer) and an inner (non-backing layer), mucoadhesive components (polyvinylpyrrolidone (PVP), Eudragit® RS100 and polyethylene oxide (PEO)) (Figure 2.5).

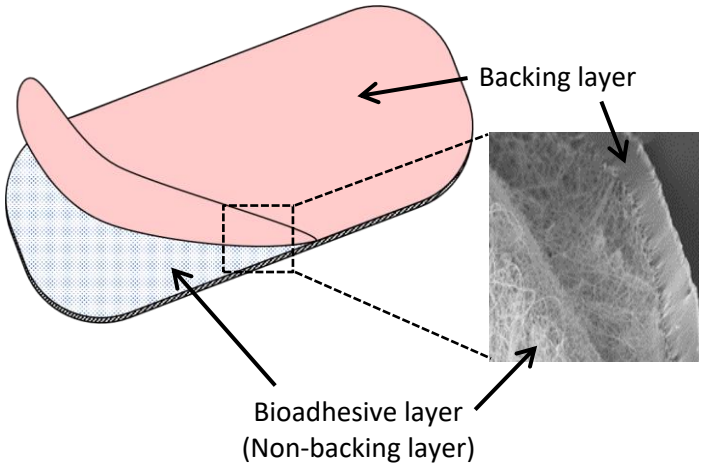

Figure 2.5: Electrospun dual – layer mucoadhesive clobetasol-17-propionate patch.

2.2.8.1 Characterisation of mucoadhesive clobetasol-17- propionate patches

2.2.8.1.1 Physical characterisations – Weight and thickness

The assessment of weight and thickness of the patch was completed on randomly selected patches from three independent batches. The weight of placebo and CP-loaded patches (25.4 x 12.7 mm^2) was measured using an electronic digital balance and an average weight of the patches calculated. The thickness of placebo and CP-loaded patches (25.4 x 12.7 mm^2) was measured using a digital micrometre at three different randomly selected areas. The average thickness of each type of patch was calculated.

2.2.8.1.2 Chemical characterisation – pH

The placebo and CP-loaded patches (25.4 x 12.7 mm^2) were placed in a tube containing distilled water and submerged for 5 minutes. The pH of the whole patch was determined using a pH meter and the average pH of each type of patch calculated.

2.2.8.1.3 Swelling index

Placebo and CP-loaded patches (25.4 x 12.7 mm^2) were placed in a pre-weighed weighing boat and weighed (W_0). The weighing boat containing the patch was submerged with excess water (5 mL) at pre-determined time intervals (30 sec – 60 minutes) until a constant weight was observed. The water was poured off and the patch was blotted with an absorbent tissue to remove any excess water. The weighing boat containing the patch was re-weighed (W_t). The same step was repeated for another interval. The percentage of patch swelling was calculated using the following equation:

$$\text{Swelling index } (\%) = \frac{W_t - W_0}{W_0} \times 100\%$$

where, W_t is the weight of the patch at time t and W_0 is the weight of the patch at time zero.

2.2.8.1.4 Scanning electron microscopy

The ultrastructure of the backing and adhesive layers of the patches were visualised using scanning electron microscopy (SEM). The patches (placebo, 1, 5 and 20 µg) were fixed in 3% glutaraldehyde for 24 hours and subsequently 1% osmium tetroxide for 1 hour. The patches were rinsed several times (6 – 8 times) in PBS (0.1 M) before dehydration in graded ethanol solutions (20, 30, 50, 60, 70, 90 and 95%) for at least 10 minutes in each. Finally, the patches were submerged in absolute alcohol, twice for 30 minutes each. Afterwards, the samples were air dried and mounted on aluminum stubs (25 mm) using silver paste and sputter coated with gold for 90 seconds with 30 mA currents. Images were captured using a scanning electron microscope (Philips XL20) at an accelerating voltage of 25 kV.

2.2.8.1.5 Drug release analysis

The release of CP from the mucoadhesive patches was determined using dissolution apparatus (Erweka DT80) in conjugation with paddle stirrers, according to Ph. Eur. method 2.9.3. In brief, the patches were attached to supports and lowered into the dissolution vessels containing dissolution medium (0.5 M phosphate buffer saline and 0.5% sodium dodecyl sulfate, pH 6.8 at 37°C). The medium was stirred at a constant rate of 100 ± 2 rpm and at pre-determined intervals (15-360 minutes) samples of dissolution fluid (2 mL) were removed and replaced with an equal volume of fresh, pre-warmed dissolution fluid. The concentration of CP in the samples of dissolution fluid was analysed by reverse phase HPLC with reference to a previously constructed calibration curve (Section 2.2.9) (Colley et al., 2018).

2.2.8.2 Cytotoxic effects of mucoadhesive clobetasol-17- propionate patches

The cytotoxic effects of placebo and CP-loaded patches (1, 5 and 20 µg/patch) were determined, analysed and interpreted based on the OECD Test Guideline 431 (OECD, 2004), as previously described in section 2.2.7.2. TEOM treated with either placebo patches or SDS (5%) were used as a negative control and positive control, respectively.

2.2.9 Preparation of calibration standards for High-Performance Liquid Chromatography

To generate a calibration curve, a series of calibration standards of CP, BV, and HV were prepared by serial dilution of the stock standard solution (100 mM) of compounds to produce solutions of a concentration of 0, 0.01, 0.05, 0.1, 1, 10 and 25 µM in Green's media. Compound analysis was performed using a Waters 2690 HPLC using a Zorbax RX-C18 250 mm x 4.6 mm column and a mobile phase composed of acetonitrile (ACN)/water: CP and BV (45% of ACN in water for 15 minutes, ramping to 100% ACN after 16 minutes) and HV (40% of ACN in water for 20 minutes, ramping to 100% ACN after 30 minutes) at 1 mL/min. UV detection was detected using Waters 486 UV/dis detector at 240 nm (CP and BV) and 244 nm (HV). For each concentration, a single injection was made to obtain the peak area for constructing the calibration curve.

2.2.10 Drug permeation analysis

2.2.10.1 Exposure of corticosteroids against the TEOM

2.2.10.1.1 Permeation evaluation of corticosteroids solution through the TEOM

As a preliminary test, TEOM were exposed to a single concentration of CP, BV, and HV (5 µM) (in solution) for one-hour. In brief, TEOM were transferred to a new plate and washed with PBS. After washing, TEOM were exposed to a single concentration of CP (5 µM) for one-hour. After one-hour exposure, media in the basolateral compartment of the inserts were collected and transferred to microcentrifuge tubes. TEOM were subsequently washed in PBS and weighed. TEOM were cut into smaller pieces (2 mm x 2mm), dissolved in collagenase IV (2 mg/mL), and centrifuged at 500xg for 5 minutes. All supernatants were collected, transferred to microcentrifuge tubes and stored at -80^{0}C before analysing.

In another experiments, (1) TEOM were exposed to a single concentration of CP (5 µM) for three different time point (10, 30 and 60 minutes). Also, (2) TEOM were exposed to CP at increasing concentrations (5, 25 and 50 µM). After the incubation, media in the basolateral compartment of the inserts were collected and all tissues were processed as previously described. The presence of compounds in the

basolateral compartment and tissues were determined using HPLC (Section 2.2.9) (Figure 2.6). The concentration of compound recovered in the TEOM was calculated by normalising to the weight of the tissue and expressed as nM per mg of tissue.

2.2.10.1.2 Topical delivery of clobetasol-17-propionate patches (1, 5 and 20 μg) for 1 hour on the TEOM

The CP-loaded patches (1, 5 and 20 μg) were applied to the TEOM. After one-hour incubation, the patches were removed and the media in the basolateral compartment of the inserts collected, transferred to microcentrifuge tubes and stored at -80^{0}C before analysing. TEOM were rinsed in PBS and weighed. The samples were analysed following procedures as previously described in section 2.2.10.1.1 (Figure 2.6).

2.2.10.1.3 Topical delivery of clobetasol-17-propionate patches (20 μg) for 4 and 24 hours on the TEOM

In this experiment, only the 20 μg CP patch was further analysed by increasing the exposure time to 4 and 24 hours. At the respective time point, both the media from the basolateral compartment of the inserts and tissues were collected. All samples were processed and analysed following procedures as previously described in section 2.2.10.1.1 (Figure 2.6).

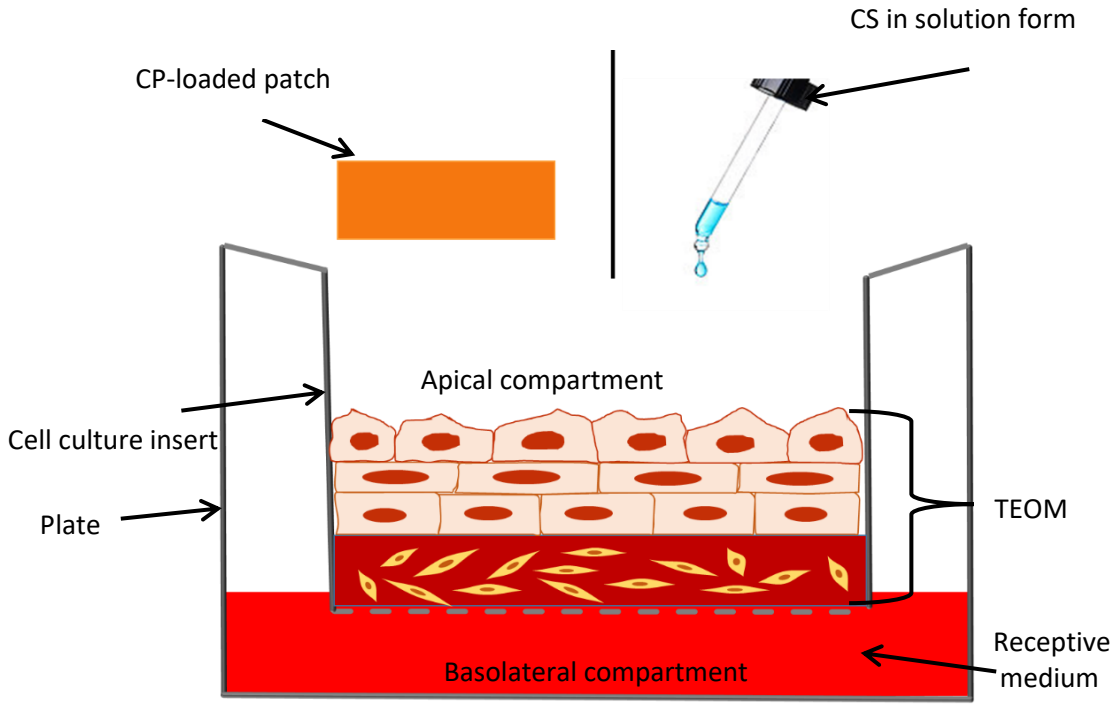

Figure 2.6: TEOM were exposed to corticosteroids (solution/patch) by topical delivery. The presence of corticosteroids in the tissues and basolateral compartment of the inserts was detected using HPLC.

2.2.11 Viability of Jurkat T cell grown in different medium

Jurkat T cells were cultured in RPMI and Green's medium (excluding the cholera toxin and hydrocortisone) to determine the viability of the cells grown in the different medium.

Jurkat T cells were seeded at 5 x 10^4 cells/well in the 6-well plate in the respective media and the viability of the cells determined every 2 days for 8 days. The trypan blue method was used to determine the viability of the cells grown in different medium and cell viability calculated using the following formula:

$$\text{Viability (\%)} = \frac{\text{Viable cells}}{\text{Total cells}} \times 100\%$$

*Total cells = Viable + dead cells

2.2.12 Stimulation of Jurkat T cells

Phytohaemagglutinin (PHA) was used as the main stimulant and Phorbol-12-myristate-13-acetate (PMA) as a co-stimulant to induce T cells to secrete interleukin-2 (IL-2). Jurkat T cells grown in Green's medium were treated with the combination of PHA and PMA at a concentration of 5 µg/mL and 100 ng/mL, respectively for 24 hours. Afterwards, Jurkat T cells were centrifuged at 250 xg for 5 minutes. The resultant cell pellets were resuspended in Green's medium and seeded in 12-well plates at a cell density of 1.0 x 10^6/mL for use in future experiments. Following stimulation, the viability of the Jurkat T cells was also measured as described in section 2.2.11.

2.2.13 Measuring IL-2 by enzyme-linked immunosorbent assay (ELISA)

The production of IL-2 was determined using a commercially available enzyme-linked immunosorbent assay (ELISA) kit following the protocol according to the manufacturer's instructions. Briefly, the capture antibody was diluted in PBS (without carrier protein) to a working concentration (4 µg/mL). Thereafter, a 96-well plate was coated with 100 µL of diluted capture antibody. The plate was then sealed and incubated overnight at room temperature. After overnight incubation with capture antibody, each well was aspirated and washed using 300 µL of wash buffer 3 times. After the last wash, the remaining wash buffer in each well was removed completely by inverting and blotting the plate on absorbent paper towels. Afterwards, 300 µL of block buffer were added to each well and incubated for 1 hour and the washing step repeated. One hundred microliters of prepared standards (0, 15.6, 31.3, 62.5, 125, 250, 500 and 1000 pg/mL) in reagent diluent and samples were pipetted into each well, sealed and incubated for 2 hours at room temperature. After 2 hours incubation, the content of each well was removed, and the washing step was carried out. 100 µL of detection antibody (100 ng/mL) in reagent diluent was added to each well, sealed, incubated for another 2 hours at room temperature and followed by a further wash step. Next, 100 µL of streptavidin-HRP (1:40) was pipetted into each well, and sealed, incubated for 20 minutes at room temperature and washed. A hundred microliters of substrate solution were then added to each well, incubated again for 20 minutes at room temperature. It is crucial to avoid the direct light during the incubation with streptavidin-HRP and substrate solution. Finally, 50 µL of stop solution was added to

each well. Prior to measurement, the plate was tapped gently to ensure thorough mixing. The measurement was determined using a microplate spectrometer set to 450 nm and corrected at 540 nm.

2.2.14 Secretion of IL-2 at different time points

After 24 hours stimulation with both stimulants, the stimulated Jurkat T cells were centrifuged at 250 xg for 5 minutes. The cell pellet was then resuspended in fresh culture media and seeded in a 12-well plate (2 mL/well) at a density of 1.0 x 10^6 cells/mL. Subsequently, the media was collected and centrifuged (500xg, 5 min) at 4, 8 and 24 hours. Jurkat T cells where the stimulants had been retained after 24 hours stimulation acted as controls. All the collected supernatants were further analysed for IL-2 by ELISA.

2.2.15 Effects of clobetasol-17-propionate patch against the IL-2 level

The construction of OLP-like model IL-2 were prepared as previously described (section 2.2.2.2) with slight modifications by incorporating the activated Jurkat T cells into the basolateral compartment medium, which the analysis was carried out at day 10 post-ALI. Prior to analysis (day 9), Jurkat T cells were stimulated with 5 µg/mL PHA and 100 ng/mL PMA for 24 hours. After 24 hours stimulation, the stimulated Jurkat T cells were collected, centrifuged (250 xg, 5 minutes) and the cell pellet was resuspended in the fresh medium. The desired number of Jurkat T cells (1.0 x 10^6 cells/mL) were seeded underneath the insert in 2 mL Green's media for each well of a 6-well plate. TEOM were grouped as follows (Table 2.11):

Table 2.11: Different treatment of the stimulated T cells.

	Treatment			
Group	**Media**	**Placebo (patch)**	**20 µg CP (patch)**	**20 µg CP (solution)**
G1	+	-	-	-
G2	-	+	-	-
G3	-	-	+	-
G4	-	-	-	+

After 4, 8 and 24 hours treatment, 500 mL of media from the basolateral compartment of the inserts was collected and centrifuged (500xg, 5 minutes). The resultant cell pellets were resuspended with 500 µL fresh media and added back to the basolateral compartment. The collected supernatants were further analysed for IL-2 by ELISA (Figure 2.7).

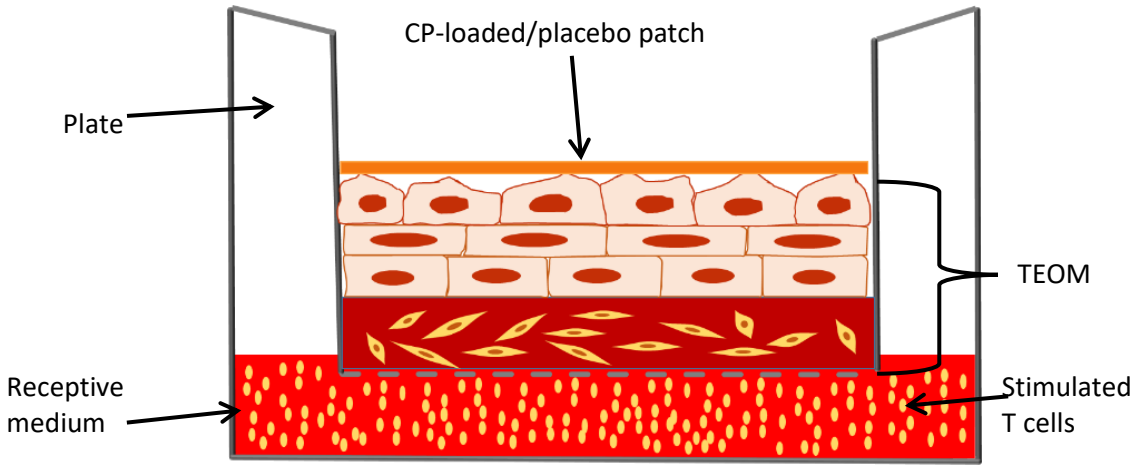

Figure 2.7: Effects of topical delivery of clobetasol-17-propionate (CP) using an electrospun patch on IL-2 level secretion by stimulated T cells in OLP-like model.

2.2.16 Data handling and statistical analysis

Data were presented as mean ± standard deviation (SD). Analysis of variance, one-way (ANOVA) was carried out to compare the differences between more than two means and differences between individual means was performed using a post-hoc test. While the comparison between two means was performed using Student's T test. A mean difference was considered significant when $*p < 0.05$, $**p < 0.001$ and $***p < 0.0001$ as compared to control. Statistical analysis was performed using Statistical Package of Social Science (SPSS) for Window version 22.0 (SPSS Inc., Chicago, IL, USA).

CHAPTER 3

DEVELOPMENT OF A FULL-THICKNESS, TISSUE ENGINEERED ORAL MUCOSA USING TERT2-IMMORTALISED ORAL KERATINOCYTES AND PRIMARY NORMAL ORAL FIBROBLASTS

3.1 Introduction

TEOM is an example of a cell-based device that requires approval from the FDA before being applied clinically (Izumi et al., 2004). The use of tissue engineered epithelial models in biological research is now widely accepted and, due to European Union legislation, are the only model system that can be used to test cosmetic products. TEOM are increasingly used in various research areas including infection (Yadev et al., 2011; Schaller et al., 2006), cancer (Colley et al., 2011; Gaballah et al., 2008; Nystrom et al., 2005), drug toxicity (Sun et al., 2006) and drug delivery (Hearnden et al., 2009). Many investigators have moved away from traditional monolayer cell culture systems to 3D oral mucosal model systems because of the high resemblance to the native oral mucosa and clinical relevance because these complex 3D models provide better, more relevant information when compared to monolayer systems (Moharamzadeh et al., 2012).

Construction of TEOM using primary oral keratinocytes and oral fibroblasts has been shown to be physiologically and histologically similar to the native oral mucosa (Yamada and Cukierman, 2007; Griffith and Swartz, 2006). Nevertheless, there are several disadvantages in constructing TEOM based on the use of human primary cells, which includes a limited supply of fresh tissue, the need for large numbers of cells, limited passaging, shorter lifespan and donor-to-donor variability (Dongari-Bagtzoglou and Kashleva, 2006: Southgate et al., 1987). In order to address these drawbacks immortalised cells are now being used to generate TEOM. Immortalisation of epithelial cells has been achieved by the over-expression of TERT-2 (Lee et al., 2004) and now oral keratinocytes derived from normal, healthy individuals have been immortalised and characterised (McGregor et al., 2002). These cells have the

advantage of having longer lifespans, accessibility, reproducibility, and ease of culture (Kassem et al., 2004; Lee et al., 2004).

The most well established immortalised oral keratinocytes are OKF6 cells and these have been used to make TEOM previously (Dongari-Bagtzoglou and Kashleva, 2006; Almela et al., 2016). However, TEOM based on OKF6 cells have not been characterized thoroughly and in some studies, these TEOM display poorly differentiated epithelium or epithelial layers that are only three to four cells thick (Almela et al., 2016; Mcleod et al., 2014). Therefore, well-characterised models developed using different immortalized keratinocytes are required. Once such possibility is the use of FNB6 immortalised oral keratinocytes. These cells are derived from normal, healthy keratinocytes isolated from buccal keratinocytes of a female and then immortalised by over-expression of TERT-2, and have been shown to be morphologically very similar to normal oral keratinocytes (McGregor et al., 2002).

The aim of this chapter was to develop and characterise TEOM using human FNB6 TERT-2 immortalised oral keratinocytes and primary normal oral fibroblast cells, and validate its similarity to normal oral mucosal tissue by analysing the histological structure, expression of structural proteins by IHC, and comparing this to native oral tissue. This validation step is crucial to ensure that the developed TEOM is suitable for using in drug toxicity and drug delivery experiments.

The specific objectives of this chapter were as follows:

- To determine the morphology of TEOM as compared to native oral mucosa using haematoxylin and eosin (H&E) and Periodic-acid Schiff (PAS) staining.
- To identify the expression of proteins involved in proliferation (Ki-67), differentiation (cytokeratin 14, cytokeratin 4 and cytokeratin 13) and adhesion (E-cadherin and Claudin-4) processes in the TEOM as compared to native oral mucosa using IHC staining.
- To examine the ultrastructure of TEOM such as tight junction-related structures (desmosomes and hemidesmosomes) using TEM.

- To evaluate the viability of TEOM for 30 days in the culture using alamarBlue®.
- To assess the electrical resistance of TEOM using transepithelial electrical resistance.
- To assess the permeability barrier of TEOM using fluorescently labelled dextrans.

3.2 Experimental procedures

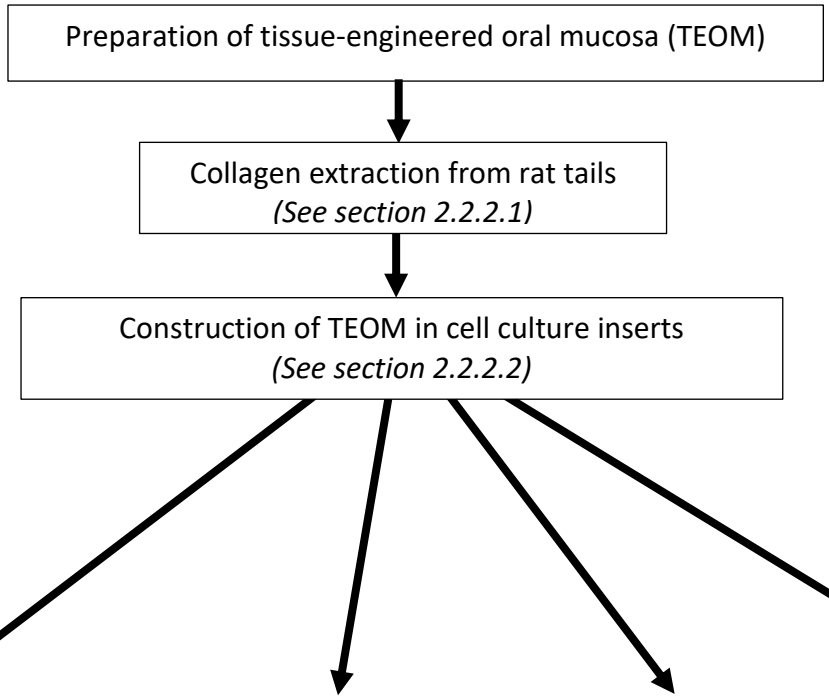

Morphological analysis	Protein expression analysis	Viability of TEOM analysis	Epithelial barrier functional analysis
• Haematoxylin and eosin (H&E) staining *(see section 2.2.3.1)* • Periodic acid-Schiff (PAS) staining *(See section 2.2.3.2)* • Transmission electron microscope (TEM) *(See section 2.2.3.3)*	• Immunohistochemical (IHC) staining *(See section 2.2.4)* ○ Differentiation markers (CK4, 14 and 13) ○ Proliferation markers (Ki67) ○ Adhesion markers (Claudin 4 and E-cadherin)	• AlamarBlue® dye *(see section 2.2.5)*	• Transepithelial electrical resistance (TEER) analysis (See section 2.2.6.1) ○ EVOM device • Permeability analysis (See section 2.2.6.2) ○ FITC-dextrans (3, 10 and 70 kDa)

3.3 Results

3.3.1 Morphology of tissue engineered oral mucosa using immortalised oral keratinocyte (FNB6) cells resembles the native oral mucosa

Histological analysis was carried out on TEOM cultured for 5, 10 and 14 days at ALI in order to investigate the basic structure of TEOM using H&E staining. Structurally, TEOM were comprised of 3 distinct layers; epithelium, basement membrane and fibroblast-populated connective tissue at all time intervals examined that resulted in the formation of a full-thickness of TEOM (Figure 3.1B-D). Generally, the histological structure of the TEOM was very similar to that observed in the native oral mucosa (Figure 3.1A), although the TEOM demonstrated a thinner epithelium. The immortalised FNB6 keratinocytes seeded onto the surface of the connective tissue equivalents differentiated into multiple stratified epithelial layers that were observed at each time point examined.

Culturing the TEOM over 14 days at ALI markedly affected the stratification pattern of the epithelium as well as its thickness (Figure 3.1B-D). After 5 days incubation, the epithelium consisted of a layer of basal cells (stratum basale) attached to the basement membrane, followed by the spinous/prickle layer (stratum spinosum) consisting of polygonal, densely packed keratinocytes that increased in size from basal layer apically. These cells became flattened to produce a non-keratinised superficial layer (stratum lucidum) (Figure 3.1B). The histology at this time point was very similar to the native buccal oral mucosa biopsy that also displayed a non-keratinised epithelium (Figure 3.1B). After 10 days incubation the epithelium retained the basal and spinous cell layers, displayed a small granular layer as well as a distinct layer of more keratinised but still nucleated stratum corneum cells in the outermost superficial layers of the epithelium, giving the appearance of parakeratinised oral epithelium (Figure 3.1C). By 14 days the most superficial epithelial layers were more keratinised but still contained nuclei (parakeratinised) whilst the spinous layer appeared to be reduced in size (Figure 3.1D). These data show that the pattern of epithelium stratification, particularly in the superficial layer, changed from non-keratinised at 5 days to a more parakeratinised layer by 10 - 14 days.

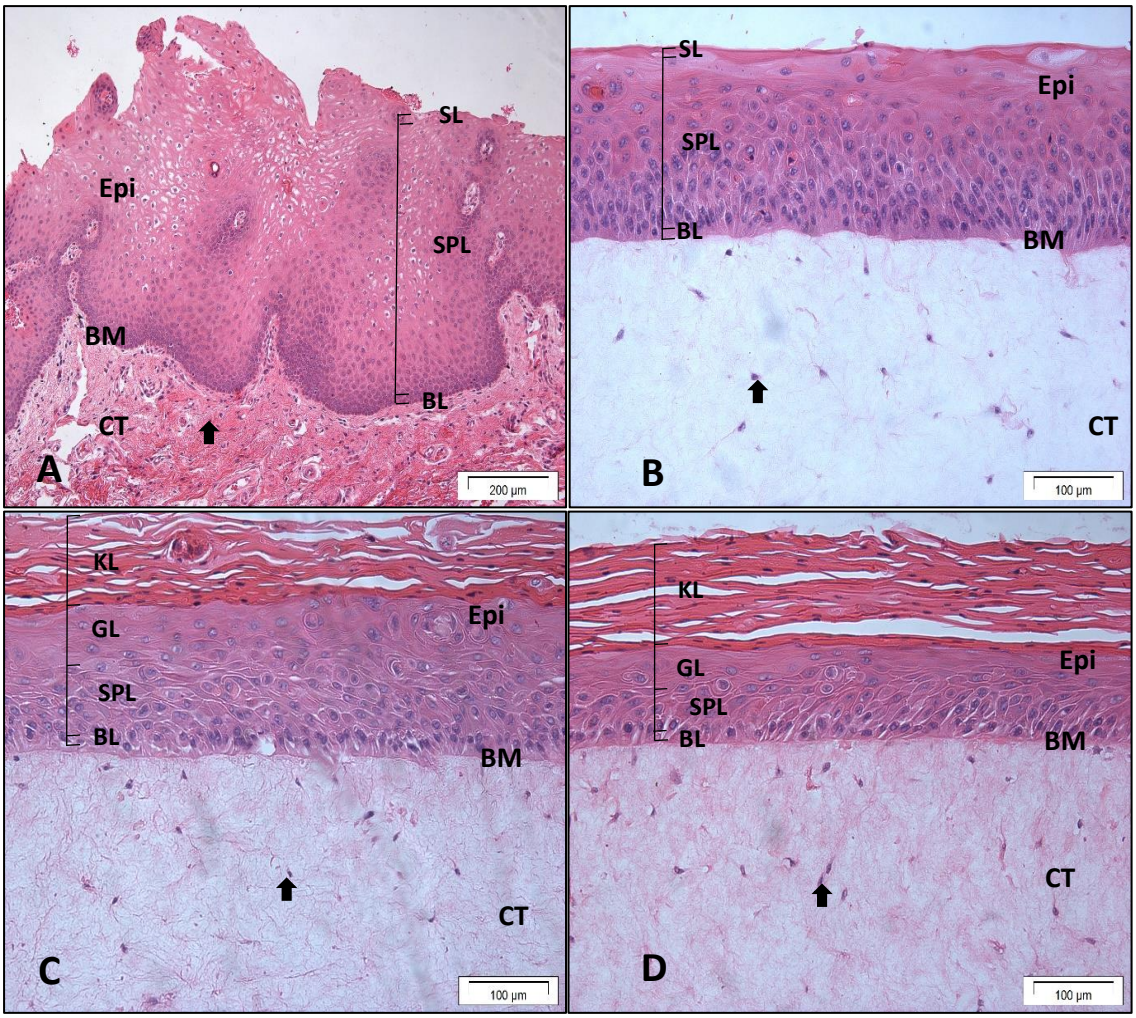

Figure 3.1: Morphology of native oral mucosa and TEOM stained using H&E staining. (A) The basic structure of native buccal oral mucosa comprises of non-keratinised epithelium (Epi), basement membrane (BM) and connective tissue (CT) - containing oral fibroblasts (Arrow). The epithelium constitutes a basal layer (BL), spinous/prickle layer (SPL) and superficial layer (SL). (B) At 5 days ALI the TEOM displays a non-keratinised epithelium that is structurally similar to the native non-keratinised buccal oral mucosa. (C) by 10 days the superficial layer is more keratinised by still contains nuclei so can be defined as parakeratinised. (D) and 14 days parakeratinised is more prominent. (KL: Keratinised layer, GL: Granular layer) (A) Scale bar = 200 µm, (B-D) Scale bar = 100 µm).

Measurement of histological images showed that the thickness of the TEOM epithelium increased significantly ($p < 0.0001$) from 5 to 10 and 14 days incubation (Figure 3.2A) but no difference was observed between 10 and 14 days (Figure 3.2A). For the keratinised epithelium, there was a significant difference in the size of the parakeratinised layer between 5 and 10/14 days because the TEOM at 5 days was non-keratinised. However, there was no significant difference between TEOM at 10 and 14 days (Figure 3.2B).

The fibroblast cells seeded into the rat-tail type 1 collagen in the TEOM were evenly able distributed within the substrate forming the connective tissue equivalents at each time interval (Figure 3.1B-D). The connective tissue equivalents in the TEOM were loosely formed whereas the connective tissue of native oral mucosa was more densely packed (Figure 3.1A).

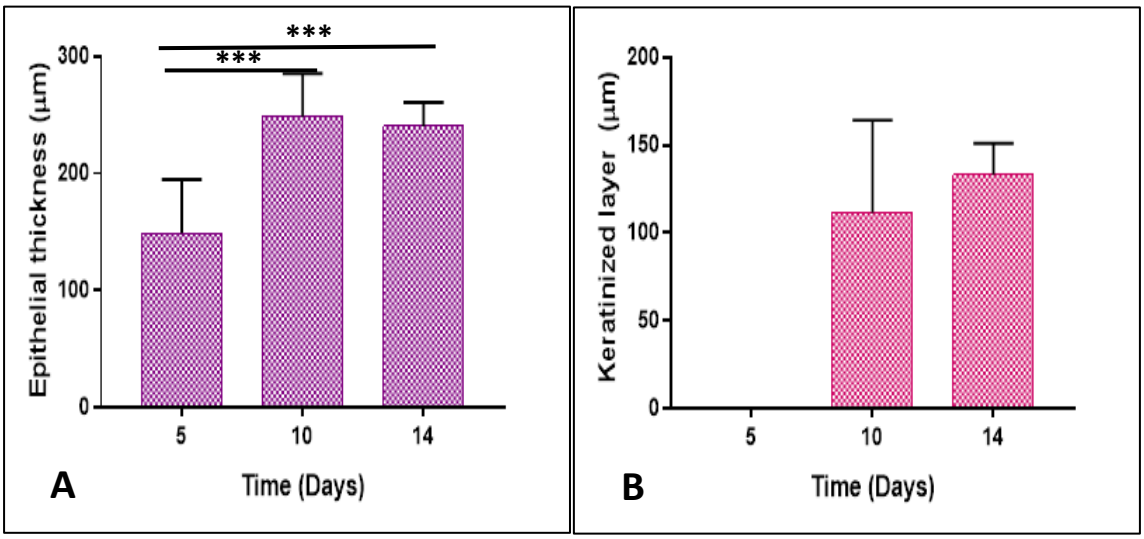

Figure 3.2: Thickness of the epithelium and keratinised layer of TEOM**.** (A) Epithelial and (B) keratinised layer thickness incubated for up to 14 days at ALI. Data were expressed as the mean ± SD for 3 independent experiments performed in triplicate. A mean difference was considered significant when * = $p < 0.05$, ** = $p < 0.001$ and *** = $p < 0.0001$ using One-way ANOVA with Tukey post-hoc multiple comparison tests.

3.3.2 Presence of basement membrane structure in TEOM

PAS staining was performed to confirm the presence of a basement membrane (arrow); a continuous thin positive pink colour staining between the epithelium and connective tissue (Figure 3.3B-D) that was similarly observed in the native oral mucosa (Figure 3.3A). Positive PAS staining was also observed in the superficial epithelial layers, in particular the parakeratinised layers, as this stain binds to glycogen within these layers.

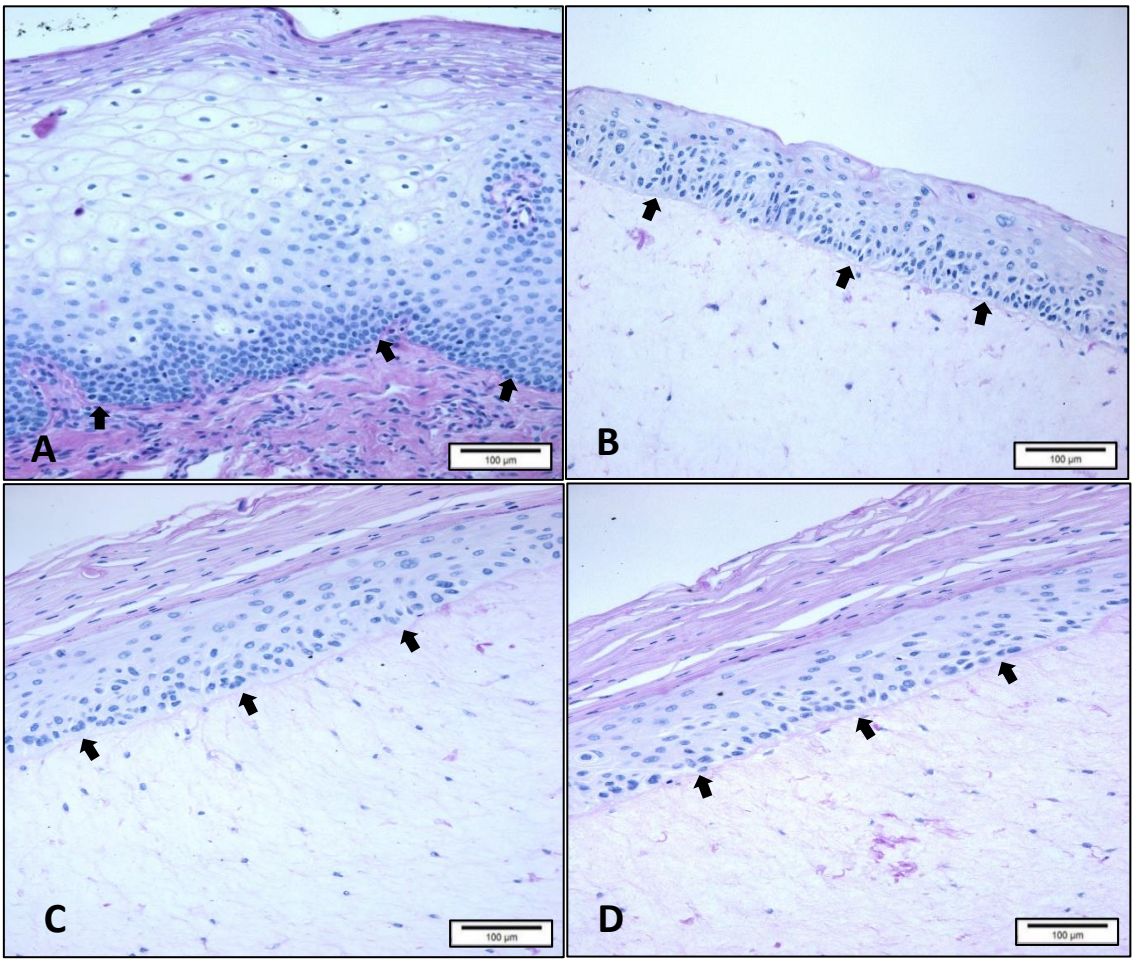

Figure 3.3: Basement membrane detected using PAS staining**.** Presence of basement membrane in (A) native oral mucosa and (B) TEOM was identified between the epithelial and connective tissue layer at (B) day 5, (C) day 10 and (D) day 14 at ALI. (Scale bar = 100 µm).

3.3.3 Preservation of the essential markers in TEOM

3.3.3.1 Cell differentiation markers

3.3.3.1.1 Cytokeratin 14

Cytokeratin 14 (CK14) is a member of the type I keratin family of intermediate filament proteins (Moll et al., 2008) and is a prototypic marker of dividing basal keratinocytes (Alam et al., 2011). Expression of CK14 in the native oral mucosa was more predominantly expressed in the basal layer than the suprabasal layer (Figure 3.4A). In contrast, the expression of CK14 in the TEOM displayed a similar level of intensity throughout the epithelium when cultured for 5 (Figure 3.4B), 10 (Figure 3.4C) or 14 days (Figure 3.4D) at ALI, respectively. For TEOM at days 10 and 14, CK14 staining was absent in the uppermost parakeratinised layers of the epithelium (Figure 3.4C-D).

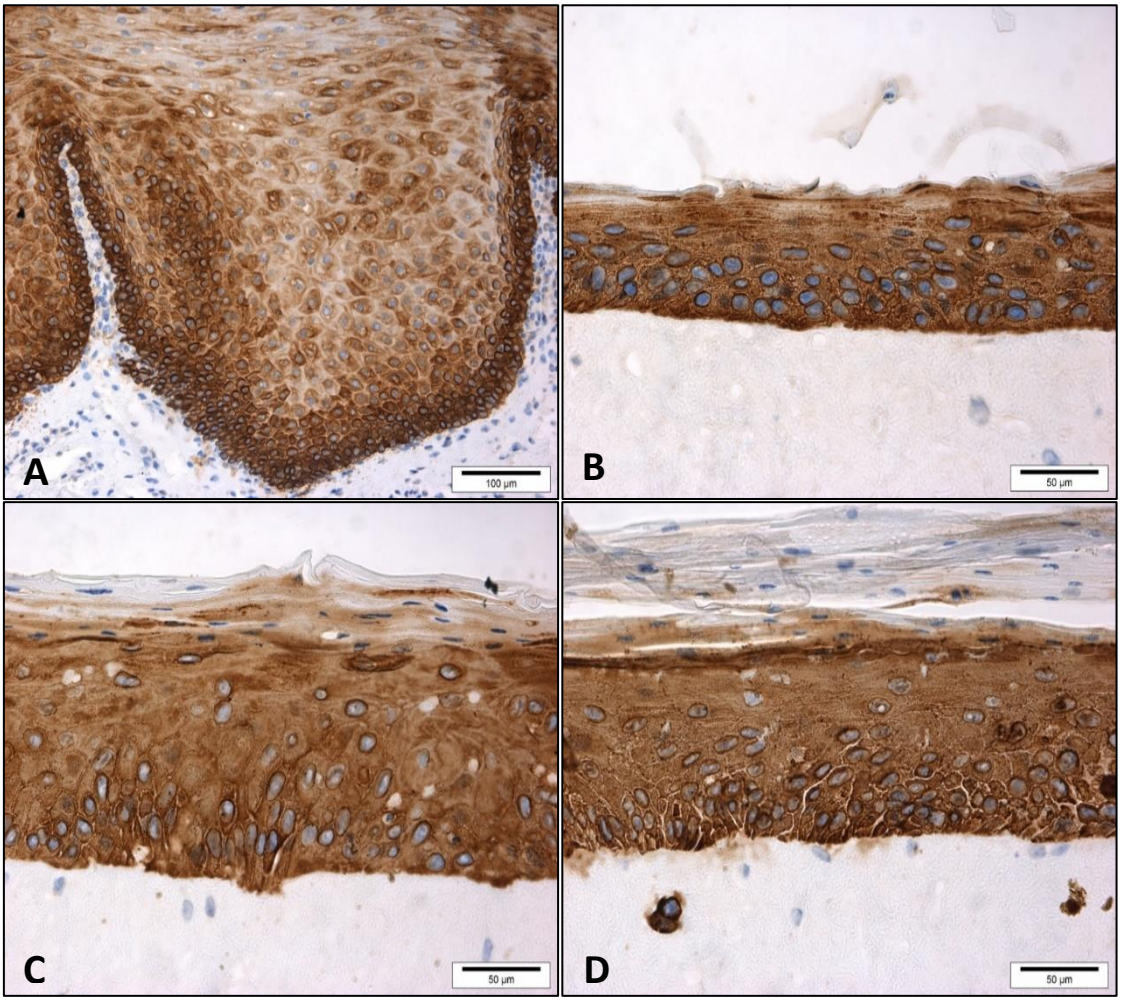

Figure 3.4: CK14 expression in native buccal mucosa and TEOM identified using IHC staining. CK14 expression was demonstrated in (A) native oral mucosa and TEOM cultured for (B) 5, (C) 10 and (D) 14 days at ALI. ((A) Scale bar = 100 µm, (B-D) Scale bar = 50 µm).

3.3.3.1.2 Cytokeratin 13 and cytokeratin 4

Cytokeratin 13 (CK13) is a type I cytokeratin that is paired with cytokeratin 4 and found in the suprabasal layers of non-keratinised stratified epithelia. CK13 expression in the native buccal mucosa was limited to the all suprabasal layers and no expression found in the basal keratinocytes (Figure 3.5A). The same pattern of CK13 staining was observed in TEOM with intense CK13 stain for all suprabasal cells with only the basal cells being CK13-negative (Figure 3.5C). Expression of CK4 was less prominent in the native oral mucosa and staining restricted to the upper spinous and superficial layers and this exact pattern of expression repeated in the TEOM (Figure 3.5B&D).

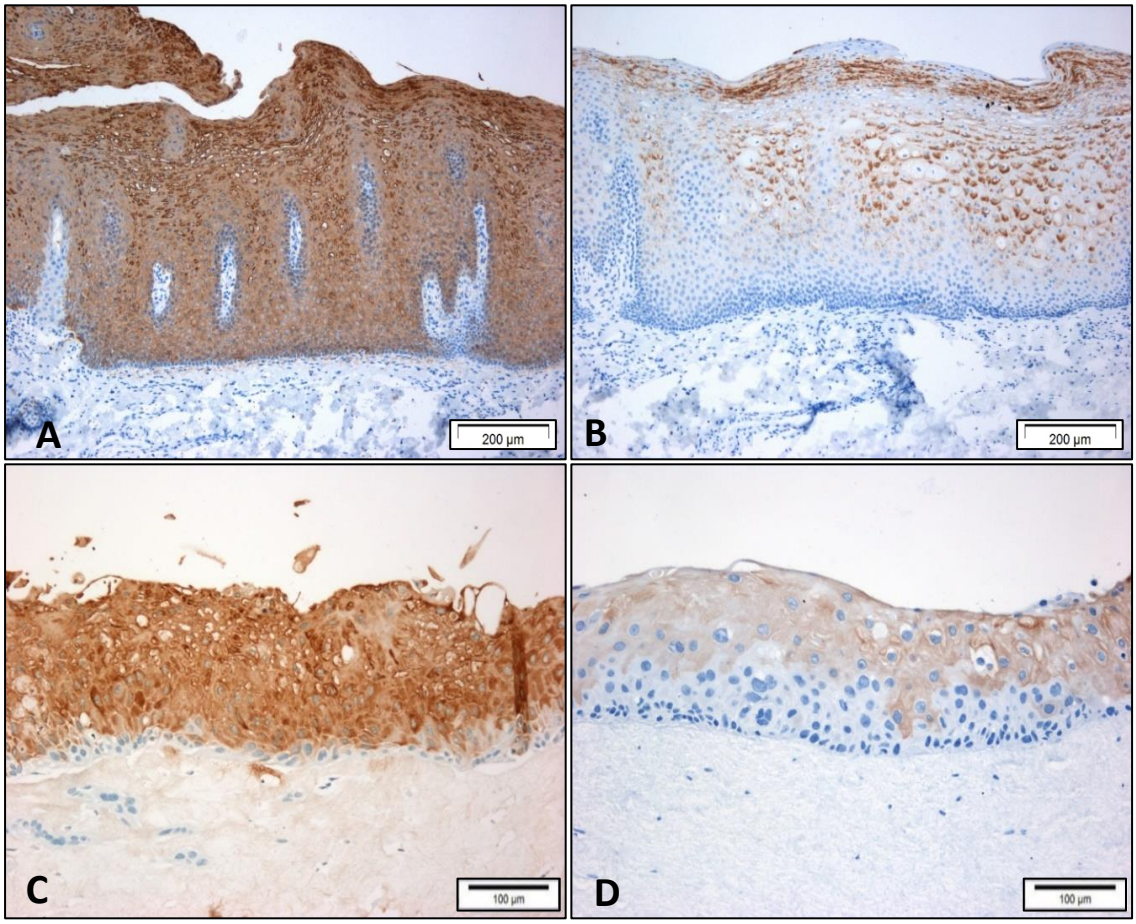

Figure 3.5: CK13 and CK4 expression in native buccal mucosa and TEOM identified using IHC staining. Expression of (A) CK13 and (B) CK4 in native oral buccal mucosa and expression of (C) CK13 and (D) CK4 in TEOM cultured for 5 days at ALI. (A&B Scale bar = 200 µm, C&D Scale bar = 100 µm).

3.3.3.2 Cell proliferation marker

3.3.3.2.1 Ki-67

Ki-67 is a protein that is only expressed during active phases of the cell cycle (Bruno and Darzynkiewicz, 1992) and is therefore, a marker for actively proliferating epithelial cells. In native oral mucosal tissue, only the basal cells are actively dividing and therefore ki-67 expression was restricted to the basal cells by IHC (Figure 3.6A). Similarly, ki-67-positive proliferating epithelial cells in the TEOM cultured for 5 (Figure 3.6B), 10 (Figure 3.6C) and 14 days (Figure 3.6D) were restricted to the basal layer and occasionally the parabasal cells. The expression of this molecule was therefore comparable to the native oral buccal mucosa.

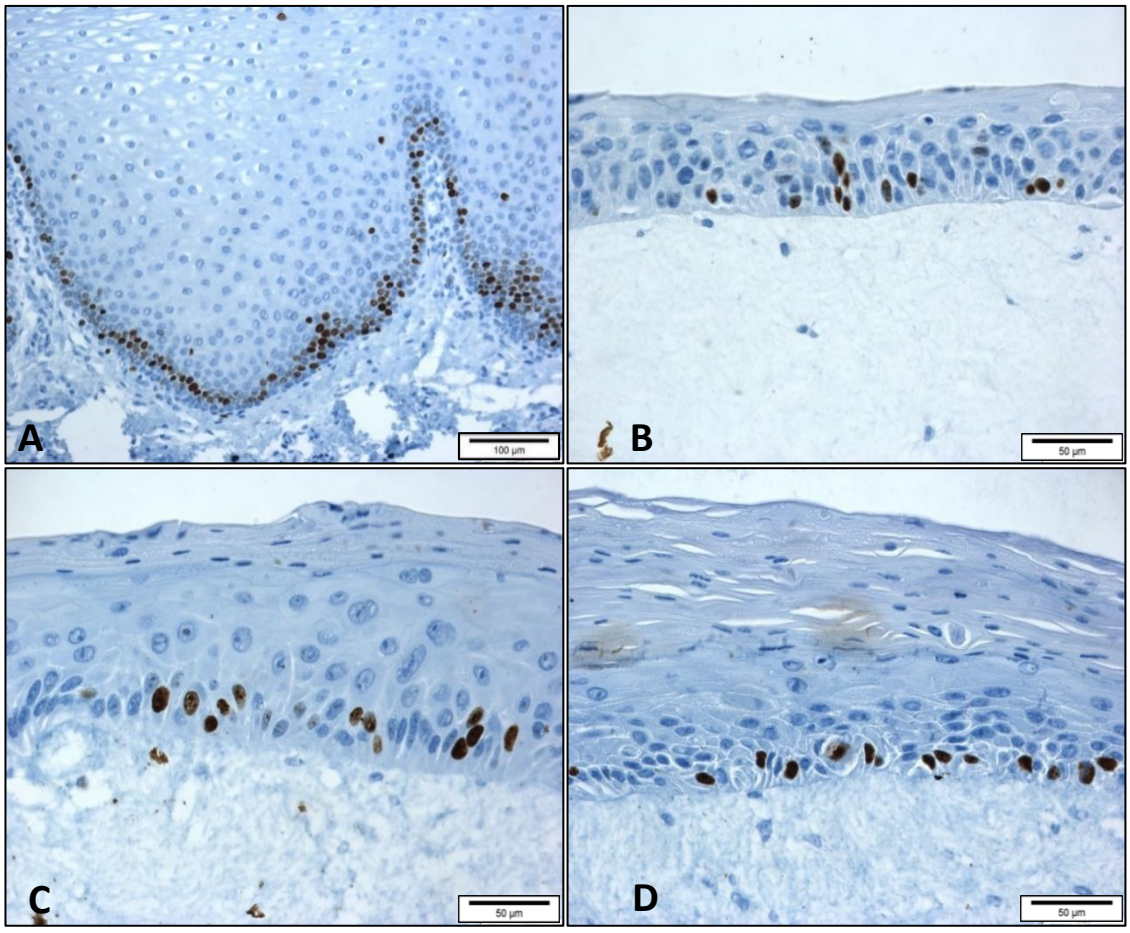

Figure 3.6: Ki-67 expression in native buccal mucosa and TEOM identified using IHC staining. Ki-67 expression is demonstrated in (A) native oral mucosa and TEOM cultured for (B) 5, (C) 10 and (D) 14 days at ALI. (A Scale bar = 100 µm, B-D Scale bar = 50 µm).

3.3.3.3 Cell adhesion markers

3.3.3.3.1 E-cadherin and Claudin-4

E-cadherin and Claudin-4 are cell adhesion proteins of the tight junctions that are located between epithelial cells. Their expression is crucial for structural integrity of the tissue. Distinctive plasma-membrane expression of both E-cadherin (Figure 3.7A) and Claudin-4 (Figure 3.8A) was observed for all the epithelium in the native oral buccal mucosa, although staining for E-cadherin was more intense than for Claudin-4. At day 5 ALI, expression of E-cadherin was also prominent and restricted to the epithelial plasma membrane (Figure 3.7B), whereas expression of Claudin-4 at this stage was more diffuse and ambiguous (Figure 3.8B). At 10 days ALI, membrane expression of E-cadherin and Claudin-4 was more pronounced and expression was not detected at the basement membrane interface or in the upper most superficial layers, which is in line with the native tissue (Figure 3.7C and Figure 3.8C). Similar observations were also seen at day 14 ALI for both E-cadherin and Claudin-4 (Figure 3.7D and Figure 3.8D). In all cases, the intensity of Claudin-4 staining was weaker when compared to E-cadherin in both TEOM and native oral mucosa.

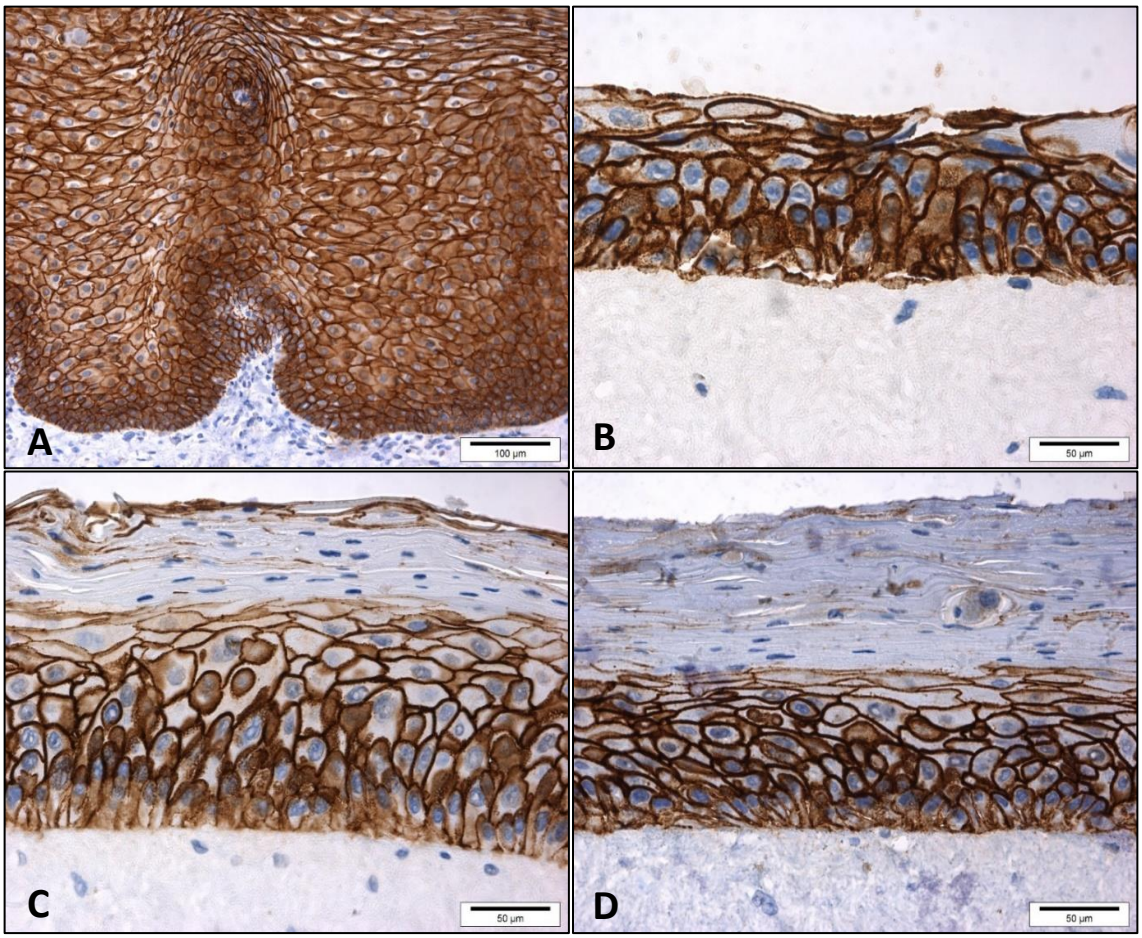

Figure 3.7: E-cadherin expression in native buccal mucosa and TEOM identified using IHC staining. E-cadherin expression was exhibited in the suprabasal layers at the plasma membrane in (A) native oral mucosa and TEOM cultured for (B) 5, (C) 10 and (D) 14 days at ALI. (A Scale bar = 100 µm, B-D Scale bar = 50 µm).

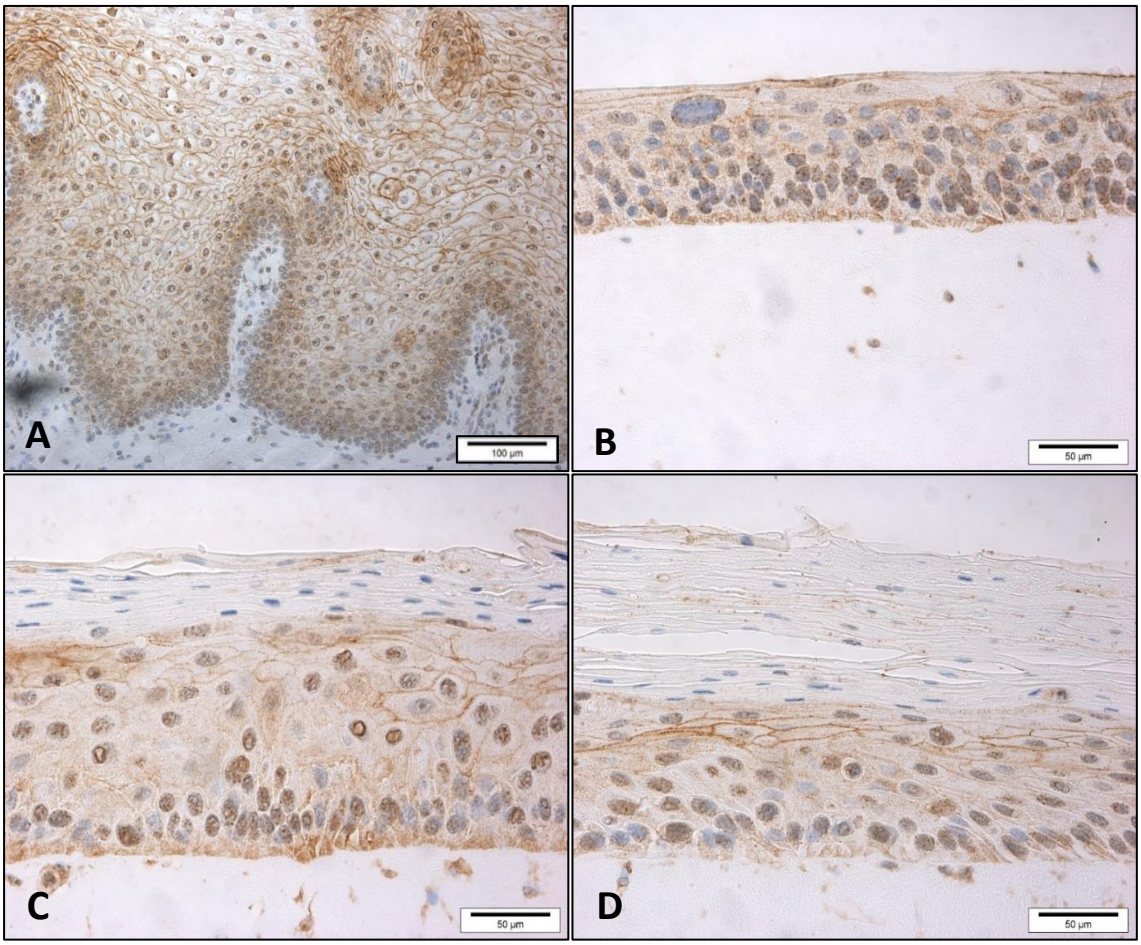

Figure 3.8: Claudin-4 expression in native buccal mucosa and TEOM identified using IHC staining. Claudin-4 expression was evident at the plasma membrane in (A) native oral mucosa and TEOM cultured for (B) 5, (C) 10 and (D) 14 at ALI. (A Scale bar = 100 µm, B-D Scale bar = 50 µm).

3.3.4 Ultra-structural analysis of TEOM by TEM

Ultrastructural analysis of the organisation of the TEOM was performed using TEM to confirm the histology and IHC staining. Figure 3.9A&B shows the flattened, elongated epithelial cell morphology in the superficial, stratum lucidium layer compared to the more rounded cell morphology in the basal cells (Figure 3.9C), confirming the histological images. Figure 3.9D shows alignment of the collagen fibres within the connective tissue component and the presence of a well-organised basement membrane separating the epithelium from the connective tissue (Figure 3.9E&F).

The structural integrity of the oral epithelium is dependent on the presence of key structural motifs that hold epithelial cells tightly together (desmosomes) and firmly connect the basal cells to the basement membrane (hemidesmosomes). Figure 3.9G shows the presence of numerous desmosome structures between adjacent epithelial cells. At higher magnification (Figure 3.9H) desmosomes exhibited a bundle of keratin intermediate filaments (tonofilaments; arrow), joining the adjacent epithelial cells by anchoring to dense plaques. Hemidesmosomes were also detected at distinct focal points where integrins connect the basal cells to the basement membrane along with anchoring fibrils (Figure 3.9 I&J).

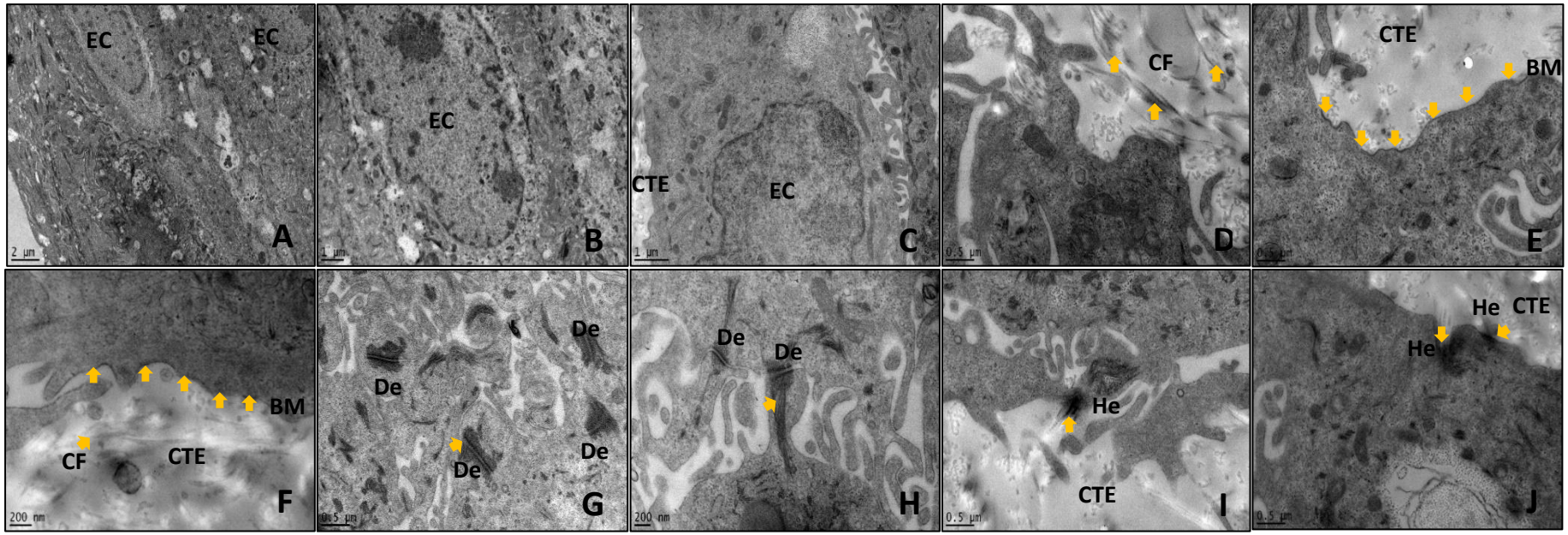

Figure 3.9: Ultrastructural organization of TEOM identified using transmission electron microscope (TEM). (A) Epithelial cells (EC) in the superficial layer (scale bar = 2 µm), (B) epithelial cell (EC) in the superficial layer at higher magnification (scale bar = 1 µm), (C) Basal epithelial cell (scale bar = 1 µm), (D) collagen fibrils (CF) (arrow) within the connective tissue (CTE) appear straight and vary in size (Scale bar = 0.5 µm), (E) basement membrane (BM) (arrows) structures between the connective tissue (CTE) and epithelium (scale bar = 0.5 µm), (F) basement membrane (BM) structures between the connective tissue (CTE) and epithelium at higher magnification (scale bar = 200 nm), (G) desmosome (De) structures and keratin filaments (tonofilaments) attach to dense plaques (Scale bar = 0.5 µm), (H) desmosomes (De) and keratin filaments (tonofilaments) (arrow) attach to dense plaque of desmosome at higher magnification (scale bar = 200 nm), (I) and (J) hemidesmosomes (He) structures anchor the basal cells to the basement membrane (scale bar = 0.5 µm).

3.3.5 The viability of TEOM was maintained up to a month

Mitochondrial metabolism of alamarBlue® by viable cells produces a fluorescent product. The levels of fluorescence are often used as an indirect measurement of cell viability and cell proliferation. The viability of TEOM was determined over time every 5 days up to 30 days at ALI using alamarBlue®. The fluorescence intensity increased in a time-dependent manner from 5 (25049.3 ± 4068.1) to 15 days TEOM reaching a maximal value (35936.2 ± 3083.6) at day 15 of ALI culture, suggesting that the cells in the TEOM are viable and increasing in number up to day 15 (Figure 3.10). Thereafter, the fluorescence values gradually decline to 16871.9 ± 3689.7 by day 30, which is significantly less that the value observed at day 15 ($p < 0.05$); Figure 3.10), but not significantly less that day 5 TEOM. These data suggest that TEOM maintain viability for up to 30 days in culture but show differences in fluorescence values that are likely to represent a loss of cell numbers as the culture progresses.

3.3.6 Electrical resistance reflects the integrity status of the epithelium of TEOM

The electrical resistance across the epithelium was measured over time using an Epithelial Voltohmmeter (EVOM) in order to determine the resistance barrier of the epithelium in the TEOM. The value of electrical resistance was expressed as mean $\Omega.cm^2$. The electrical resistance across the epithelium of TEOM increased gradually from day 5 (92.4 ± 8.2 $\Omega.cm^2$) to day 20 ALI culture where it reached the maximal electrical resistance (155.8 ± 13.3 $\Omega.cm^2$). The TEER was significantly increase at day 20 compared to day 5 ($p<0.05$) suggesting that the integrity of the tissue increases during this period (Figure 3.11). Thereafter, the TEER gradually declined to 114.03 ± 5.4$\Omega.cm^2$ by day 30, a significant decrease ($p<0.05$) compared to values obtained at day 20, although still remaining above 100 $\Omega.cm^2$ and much higher than compared to the measurement taken on day 5 (Figure 3.11).

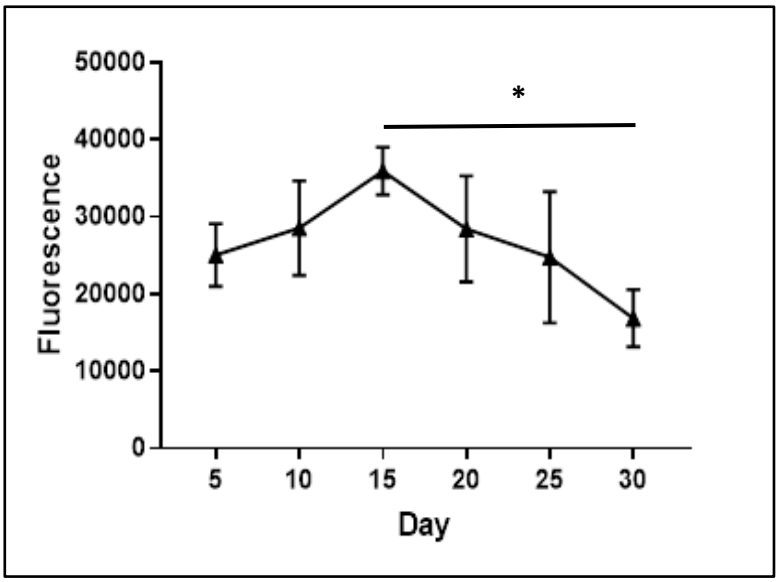

Figure 3.10: Viability profile of the TEOM determined using alamarBlue® for 30 days in the cultures. TEOM were cultured at ALI for up to 30 days and viability indirectly measured by reduction of alamarBlue® at indicated time points. The maximal viability is reached at day 15. Data were expressed as the mean ± SD for 3 independent experiments performed in triplicate. A mean difference was considered significant when *p < 0.05, **p < 0.001 and ***p < 0.0001 using One-way ANOVA with Tukey post-hoc multiple comparison tests.

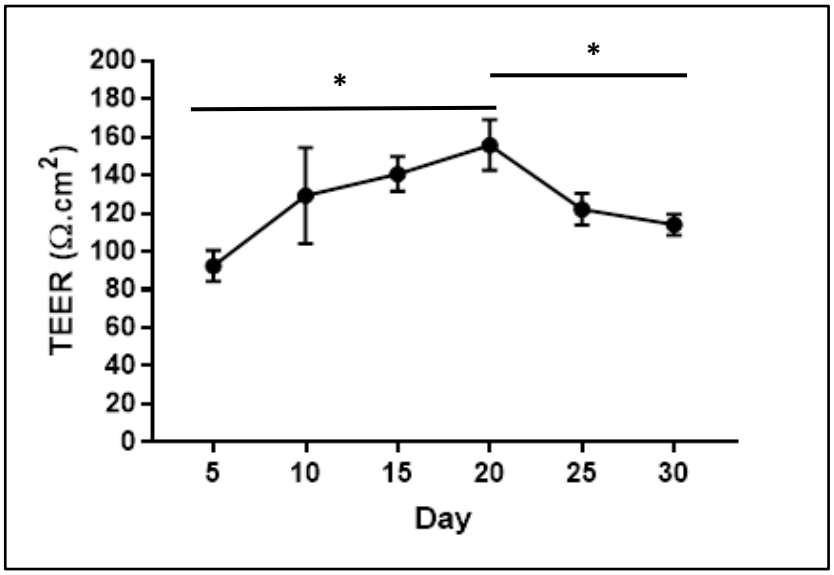

Figure 3.11: TEER profile of TEOM measured using an Epithelial Voltohmmeter (EVOM) over 30 days at ALI culture. The maximal viability is reached 155.8 $\Omega.cm^2$ at day 20. Data were expressed as the mean ± SD for 3 independent experiments performed in triplicate. A mean difference was considered significant when *p < 0.05, **p < 0.001 and ***p < 0.0001 using One-way ANOVA with Tukeypost-hoc multiple comparison tests.

3.3.7 Integrity status of the epithelium influences the permeability of FITC-dextrans and electrical resistance profile

The permeability across the TEOM was performed using three different fluorescently labelled dextrans of increasing molecular weight (3, 10 and 70 kDa). Dextrans at 3 kDa pass easily through the epithelium, 10 kDa less so, whereas 70 kDa dextrans have much restricted diffusion (Hoogstraate et al., 1994). Firstly, TEOM were exposed to fluorescent dextrans for up to 300 minutes (Figure 3.12). The amount of each fluorescently labelled dextran that passed through the TEOM increased in a time-dependent manner. From 60 minutes onwards, significantly ($p < 0.05$) more 3 kDa dextran was able to diffuse through the TEOM than either the 10 or 70 kDa fluorescent dextran. The permeability of the TEOM was 3>10>70 kDa at each time point tested. After 5 hours exposure, the amount of fluorescent 3, 10 and 70 kDa dextran that had permeated through the TEOM was approximately 17, 6 and 3 %, respectively (Figure 3.12).

Secondly, the permeability of TEOM was assessed by treating the TEOM using sodium dodecyl sulphate (SDS; 5%), a detergent that is known to disrupt the barrier of the epithelium in TEOM and evaluating the loss of permeability/integrity of the tissue by evaluating both the TEOM TEER and dextran permeability. It was noted that the impairment of epithelium barrier in the SDS treated group displayed significantly ($p < 0.05$) increased permeability to all sizes of fluorescently labelled dextrans when compared to PBS treated, suggesting nearly complete loss of the permeability barrier of the TEOM epithelium (Figure 3.13A). Similarly, the TEER value was significantly reduced ($p < 0.05$) in the SDS, compared to PBS control treated TEOM (Figure 3.13B). Histologically, the treatment of TEOM with SDS (5%) caused tissue decellularisation with loss of integrity of all cells in both the epithelium and connective tissue. The detachment of the epithelia from the connective tissue is also evident in many parts of the TEOM, virtually destroying the structure of TEOM (Figure 3.14).

Taken together, these data show that when the epithelial barrier is maintained, the permeation of all sizes of dextrans was low, especially the permeation of larger molecules such as 70 kDa dextran, whilst at the same time the TEER value increased.

In contrast, the addition of detergent to the TEOM completely disrupted the tissue architecture, allowing complete permeation of the tissue to all dextrans and decreased electrical resistance. These data show that the TEOM have good integrity and are relatively impermeable.

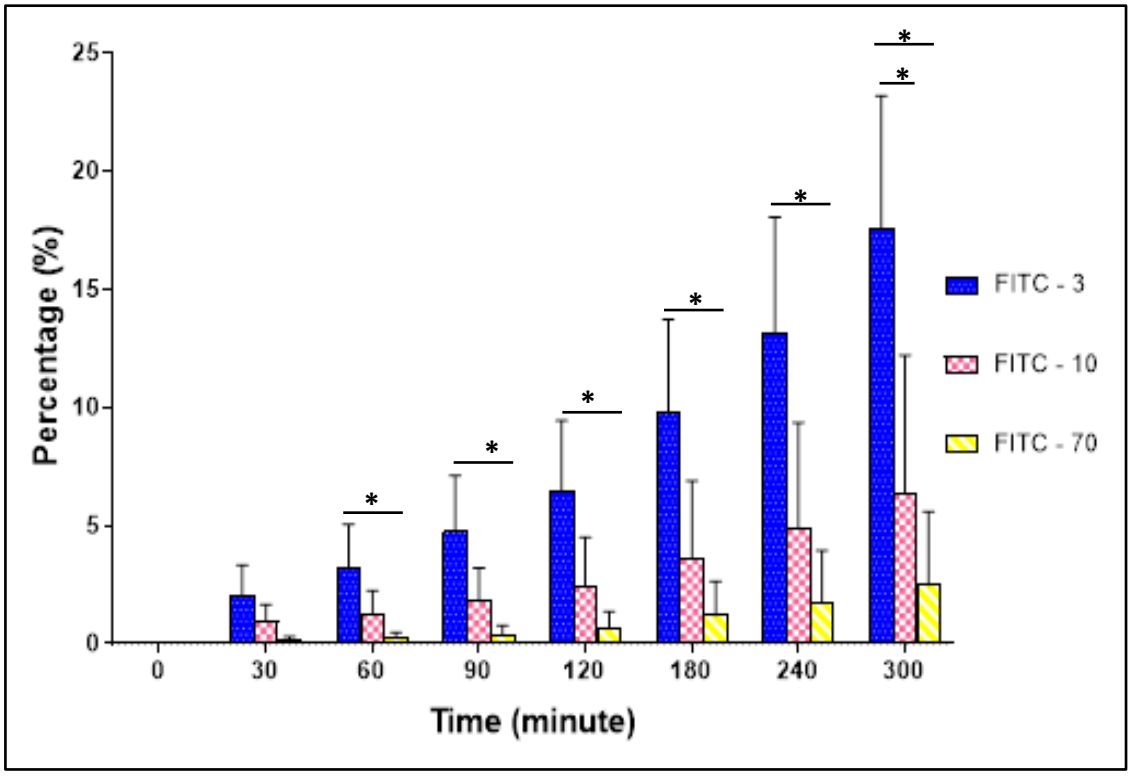

Figure 3.12: Permeability analysis of fluorescently labelled dextrans (3, 10 and 70 kDa) across the epithelium of TEOM. The permeability of TEOM against fluorescently labelled dextrans was increased in a size-dependent manner over time, particularly the permeability of TEOM against smaller (3 kDa) molecules. Data were expressed as the mean ± SD for 3 independent experiments performed in triplicate. A mean difference was considered significant when *$p < 0.05$, **$p < 0.001$ and ***$p < 0.0001$ using One-way ANOVA with Tukey post-hoc multiple comparison tests.

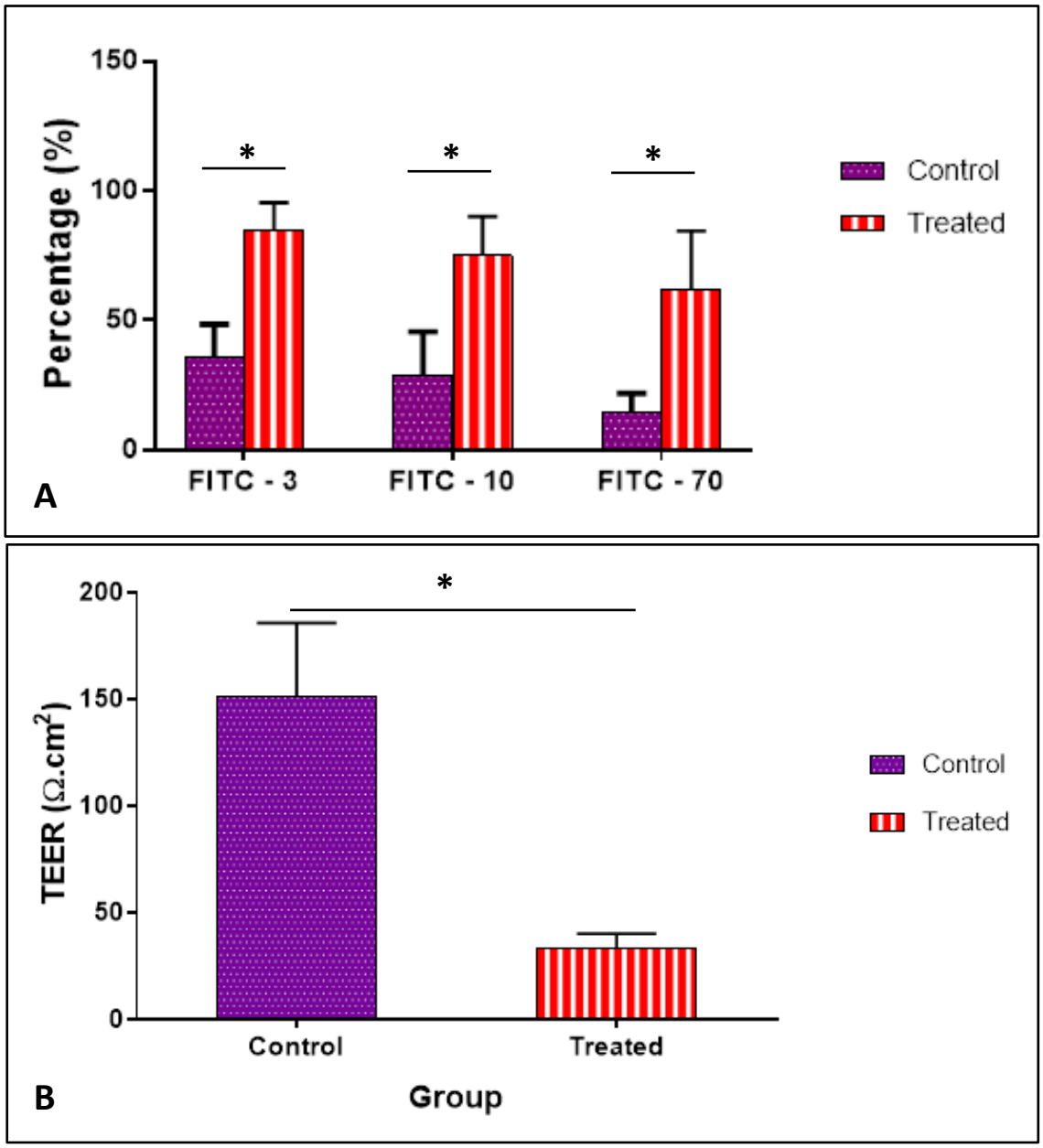

Figure 3.13: Comparison of the permeability and TEER value in TEOM between control and 5% SDS treated tissue. (A) The permeability of TEOM is decreased against fluorescently labelled dextrans in a size-dependent manner when the barrier is maintained and concurrently, (B) elevation of TEER value is observed. Data were expressed as the mean ± SD for 3 independent experiments performed in triplicate. A mean difference was considered significant when *$p < 0.05$, **$p < 0.001$ and ***$p < 0.0001$ using One-way ANOVA with Tukey post-hoc multiple comparison tests.

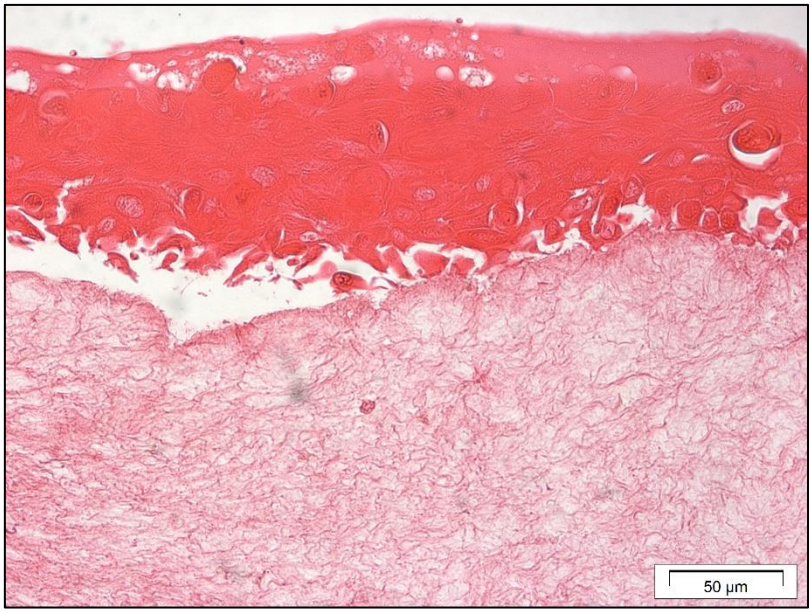

Figure 3.14: Morphology of TEOM treated with 5% SDS. The decellularisation of the epithelial and fibroblast cells and the detachment of the epithelium layer from the connective tissue of the TEOM can be been observed.

3.4 Discussion

Construction of a reliable TEOM that retains the structure, differentiation status and permeability of native oral mucosa remains a major challenge to investigators. Construction of a TEOM using immortalised keratinocytes whilst maintaining the viability, epithelial barrier functions and biological properties over a period of culture were the main driving force for the experiments described in this chapter. Extensive characterisation was performed to ensure that the TEOM was a reliable replica of oral mucosa and to ensure that it was fit to be used for downstream applications such as drug toxicity and drug delivery that are conducted over a long period of time.

In the present work, the development of TEOM was based on the utilisation of FNB6 cells and primary NOF, while the connective tissue scaffold was comprised of rat-tail type I collagen. The TEOM were cultured using commercially available culture inserts which contained a 0.4 μm porous membrane that permitted supply of nutrients to the basal side of the tissue and is commonly used for culture of 3D models (Chen et al., 2015; Sanchez-Quevedo et al., 2007; Geroski and Hadley, 1992). The design of the culture inserts also permitted culture at an ALI (Bayar, 2012; Sanchez-Quevedo et al., 2007; Reichl and Muller-Goymann, 2003; Richard et al., 1991). It has been reported that culture at ALI results in oxidative stress that produces a change in the cellular glutathione system (Kameyama et al., 2003; Tammi and Jansen, 1980), stimulating epithelial proliferation and differentiation (Bayar, 2012; Sanchez-Quevedo et al., 2007; Kameyama et al., 2003; Izumi et al., 1999).

The construction of a full-thickness TEOM based on immortalised oral keratinocytes and primary oral fibroblasts successfully generated a multi-layered epithelium consisting of stratified and differentiated epithelial cells that was histologically similar to the native oral mucosa. The thickness of the epithelium increased over time but was still thinner than native oral mucosa. Despite the difference in the epithelial thickness between native oral mucosa and TEOM, the structure and pattern of epithelial stratification were very comparable, which has been observed in previous studies (Buskermolen et al., 2016; Kinikoglu et al., 2009; Izumi et al., 2000). The interactions between keratinocytes, fibroblasts and the surrounding stroma are

thought to be the main influence over the thickness of the epithelium (Moharamzadeh et al., 2012; Liu et al., 2011; Costea et al., 2005). It may be that the factors in the *in vitro* model may not exactly replicate the *in vivo* situation, leading to slightly thinner epithelia.

Interestingly, the TEOM displayed increased levels of keratinisation along with visible signs of epithelial shedding the longer they were cultured at ALI. Histologically, a shorter incubation time of TEOM at ALI displayed as a non-keratinised epithelium. While longer incubation time demonstrated a keratinised epithelium, with nuclei being retained in the superficial layer (parakeratinised), indicating the parakeratosis (Bayar et al., 2012). This is intriguing as the immortalised keratinocytes are derived from the buccal mucosa, a non-keratinised area of the oral mucosa. The fibroblasts used in this study were mainly from gingival tissue, an area of keratinised epithelium. It is plausible that factors released from these fibroblasts influence the oral keratinocytes and push them toward a more keratinised, albeit parakeratinised status. This transformation has also been observed by Izumi et al., 2000 and suggests that the origin of cells plays a key role in keratinisation. In addition, other studies also reported keratinised epithelium in TEOM as early as 7 days incubation at ALI (Bayar et al., 2012; Izumi et al., 2000), which similar to these findings showing keratinisation at day 10. However, the epithelium of TEOM in these studies showed only a few epithelial layers thick that were not well differentiated (Bayar et al., 2012; Izumi et al., 2000), possibly due to the lack of fibroblasts in these models. A recent study constructed a TEOM using entirely immortalised of oral keratinocytes and fibroblasts derived from gingival biopsies (Buskermolen et al., 2016). Here the full-thickness TEOM displayed a keratinised epithelium after 10 days at ALI, which is in line with the findings in this study. The data presented here are also in line with another recent study published using immortalised FNB6 keratinocytes and primary gingival fibroblasts. Although less characterised than the data presented here, these TEOM displayed non-keratinised epithelium (Jennings et al., 2016) and were structurally comparable to the TEOM in this study. In addition, other researchers have generated TEOM using immortalised oral keratinocytes derived from the floor of the mouth (OKF6-TERT2). These cells

appear to produce poorly differentiated epithelium, sometimes only a few layers thick (Almela et al., 2016; McLeod et al., 2014 and Dongari-Bagtzoglou and Kashleva, 2006).

The presence of non-keratinocytes, such as melanocytes (Yamazaki et al., 1991), Langerhans cells (Terris et al., 1995), Merkel cells (Harmese et al., 1999) and lymphocytes (Squier and Kremer, 2001) can also be found in the oral mucosa. These cells constitute approximately 10% of the oral epithelium in both non-keratinised and keratinised epithelium (Squier and Kremer, 2001; Squier and Finkalstein, 1998). All these cells, except Merkel cells, lack desmosomal attachments to neighbouring cells. Therefore, the cytoplasm of these cells shrink around the nuclei to generate a clear halo effect during the histologic processing. It is highly unlikely that these cells survive the isolation and culture process when keratinocytes are generated from tissue biopsies and therefore are not likely to be in the TEOM. Indeed, lack of other cell types is a criticism of TEOM and the development of advanced models to include immune cells is warranted.

PAS staining and TEM analysis confirmed the presence of a basement membrane between the epithelium and connective tissue. The basement membrane is a region of attachment that is required as a mechanical support to endure the sheer stress occurred in the oral mucosa (Dodla and Velmurugan, 2013; Shinkar et al., 2012; Feinberg et al., 2005). The interplay of keratinocytes and fibroblasts together with the basement membrane components such as collagen type IV and laminin 5 are essential for the formation of functional basement membrane (Laverdet et al., 2014; Stephens and Genever, 2007; Marrionet et al., 2006). Keratinocytes are the main source of collagen type IV (Chen et a., 2002) and laminin 5 (Amano et al., 2001), in the absence of fibroblasts, whereas fibroblasts are the main source of collagen type IV in the presence of keratinocytes (Smola et al., 1998). The basement membrane also acts as a rate-limiting factor that affects the movement of the molecules in a size-dependent manner from the epithelium to the connective tissue and its presence is therefore important when analysing the movement of drugs across the tissue (Vllasaliu et al., 2014; Rathbone and Tucker, 1993).

A scaffold, as an artificial supporting structure for growing the cells, is another essential component for generation of TEOM. An ideal scaffold should be non-toxic (MacNeil, 2007), have porosity (Will et al., 2008; Muschler et al., 2004), biodegradability (Palsson and Bhatia, 2004), biostability (Ma et al., 2003), biocompatibility and the ability to mimic the native structure of the oral mucosa (Moharamzadeh et al., 2007). Collagen-based scaffolds possess most of these qualities (Parenteau-Bareil et al., 2010). In this study, the connective tissue scaffold was based on collagen I from rat tails that is widely utilised by researchers as it bio-mimics the human extracellular matrix (Parenteau-Bareil et al., 2010; Shoulders and Rainers, 2009; Moharamzadeh et al., 2007). The fibroblasts in this study had proliferated, migrated and distributed evenly within the collagen-based connective tissue, similar to a previous study (Almela et al., 2016). It had been reported that this type of scaffold provides a suitable substrate for a communication between epithelial and fibroblasts cells, it avoids epithelial cell invasion and island formation in sub-epithelial layers (Moharamzadeh et al., 2007; MacCallum and Lillie, 1990). Thus far, collagen-based materials have shown favourable results in producing the TEOM in other studies (Luitaud et al., 2007). However, there are some drawbacks in using these types of scaffold including relatively weak mechanical properties (Roy et al., 2010), stability and degradation (Chen et al., 2005), and collagen contraction mediated by fibroblasts (Schoop et al., 1999; Bach et al., 2001; Chinnathambi et al., 2003). Occasionally, these features were observed in this study.

IHC staining of TEOM showed that these 3D models expressed a cytokeratin profile (differentiation markers) equivalent to that observed in the native oral mucosa (Yadev et al., 2011) and by other TEOM (Yadev et al., 2011; Moharamzadeh et al., 2007; Dickson et al., 2000). The expression of the cytokeratins reflects the differentiation stage of keratinocytes within different layers of the epithelium (Moharamzadeh et al., 2007; Vaidya et al., 2000). CK14 is a differentiation marker that helps in maintaining cell shape and provides resistance to mechanical stress (Alam et al., 2011; Jacques et al., 2009). In this study, CK14 was expressed in the entire epithelium of TEOM, consistent with previous studies either developed using immortalised or primary-based cells (Jennings et al., 2016; Yadev et al., 2011). CK14 expression in TEOM was

only partially in accordance to staining seen in the native oral mucosa (Blumenberg and Tomic-canic, 1997), where it is predominantly expressed in the basal cells and expression is gradually reduced as the cells move upward and differentiate in the suprabasal layer (Rao et al., 2014; Alam et al., 2011; Jacques et al., 2009; Moll et al., 2008) of the non-keratinised and keratinised epithelium (Rao et a., 2014; Jacques et al., 2009; Presland and Dale, 2000). This may be due to the difference in the level of maturity of the epithelium between native oral mucosa and TEOM that only been developed over a few weeks. CK13 and CK4 are important components of the stratified squamous mucosal epithelium. Both CK13 and CK4 were expressed in suprabasal layers only of TEOM. Expression was directly in line with native mucosa where these cytokeratins are predominantly expressed in the suprabasal layers of non-keratinising stratified squamous epithelium such as the buccal mucosa (Sanchez-Quevedo et al., 2007; Vaidya et al., 2000; Pang et al., 1993). Previously studies have reported the expression of CK13 in immortalised or primary-based TEOM (Buskermolen et al., 2016; Jennings et al., 2016). However, this study is the first to report the expression of CK4 in TEOM.

Ki-67, a cell proliferation marker, was confined predominantly in the basal layer in both TEOM and native tissue, which is in agreement with previously studies (Yoshizawa et al., 2004; Izumi et al., 2000). The results indicate that the TEOM has the capability of self-renewal (Kinikogklu et al., 2009). These findings are consistent with previous studies of TEOM generated using immortalised or primary cells (Buskermolen et al., 2016; Jennings et al., 2016; Yadev et al., 2011; Dongari-Bagtzoglou and Kashleva, 2006; Izumi et al., 2000).

E-cadherin and Claudin-4 are molecules that form the tight junctions (De Vicente et al., 2015), confined in the cell membrane of the epithelial cells (Costea et al., 2005), and are essential for preserving the integrity of the epithelium (De Vicente et al., 2015). E-cadherin and Claudin-4 were positive in all epithelial layers of the native oral mucosa and in the TEOM of the non-keratinised epithelium. Likewise, staining was observed in basal, spinous and granular layer of the TEOM of keratinised epithelium, but no staining was observed in the keratinised layer of 10 and 14 days TEOM (Ye et

al., 2000), suggesting loss of contacts between cells as they moved upward to the more differentiated cells in the superficial layer. The expression of E-cadherin in immortalised and primary-derived TEOM had been reported in previous studies (Buskermolen et al., 2016; Jennings et al., 2016; Dongari-Bagtzoglou and Kashleva, 2006). While there was no report thus far on the expression of Claudin-4 in immortalised and primary-derived TEOM. The IHC results indicate that TEOM developed using immortalised (FNB6) cells exhibit a normal expression pattern of important proliferation, structural and integrity molecules that are comparable to the native oral mucosa.

TEM analysis also validated the presence of ultrastructural organisation located in the cell membrane of the epithelial cells particularly the intercellular junction-related structures such as desmosomes and hemidesmosomes that bind cells to the basement membrane, all of which are important in cell-cell adhesion, regulation of epithelial permeability and barrier function (Squier and Brogden, 2011: Kinikoglu et al., 2009; Niessen, 2007). Abundant desmosomes were identified, indicating strong adhesion between cells in the epithelium of TEOM (Minin and Moldaver, 2008). The presence of hemidesmosomes and associated dense plaques reveals that basal cells were strongly attached to the underlying connective tissue (Borradori and Sonnenberg, 1999), suggesting that the TEOM can resist functional stresses (Izumi et al., 2004). The presence of these structures confirms the well-developed integrity of the epithelium in the TEOM. Collagen fibrils were also detected deeper in the connective tissue equivalents of TEOM. The collagen fibrils were orientated straight, varying in size and loosely organised, and as a result, produced less densely packed connective tissue than native tissue. Nevertheless, the integrity of the connective tissue in TEOM remained intact; a finding also had been observed by Kinokoglu et al., 2009.

It is crucial that the TEOM remain viable and keep their function throughout the course of development (Izumi et al., 2004) before being introduced in down-stream applications. Therefore, the viability of TEOM was assessed over time for up to 30 days. It was noted that the viability of the TEOM remained stable up to 3 weeks in culture before the viability started to decline; data that is consistent with a previous

report (Antoni et al., 2015). A recent study showed that the viability of oral mucosal-bone equivalents, representing the alveolar bone with an overlying mucosa was preserved for a longer time (3 months) (Almela et al., 2016). This might be due to a variety of cell type in the cultures and the method used in culturing the substitutes, which differs from the model system in this study.

The epithelium serves as a dynamic barrier that selectively restricts the movement of molecules across the epithelial layers (Rodgers and Fanning, 2011). The epithelial barrier function of the TEOM was assessed employing two methods: (i) electrical resistance using a TEER device and (ii) dye tracing method by fluorophotospectrometry. Firstly, the TEOM was assessed using a non-invasive TEER device. Here, the TEER profile reached its highest value at day 20 (155.8 $\Omega.cm^2$) before declining in subsequent days. Previously, TEER measurement of the immortalized cells derived from different origin showed TEER value of 28.2 ± 1.3 $\Omega.cm^2$ and 200 $\Omega.cm^2$ for human brain endothelial cell (hCMEC/D3) and human immortalized colon cell (HCEC), respectively. Kimura et al., found that the highest TEER values of human oral mucosal models on insert membranes were 134.8 ± 7.0 $\Omega.cm^2$ at day 7 (Kimura et al., 2002). Jacobsen et al., reported a maximal TEER value of 68.2 ± 2.3 $\Omega.cm^2$ using TR146-based models at day 29 (Jacobsen et al., 1995). However, Nielsen & Rassing (1999) showed a larger variance of TEER value of 272 ± 132 $\Omega.cm^2$ using the same model and incubation time. Several studies demonstrated TEER values obtained from blood-brain-barrier (BBB) models (Lippmann et al., 2014) pulmonary model (Mathias et al., 2002) and GI tract model (Hilgendorf et al., 2000) exhibited higher TEER values as compared to data in this study. It is suggesting that the variability of TEER values of the models from different origin probably partly because of the varied composition of the tight junctions (desmosomes/hemidesmosomes) exist in each type of tissue. There are no reference values of TEER for native oral mucosa published elsewhere, probably because of the difficulty in getting the biopsies in sufficient sizes for TEER measurement.

Epithelial barrier functions of TEOM were also evaluated using dextrans with different molecular weight (3, 10 and 70 kDa), to determine the size of molecules that can

permeate across the TEOM. Data presented in this study show that the permeability of TEOM was dextran size and time-dependent manner. Dextrans, as a model hydrophilic compounds, demonstrated that the smaller molecules especially 3 kDa were the most permeable, indicating that any hydrophilic drugs with a molecular weight of 3 kDa may be able to pass through the epithelial barrier of the TEOM. Previous studies reported that the permeation of dextran against porcine buccal mucosa was restricted to lower than 20 kDa through the paracellular route (Sandri et al., 2006; Hoogstraate et al., 1994), which is consistent with the findings reported here and suggest that TEOM display similar permeation to native tissue. It was also revealed that the permeability of TEOM against dextrans increased when the barrier function was impaired, regardless the size of molecules. As a result, the electrical resistance was also reduced. These phenomena occurred as a direct result of the loss of key structures that preserves the barrier of the epithelium such as basement membrane and tight junction-related structures (desmosomes and hemidesmosomes) upon treatment with a detergent (SDS) widely known for its cell destructive properties.

3.5 Summary

In summary, the data presented in this chapter show that TEOM based on immortalised buccal oral keratinocyte and primary normal oral fibroblasts are histologically and structurally equivalent to the native oral buccal mucosa. In addition, despite the use of immortalised keratinocytes, these TEOM display preserved expression of essential proteins involved in proliferation, differentiation and cell-cell, cell-basement membrane adhesion processes. These TEOM are a clear advancement on those developed using primary cells where the availability of these primary cells is limited.

Moreover, these TEOM displayed longevity with good barrier and permeability properties, crucial aspects when TEOM are used in down-stream applications. Based on these results, the TEOM demonstrated robust characteristics that are highly desirable for testing candidate drugs and drug delivery systems intended for administration to the oral mucosa. The data strongly indicates that this TEOM has

potential to be utilised in a variety of research and pre-clinical settings and as an attractive alternative *in vitro* model system to rival animal models.

CHAPTER 4

CYTOTOXIC POTENCY OF CORTICOSTEROIDS AGAINST ORAL KERATINOCYTES AND FIBROBLASTS GROWN AS MONOLAYERS OR TEOM

4.1 Introduction

Corticosteroids are generally used for the treatment of inflammatory and autoimmune disorders in dermatology, such as psoriasis and atopic dermatitis (Kwatra and Mukhopadkyay, 2018; Alexandre et al., 2015), and mucosal disorders such as OLP (Córdova et al., 2014) and aphthous stomatitis (Scully and Porter, 2008). Corticosteroids have been categorised based on their potency using the vasoconstriction or skin-blanching assay (McKenzieE and Stoughton, 1962), which have been used as the gold standard in determining the anti-inflammatory efficacy of these drugs, and where it has been suggested that vasoconstriction is correlated with anti-inflammatory effects (Kwatra and Mukhopadkyay, 2018). However, often simpler *in vitro* assays are performed in pre-clinical screening. Cytotoxicity assays such as the MTT assay, measure the effect of a compound on cell mitochondrial metabolism as a surrogate marker for cell viability (Graham-Evans et al., 2003) and are widely used in *in vitro* toxicology studies as a tool to provide predictive evidence of compound safety (Miret et al., 2006). The MTT assay (or other such derivatives) has been used in countless studies as a measure of cell toxicity, particularly in monolayer studies for numerous cell types, including oral keratinocytes (Ji et., 2016; Alexandre et al., 2015; Chen et al., 2012). Moreover, the MTT assay is currently used to define compound irritation and corrosion on the tissue engineered skin (OECD guideline 3 and European Centre for the Validation of Alternative Methods, ECVAM) as a model system in the cosmetic industry to replace animal models.

The efficacy of a corticosteroid is related to its level of potency and capability of the drug to reach its target site (Wiedersbeg et al., 2008; Federman et al., 1999). The potency of corticosteroids is influenced by several factors including chemical structure and concentration (Wiedersbeg et al., 2008; Hengge et al., 2006; Kansky et al., 2000;

Pershing et al., 1994; Stoughton, 1987). Formulation of corticosteroids using different vehicles may also influence their clinical efficacy (Uva et al., 2012; Schoepe et al., 2006). These also play a significant role in their absorption to reach the site of action, influencing their bioavailability and potency (Mehta et al., 2016; Wiedersbeg et al., 2008; Poulsen and Rorsman, 1980; Ayres and Hooper, 1978). Corticosteroids have been formulated in a variety of conventional vehicles such as ointments, creams, gels, lotions and foams (Mehta et al., 2016).

Monolayer cell culture, which is the conventional cytotoxicity model system, has widely been utilised to determine the safety profile of compounds. Nevertheless, the data obtained from monolayer cultures is still debatable due to the dissimilarities in the structure and physiology found in normal human tissue compared to cells grown as sheets on tissue culture plastic. As a result, most of the tested compounds give unsatisfactory, misleading and non-predictive data for *in vivo* responses (Sun et al., 2006). Due to the limitations in monolayer cultures, 3D model systems have been introduced as the promising model system for cytotoxicity testing as these systems are more structurally and physiologically relevant (Fang and Eglen, 2017; Edmondson et al., 2014). Monolayer and 3D culture systems often display different drug sensitivities, where 3D model systems are usually more resistant to therapeutic agents compared to monolayer cultures (Edmondson et al., 2014). The difference in resistance to therapeutic agents in 3D models is likely mediated by the complex, multi-cellular 3D structure, as well as differences in the expression of proteins involved in growth and survival (e.g. EGFR family of receptors), drug transporters (e.g. P-glycoprotein) and drug metabolising enzymes (e.g. CYP3A4) (Breslin and O'Driscoll, 2016; Edmondson et al., 2014) that appear to be increased in 3D compared to 2D cell culture.

The aim of the work conducted in this chapter was to determine the cytotoxic effects of seven topical corticosteroids representing different levels of potency on both monolayer culture of immortalised oral keratinocyte (FNB6), primary NOF and TEOM. The specific objectives of this study were as follows:

- To determine the cytotoxic effect of seven corticosteroids with increasing concentrations against FNB6 and NOF cells after 72 hours of incubation using an MTT assay and rank the potency of these corticosteroids based on the IC_{50} values.
- To choose three corticosteroids for further investigation representing high, medium and low potency and further analyse the cytotoxic effect of these compounds at increasing concentrations against FNB6 and primary NOF cells after 24 and 48 hours of incubation period using MTT assay.
- To evaluate the cytotoxic effect of the three selected corticosteroids at increasing concentrations against TEOM using an MTT assay based on the OECD Test Guideline 431.
- To optimise the permeation of corticosteroids against TEOM after one-hour exposure to a single concentration.

4.2 Experimental procedures

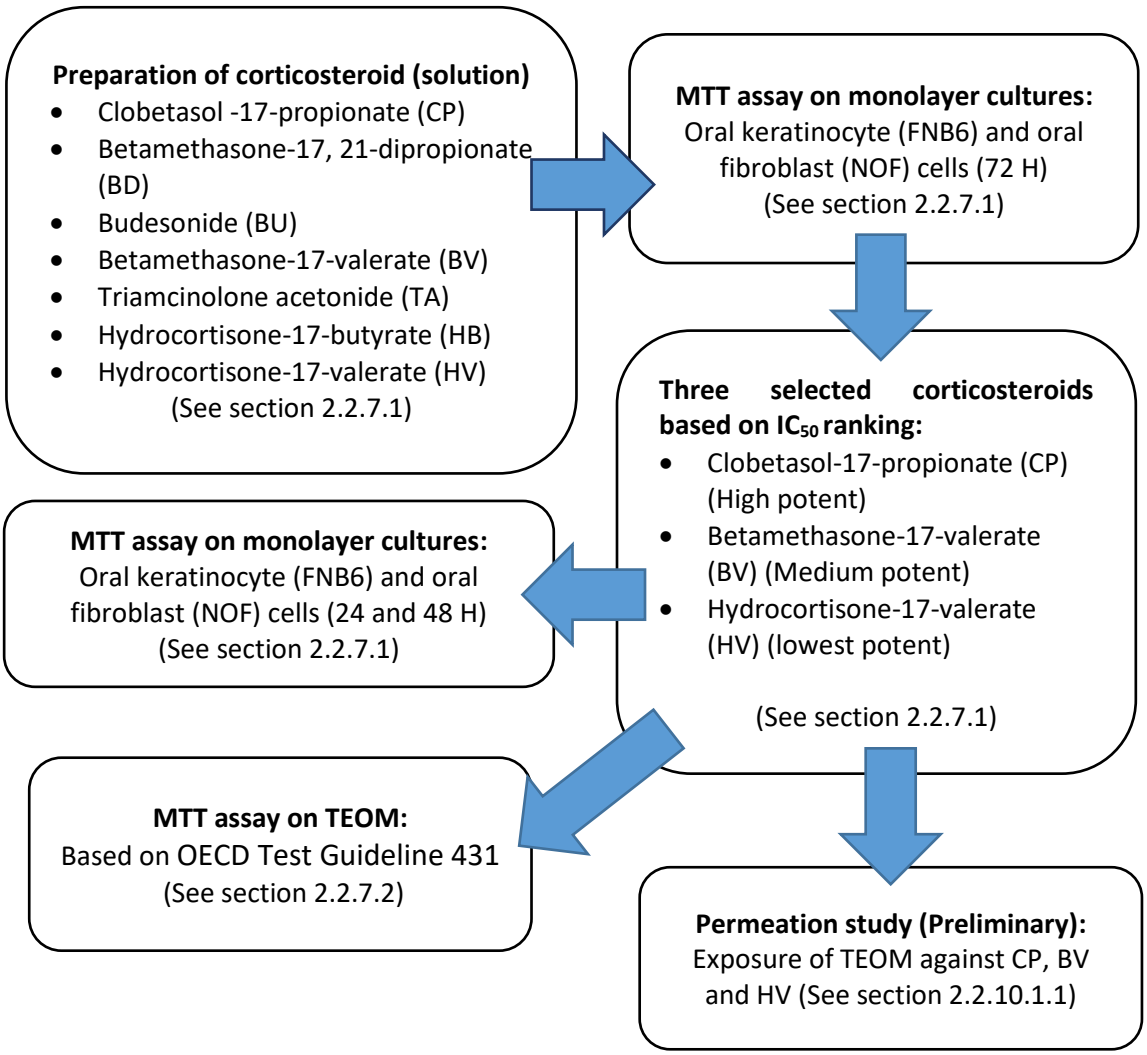

4.3 Results

4.3.1 Corticosteroids cytotoxicity against oral keratinocytes and fibroblasts is dose-dependent

The cytotoxic potency of seven topical corticosteroids often used to treat OLP and representing different levels of potency were tested against immortalised FNB6 and primary human NOF cells using an MTT assay. IC_{50} values, defined as the corticosteroid concentration that was cytotoxic to 50% of the cells were obtained from dose-response curves. FNB6 cells exposed to all seven corticosteroids for 72 hours showed concentration-dependent cytotoxicity profiles, presenting typically as sigmoid-shaped curves (Figure 4.1), allowing IC_{50} values to be calculated. Some of the curves, in particular for BD, displayed viability levels above 100% for cells treated with the drug at low concentrations, although the increases in cell viability at these concentrations were not statistically significant compared to untreated controls (Figure 4.1). According to Lopez-Garcia et al., (2014) cell viability above 80%, within 80-60%, 60 – 40% or below 40% are considered as either non-cytotoxic, weak, moderate or having strong cytotoxicity, respectively. From the findings, the range of concentrations for each corticosteroid that showed strong cytotoxicity against FNB6 cells are as follows: 50-500 µM (CP), 100-500 µM (BD and BU), 250-500 µM (BV and HB), and 500 µM (TA and HV) (Figure 4.1). The IC_{50} values for each corticosteroid against FNB6 cells are provided in Table 4.1. The most potent corticosteroid with the greatest toxicity was CP with an IC_{50} of 32.1 ± 0.9 µM whereas the least potent in terms of toxicity to FNB6 cells was HB with an IC_{50} of 340.9 ± 20.3 µM. The ranking of corticosteroid cytotoxic potency against FNB6 keratinocytes was: CP > BU > BD > BV > TA > HV > HB.

Similar concentration-response profiles were observed when the corticosteroids were tested against NOF cells for cytotoxicity and once again cytotoxicity profiles presented typically as sigmoid-shaped curves (Figure 4.2). The IC_{50} values for each corticosteroid against NOF cells are provided in Table 4.1. Similar to FNB6 cells, the most potent in terms of cytotoxicity was CP with an IC_{50} of 40.3 ± 2.1 µM, whereas, in contrast to FNB6 cells, the least cytotoxic corticosteroid for NOF cells was HV with an IC_{50} of 314.3

± 52.1 µM. The ranking of corticosteroid cytotoxic potency against NOF was: CP > BD > BV > BU > TA > HB > HV.

The potency of CP, BD, BU, TA, BV and HV were greater (i.e. caused more cytotoxicity) for FNB6 cells than for NOF cells, suggesting that keratinocytes are more affected by these corticosteroids than fibroblasts in a like-for-like comparison. HB was more toxic toward NOF cells than FNB6 cells, although cytotoxicity levels were low for both cell types (Table 4.1).

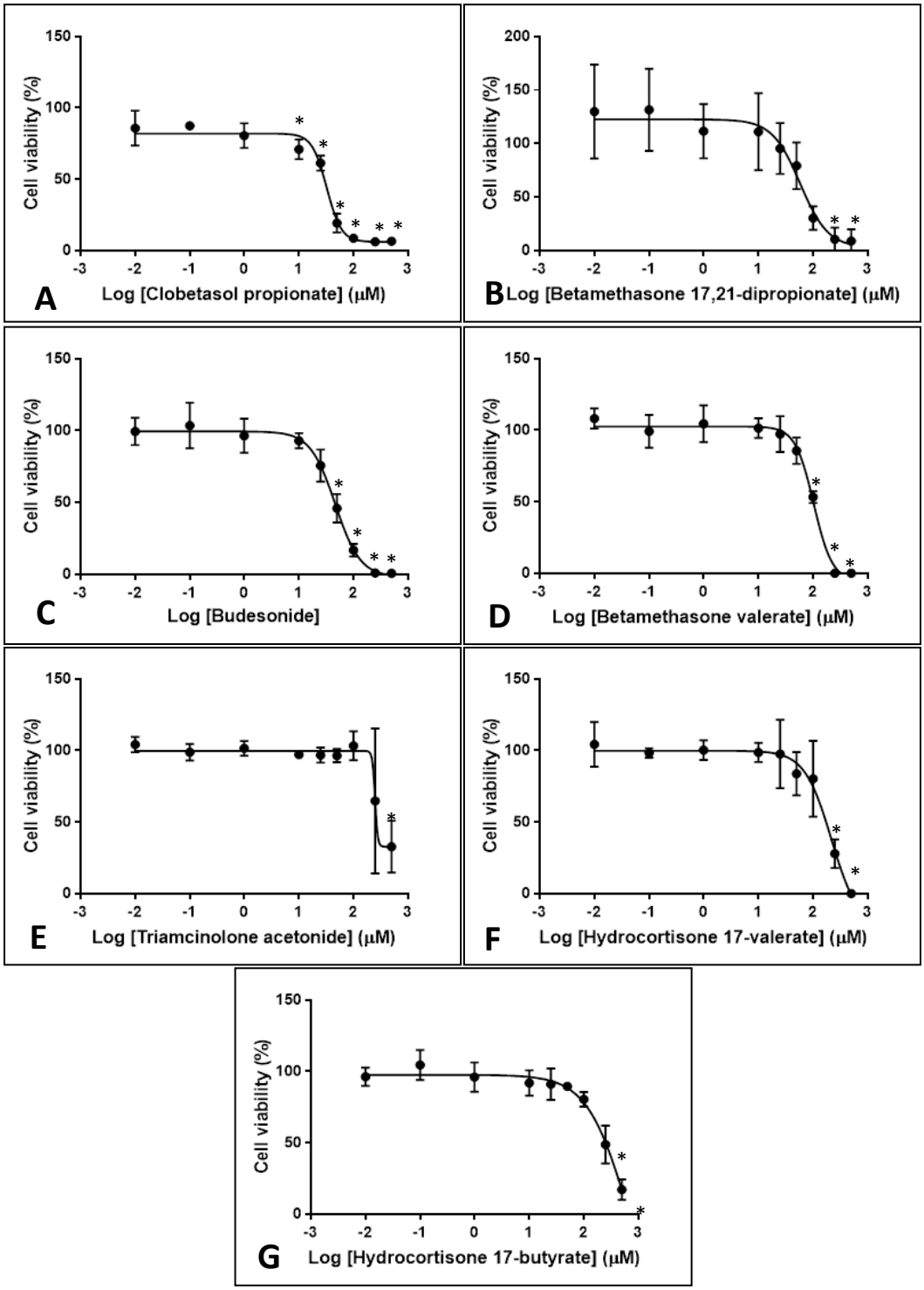

Figure 4.1: The IC_{50} values for human normal keratinocytes (FNB6) cells treated with increasing concentrations of corticosteroids: (A) clobetasol-17-propionate (CP), (B) betamethasone-17, 21-dipropionate (BD), (C) budesonide (BU), (D) betamethasone-17-valerate (BV), (E) triamcinolone acetonide (TA), (F) hydrocortisone-17-valerate (HV) and (G) hydrocortisone-17-butyrate (HB) from 0.01 to 500 μM for 72 hours. Cell viability was measured by MTT assay. Each value represents the mean ± SD of three independent experiments with each experiment performed in triplicate. *$p < 0.05$ indicative of significant differences as compared to control analysed using One-way ANOVA with Tukey post-hoc multiple comparison tests.

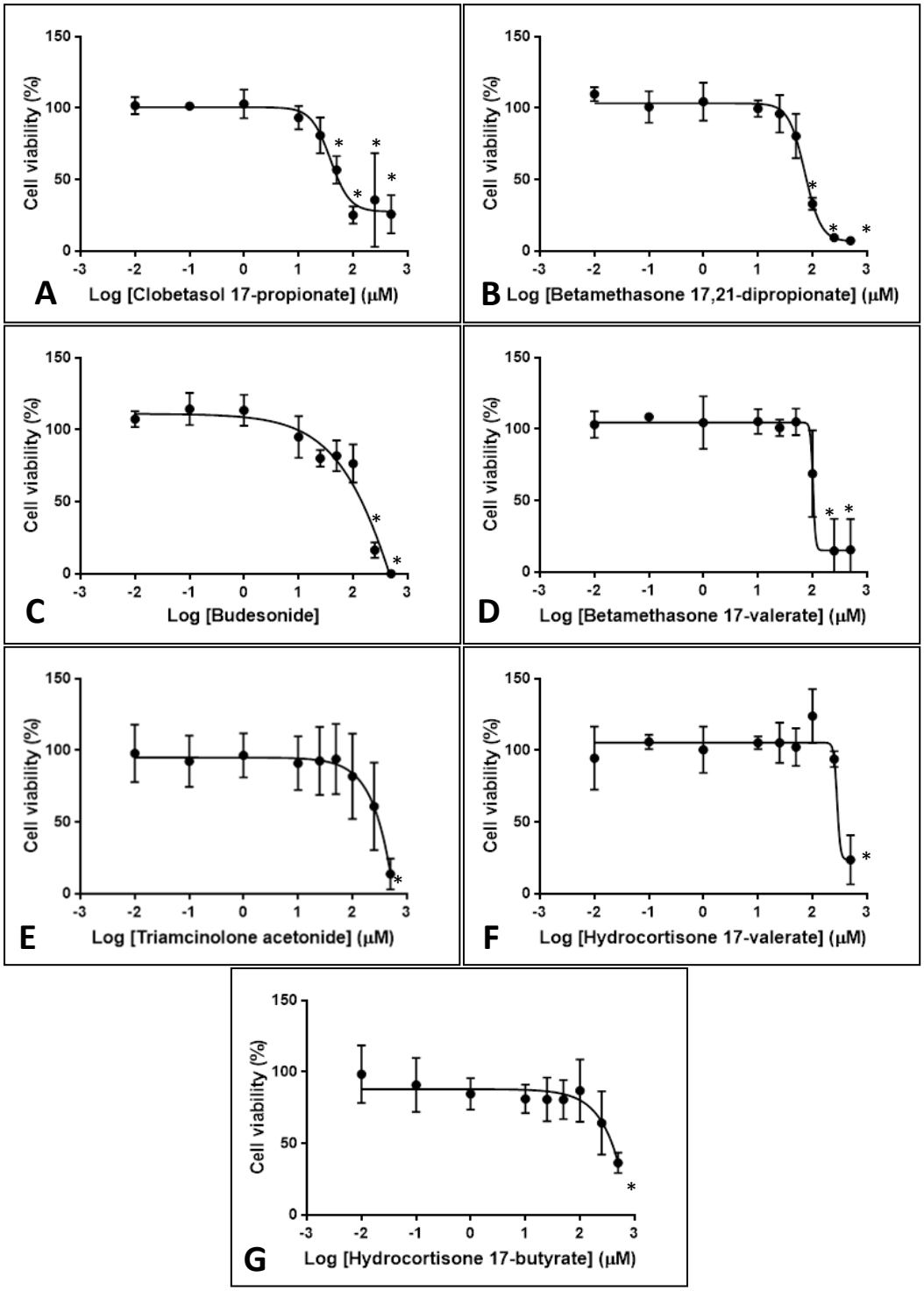

Figure 4.2: The IC_{50} values for primary human normal oral fibroblast (NOF) cells treated with increasing concentrations of corticosteroids: (A) clobetasol-17-propionate (CP), (B) betamethasone-17,21-dipropionate (BD), (C) budesonide (BU), (D) betamethasone-17-valerate (BV), (E) triamcinolone acetonide (TA), (F) hydrocortisone-17-valerate (HV) and (G) hydrocortisone-17-butyrate (HB) from 0.01 to 500 μM for 72 hours. Cell viability was measured by MTT assay. Each value represents the mean ± SD of three independent experiments with each experiment performed in triplicate. *$p < 0.05$ indicative of significant differences as compared to controls analysed using One-way ANOVA with Tukey post-hoc multiple comparison tests.

Table 4.1: The IC_{50} values for FNB6 and NOF cells treated with different corticosteroids for 72 hours reveals different levels of potency. Each value represents the mean ± SD of three replicates. A mean difference was considered significant when *p < 0.05, **p < 0.001 and ***p < 0.0001 as compared to clobetasol 17-propionate (known as the most potent corticosteroids) using One-way ANOVA with Tukey post-hoc multiple comparison tests.

	IC_{50} value (µM) (Mean ± SD)	
Cell type / Drugs	**Oral keratinocyte (FNB6) cells**	**Oral fibroblast (NOF) cells**
Clobetasol-17-propionate	32.2 ± 0.9	40.3 ± 2.1
Budesonide	46.4 ± 5.2	150.9 ± 17.7*
Betamethasone-17,21-dipropionate	59.2 ± 5.9	74.8 ± 1.71
Betamethasone-17-valerate	92.8 ± 17.3	103.7 ± 7.2
Triamcinolone acetonide	194.8 ± 41.6***	259.5 ± 24.3***
Hydrocortisone-17-valerate	261.3 ± 28.9***	314.3 ± 52.1***
Hydrocortisone-17- butyrate	340.9 ± 20.3***	246.4 ± 29.4***

4.3.2 The cytotoxic potency of corticosteroids is more pronounced in a concentration rather than time-dependent manner

Based on the initial screening experiments of seven corticosteroids for 72 hours, three corticosteroids identified as having strong (CP), moderate (BV) or mild (HV) potency were selected to take forward for further experiments. FNB6 keratinocytes or NOF were cultured with each of these three corticosteroids for 24, 48 and 72 hours at increasing concentrations to determine if the cytotoxic response was time-dependent.

Similar to data obtained for 72 hours, the exposure of CP, BV and HV against FNB6 cells caused a concentration-dependent reduction in cell viability at all time-points tested (Figure 4.3A-C). The results displayed in figure 4.3 show that for CP, BV and HV the IC_{50} tended to be greater at 24 hours compared to values at 48 hours, suggesting that these drugs are less toxic at shorter incubations, although this was not statistically significant. For CP and BV, the IC_{50} values at 48 hours were very similar to 72 h (≈ 31 µM (CP), ≈ 93 µM (BV)), suggesting equal FNB6 cells cytotoxicity between these two time-points, whereas cytotoxicity appears lower after 72 hours (≈ 261 µM) for HV than at 48 hours, although again these values were not statistically significant (Figure 4.3).

A similar trend was also observed for the time-dependent cytotoxicity effects of these three compounds (CP, BV, HV) against NOF cells (Figure 4.4A-C). Once again there was a concentration-dependent cytotoxic effect on NOF cells at all time-points tested. NOF cells also displayed IC_{50} values less than those observed for FNB6 cells for CP and BV but not for HV, at all time-points examined, once again suggesting that FNB6 cells are more sensitive to the effects of the more potent corticosteroids than NOF cells. For CP, the IC_{50} value at 24 (113.4 µM) hours was much higher than for both 48 and 72 hours (52.7 µM (48 h) and 40.3 µM (72 h)) suggesting that this corticosteroid has a time-dependent effect on NOF cells cytotoxicity, whereas this trend was not observed for both BV or HV (Figure 4.4A-C).

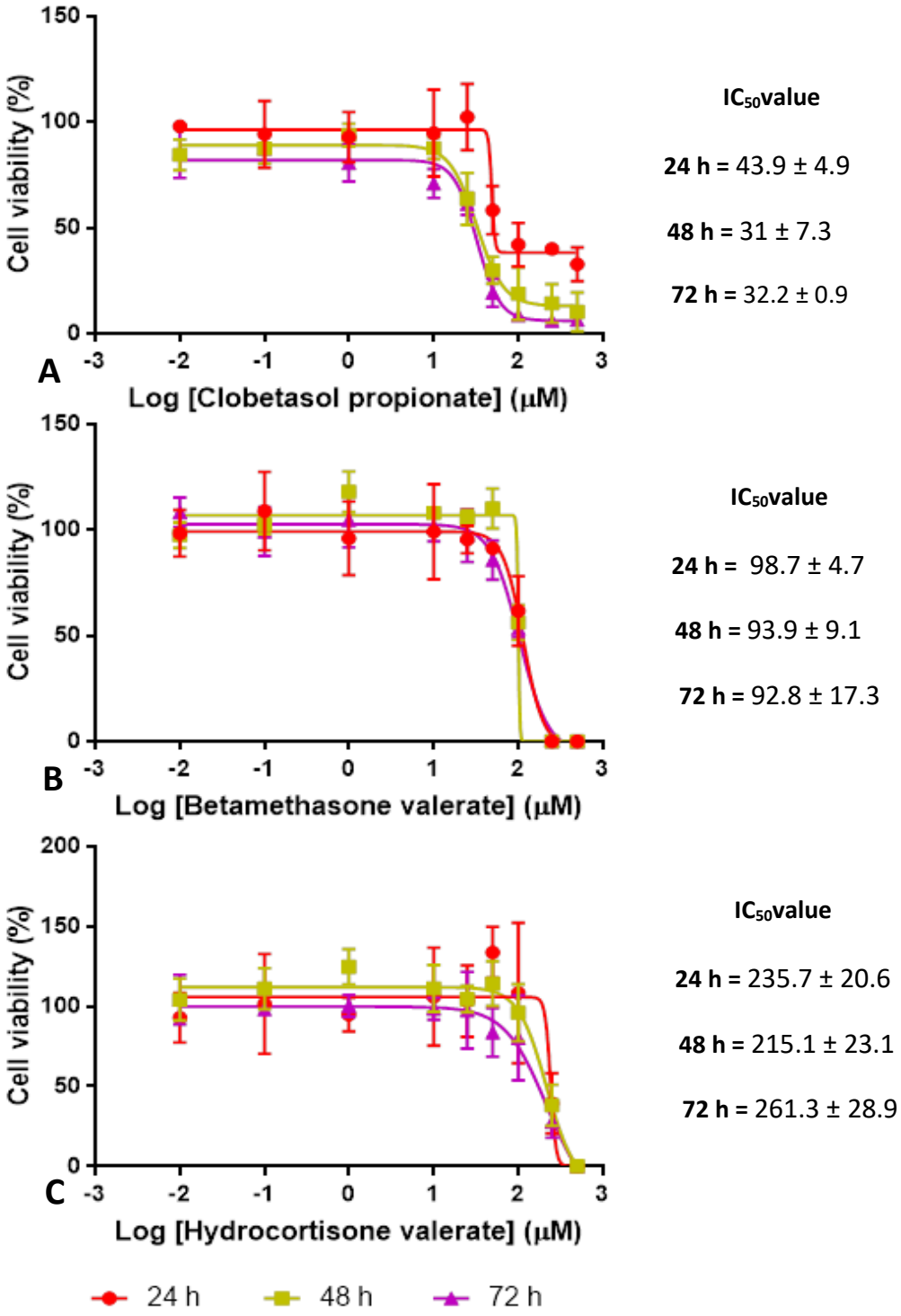

Figure 4.3: The IC_{50} values for human normal keratinocytes (FNB6) cells treated with increasing concentrations of (A) clobetasol-17-propionate, (B) betamethasone-17-valerate and (C) hydrocortisone-17-valerate (0.01 to 500 µM) against FNB6 cells for 24, 48 and 72 hours. Cell viability was detected using an MTT assay. Data were expressed as the mean ± SD for 3 independent experiments performed in triplicate. There was no significant difference between different incubation time for each compound analysed using One-way ANOVA with Tukey post-hoc multiple comparison tests.

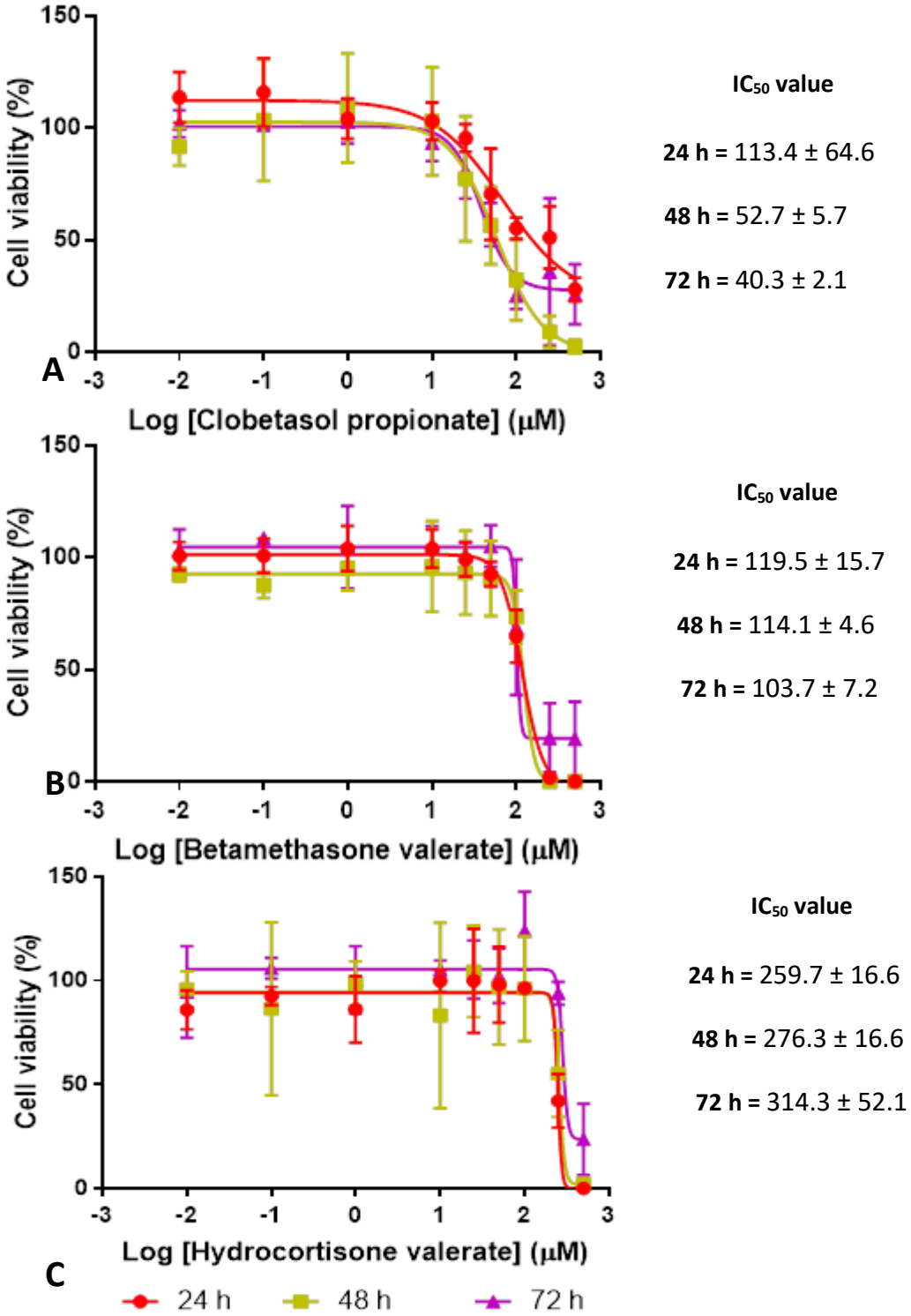

Figure 4.4: The IC_{50} values for primary human normal oral fibroblast (NOF) cells treated with increasing concentration of (A) clobetasol-17-propionate, (B) betamethasone -17-valerate and (C) hydrocortisone -17-valerate (0.01 to 500 µM) against NOF cells for 24, 48 and 72 hours. Cell viability was detected using an MTT assay. Data were expressed as the mean ± SD for 3 independent experiments performed in triplicate. There was no significant difference between different incubation time for each compound analysed using One-way ANOVA with Tukey post-hoc multiple comparison tests.

4.3.3 Effect of corticosteroids on TEOM viability

CP, BV and HV, each representing strong, medium and low potency corticosteroids respectively were used to test the cytotoxic effects of these drugs on TEOM (that are composed of both FNB6 and NOF cells). In these experiments, corticosteroids were added topically to the surface of the TEOM, incubated for 1 hour, removed, incubated further for 42 hours and then the viability of the tissue measured using an MTT assay based on the OECD Test Guideline 431 protocol that is used as an industrial standard to identify potentially irritant compounds using tissue-engineered skin. Figure 4.5A-C shows the concentration-dependent effect of these three corticosteroids on TEOM. In these experiments, 5% SDS was used as a positive control as this compound is known to destroy the tissue, causing complete loss of cell viability, whereas untreated TEOM served as negative controls displaying 100% viability. Exposure of TEOM to CP caused a concentration-dependent loss of tissue viability with gradual reduction. The viability of TEOM at 5, 50, 100, 200 and 400 µM CP were 78.7 ± 0.08% ($p < 0.05$), 75.8 ± 2.38% ($p < 0.001$), 69.8 ± 4.05% ($p < 0.0001$), 65.3 ± 6.25% ($p < 0.0001$) and 52.5 ± 8.44% ($p < 0.0001$), respectively as compared to control.

Likewise, exposure of TEOM to BV had a similar pattern of viability reduction where the viability of TEOM decreased gradually as the concentration of BV was increased. The reduction of TEOM viability at 5 µM (87.4 ± 7.01%) and 50 µM (87 ± 6.42%) was not significant as compared to controls. The viability of TEOM at 100, 200 and 400 µM was significantly decreased further to 82.7 ± 8.11% ($p < 0.05$), 71.2 ± 6.55% ($p < 0.001$) and 68.4 ± 3.22% ($p < 0.0001$), respectively as compared to controls.

In contrast, TEOM cultured with 5-50 µM HV had little effect on viability and ≈99% viability values were close to untreated controls. However, as the concentration of HV was increased the viability of TEOM decreased. Incubating TEOM with 100, 200 and 400 µM decreased TEOM viability by 71.9 ± 7.21%, 65.9 ± 7.08% and 71.8 ± 7.62% respectively, all significantly decreased from untreated controls ($p < 0.05$). Exposure of TEOM to 5% SDS (positive control) lead to a dramatic and significant reduction ($p < 0.0001$) in TEOM viability in all cases tested.

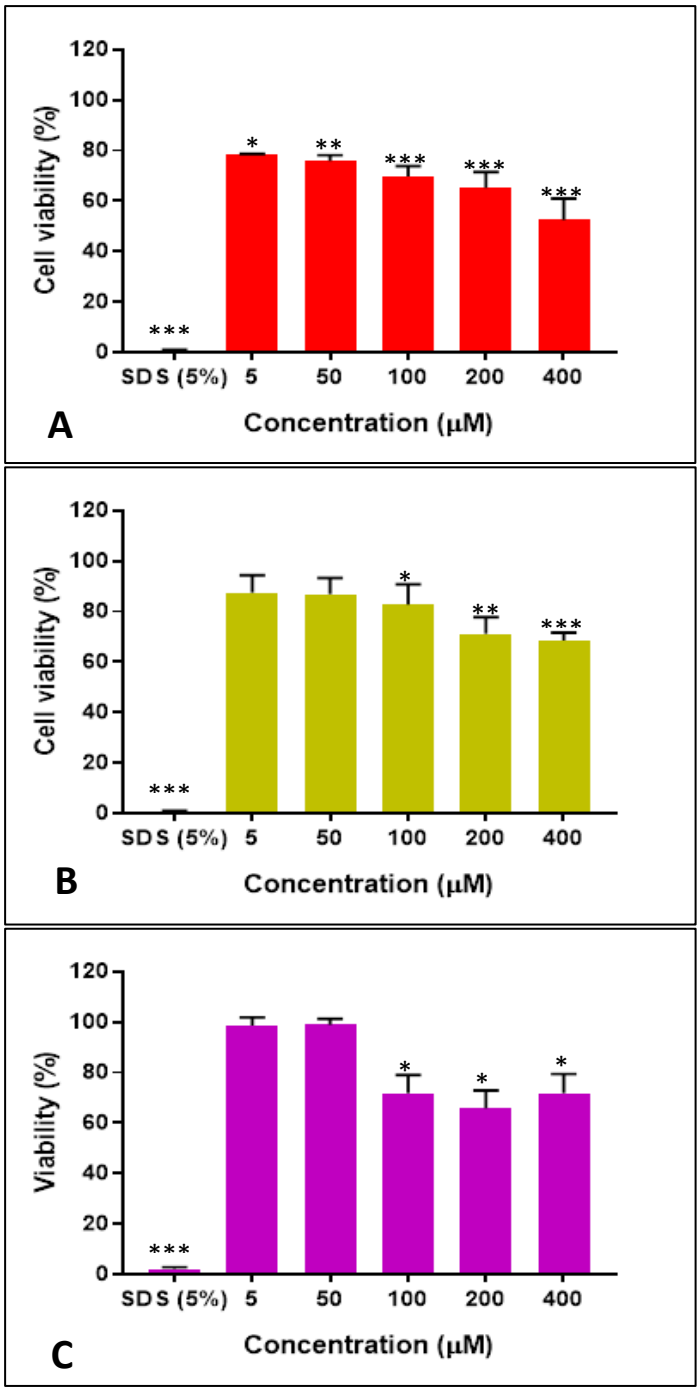

Figure 4.5: The cytotoxic potency of different corticosteroids on TEOM. TEOM were incubated with increasing concentrations (5 to 400 µM) with (A) clobetasol-17-propionate, (B) betamethasone-17-valerate and (C) hydrocortisone-17-valerate. TEOM viability was measured using an MTT assay. Data were expressed as the mean ± SD for 3 independent experiments performed in triplicate. A mean difference was considered significant when *$p < 0.05$, **$p < 0.001$ and ***$p < 0.0001$ as compared to controls using One-way ANOVA with Tukey post-hoc multiple comparison tests.

It must be noted that none of the corticosteroids tested reduced the viability of the TEOM to less than 50%, even at the highest concentrations tested. This is particularly important because the OECD guidelines for irritancy and corrosive testing on tissue-engineered skin state that compounds that reduce tissue viability by more than 50% can be considered as an irritant, whereas compounds that reduce tissue viability by less than 50% can be considered as non-irritant and therefore safe. Using these definitions, the data provided here show that at the concentrations tests all the corticosteroids would be deemed safe by OECD guidelines.

Figure 4.6 shows a comparison of cytotoxic potency between three corticosteroids (CP, BV and HV). At low corticosteroid concentrations (5 µM), there was a significant reduction in TEOM viability between CP and HV, with CP being most potent ($p < 0.05$), although viability levels were not different for CP and BV at this concentration. At 50 µM there was a significant difference ($p < 0.05$) in TEOM viability between at three corticosteroids with CP having the greatest effect on TEOM viability (75.8 ± 2.4%), followed by BV (87 ± 6.4%) then HV (98.9 ± 2.4%). This is agreement with data on monolayers showing that the potency of CP > BV > HV is also the same for TEOM. TEOM incubated with concentrations of 100-400 µM displayed similar potency levels for all corticosteroids tested.

Interestingly, the viability of TEOM was above 50% at all concentrations tested for all corticosteroids and therefore IC_{50} values (the value at which 50% tissue viability would be observed) could not be determined accurately. These data infer that the IC_{50} values for TEOM is greater than 400 µM for corticosteroids tested. This is a huge difference to the same corticosteroids when cells were treated as monolayers (Table 4.2) and suggests that monolayer cultures are more sensitive to the actions of drugs than TEOM, which are structurally and histologically more similar to native tissue.

Table 4.2: The summary of the IC_{50} values of FNB6 monolayer, NOF monolayer and TEOM for clobetasol-17-propionate, betamethasone-17-valerate and hydrocortisone-17- valerate.

Model system / Compound	FNB6 monolayer	NOF monolayer	TEOM
Clobetasol-17-propionate	43.9 ± 4.9 (24 h)	113.4 ± 64.6 (24 h)	> 400 µM
	31 ± 7.3 (48 h)	52.7 ± 5.7 (48 h)	
	32.2 ± 0.9 (72 h)	40.3 ± 2.1 (72 h)	
Betamethasone-17-valerate	98.7 ± 4.7 (24 h)	119.5 ± 15.7 (24 h)	> 400 µM
	93.9 ± 9.1 (48 h)	114.1 ± 4.6 (48 h)	
	92.9 ± 17.3 (72 h)	103.7 ± 7.2 (72 h)	
Hydrocortisone-17-valerate	235.7 ± 20.6 (24 h)	259.7 ± 16.6 (24 h)	> 400 µM
	215.1 ± 23.1 (48 h)	276.3 ± 16.6 (48 h)	
	261.3 ± 28.9 (72 h)	314.3 ± 52.1 (72 h)	

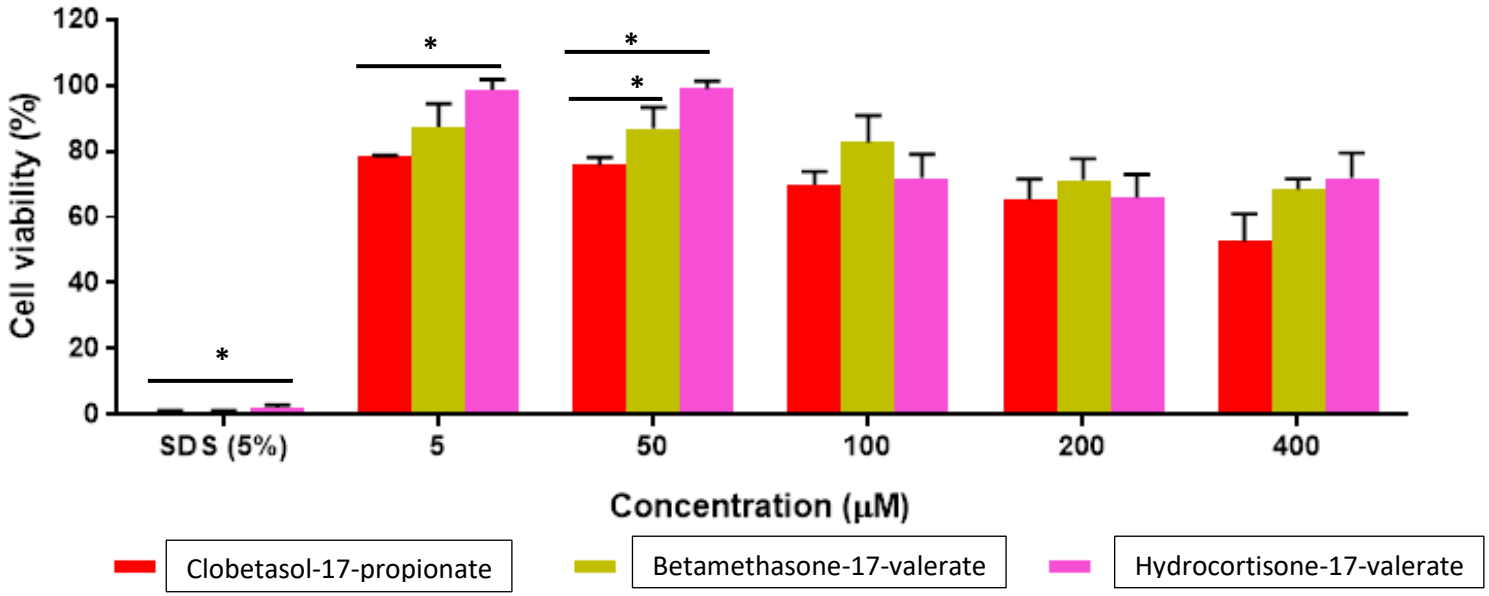

Figure 4.6: Comparison of the cytotoxic potency between clobetasol-17-propionate, betamethasone-17-valerate and hydrocortisone-17-valerate at increasing concentrations (5 to 400 µM) against TEOM. Data were expressed as the mean ± SD for 3 independent experiments performed in triplicate. A mean difference was considered significant when *$p < 0.05$, **$p < 0.001$ and ***$p < 0.0001$ using One-way ANOVA with Tukey HSD of post-hoc multiple comparison tests.

4.3.4 Different corticosteroids with varying levels of potency showed a different pattern of permeation into TEOM

A comparison of tissue permeation of the three different corticosteroids (CP, BV and HV) at 5 µM, each having different levels of potency was performed after one-hour exposure. The levels of corticosteroids in the TEOM tissue and in the medium bathing the basolateral compartment (and therefore had traversed the tissue) were measured by HPLC. Data presented in figure 4.7 show that CP was highest in the TEOM tissue at approximately 2.59 ± 0.25 nM/mg and this was significantly greater ($p < 0.0001$) than the levels for both BV (0.299 ± 0.05 nM/mg) and HV (0.297 ± 0.03 nM/mg; Figure 4.7A). In contrast, the amount of CP accumulating in the basolateral compartment of the tissue culture system was significantly lower (111 ± 11.63 nM) compared to HV (215.3 ± 36.6 nM) ($p < 0.001$) but comparable to BV (85 ± 18.59 nM; Figure 4.7B). These data indicate that after one-hour CP is mainly retained in the tissue with little drug entering the medium, whilst HV rapidly crosses the tissue and is found at higher concentrations in the medium. This difference in tissue penetration is likely to reflect the different physiochemical properties of the different corticosteroids, such as the addition of halogen molecules to the chemical structure.

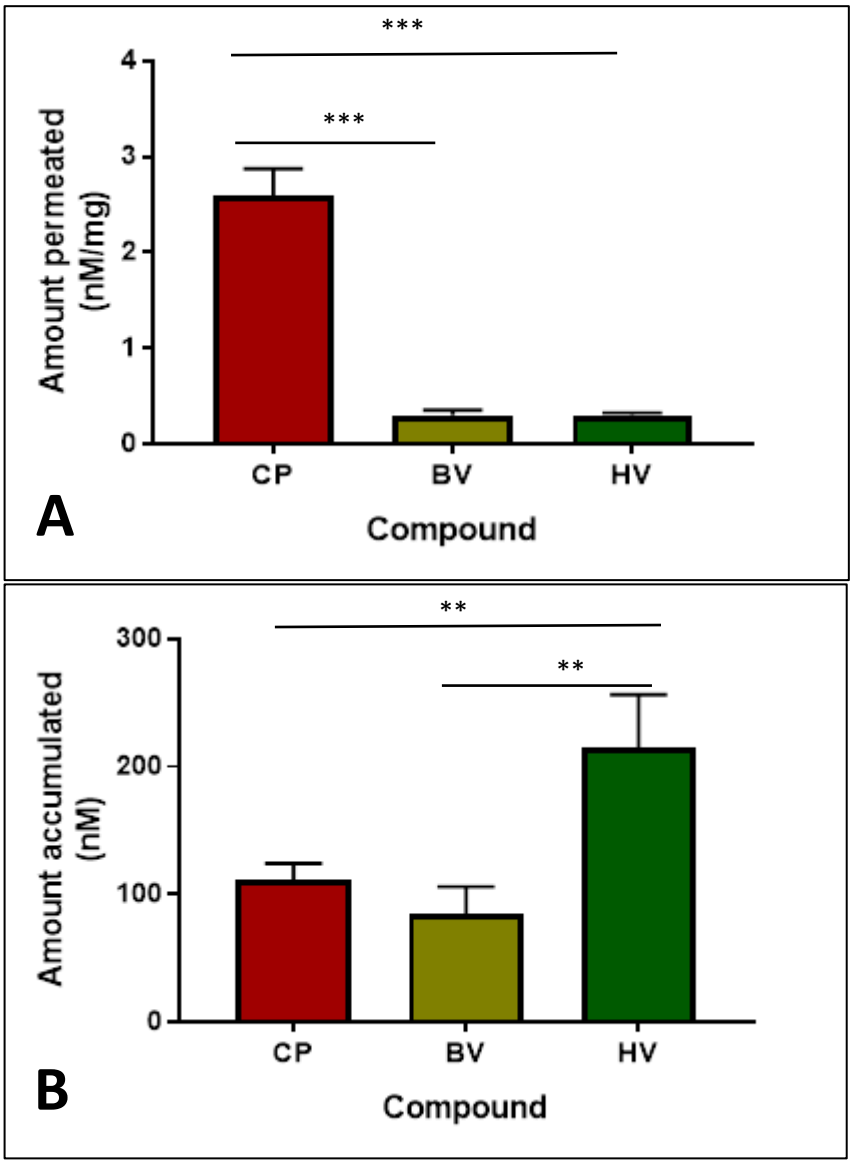

Figure 4.7: Different permeation pattern of CP, BV and HV in (A) the tissue and in (B) the basolateral compartment after 1 hour. Data are expressed as the mean ± SD for 3 independent experiments performed in triplicate. A mean difference was considered significant when *$p < 0.05$, **$p < 0.001$ and ***$p < 0.0001$ using One-way ANOVA with Tukey post-hoc multiple comparison tests.

4.4 Discussion

In this chapter, the cytotoxic potency of corticosteroids was assessed against oral keratinocytes and fibroblasts cultured as monolayers and as 3D TEOM. Oral keratinocytes and fibroblasts were utilised, as these cells are the major constituent cells that make up the oral mucosa and are therefore clinically relevant. FNB6 cells are immortalised keratinocytes (McGregor et al., 2002) and are suitable substitutes for primary oral keratinocytes because these cells can be easily grown and passaged indefinitely and, as shown in the previous chapter, generate a stratified squamous epithelium that is histologically similar to native oral epithelium when cultured in tissue models.

In monolayer culture, the effects of seven corticosteroids were examined against FNB6 and NOF using the MTT assay; a method that is commonly employed for the determination of cell cytotoxicity or viability following exposure to toxic substances (Sathisha et al., 2008; Ulukaya et al., 2008). All corticosteroids tested reduced viability of both cell types in a concentration-dependent manner. The level of potency was similar for both cell types, which was generally CP > BD > BV > BU > TA > HB > HV. This level of potency is in agreement with evaluation of these drugs in a clinical setting. For example, CP is known to be one of the most potent topically applied corticosteroids clinically available. Betamethasone is often classified as having moderate-to-potent potency, whilst hydrocortisone has mild-to-moderate potency (National Eczema Society, 2016). This shows that the data generated for monolayers, as far as cytotoxicity is concerned, is clinically representative. The data presented here do not measure the immunological action of these corticosteroids, which may be different in potency.

This study also revealed that some corticosteroids, when used at lower concentrations, caused an apparent increase in cell viability, while at higher concentrations they exhibited cytotoxicity and loss of cell viability. These findings are in agreement with previous work performed by Alexandre and co-workers (Alexandre et al., 2015). The apparent increased cell viability at lower concentrations is associated with increased cell metabolism as a cell stress response toward the toxic compound.

Addition of a foreign chemical to cells often stimulates these cells to increase membrane pumps in order to transport these chemicals out of the cells thereby promoting cell survival (Fulda et al., 2010). This process requires additional ATP that is supplied by increased cell metabolism. This increase in mitochondrial metabolic output also reduces MTT into a colour product; therefore, increases in MTT may be due to increased metabolism due to a toxic response rather than alterations in cell number. At higher compound concentrations the toxic effects of the chemical affect the cells quicker than the cells response and so a decrease in viability is observed. Although not performed, a trypan blue exclusion assay could have been undertaken to show that the effects of the corticosteroids were due to toxicity and not on metabolism or cell proliferation.

Previously, the potency of corticosteroids was classified based on the vasoconstrictor assay as the gold standard, which uses skin pallor as a measure of drug potency (McKenzie and Stoughton, 1962). In addition, the potency of a compound could also be determined either using a single-dose technique or dose-response curve (Van Rossum, 1962). Alexandre et al., 2015 determined the potency of corticosteroids against keratinocyte cells based on a single concentration (used the highest concentration) (Alexandre et al., 2015). On contrary, in this study, the potency of CS in monolayer cultures was determined using IC_{50} value as an indicator of toxicity obtained from dose-response curve, which is therefore more scientifically determined and so informative.

The potency of corticosteroids has also been characterised by their formulation. (Wiedersberg et al., 2008; Ference and Last, 2009) based on WHO classification. In this classification, corticosteroids have been categorised into seven potency classes ranging from super-potent (class I) to least potent (class VII) (Habif, 1990). The same drug can also be classified in different potency classes depending on the formulation of the drug (World Health Organisation, 2018). In contrast, the British National Formulary (BNF) recommended only four classes ranging from mild to potent and here the drugs are classified regardless of the formulation used (British National Formulary,

2016). Our findings showed that most of the corticosteroids that were ranked based on their toxic potencies *in vitro* are similar with aforementioned classification.

The monolayer result revealed that CP was the most cytotoxic and potent compound where it showed strong cytotoxicity (<40% of cell viability) at low concentrations and also exhibited the lowest IC_{50} value against both cell types as compared to other corticosteroids. In contrast, Alexandre and co-workers reported that BD was the most potent corticosteroid when incubated with human immortalized non-tumorigenic skin keratinocytes (HaCaT). This discrepancy may be due to the different method applied in assessing the cytotoxicity of corticosteroids. Here, Alexandre et al., determined potency using the percent viability of cells when using corticosteroids at a single highest concentration only (Alexandre et al., 2015). In contrast, this study used a dose-response to generate IC_{50} values as an indicator of cytotoxic and potency to rank the corticosteroids. Similar to our data Alexandre et al., showed that HB and HV were among the least potent corticosteroids as evidenced by high IC_{50} values as compared to other compounds (Alexandre et al., 2015).

CP, BV and HV that represent different classes of potency were selected for further evaluation against both cell types and TEOM. In monolayer cultures, exposure of these compounds at increasing times against both keratinocytes and NOF had no substantial effects indicating that the action of the corticosteroids appeared not to be time-dependent. These data suggest that higher concentrations of corticosteroids induce rapid cytotoxicity, whereas cells can tolerate lower levels and indicate that drug concentration rather than incubation time is more important. The cytotoxic potency of CP, BV and HV was also assessed against TEOM in a concentration-dependent manner. CP was the most potent compound as compared to BV and HV, which is in line with the monolayer culture results. Previously, it has been demonstrated that the IC_{50} values of compounds tested on 3D models are higher than for monolayer cultures (Moharamzadeh et al., 2015, Sun et al., 2006). Although IC_{50} values of corticosteroids against TEOM were higher than in monolayer cultures, a direct comparison of drugs efficacy between monolayer culture and TEOM cannot be drawn as both systems were exposed at different concentrations and incubation times. As far as known, this is the

first study to measure the cytotoxicity of corticosteroids on TEOM. Our findings determined CP as a non-irritant corticosteroid based on a TEOM viability of >50% and in accordance with the OECD guidelines.

A comparative permeation analysis was conducted between corticosteroids representing different levels of potency to investigate any differences in their penetration capability. Interestingly, a differential permeation pattern was found between CP, BV and HC, suggesting that the physicochemical properties of these molecules such as the molecular weight and lipophilicity characteristics influence tissue absorption (Sudhakar et al., 2006). Generally, drugs with molecular weight less than 500 Da are easily transported through tissue (Uva et al., 2012; Bos and Meinardi, 2000) and all the molecular weight of the tested compounds are below 500 Da. Esterification and addition of components such as valerate or propionate enhances the lipophilicity of the corticosteroid proportionally, increasing their tissue absorption (Kwatra and Mukhopadhyay, 2018; Gual et al., 2015; Kansky et al., 2000; Thorburn and Ferguson, 1994; Ponec et al., 1986). Indeed, CP exhibited higher tissue penetration than BV, which was also greater than HV. Moreover, chemical modification also enables molecules to be held for longer within the mucosal tissue, providing a reason as to why HV passed through the TEOM into the receptive medium quicker than both CP and BV.

4.5 Summary

Data presented in this chapter demonstrates that the ranking of cytotoxic potencies based on the IC_{50} exhibited very similar ranking to the potency levels based on the vasoconstrictor assay that is still used in clinical practice as the gold standard in potency assessment. In addition, potency levels found in the monolayer and TEOM experiments were in line with potency ranks described by WHO and BNF for the corticosteroids tested. Importantly, we found that cytotoxicity levels were much higher for keratinocyte and fibroblast monolayers than observed for TEOM and this is in line with clinical data. TEOM showed good sensitivity in dose-dependent toxicity models, displaying decreased viability with increasing corticosteroid concentration.

Preliminary study of corticosteroids permeation showed that CP displayed higher tissue penetration and retention through the TEOM. Taken together, these data provide good evidence that TEOM are the most suitable *in vitro* experimental model to perform drug toxicity and drug activity studies, and therefore will be taken forward for use as experimental models in the next chapters.

CHAPTER 5

ORAL PATCH CHARACTERISATION AND CYTOTOXICITY

5.1 Introduction

A drug formulation should have the capability in delivering an active compound to the affected site at a therapeutically relevant dose without discomfort and adverse effects (Zhang and Smith, 2010). Formulation strategies for oral mucosal delivery have gained considerable attention because this site offers advantages including sustained release, targeted drug delivery and prolonged contact time with enhanced drug absorption (Mojtahedi et al., 2017; Paderni et al., 2012). These features of mucoadhesive drug delivery would be beneficial for oral mucosal diseases such as OLP and RAS. Studies have shown that high-potency topical corticosteroids are a good treatment for these lesions. For example, patients presenting with OLP showed a 95% improvement following 2 months of therapy with CP (Conrotto et al., 2006) and patients with RAS showed complete remission with no major adverse effects after treatment with this corticosteroid (Lozada-Nur et al., 1991).

Currently, CP has been formulated as topical preparations such as ointment or emollient cream that have minimal oral bioavailability and low aqueous solubility (Varoni et al., 2012). These preparations have been designed for application to the skin and not the oral mucosa, so these dosage forms in addition to mouthwashes that are administered topically to the oral cavity generally have unpredictable absorption and distribution due to saliva flow and mechanical factors within the oral cavity (Reddy et al., 2011). CP has also been formulated in nanoencapsulation formulations including lecithin/chitosan nanoparticles (Senyigit et al., 2010), polymer-coated lipid nanocapsules (Fontana et al., 2011), liposomes (Rao and Murthy, 2005), lipid nanoparticles (Hu et al., 2006) and nanostructured lipid carriers (Silva et al., 2012) with the intention to improve the safety of the corticosteroids by increasing the accumulation of the drug in the skin while lowering the permeation of the drug to reduce systemic side effects (Silva et al., 2012; Senyigit et al., 2010). Recently, oral

patches as a mucoadhesive device have been developed using electrospinning technology (Santocildes-Romero et al., 2017). These patches comprise of an outer hydrophobic backing layer and a highly mucoadhesive inner layer, with each layer being manufactured from FDA-approved polymer formulations. These patches may dramatically improve oral mucosal drug delivery by prolonging the residence time between the drug and the mucosal lesion providing localised controlled drug delivery.

The purpose of the experiments performed in this chapter was to characterise oral patches loaded with CP. The specific objectives of this study were as follows:

- To examine the physicochemical characteristics (weight, thickness and pH) of the oral patches.
- To evaluate the swelling capability of placebo and CP-loaded patches
- To assess the surface morphology of placebo and CP-loaded patches using SEM.
- To determine the cytotoxicity effects of placebo and CP-loaded patches using TEOM generated in chapter 3 following the OECD guidelines.
- To investigate the morphology of the TEOM following treatment with placebo and CP-loaded patches.

5.2 Experimental procedures

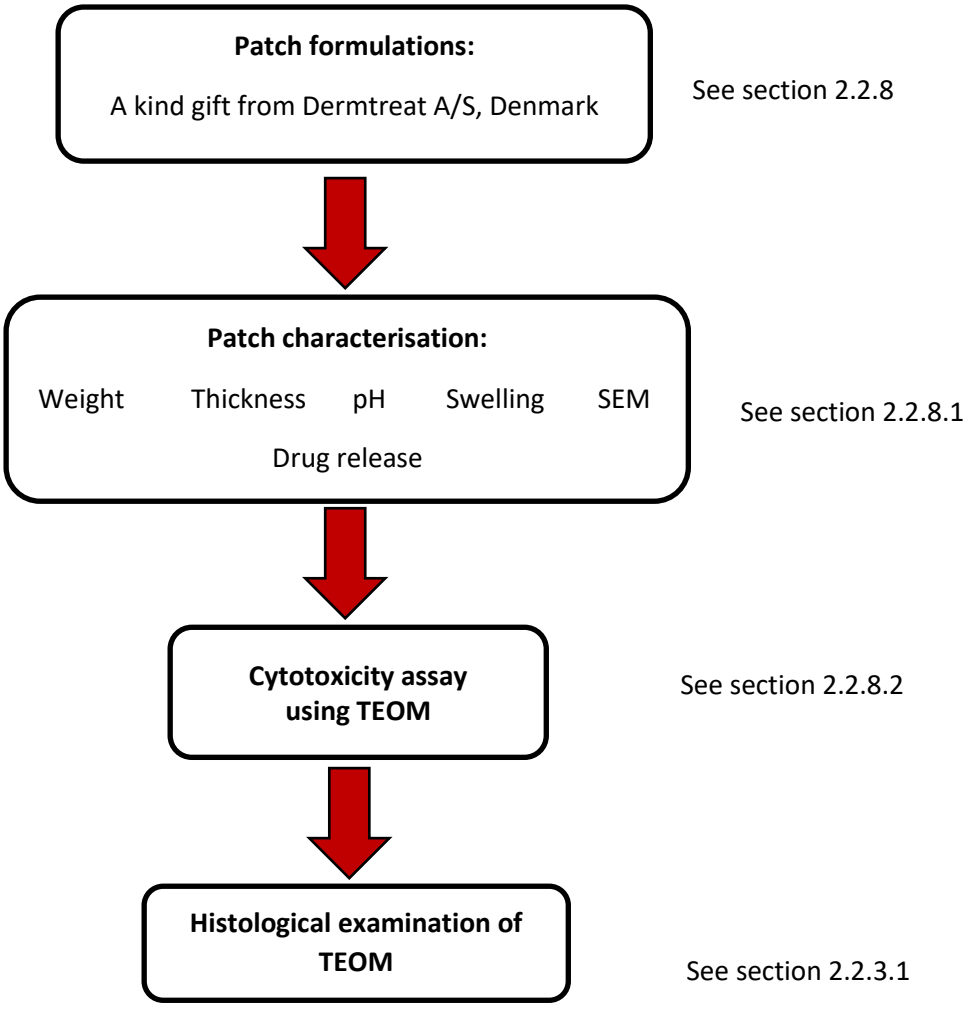

5.3 Results

5.3.1 Physicochemical characterisation

The physicochemical characteristics of mucoadhesive oral patches were assessed using 3 different batches made on different days. Dermtreat A/S provided both placebo and CP-loaded oral mucosal patches. The amount of CP within each of the patches (1, 5 or 20 μg per patch, respectively) was calculated by Dermtreat A/S using HPLC analysis prior to shipment. The average weight of the placebo patch was 55.3 ± 5.18 mg, while CP-loaded patches had an average weight of 67.4 ± 5.1 mg, 59 ± 3.72 mg and 53.3 ± 3.3 mg for 1 μg, 5 μg and 20 μg patches, respectively (Figure 5.1A). The weight of the patches between samples and batches was not significantly different. The average thickness of the placebo patch was 0.43 ± 0.03 mm, while the average thickness of CP-loaded patches was 0.51 ± 0.05 mm, 0.36 ± 0.02 mm and 0.45 ± 0.03 mm for the 1 μg, 5 μg and 20 μg patch, respectively (Figure 5.1B). In addition, the pH values between the different types of patches, either placebo or loaded with CP, were consistently between 8.0 and 8.1 for the placebo as well as different CP concentrations (Figure 5.1C).

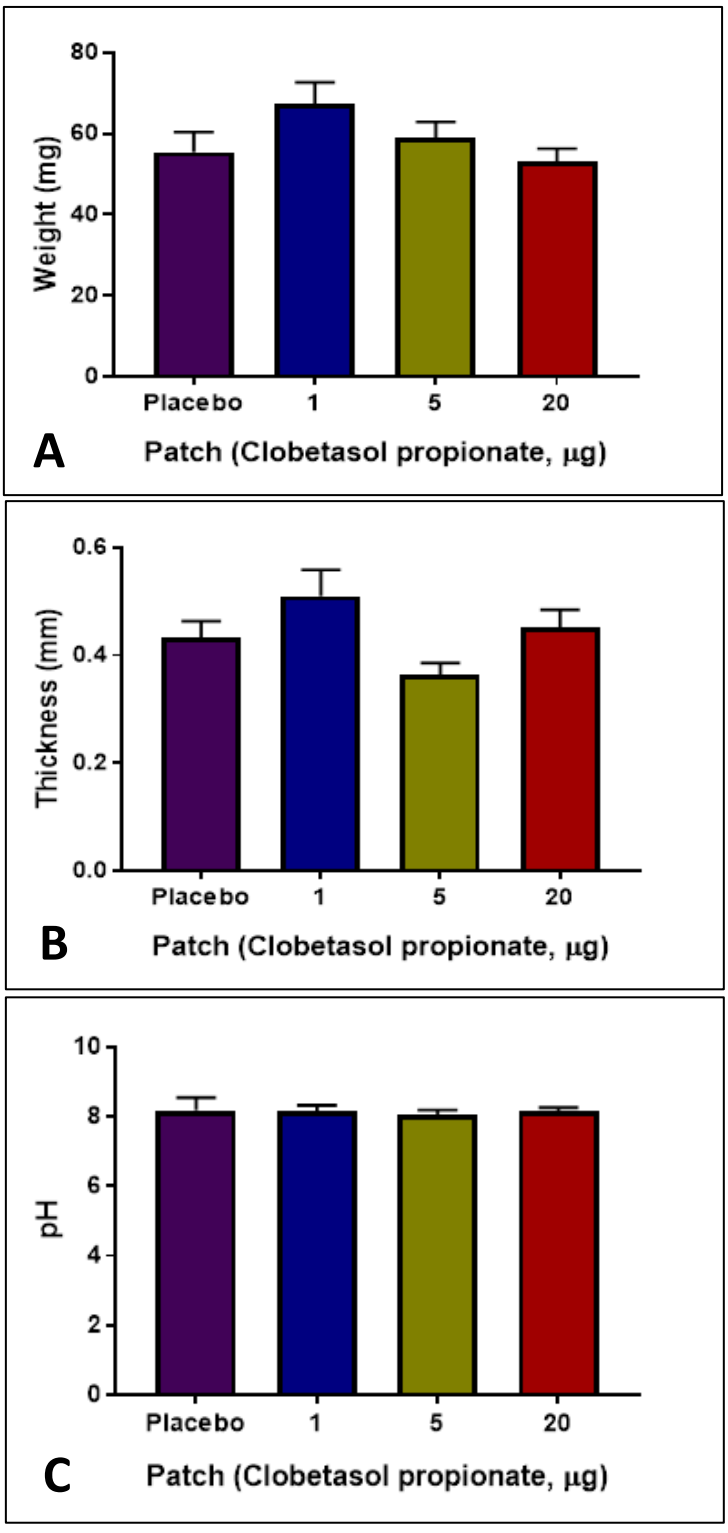

Figure 5.1: Mucoadhesive placebo and CP-loaded (1, 5 and 20 µg) patches are characterised from three different batches for (A) weight (B) thickness and (C) pH. Data were expressed as the mean ± SD for 3 independent experiments performed in triplicate. There was no significant difference for (A) weight (B) thickness and (C) pH between each type of patch, analysed using One-way ANOVA with Tukey post-hoc multiple comparison tests.

5.3.2 Swelling profile of patches

The speed of hydration for polymer-based patches is crucial for their adhesiveness; therefore, patch swelling was examined over time. The degree of swelling for placebo patches was fast with patches taking on 50% of their weight within 3 minutes. This was followed by a steady swelling rate where patches increased in weight by 65% after 60 minutes. The degree of swelling for the CP-loaded patches was slightly slower, although not significantly, as compared to the placebo patches. The 1 µg CP patches increased 50% of its weight within 24 minutes, while both the 5 and 20 µg CP patches took 14 minutes to increase to this weight. Overall, both placebo and CP-loaded patches increased in weight by approximately 70% of their own weight within 60 minutes (Figure 5.2).

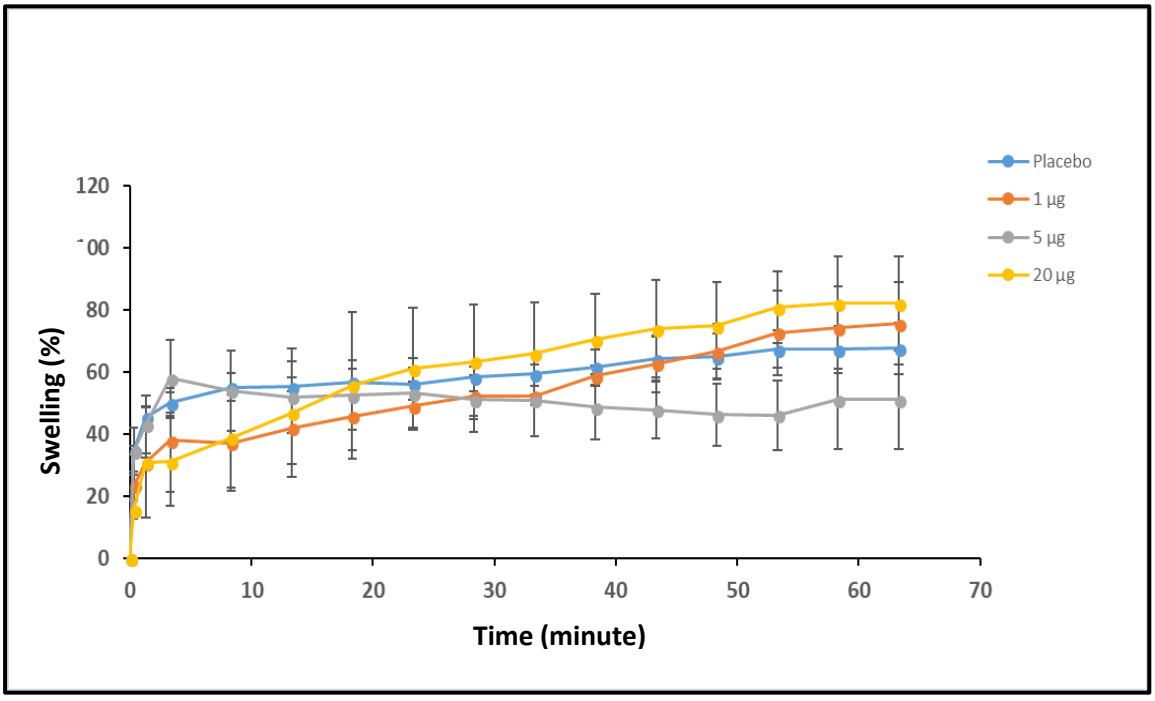

Figure 5.2: Swelling pattern profile of placebo and CP-loaded patches. Data were expressed as the mean ± SD for 3 independent experiments performed in triplicate.

5.3.3 Surface morphological analysis of oral patches

SEM analysis of the oral patches showed that the PCL backing layer exhibited a smooth surface for both placebo and CP-loaded patches (Figure 5.3A). SEM images of the electrospun mucoadhesive layer showed that the inner surface of the patches displayed nanofibers that were homogeneous in number, alignment and diameter regardless of whether they were loaded with CP or placebo (Figure 5.3B). SEM cross sectional analysis also revealed that the PCL backing layer was adhered tightly to the mucoadhesive layer (Figure 5.3C).

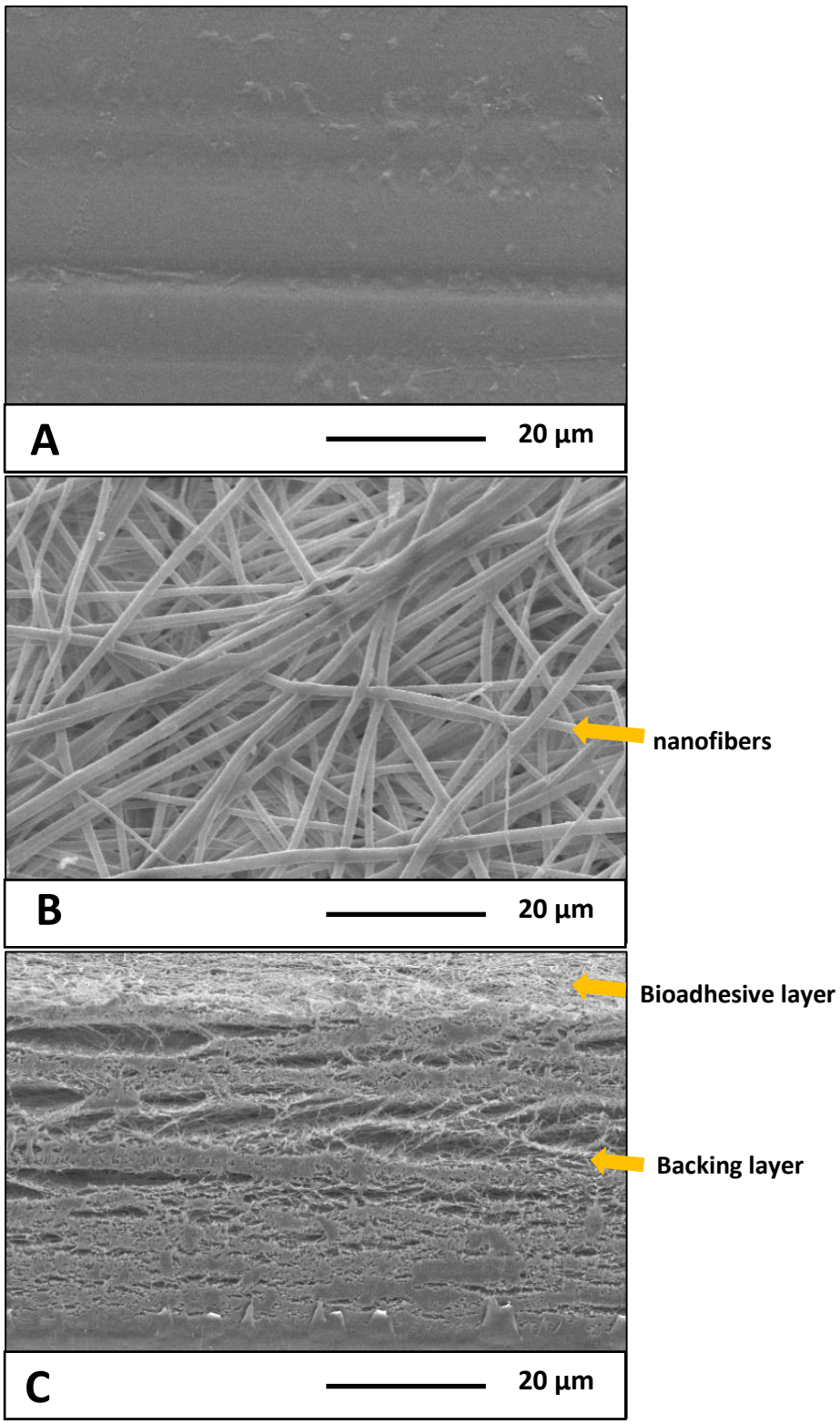

Figure 5.3: Representative surface images of placebo and CP-loaded patches analysed using a scanning electron microscopy (SEM). Images revealed (A) a smooth PCL impermeable backing layer, (B) a homogenous bioadhesive layer of the patch containing nanofibers and (C) a cross section of patch showing tight adherent between the impermeable backing layer and bioadhesive layer. Scale bar = 20 µm.

5.3.4 Drug release profile of CP-loaded patches

Next, the ability of the electrospun oral patches to release CP over time into a receiver liquid was examined by HPLC analysis. There was no significant difference in the drug release profiles for patches loaded with 1, 5 and 20 µg of CP over time. After 6 hours, it was observed that all patches loaded with a different dose of CP had released the drug slowly in a sustained manner with approximately 20%, 50% and 80% of CP released after incubation for 30, 180 and 360 minutes, respectively (Figure 5.4).

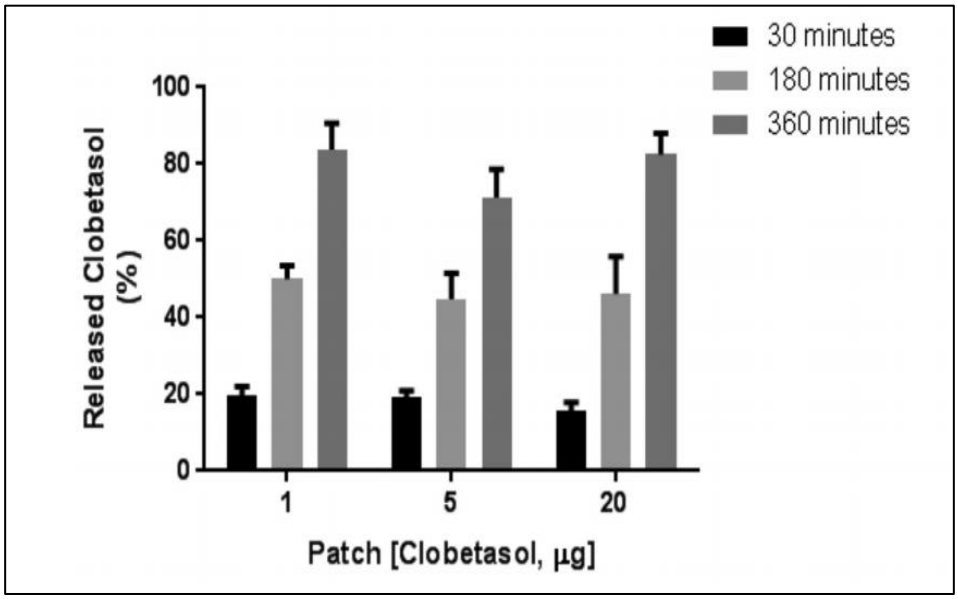

Figure 5.4: Sustained release profile of patches loaded with increasing doses of clobetasol 17-propionate (1, 5 and 20 µg) over a 6-hour period. Data are expressed as the mean ± SD for 3 independent experiments performed in triplicate.

5.3.5 Cytotoxicity profile following treatment with patches against TEOM

To ensure that the oral patches are not toxic to oral mucosa, a MTT cytotoxicity assay was performed for the placebo patch against TEOM following OECD guidelines. MTT analysis showed that the viability of TEOM following one-hour exposure to the placebo patch (90 ± 2.3%) was similar to the medium alone control (100%) suggesting that the polymers used to make the patches are non-toxic to the oral mucosal tissue (Figure 5.5A). In contrast, treatment with 5% SDS, used as a positive control, caused a significant reduction in cell viability (2.3 ± 1.0 %, $p < 0.0001$; Figure 5.5A). There was a non-significant reduction in viability of TEOM following treatment with CP-loaded patches to 76.8 ± 10.3%, 71.2 ± 18.4% and 74.6 ± 24.4% for the 1, 5 and 20 µg patches, respectively (Figure 5.5B). According to the OECD irritancy assay guidelines, the placebo and CP-loaded patches can be considered as non-irritant as the viability of TEOM is above the 50% threshold.

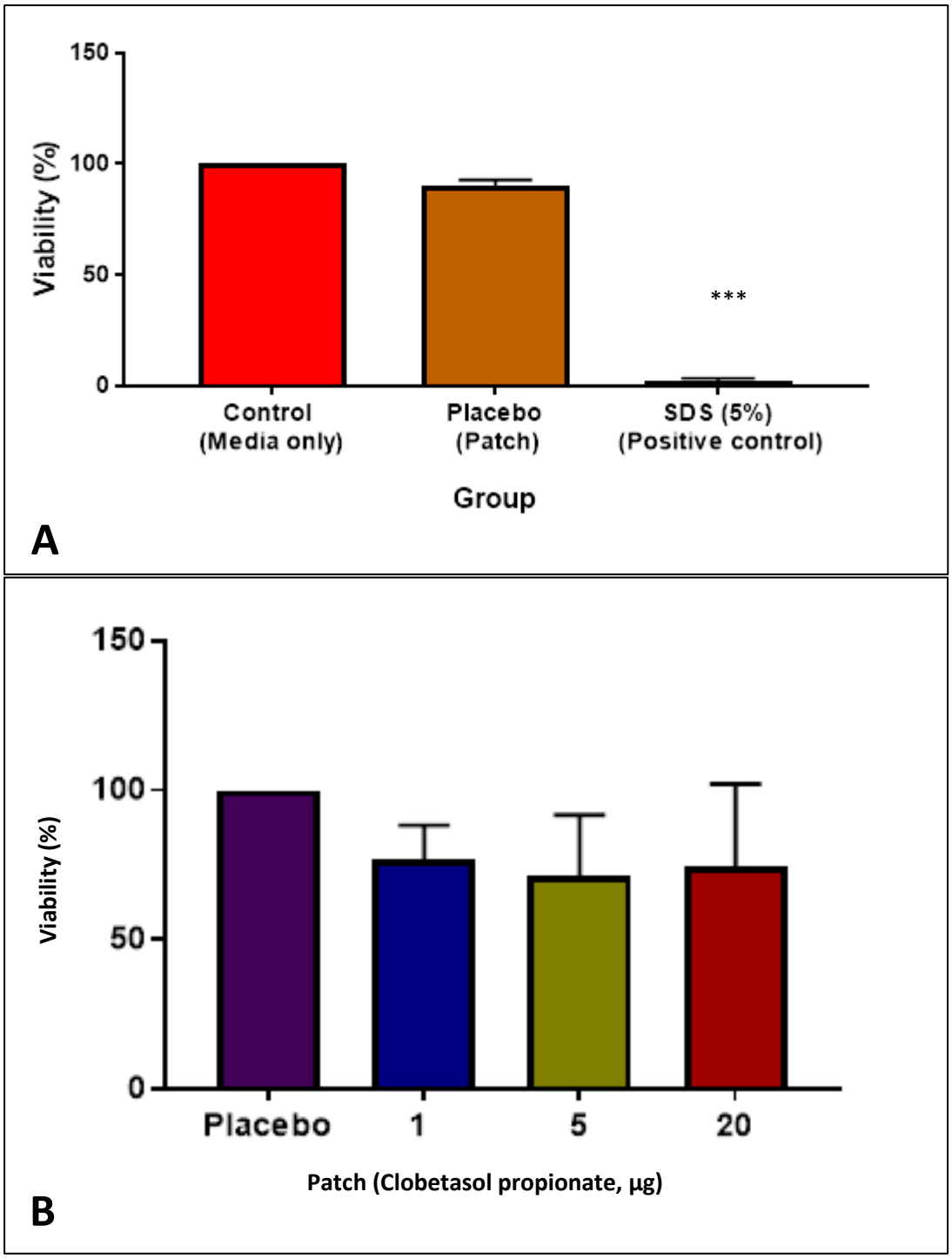

Figure 5.5: Cytotoxicity assay of placebo and CP-loaded patches against TEOM using an MTT assay. (A) placebo patches do not cause cytotoxicity compared to control (media only); SDS treatment was used as positive control. (B) CP-loaded patches showed a small reduction of viability as compared to placebo patches but were not considered cytotoxic/irritant as the percentage is above 50% according to OECD guideline. Data were expressed as mean ± SD for 3 independent experiments performed in triplicate. A mean difference was considered significant when *$p < 0.05$, **$p < 0.001$ and ***$p < 0.0001$ using One-way ANOVA with Tukey post-hoc multiple comparison tests.

5.3.6 Morphological examination following treatment with patches against TEOM

Data from the MTT cytotoxicity assay was supported by histological examination of the TEOM in the absence or presence of the oral patch. The morphology of TEOM that had placebo or CP-patch treatment was less well defined than the TOEM treated with medium alone, with some slight changes evident in keratinocyte morphology and loss of the superficial layers making the epithelium thinner than controls. This may be because these uppermost layers have been lost upon removal of the patch before fixing and histological processing. There is no evidence of damage or loss of integrity of the epithelium following treatment with placebo compared to CP-loaded patches with all these models displaying a full thickness, stratified squamous epithelium (Figure 5.6). In contrast, treatment of TEOM with 5% SDS as a positive control caused complete decellularisation of the TEOM with mucosal models displaying a complete loss of nucleated cells, loss of epithelial attachment to the connective tissue and loss of fibroblast viability in the connective tissue (Figure 5.6B).

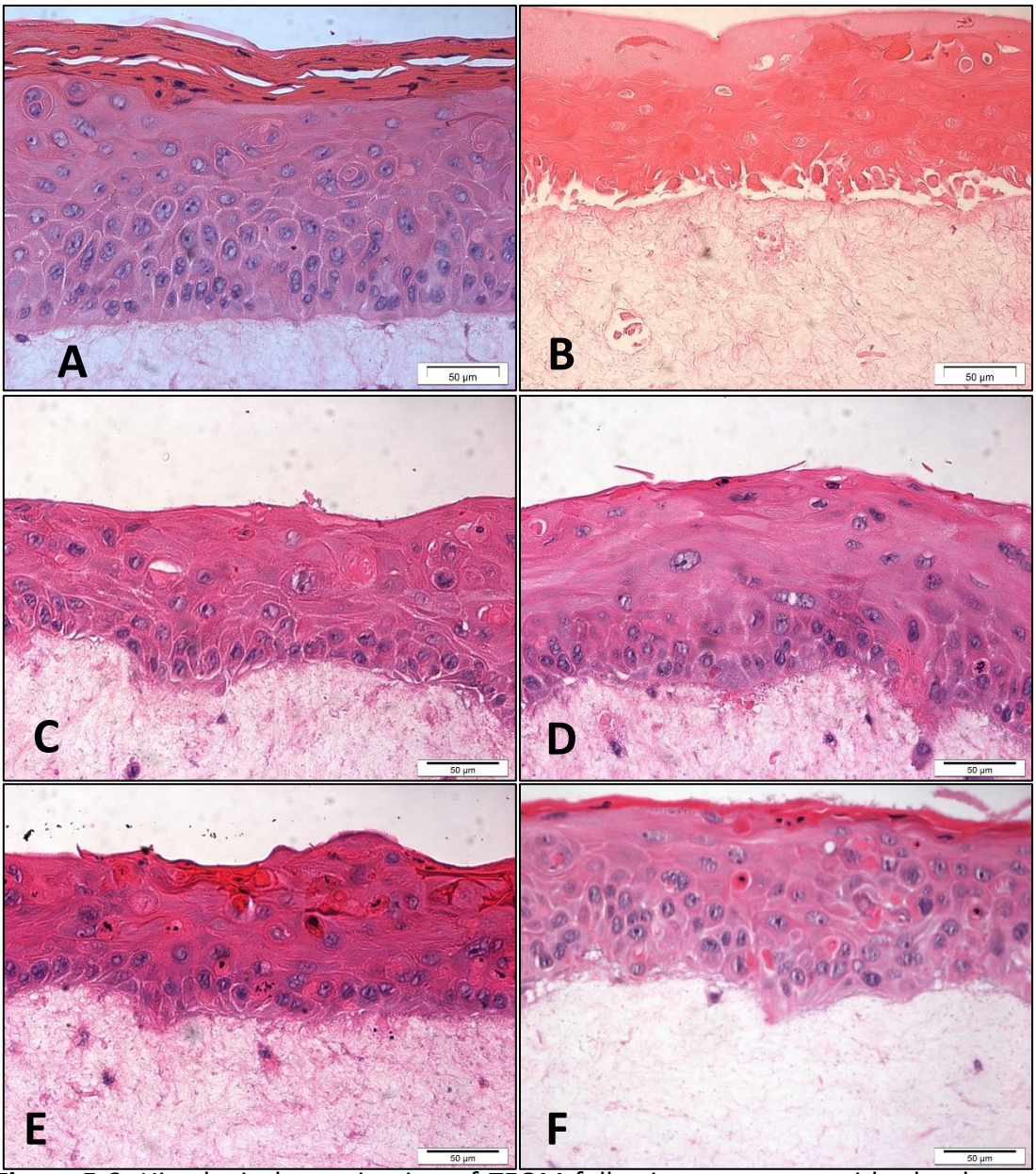

Figure 5.6: Histological examination of TEOM following treatment with placebo or CP-loaded patches performed using H&E staining. (A) TEOM treated with medium alone control shows complete integrity and a full-stratified squamous epithelium whilst treatment with (B) 5% SDS caused complete loss of viability with decellularisation. Treatment with (C) placebo control patch or (D) 1 µg (E) 5 µg and (F) 20 µg patches showed similar histology to medium only controls, suggesting no damage to the epithelium.

5.4 Discussion

Corticosteroids applied topically are commonly used for the treatment of mucosal lesions (Mehdipour and Zenouz, 2012) and CP, as a potent topical corticosteroid, has been shown to effectively treat mucosal lesions including OLP and RAS (Bagan et al., 2012; Belenguer-Guallar et al., 2014). Thus, CP was selected as the model corticosteroid to be formulated as an oral patch intended for localised, controlled drug delivery to the oral mucosa. In previous studies, CP has been formulated as nanosystems intended for drug delivery to the skin, including polymer-coated nanocapsules (Fontana et al., 2011), lipid nanoparticles (Kalariya et al., 2005) and lecithin/chitosan nanoparticles (Senyigit et al., 2010). This is the first study to use corticosteroid-loaded electrospun patches for oral drug delivery.

The CP-loaded patches were formulated with 1-20 μg/patch doses based on the current dosing regimens of gels or creams used in the topical delivery for treatment of dermal inflammatory lesions. These topical preparations that contain 0.05% CP when applied as a fingertip unit to treat and area of 1.33 – 2.5 μg/cm^2. In order to produce the same dosage, 3.1 cm^2 patches were manufactured with 0.0004%, 0.002% or 0.008% CP to produce CP-loaded patches that contained total drug content of 1, 5 and 20 μg/patch, respectively when analysed by HPLC.

Current oral drug formulations have poor residence time resulting in inefficient drug delivery to target tissue. To address this Santocildes-Romero and colleagues (2017) have recently developed an innovative dual-layered electrospun mucoadhesive patch made from adhesive polymers in order to improve the adhesion of the patch to the biological surfaces whilst also controlling drug release. The use of electrospun nanofibres has the advantage of increased surface area and high porosity (Zafar et al., 2016; Ramakrishna et al., 2006). The patches, recently developed by Dermtreat A/S in collaboration with researches at The School of Clinical Dentistry, are a complex mucoadhesive electrospun dual-layer system comprised of an impermeable backing layer made of thermally-treated PCL nanofibres and a bioadhesive layer made from Eudragit®RS100, PVP and PEO nanofibers (Santocildes-Romero et al., 2017). Differential thermal and X-ray diffraction analysis show that the CP within the

electrospun patches is in an amorphous rather than crystalline state. The amorphous state possesses several advantages over a crystalline state including enhanced solubility, increased dissolution rate and enhancing drug delivery (Colley et al., 2018).

The placebo or CP-loaded mucosal patches had no significant effects on any of the physicochemical properties studied including weight, thickness or pH. The patches exhibited a uniform and consistent weight and thickness. Furthermore, the pH of the placebo and CP-loaded patches was between 8 - 8.2 which is slightly alkali than the pH of saliva (5.6 – 7.9). However, the slight deviation was insufficient for the patches to cause irritation or cytotoxicity in a human volunteer study (Colley et al., 2018). The nanofibre structures of all types of patches analysed was homogenous with no apparent defects observed under scanning electron microscopy.

Nanofibre swelling is an essential property for mucoadhesion as successful patch adhesion is dependent on the rapid hydration and gelation once the patch is applied to the moist mucosal surface (Smart, 2005). This study showed that all patches demonstrated extremely quick swelling that was maintained for up to 60 minutes, suggesting that the patches had a profile suitable for rapid and prolonged residence to mucosal surfaces. In a volunteer human study, Colley et al., (2018) observed that when the placebo patches were applied with gentle pressure, they adhered quickly to the gingival, buccal mucosa, and tongue epithelium that are common sites for OLP and RAS lesions. The residence time of the placebo patches was 118, 93 and 43 minutes for gingivae, buccal mucosa and tongue, respectively (Colley et al., 2018). From these data, it could be suggested that the adhesion strength is correlated to the level of epithelial keratinisation in a different region of the oral mucosa. In a previous study, oral patches made from thiolated-chitosan sulphate blended with polyvinyl alcohol (PVA) exhibited rapid swelling properties but only adhered to human buccal mucosa for approximately 5 minutes (Samprasit et al., 2015), suggesting that the polymer blend produced by electrospinning could increase the surface area, crucial for the adhesion to human mucosal surfaces. In other studies, *in vivo* adhesion analysis on adhesive films manufactured using various polymers and blends showed various residence times either at similar times or lower as compared to the Colley et al study

(Kumria et al., 2016; Yehia et al., 2009; Perioli et al., 2004). The presence of food whilst wearing the oral patch may reduce the adhesiveness of the patch, which must be taken into consideration in future studies or clinical trials.

Drug release of CP from loaded patches was initially fast and then the drug was released in a sustained manner. Approximately 80% of the loaded CP was released from the patch within 360 minutes. Previously, it was reported that the release of the antihistamine diphenhydramine from PVA electrospun patches was rapid with almost 86% of the drug released after 3 minutes (Dott et al., 2013). While a patch manufactured using PCL electrospun fibres containing dexamethasone exhibited 50% drug release after 20 minutes and 100% after 90 minutes. In contrast, dexamethasone manufactured within poly(L-lactic) acid fibres showed a much slower release profile with 100% release after 1 month (Vacanti et al., 2012). In another study, α-mangostin incorporated into thiolated chitosan (CS-SH) blended with polyvinyl alcohol (PVA) as the mucoadhesive polymers exhibited rapid burst release from the nanofibres regardless of the concentration. The release of the compound reached 80% within 60 minutes and the release completed within 240 minutes (Samprasit et al., 2015). These data suggest that the polymer blend is crucial in determining the drug release profile from oral patches, with slight differences in polymer mix allowing rapid or sustained drug release. Moreover, the addition of Eudragit RS100 to electrospun nanofibres has been shown to prolong the release of drugs for up to several hours compared to nanofibres alone (Colley et al., 2018; Karthikeyan et al., 2012), indicating that the presence of this polymer in electrospun nanofibres can improve sustained release of the drug as compared to previous drug-loaded systems.

TEOM was used to assess the potential irritancy and toxicity of unloaded or CP-loaded patches. Following the European Union directive on the use of animals for cosmetic testing, effectively banning their use; tissue engineered skin models have become the principle way of testing drug toxicity. There are now several OECD protocols for the standardised use of tissue engineered skin models for compound irritancy and toxicity testing. Several laboratories have extensively validated these tests, which include use of MTT as a cell viability marker, across Europe and the US. However, to date, there is

no official way to test drugs aimed at the oral mucosa. Since oral mucosal models are very similar to those of the skin it was decided to use the OECD skin irritancy test but instead using tissue engineered oral mucosa to test if CP-loaded oral patches were cytotoxic or irritant. Interestingly, using the exact methodology for skin irritancy testing, CP-loaded patches containing up to 20 µg of CP were found not to be irritant as defined by OECD guidelines, which state that a compound is not irritant/toxic if the viability of the tissue engineered model is maintained above 50% (OECD, 2015). These cytotoxicity data suggest that even at high doses CP-loaded patch do not damage the structure and integrity of the epithelium and so their use can be considered for the treatment or oral lesions.

Skin atrophy is the most common adverse effect following treatment with topical glucocorticoids and relies on level of drug potency, duration of exposure, frequency of application and concentration of treatment (Schoepe et al., 2006; Rhen and Cidlowski: 2005). Irreversible adverse effect of glucocorticoid-induced skin atrophy is characterised by a fragile, thinned skin and diminished barrier function (Uva et al., 2012; Schoepe et al., 2006). Histopathological analysis shows that exposure of mucosa with CP results in markedly thinner epithelium (Schoepe et al., 2006; Mills and Marks, 1993), attributable to cellular atrophy where the size of keratinocytes is reduced (Kolbe et al., 2001; Delforno et al., 1978). Glucocorticoids also reduce the intercellular lipid in the upper epidermal layers by diminishing lipids synthesis such as ceramide, cholesterol and fatty acids (Kolbe et al., 2001; Sheu et al., 1997). As a consequence, these changes cause increased permeability and water loss (Kolbe et al., 2001), indicators of disruption of skin barrier function (Kao et al., 2003).

In addition to their actions on epithelial cells, glucocorticoids can also reduce fibroblast numbers in the connective tissue (Schoepe et al., 2006; Kolbe et al., 2001; Saarni and Hopsu-Havu, 1978), resulting in dysregulated ECM turnover (e.g. collagen, proteoglycans and elastin) (Nuutinen et al., 2001; Cutroneo et al., 1981) leading to the decreased dermal thickness and disruption of the tensile strength and elasticity of the skin. Previously, glucocorticoid-induced skin atrophy had been assessed in animal models such as rats, mice, pigs and dogs where marked epidermal and dermal thinning

had been observed (Schoepe et al., 2006). Although the skin is different to the oral mucosa the tissues have many similarities, and so it is believed that the adverse actions of corticosteroids on the oral mucosa are similar to those observed for the skin (Mehdipour and Zenouz, 2012).

Histological data for patch-treated TEOM appear to show slight differences in keratinocyte histology compared to medium alone controls but this may be due to loss of the uppermost-stratified epithelium during processing. There was no difference in the epithelial histology of placebo versus CP-loaded patches. The CP-treated TEOM was examined over a relatively short period of time so any CP-induced changes in tissue morphology may not have yet occurred. Moreover, tissue integrity or permeability using TEER or dextran was not assessed. It would be interesting to examine the long-term effects of CP use on TEOM in terms of TEER, permeability, keratinocyte and fibroblast proliferation, epithelial thickness and so further detailed dose and time-dependent studies are warranted in this area.

5.5 Summary

In conclusion, the data presented in this chapter show that the corticosteroid, CP can be effectively incorporated into electrospun polymer fibres and made into a mucoadhesive patches that have consistent properties. Moreover, these patches can rapidly release the steroid, suggesting that they have properties favourable for oral mucosal patches to target oral lesions like OLP and RAS. However, data showing that the drug is released into the mucosal tissue and is able to exert its effects on target T cells is lacking and so these studies are the subject of the next chapter.

CHAPTER 6

EVALUATION OF THE PERMEATION AND IMMUNOSUPPRESSIVE PROPERTIES OF CORTICOSTEROIDS *IN VITRO* USING TEOM

6.1 Introduction

OLP is an autoimmune disease that affects the stratified squamous epithelium where auto-cytotoxic T lymphocytes trigger apoptosis of epithelial cells leading to chronic inflammation and pathology (Schlosser, 2010; Scully and Carrozzo, 2008). The host inflammatory response is the primary defence mechanism triggered following injury or infection (Coutinho and Chapman, 2011) and as part of this response T cells are activated and recruited to the sites of inflammation (Rauch et al., 2009). The activated T cells are known to produce mediators such as IL-2, an important regulator of lymphocyte proliferation and differentiation into effector T cells, via activation of the transcription factors NFAT, NFκB and AP-1 (Bianchi et al., 2000). IL-2 is an important biomarker used as an indicator of several pathological conditions including multiple sclerosis, rheumatoid arthritis and systemic lupus erythematous (Sedighi et al., 2014).

The anti-inflammatory and immunosuppressant effects of corticosteroids are remarkably efficient at managing the manifestations of inflammatory and autoimmune conditions (Coutinho and Chapman, 2011; Chatham and Kimberly, 2001). Corticosteroids such as CP elicit both anti-inflammatory and immunosuppressant effects on many types of immune cells including T cells (Chatham and Kimberly, 2001). They act by binding to intracellular glucocorticoid receptors that then bind to regulatory sites on the DNA, altering gene transcription in favour of an anti-inflammatory response, such as increased expression of phospholipase A2 inhibitory proteins that reduce the release of arachidonic acid as well as decreasing cytokine secretion, such as IL-2 (Kwatra and Mukhopadhyay, 2018).

The work described in this chapter aim to develop an oral mucosal diseased model representing OLP in order to assess the absorption and immunosuppressant properties of CP both as a free solution or in patch-loaded form. The specific objectives of this study were as follows:

- To assess the distribution and penetration capability of CP (solution form) using TEOM in both a time (10, 30 and 60 minutes) and concentration (5, 25 and 50 µM) dependent manner using HPLC.
- To assess the distribution and penetration capability of CP (patch form) in different doses 1 µg (1 hour), 5 µg (1 hour) and 20 µg (1, 4 and 24 hours) in TEOM using HPLC.
- To evaluate the viability of a T cell line (Jurkat) in different growth media using a trypan blue exclusion assay.
- To determine the optimal concentration of PMA and PHA as stimulants for activating T cells using an IL-2 ELISA.
- To investigate IL-2 secretion by activated T cells over time (4, 8 and 24 hours) using ELISA.
- To establish the OLP-like model by incorporating the activated T cells.
- To investigate the inhibitory effects of CP against IL-2 secretions using ELISA.

6.2 Experimental procedures

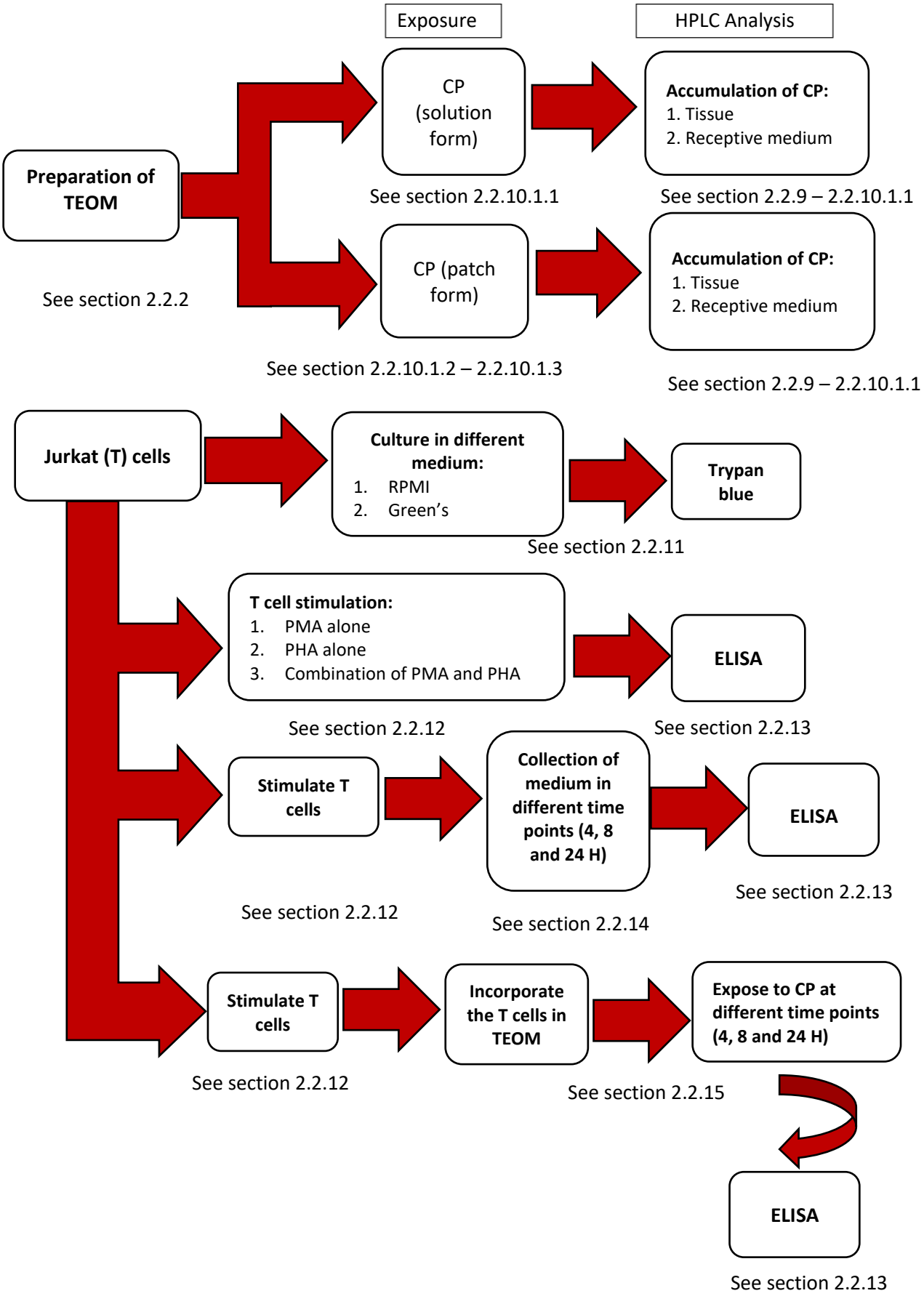

6.3 Results

6.3.1 Permeation of CP into TEOM in solution form was time and concentration-dependent manner

TEOM were exposed to a single dose of CP (5 µM) at increasing exposure times (10, 30 and 60 minutes) and the presence of CP within the tissue and receptive medium of the basolateral compartment of the transwell culture analysed using HPLC. Accumulation of CP increased steadily in a time-dependent manner in both the tissue and receptive medium. In the tissue, the CP concentration measured after 10 minutes exposure was 6.08 ± 1.66 nM/mg that increased to 8.03 ± 1.81 nM/mg and 10.89 ± 0.1 nM/mg after 30 and 60 minutes, respectively (Figure 6.1A). The presence of CP in the receptive medium of the basolateral compartment of the culture system could not be detected after 10 minutes exposure but 21.67 ± 12.18 nM was detected after 30 minutes and this increased to 91.5 ± 7.51 nM after 60 minutes (Figure 6.1B). For all subsequent permeation tests, the TEOM was exposed for one hour, as this was the optimal incubation time in detecting the presence of CP in the tissue and receptive medium.

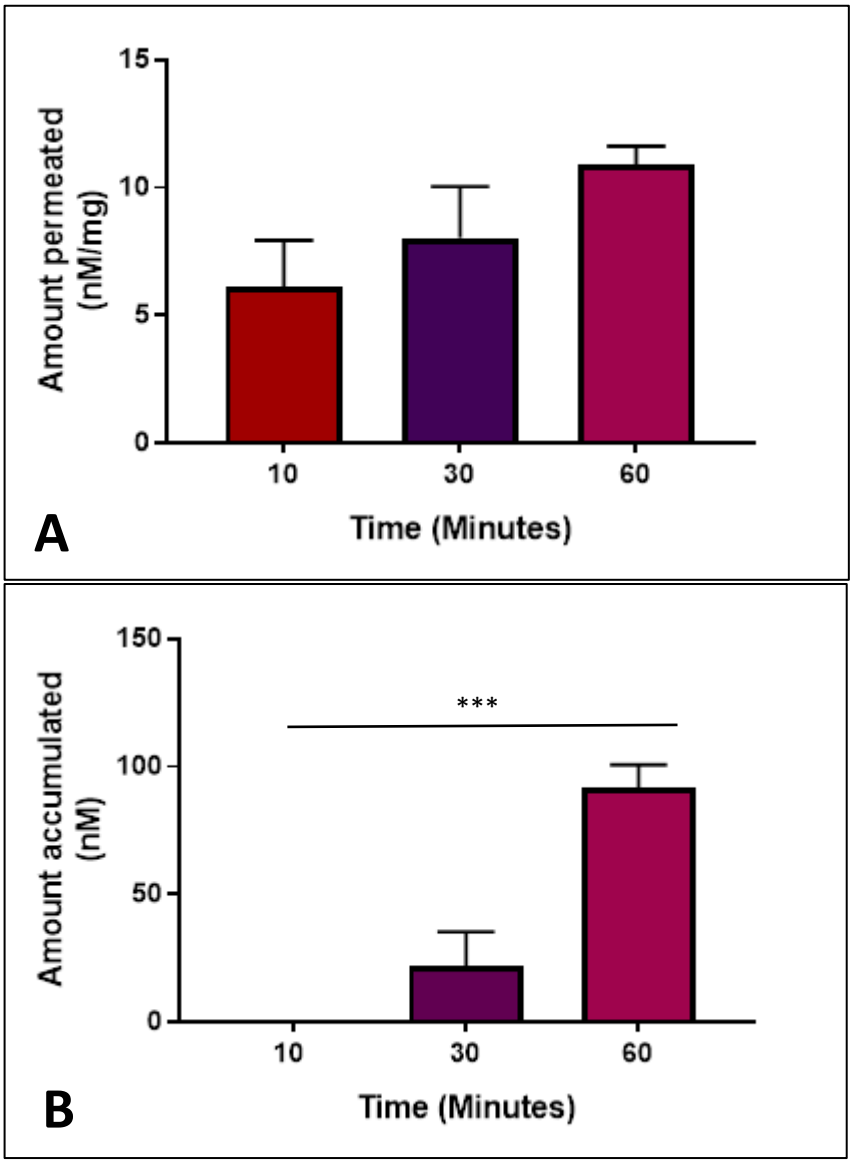

Figure 6.1: Time-dependent increase in the amount of CP within (A) TEOM tissue and (B) in the receptive medium of the basolateral compartment after 10, 30 and 60 minutes exposure to CP (solution). Data are expressed as the mean ± SD for 3 independent experiments performed in triplicate. A mean difference was considered significant when *$p < 0.05$, **$p < 0.001$ and ***$p < 0.0001$ using One-way ANOVA with Tukey post-hoc multiple comparison tests.

To determine the effects of drug concentration on permeation, TEOM were exposed to increasing concentrations of CP (5, 25 and 50 µM) for one hour. HPLC analysis revealed that the accumulation of CP in both the tissue and receptive medium increased in a concentration-dependent manner. The CP levels measured in the tissue were approximately 0.84 ± 0.14 nM/mg after 5 µM exposure and increased to 1.5 ± 0.21 nM/mg at 25 µM. At 50 µM, the CP levels increased significantly to 4.21 ± 0.37 nM/mg ($p < 0.0001$) compared to the CP levels at 5 and 25 µM (Figure 6.2A). CP accumulation in the receptive medium of the basolateral compartment was approximately 87.67 ± 12.14 nM after exposure to 5 µM, increasing significantly to 192.33 ± 18.55 nM ($p < 0.05$) with 25 µM exposure as compared to the CP level at 5 µM. Moreover, the level of tissue CP after 50 µM exposure was drastically increased (889.33 ± 22.51 nM; $p < 0.0001$) as compared to the CP levels at 5 and 25 µM (Figure 6.2B).

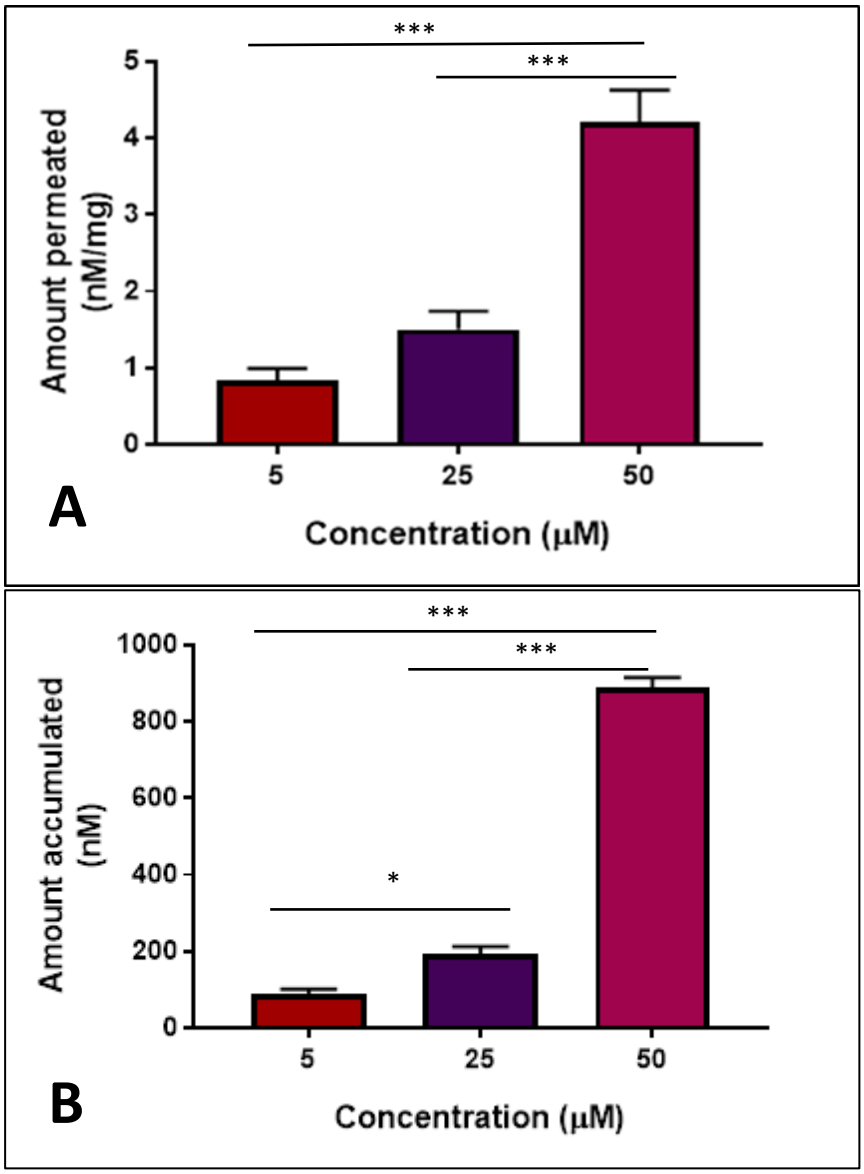

Figure 6.2: Amount of CP in the (A) TEOM tissue and (B) the receptive medium of the basolateral compartment after one-hour exposure with 5, 25 and 50 µM CP (solution). The amount of CP detected in tissue and receptive medium increased in a concentration-dependent manner. Data are expressed as the mean ± SD for 3 independent experiments performed in triplicate. A mean difference was considered significant when *$p < 0.05$, **$p < 0.001$ and ***$p < 0.0001$ using One-way ANOVA with Tukey post-hoc multiple comparison tests.

6.3.2 The penetration of clobetasol-17-propionate delivered via loaded mucoadhesive patches through TEOM was concentration and time-dependent

CP-loaded mucoadhesive patches containing 1, 5 and 20 µg of active drug were applied to the epithelial surface of TEOM for one hour. The concentration of CP that had permeated into the tissue was measured by HPLC and found to be 0.04 ± 0.04 nM/mg from the 1 µg patch, increasing to 0.06 ± 0.07 nM/mg when a 5 µg patch was applied to the TEOM and to 0.15 ± 0.14 nM/mg from the 20 µg patch (Figure 6.3A). Interestingly, CP was only detected in the receptive medium when a 20 µg patch was applied to the epithelium, the amount detected was low at 5.33 ± 8.26 nM (Figure 6.3B). For all subsequent experiments, only the 20 µg patch was used as this concentration showed the capability in penetrating and traversing the TEOM and reached to the basolateral compartment within 1 hour. Although it is the highest concentration, this CP-patch did not induce toxicity in the TEOM, which was confirmed in the previous chapter.

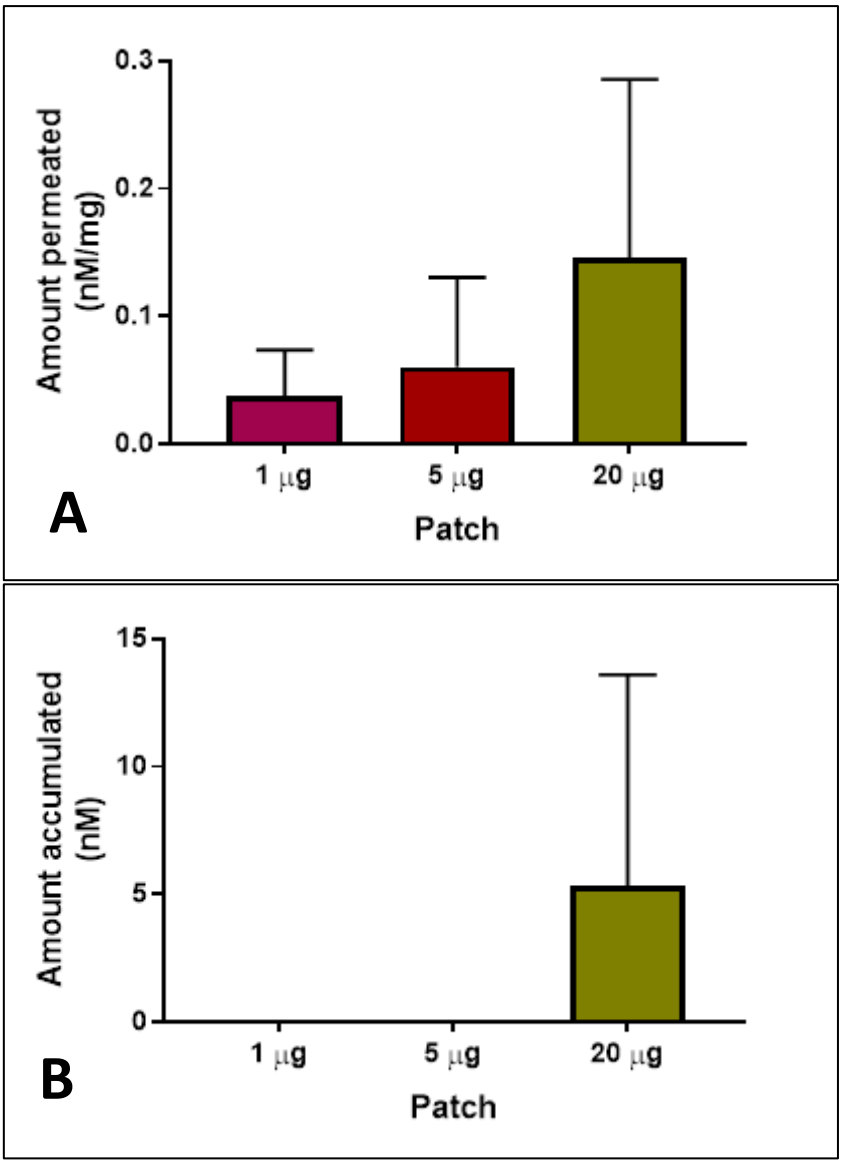

Figure 6.3: The amount of CP in (A) the TEOM tissue and (B) in the receptive medium of the basolateral compartment after one-hour exposure to either a 1, 5 or 20 μg CP-loaded patches. The amount of CP detected increased in a concentration-dependent manner in the tissue. Whilst the presence of CP was only detected in the receptive medium when a 20 μg CP patch was applied to the TEOM. Data are expressed as the mean ± SD for 3 independent experiments performed in triplicate. A mean difference was considered significant when *$p < 0.05$, **$p < 0.001$ and ***$p < 0.0001$ using One-way ANOVA with Tukey post-hoc multiple comparison tests.

The capability of CP released from the 20 µg patch in penetrating the tissue was further analysed by applying the patch topically to the surface of the TEOM for two additional time points, 4 and 24 hours. In general, the data in figure 6.4 shows that the amount of CP detected in the tissue and receptive medium increased when the incubation time was extended. The amount of CP detected in the tissue was approximately 0.22 ± 0.11 nM/mg after 1-hour exposure. It increased slightly to 0.25 ± 0.03 nM/mg after 4 hours exposure and the amount of CP detected was significantly increased ($p < 0.05$) to 0.94 ± 0.13 nM/mg after 24 hours incubation (Figure 6.4A). Similarly, the amount of CP present in the receptive medium was 16 ± 18.48 nM after 1 hour exposure and increased to 31 ± 2.31 nM after 4 hours incubation and then significantly increased to 94.5 ± 5.2 nM ($p < 0.05$) after 24 hours incubation (Figure 6.4B).

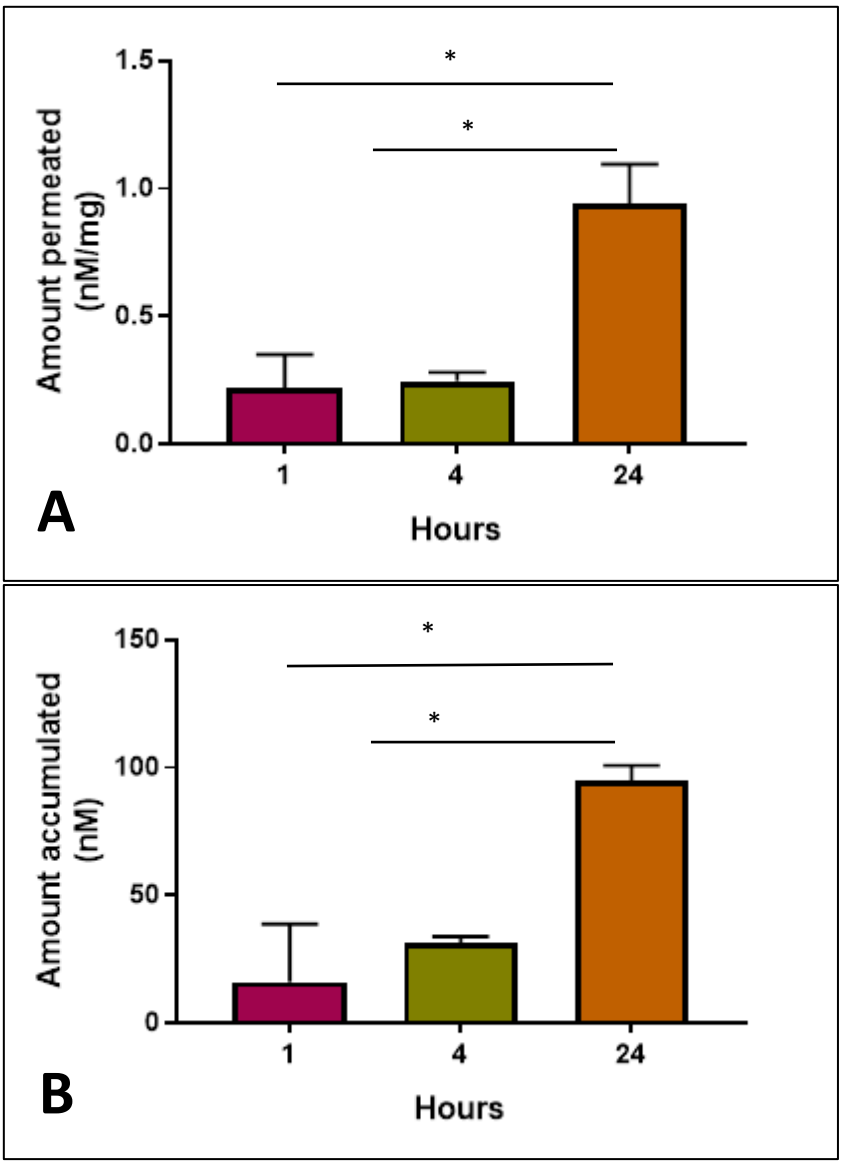

Figure 6.4: The amount of CP in (A) the TEOM tissue and (B) in the receptive medium of the basolateral compartment when a 20 µg CP patch was applied topically for either 1, 4 and 24 hours. The amount of CP detected increased in a time-dependent manner in both the tissue and receptive medium. Data are expressed as the mean ± SD for 3 independent experiments performed in triplicate. A mean difference was considered significant when *$p < 0.05$, **$p < 0.001$ and ***$p < 0.0001$ using Independent T-test.

6.3.3 Culture of Jurkat T cells in different medium

The experimental plan was to develop a tissue engineered mucosal model to incorporate T cells in order to assess the biological effects of topically applied CP. However, Jurkat T cells (the cell line to be used) are routinely cultured in different medium (RPMI) to TEOM (Green's medium). RPMI is the standard culturing medium for Jurkat T cells. Therefore, the viability of Jurkat T cells grown in RPMI medium was compared with cells grown in Green's medium that is commonly used for culturing TEOM and required for epithelial differentiation. Jurkat T cell viability was assessed for up to 8 days in continuous culture (Figure 6.5).

The viability of the Jurkat T cells cultured in Green's medium was 95.17 ± 3.35%, 90.41 ± 3.42%, 86.14 ± 2.11%, 91.08 ± 1.12% at day 2, 4, 6 and 8 respectively. While the viability of the Jurkat T cells cultured in RPMI was 96.34 ± 4.14, 87.36 ± 1.53%, 89.51 ± 1.43%, 88.15 ± 0.1% at day 2, 4, 6 and 8 respectively. A significant difference in Jurkat T cell viability was observed at day 6 ($p < 0.05$) and 8 ($p < 0.05$) when compared between both media. Overall, the percentage of Jurkat T cell viability cultured in both media was maintained above 86% at all time points tested.

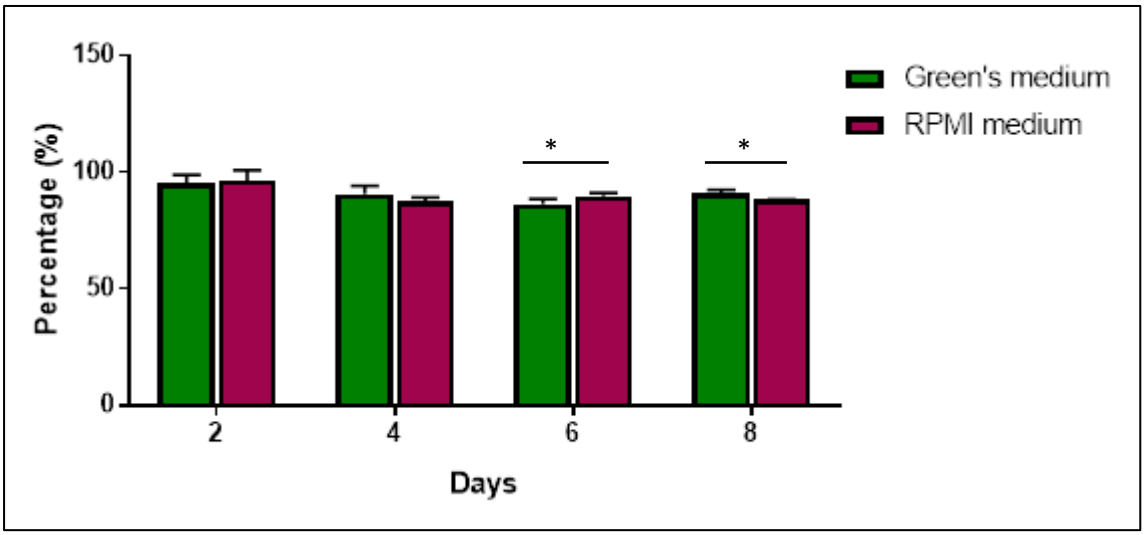

Figure 6.5: Jurkat T cell viability when grown in RPMI and Green's medium cultured for 8 days. The data shows that culture in Green's medium was comparable with RPMI medium. Data are expressed as the mean ± SD for 3 independent experiments performed in triplicate. A mean difference was considered significant when *$p < 0.05$, **$p < 0.001$ and ***$p < 0.0001$ using student T-test.

6.3.4 Activation of Jurkat T cells was more pronounced using a combination of PHA and PMA compared to a single stimulant alone

Jurkat T cells can be activated and induced to secrete IL-2 either by direct activation of the T cell receptor using stimulating monoclonal antibodies or indirectly by stimulating the protein kinase C signal transduction pathway using PMA, PHA or a combination of these two molecules. Jurkat T cells at a cell density of 1.0 x 10^6/mL were stimulated with PHA and PMA alone or with combinations of these two stimulants for 24 hours. Optimisation of the most suitable concentration required to activate the Jurkat T cells (quantified by IL-2 release) without causing cell toxicity was performed. As a preliminary study, concentrations of 1 µg/mL PHA and 50 ng/mL PMA were used as recommended in the literature (Manger et al., 1986). However, these concentrations either added alone or in combination failed to activate the cells to release IL -2 (data not shown).

Further optimisation was therefore performed with various doses of the two stimulants. Two concentrations of PHA (2 and 5 µg/mL) and a single PMA concentration (100 ng/mL) were tested for their ability to activate Jurkat T cells. By measuring the release of IL-2, it was shown that PHA alone at 2 and 5 µg/mL activated the cells with IL-2 secretion measured at 13.01 ± 20.16 pg/mL and 264.31 ± 34.83 pg/mL, respectively. PMA alone (100 ng/mL) had no effect on T cell IL-2 secretion. However, when a combination of PHA and PMA was applied the secretion of IL-2 was significantly increased. The combination of 2 µg/mL PHA and 100 ng/mL PMA increased the release of IL-2 73-fold to 962.03 ± 153.41 pg/mL ($p < 0.0001$). Furthermore, elevation of PHA concentration to 5 µg/mL and co-stimulation with 100 ng/mL PMA induced IL-2 secretion by a further 6-fold to 1626.34 ± 311.36 pg/mL ($p < 0.0001$). As a result, the co-stimulation of Jurkat T cells with 5 µg/mL PHA and 100 ng/mL PMA was selected as the optimal concentrations to activate Jurkat T cells to secrete high levels of IL-2 and therefore used for subsequent experiments (Figure 6.6).

In addition, cell viability was determined to ensure that there was no adverse cytotoxic effect caused to the Jurkat T cells when the stimulants were applied. Cell viability was maintained above 82% after exposure to PMA and PHA when applied either alone or

in combination with no statistically significant different between all groups of stimulants investigated (Figure 6.7).

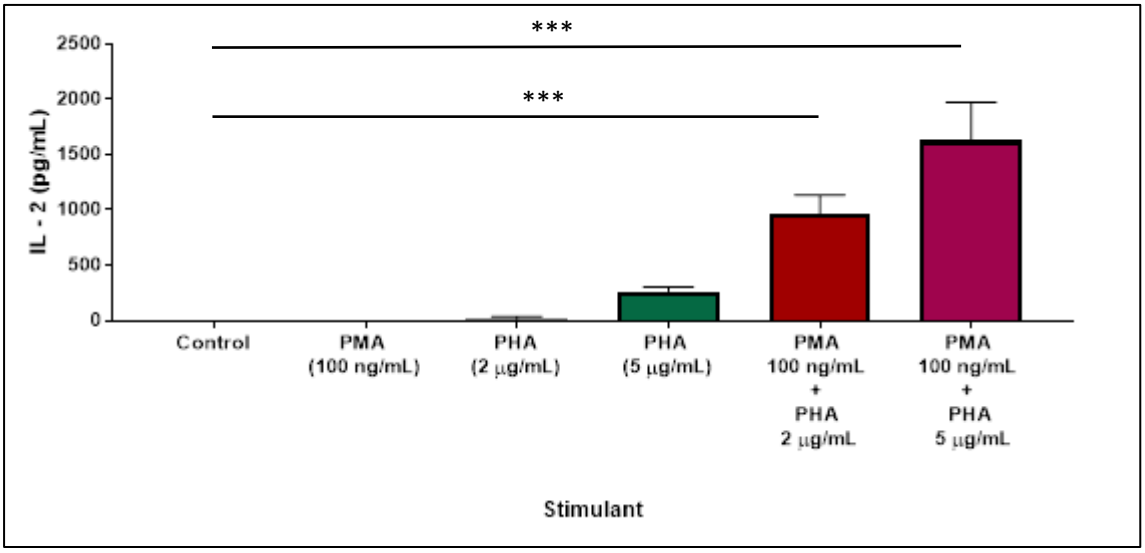

Figure 6.6: The activation of Jurkat T cells was tested by stimulation with PHA as a main stimulant and PMA as a co-stimulant. Stimulation of Jurkat cells was conducted either using a single or combination of the two compounds for 24 hours. The co-stimulation of Jurkat cells induced a significant increase of IL-2 secretions compared to stimulation with either PHA or PMA alone. Therefore, the co-stimulation of PHA and PMA at 5 μg/mL and 100 ng/mL, respectively were chosen as the optimal concentration to activating Jurkat cells. Data are expressed as the mean ± SD for 3 independent experiments performed in triplicate. A mean difference was considered significant when *$p < 0.05$, **$p < 0.001$ and ***$p < 0.0001$ using One-way ANOVA with Tukey post-hoc multiple comparison tests.

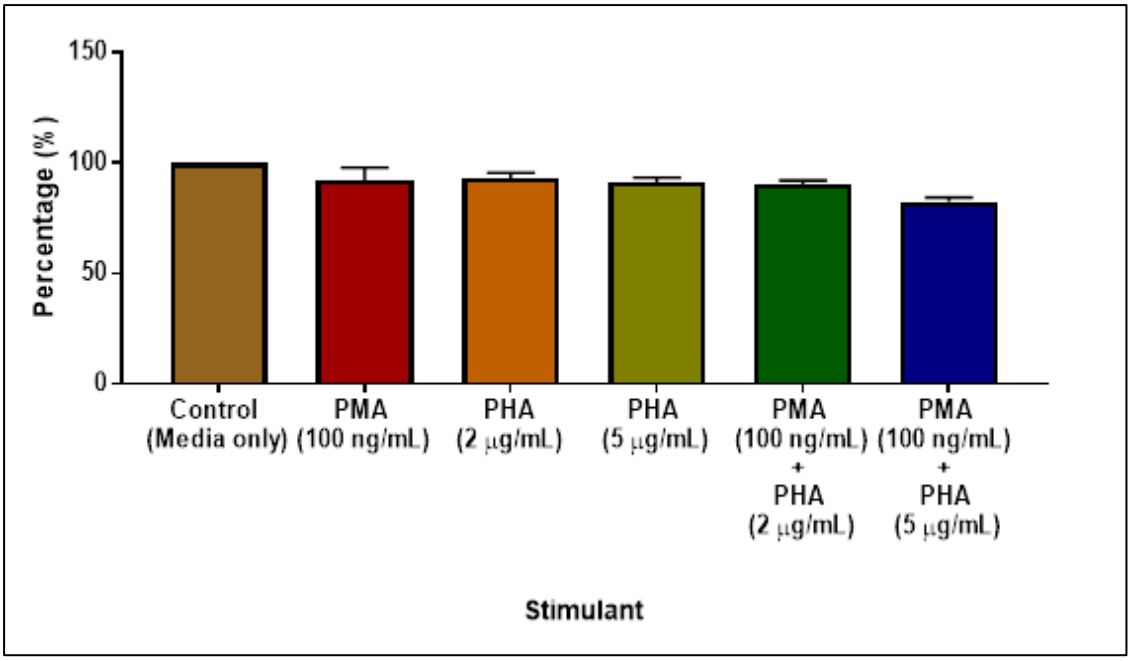

Figure 6.7: The effect of the different concentrations of the stimulants either applied alone or in combination on cell viability measured. No significant different between each group was observed, with cell viability remaining above 82% for each group tested. Data are expressed as the mean ± SD for 3 independent experiments performed in triplicate. A mean difference was considered significant when *$p < 0.05$, **$p < 0.001$ and ***$p < 0.0001$ as compared to control (media only) using One-way ANOVA with Tukey post-hoc multiple comparison tests.

6.3.5 Sustained IL -2 release from activated T cells over time with stimulants

The efficiency of activated Jurkat T cells to sustain release of IL-2 post-24 hours stimulation was investigated with IL-2 being measured after 4, 8 and 24 hours once the stimulants were removed. This analysis was crucial to ensure that the Jurkat T cells are able to release of IL-2 in a sustained manner prior to another experiment being conducted particularly in assessing the efficiency of CP treatment against IL-2 levels experiment. The data showed the secretions of IL-2 were 799.67 ± 114.74 pg/mL, 713 ± 98.77 pg/mL, 664.79 ± 98.27 pg/mL after 4, 8 and 24 hours, respectively. IL-2 secretions were decreasing over time. However, the reduction of IL-2 levels was slight and insignificant different between each time point (Figure 6.8).

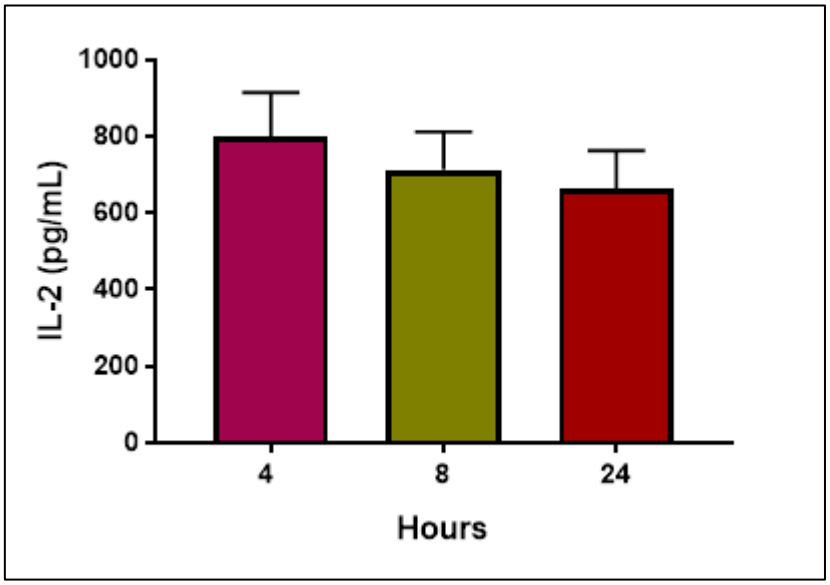

Figure 6.8: The level of IL-2 secretion by activated Jurkat T cells following 24 hours of stimulation was assessed over time. The insignificant reduction of IL-2 levels was observed in a time-dependent manner. Data are expressed as the mean ± SD for 3 independent experiments performed in triplicate and analysed using One-way ANOVA with Tukey post-hoc multiple comparison test.

6.3.6 Clobetasol-17-propionate-mediated inhibition of IL-2 production by the activated Jurkat T cells in OLP-like model

To model OLP *in vitro*, Jurkat T cells were stimulated with a combination of PMA and PHA as previously described, the stimulant removed and the activated cells then added into the basolateral compartment of the TEOM. The TEOM were treated with different treatment strategies; namely control (media only, no patch), placebo (patch), 20 µg CP (patch) and 20 µg CP (solution) for 4, 8 and 24 hours and then the levels of IL-2 measured in the medium of the basolateral compartment of the tissue culture model where the Jurkat T cells resided.

Data in figure 6.9 shows that IL-2 levels in the basolateral compartment of TEOM treated with medium alone were elevated and constant at 427.17 ± 53.58 pg/mL over 24 hours, showing that the activated T cells secrete significant amounts of IL-2 over this time period. The treatment of both the CP-loaded patch and CP solution reduced the level of IL-2 in a time-dependent manner, but only significant reduction was observed following treatment with CP solution after 24 hours treatment compared to IL-2 level after 4 hours treatment ($p < 0.05$). Interestingly, treatment with just a placebo patch containing no CP reduced the levels of IL-2 in the receptive medium that was significant ($p < 0.05$) at 4 hours but not so at 8 or 24 hours when compared to the medium only control (Figure 6.9).

After 4 hours treatment, both the 20 µg CP-loaded patch and 20 µg CP added in solution form significantly ($p < 0.05$) reduced the IL-2 levels secreted by activated Jurkat T cells to 352.94 ± 65.57 and 319.72 ± 54.80 pg/mL, respectively, in the basolateral compartment compared to TEOM treated with control medium alone (528.28 ± 43.38 pg/mL). In contrast, no significant difference in IL-2 levels was observed between the CP-treated TEOM and the placebo patch treated TEOM (390.06 ± 41.17 pg/mL) at this time point (Figure 6.9). By 8 hours, levels of IL-2 in the basolateral compartment of both the CP-loaded patch (261.83 ± 23.18 pg/mL) ($p < 0.05$) and the CP solution (230.64 ± 2.16 pg/mL) ($p < 0.001$) treated TEOM were significantly lower than the medium only control (421.83 ± 57.38 pg/mL) and more importantly the placebo control patch treated TEOM (356.50 ± 44.18 pg/ml) (Figure

6.9). The reduction in IL-2 levels in the CP treated groups continued in a time dependent manner and by 24 hours the level of IL-2 in the basolateral compartment had declined further to 230.17 ± 98.36 pg/mL for the CP-loaded patch and 164.61 ± 62.29 pg/mL for the CP applied in solution form. These levels were significantly lower ($p < 0.05$) than those of both the medium only control (427.17 ± 53.38 pg/mL) and importantly, the placebo patch treated TEOM (376.61 ± 10.96 pg/mL) (Figure 6.9). These data show that CP either delivered in solution or in patch form penetrate and cross the TEOM models, enter the basolateral compartment where the T cells reside and then exert their anti-inflammatory actions by inhibiting IL-2 release from the activated T cells. These anti-inflammatory actions appear to take in excess of 4 hours, most likely due to the time taken for the corticosteroid to affect IL-2 gene transcription and protein translation.

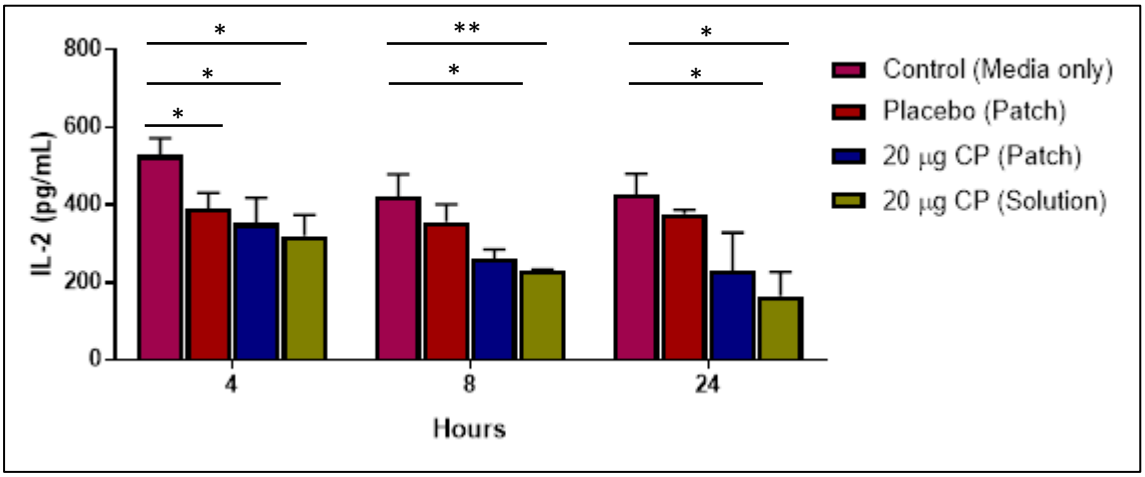

Figure 6.9: Treatment of OLP-like model using either media alone (control) placebo (patch), 20 µg CP (loaded-patch) or 20 µg CP (solution) at (A) 4, (B) 8 and (C) 24 hours. Data are expressed as the mean ± SD for 3 independent experiments performed in triplicate. A mean difference was considered significant when *$p < 0.05$, ** $p < 0.001$ and ***$p < 0.0001$ as compared to control (media only) using One-way ANOVA with Tukey post-hoc multiple comparison tests.

To confirm that the CP had penetrated and traversed the TEOM, the levels of CP in the medium of the basolateral compartment was also measured at each time-point. After treatment with the 20 μg CP-loaded patch, the amount of CP detected after 4, 8 and 24 hours was 0.016 ± 0.002 μM, 0.032 ± 0.003 μM and 0.08 ± 0.003 μM, respectively (Figure 6.10A). After treatment with the 20 μg CP in solution, the amount of CP detected was significantly higher with 0.49 ± 0.02 μM, 1.19 ± 0.03 μM and 2.35 ± 0.09 μM after 4, 8 and 24 hours, respectively (Figure 6.10B). Although the accumulation of CP increased overtime for both CP treatments, the amount of CP measured in the medium of the basolateral compartment when delivered in solution form was significantly greater ($p < 0.0001$) than when the CP was delivered in patch form at all time points tested, although the amount of CP in the patch and solution are not comparable, with solution containing more CP. These data show that the CP is able to traverse the TEOM models in both solution and patch form although levels are much higher when CP is applied as a solution. However, even though CP is in greater quantity when delivered in solution form in the basolateral compartment, data in figure 6.9 show that both CP solution and patch-loaded CP decreased IL-2 levels to a similar degree. These data indicate that the levels delivered by the CP-loaded patches are enough to have a functional effect on T cells by promoting an anti-T cell response.

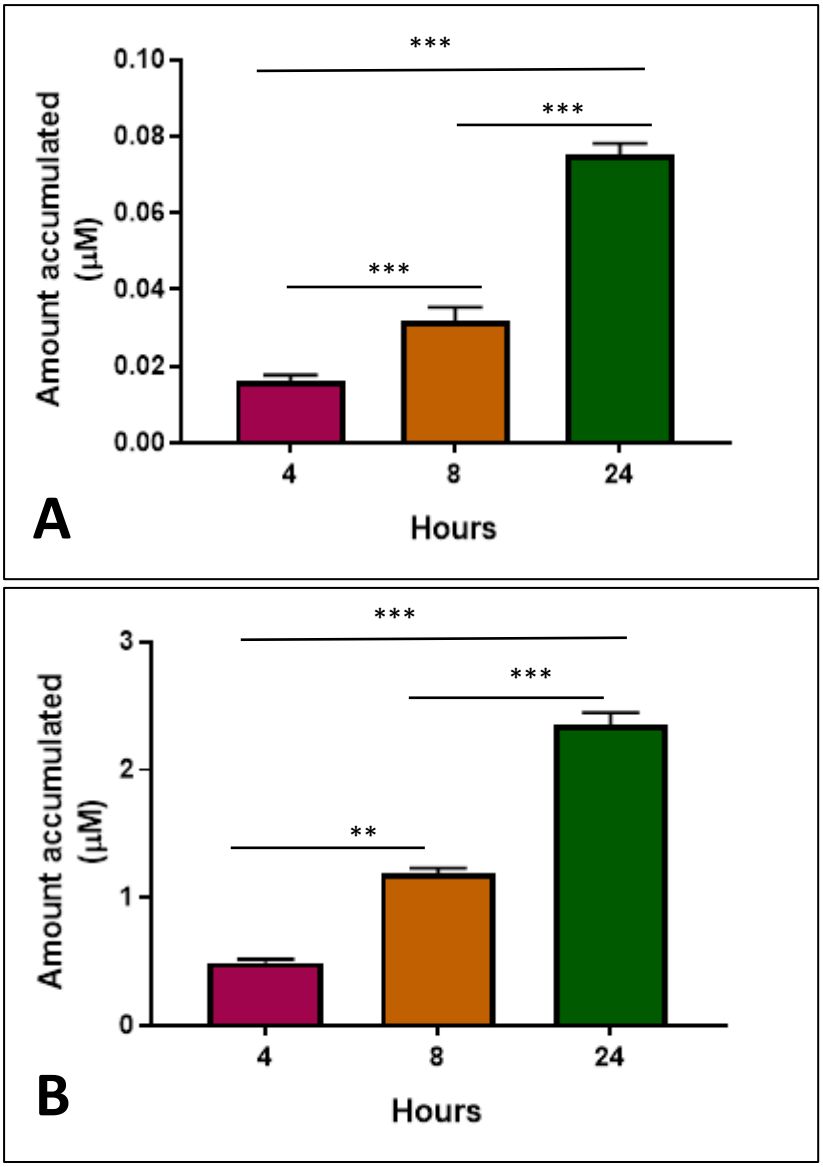

Figure 6.10: Accumulation of CP in the basolateral compartment medium increased after 4, 8 and 24 hours exposure for both treatments using (A) 20 µg CP (patch) and (B) 20 µg CP (solution). The penetration capability of 20 µg CP delivered in (solution) was greater compared to the 20 µg CP (patch). Data are expressed as the mean ± SD for 3 independent experiments performed in triplicate. A mean difference was considered significant when *$p < 0.05$, **$p < 0.001$ and ***$p < 0.0001$ using One-way ANOVA with Tukey post-hoc multiple comparison tests.

6.4 Discussion

In the past several approaches for assessing drug transport across the oral mucosa have been performed including use of animals or healthy human volunteers (Sohi et al., 2010), excised animal tissues (Hoogstraate et al., 1993), cell cultures (Nielsen and Rassing, 1999) and reconstituted tissue models (Odraska et al., 2011; Sohi et al., 2010). In this study, the permeation of corticosteroid had been optimised using TEOM based on FNB6 immortalised keratinocytes as a reproducible model system to assess drug delivery (chapter 4). To our knowledge, these are the first studies performed to assess drug delivery using an immortalised keratinocyte cell-based TEOM.

Absorption of molecules through the oral mucosa occurs mainly by passive diffusion via either paracellular or transcellular pathways (Sudhakar et al., 2006; Rossi et al., 2005). These pathways, for drug absorption into the oral mucosa, rely on the lipophilicity of the drug (Deneer et al., 2002); the paracellular pathway favours hydrophilic and small molecules (≤ 300 Da) whilst the transcellular pathway is preferential for lipophilic molecules (Rossi et al., 2005, Patel et al., 2011). CP is a lipophilic molecule with a molecular weight of 466.97 g/mol (Barange and Asghar, 2017) and therefore, the transcellular pathway is the likely dominant pathway for its transport.

In this study, the transport of CP either in solution or patch form into and across the TEOM was assessed. The penetration capabilities of CP and its distribution were determined in the tissue and receptive medium of the basolateral compartment of the transwell tissue culture system using HPLC. At lower concentrations, the CP in solution form was detected in the TEOM tissue but it did not penetrate to reach the receptive medium after 10 minutes exposure. It is revealing that this duration of treatment was the minimal time for the CP to be detected in the tissue. However, when a higher concentration was applied at the same time point, the CP was detected in both the tissue and the receptive medium. Accumulation of CP into the TEOM tissue and receptive medium was both time and concentration dependent. In contrast, the minimal contact time of CP in the patch form that was sufficient to be detected in the tissue was one hour for all concentrations analysed. Results also demonstrated that

only CP released from 20 µg patches accumulated in the receptive medium after one-hour exposure. Studies examining the adsorption of CP into any epithelial tissue are sparse. Previous CP permeation tests on porcine skin showed that the minimal time for the drug to permeate the skin was 3 hours and the accumulation of drug increased up to 6 hours yet no CP was detected in the receptive medium after 6 hours, irrespective of dosage form being used (Silva et al., 2012; Senyigit et al., 2010). Compared to the TEOM model system structure, it can be postulated that the complexity, thickness and keratinisation of the porcine skin limited the transport of CP, regardless of the physicochemical properties of the molecule (Kulkarni et al., 2009), increasing the duration of time for the compound to penetrate and traverse the tissue. The penetration of CP into the TEOM was fast, irrespective of being in the soluble or patch-loaded formulation as the drug permeated the tissue in 10 minutes. This is likely to be due to a combination of the high lipophilicity of CP and the lack of keratinisation and lower level of permeability barrier in the TEOM than found in porcine skin.

Previously, researchers have utilised Jurkat T cells, originally isolated from a patient with leukaemia, as a surrogate for normal T cells in experimental studies (Basak and Banerjee; 2016; Seggewiss et al., 2005; Yiemwattana et al., 2012). Although Jurkat T cells differ in some aspects from normal peripheral blood T cells, they serve as a good model cell system and profit from ease of culture and the lack of requirement to isolate the cells from peripheral blood. Previous studies have shown that these cells can be activated using PHA or PMA either singularly or as a combination with various concentrations and incubation periods described in the literature (Basak and Banerjee, 2016; Fernández-Riejos et al., 2008). Analysis in this study showed that Jurkat T cells treated with a combination of PHA and PMA cultured in Green's medium caused a marked activation of the cells, inducing significant levels of IL-2 secretion that were consistent over time up to 24 hours. Thereby, indicating that this type of activation, although not entirely realistic of T cell activation in OLP, is sufficient enough to examine activated T cell responses to corticosteroids in an OLP-like TEOM model.

Activated T cells were added to the lower chamber of a transwell system with the upper well containing the TEOM in order to mimic *in vitro* OLP, or at least a T cell mediated mucosal immune disease. OLP is associated with T cell-mediated immunity (Sato et al., 2015). Therefore, the OLP-like model was developed using activated IL-2 releasing T cells since elevated expression of IL-2 levels has been reported in OLP lesions previously (Piccinni et al., 2014; Hasseus et al., 2001). Increased IL-2 levels also reflect the immune dysregulation status that is associated with the immunopathogenesis of OLP (Alikhani et al., 2017; Lu et al., 2015). IL-2 is essential for the development, proliferation and survival of T cells (Gutsol et al., 2015) and mediates its effects by binding to the IL-2 receptor (IL-2R) on T cells in an autocrine manner (Lu et al., 2015). The decreased expression of a few cytokines relevant to inflammatory diseases, including IL-2, following treatment with CS had been reported in several previous studies (Uva et al., 2012; Bianchi et al., 2000; Barnes, 1998). In general, the therapeutic effect of corticosteroids includes the depletion of circulating T cells which results in the inhibition of IL-2 secretion as well as signal transduction via the IL-2R (De Jong et al., 1999; Paliogianni et al., 1993). Other immunosuppressive agents besides CP such as dexamethasone and cyclosporin A are also reported to inhibit T cell IL-2 secretion (Lu et al., 2015; Malek, 2008), suggesting that IL-2 is a useful biomarker which can be used to evaluate the efficiency of immunosuppressive molecules.

The results described in this chapter revealed that the efficiency of CP in reducing IL-2 levels in the *in vitro* TEOM OLP model was comparable between patch-loaded CP and that delivered in solution, despite a greater amount of CP entering the basolateral lower chamber for solution than the patch form as determined by HPLC analysis. It can be postulated that the smaller amount of CP delivered in the patch form was still sufficient to inhibit the level of T cell secreted IL-2, which may reflect the potency of CP. In addition, the formulations of CP showed different absorption characteristics where tissue absorption of CP in solution was rapid whereas patch-loaded CP exhibited a slower tissue uptake. This difference in rate of tissue absorption is likely due to the release profile characteristics of the patch-loaded CP compared to CP free in solution. In a soluble form CP is freely mobile and which allows fast and direct

absorption (Chillistone and Hardman, 2017; Gautami, 2016). In contrast, in the patch-loaded form, CP is held within the polymer fibers in an amorphous form (Colley et al 2018). Hydration and collapse of the polymer complex is required in order for the CP to be released that is in part controlled by levels of RS100. Therefore, patch-loaded drugs are delivered much more slowly to tissues than drugs in free solution (Gilhotra et al., 2014; Boddupalli et al., 2010: Artusi et al., 2003). Indeed, the ability to control the rate of drug release is a distinct advantage for treating oral lesions.

The disappearance or lower drug recovery in the tissue or receptive medium might be due to its biotransformation into metabolites when catalysed by cytochrome P450 enzymes that likely exist in the epithelium of the tissue (Smith et al., 2017; Zanger and Schwab, 2013). Noteworthy, the treatment of TEOM with the placebo patch also reduced IL-2 levels significantly compared to TEOM treated with buffer alone after 4 hours. The reason for this is uncertain, as the patches contain no previously detected bioactive molecule. It is plausible that polymers derived from the mucoadhesive layer may traverse the epithelium to directly affect T cells, although the size of these polymers make this unlikely, or activate the epithelium which then responds by secreting a factor that can inhibit IL-2 secretion from T cells. Further research is required to ascertain the reason for this finding.

A major limitation of this study was the efficiency of the extraction procedure used for quantifying the amount of compound in the TEOM; which sometimes caused low recovery of the compound and was largely responsible for the large standard deviation in the individual datasets. It was troublesome to get a clear separation between the supernatant and cell pellets. The interference of the cell residue impacted the HPLC analysis, which occasionally caused failure of the instrument. To address this issue, tissue supernatants were filtered to remove any cell residue and minimise the occurrence of the problem. It was previously reported that the interaction between analytes, lipids and proteins may cause low drug recovery (Silva et al., 2012). In addition, only reduction of IL-2 as a marker of T cell activation was measured. Although a good marker, several others are available including the cell surface marker CD69 along with other cytokines. Time permitting, it would have been

advantageous to measure a decrease in the expression or secretion of other activation markers as well decreased activation of signal transduction pathways such as NFκB, AP-1 and NFAT.

6.5 Summary

In this chapter an *in vitro* model of OLP was created using TEOM with underlying activated T cells secreting IL-2 in order to show the efficacy of topically delivered CP, with particular emphasis on electrospun patch-loaded CP as a drug delivery system. The amounts of CP that permeated into the tissue and accumulated in the receptive medium increased in a time and dose-dependent manner, irrespective of CP formulation. CP-loaded patches released the drug into tissue and receptive medium that was in sufficient levels to decrease T cell activation, if placed onto a lesion *in vivo*, this is highly likely to result in targeted therapy with the ability to reduce T cell activation in the connective tissue as well as in the basal epithelium, sites where activated T cells are known to cause pathology in OLP and other inflammatory oral lesions.

CHAPTER 7

GENERAL DISCUSSION, CONCLUSION AND FUTURE WORK

7.1 General discussion

The standard procedure in drug development typically starts with the screening of a candidate compound in pre-clinical studies prior to clinical trials, which are finally followed by commercialisation of the compound (Breslin and O'Driscoll, 2013; DiMasi and Grabowski, 2007). In pre-clinical studies there are several alternative biological model systems that are commonly used including various forms of two-dimensional (2D) cell culture and animal models (Gazdar et al., 2016; Denayer et al., 2014). However, each of these model systems has drawbacks that have contributed to the low success rate (≈10%) of tested compounds in clinical trials (Denayer et al., 2014). Most tested compounds fail due to their low efficacy and/or undesirable toxicity (Hopkins, 2008), mainly because the pre-clinical experimental systems failed to provide sufficient critical information that is required for prediction of drug efficacy and safety (Brajša et al., 2016; Kim, 2005). In order to reduce the considerable costs associated with clinical trials, it is best to eliminate test compounds that are less efficient or show undesirable toxicity as early as possible, ideally prior to animal testing (Edmondson et al., 2014).

One way to address the limitations observed in 2D and animal model systems is by establishing 3D culture systems. If developed and validated correctly, these model systems can accurately mimic the *in vivo* conditions by enabling cells to interact in a biological environment that better reflects native tissues both structurally and physiologically. Such 3D environments drastically differ from 2D model systems where cell often grow as monolayer cultures on plastic surface that are far removed from *in vivo* conditions (Antoni et al., 2015; Edmondson et al., 2014). Animal models are commonly employed over *in vitro* models because, being living organisms, it is supposed that these better reflect the human *in vivo* situation (Antoni et al., 2015). However, the use of experimental animal models is associated with ethical issues, as

well as unpredictable responses that may be far removed by those experienced by humans due to species variation. They can also be costly and time-consuming (Langhan, 2018; Antoni et al., 2015; Sivaraman et al., 2005). *Ex vivo* human tissue can also act as a model system and this is biologically closest to the *in vivo* situation. However, problems encountered include maintaining tissue viability and access to tissue making this model difficult for routine testing purposes (Antoni et al., 2015). Tissue engineered 3D model systems offer a solution in terms of ethical and economic reasons as well as minimising the use of animals in research. It is argued that these models also provide more predictive data for *in vivo* tests prior to clinical trials (Edmondson et al., 2014).

Most tissue engineered model systems use primary human cells, but like human tissue access to these is restricted and data in repeat experiments may vary widely due to genetic background differences of the cell donors. More recent research has moved to use immortalized human cells that can proliferate almost indefinitely whilst retaining the morphology of normal cells, usually by over-expression of TERT-2, although such studies for the oral mucosa are limited (Buskermolen et al., 2016; Jennings et al., 2016; Dongari-Bagtzoglou and Kashleva, 2006).

Data provided in chapter 3 demonstrate that full-thickness TEOM can be successfully constructed from FNB6 oral keratinocytes. These TEOM display a histological structure that is very similar to the normal oral mucosa, having a stratified squamous epithelium, basement membrane and connective tissue. Indeed, it seems that FNB6 TEOM exhibit better growth and differentiation of the epithelial layers when compared to the TEOM constructed using other oral mucosal immortalised cells (Buskermolen et al., 2016; Dongari-Bagtzoglou and Kashleva, 2006). FNB6 TEOM also showed normal expression of proteins involved in keratinocyte differentiation (CK4, CK13 and CK14) and proliferation (Ki-67) processes within different layers of the epithelium, confirming that cell immortalisation does not cause any alteration in mucosal epithelial biology.

The crucial aspect to this study, which is largely based on drug delivery into and across the mucosa, was to ensure that the epithelial integrity and permeability barrier function of the TEOM are present. Data in chapter 3 showed that the TEOM displayed a normal expression pattern of structural and integrity molecules such as E-cadherin and Claudin-4, which form tight junctions (De Vicente et al., 2015). TEOM also displayed intercellular junction-related structures such as desmosomes as well as hemidesmosomes that are important in cell to basement membrane adhesion (Squier and Brogden, 2011: Kinikoglu et al., 2009; Niessen, 2007). In addition, data obtained for TEER and permeability against dextrans confirmed the integrity status of the TEOM, showing that TEOM constructed of immortalised FNB6 cells are fit to be used for drug delivery experiments, particularly if long-duration experiments are intended.

Corticosteroids are the treatment used for mucosal lesions such as OLP (Córdova et al., 2014) and RAS (Scully and Porter, 2008). To date several types of corticosteroids are used in treatment regimes, with these corticosteroids ranging from mild to very potent. However, the increasing level of potency of the corticosteroid used has been associated with increasing degree of side effects (McKenzie and Stoughton, 1962). This assertion was exemplified in data provided in chapter 4, which showed that highly potent corticosteroids such as CP had a lower IC_{50} values towards oral keratinocytes and fibroblasts than milder corticosteroids. In fact, data provided in chapter 4 showed that there was a distinct correlation between potency of corticosteroid as defined in the British National Formulary and toxicity towards oral keratinocytes, fibroblasts and TEOM. However, most notably the toxicity toward TEOM was lower than for monolayer cultures because of its multilayered nature and permeability barrier that are absent in 2D systems. This highlights the usefulness of TEOM over monolayer culture, suggesting that TEOM is the most appropriate *in vitro* experimental model to use in order to predict the response of drugs as close to *in vivo* conditions.

The current oral drug delivery systems for corticosteroids such as mouthwashes, creams or ointments are dramatically affected by the conditions in the oral cavity, such as saliva flow rate and mechanical forces causing the drug to have minimal

contact time with the oral lesion. This inevitably leads to inefficient drug absorption and distribution (Madhav et al., 2012; Sankar et al., 2011).

Development of electrospun mucoadhesive oral patches has given rise to the prospect of drug delivery via drug-loaded patches (Santocildes-Romero et al., 2017). The use of mucoadhesive oral patches with a protective backing layer will ensure that delivery of the drug is unaffected by the conditions of the oral cavity with unidirectional release of drug directly to the lesion (Patel et al., 2011; Alur et al., 1999). This may increase lesion healing and thus increase patient compliance because it is a more convenient route of administration (Satheesh Madhav et al., 2012). The absorption of the drug is likely to be improved and so frequency of dosing could be reduced as well as off-target and systemic side effects of the drug (Sankar et al., 2011; Patel et al., 2011; Alur et al., 1999). The side effects of corticosteroids are unavoidable, irrespective of their potency level, but this may be controllable. Thus, the use of highest potent corticosteroids (e.g. CP) in a clinical setting is sensible as long as the dose of the drug and the duration of the treatment are controlled (Stanbury and Graham, 1998). Data provided in chapter 5 show that CP-loaded patches are homogeneous as far as physical characteristics are concerned, are non-toxic and can be manufactured with increasing drug content. Moreover, the drug is released efficiently from the patches in a time and dose-dependent manner. Recently published data also demonstrate their adhesiveness to human buccal, gingival and tongue mucosa in a first human study, where the patches were acceptable to wear over prolonged periods (Colley et al., 2018). Moreover, the patches rapidly hydrate and swell upon contact with aqueous solution such as saliva, which not only causes their mucoadhesiveness but also initiates drug release from the polymers. Data in chapter 5 show that CP was released from the patch into the TEOM in a time and dose-dependent manner. These data are the first to show electrospun polymer patch delivery of a corticosteroid to TEOM in pre-clinical experiments.

The development of a disease model TEOM to test novel therapeutic formulations is an attractive approach. Experiments in chapter 6 showed the use of a simple adaptation of the TEOM system by the addition of activated T cells at the basolateral

surface of the connective tissue. Although a similar model was used to mimic atopic dermatitis (Sriram et al., 2018), this is the first to be developed to mimic oral lesions such as OLP. Ideally the T cells should reside just below the basement membrane in the connective tissue and be dispersed within the lower epithelium where they exert their cytotoxic effects causing epithelial cell destruction. However, due to time limitations, the activated T cells were placed in the receptive medium basolateral to the connective tissue. It is highly likely that more complex models will be developed in future.

The use of the OLP-like TEOM model constructed in this study provided a good assay in providing evidence for the efficacy of immunosuppressant effects of corticosteroids particularly patch-loaded CP for OLP treatment. Such a tissue engineered OLP model may be suitable to be utilised to study the more mechanistic aspects of the disease, instead of using animal experimental models (Van De Worp et al., 2010; Yamada and Cukierman, 2007). While the use of IL-2 as a biomarker for OLP may be valuable in diagnosing the status of the disease with greater ease and accuracy and at a lower cost. Importantly, data in chapter 6 show that CP-loaded patches were able to reduce the activation status of activated T cells by significantly reducing IL-2 levels. Moreover, this was achieved at much lower doses than that for CP in a solution. Some of the data provided in this thesis have been instrumental in the development of the novel electrospun patch drug delivery system. Data provided by the TEOM model was mirrored by those observed using a mini-pig model, validating its usefulness in drug delivery research (Colley et al., 2018). Indeed, the use of TEOM as a model assay system has strengthened the case for the use of such a novel delivery formulation for oral lesions. At present, the CP-drug loaded oral patches have entered phase 2 clinical trials and data from these are expected in 2019.

7.2 General conclusion

The *in vivo*-like conditions of 3D model systems has broadened the opportunities to new, highly versatile assay systems in the various field of research. As proven, this study has extended the applications of TEOM in drug delivery and toxicity as well as in therapeutic applications that have been used to assess the use of corticosteroids for OLP treatment. As a more humane alternative, the use of TEOM allows experiments to be performed on tissue that more accurately mimics the human *in vivo* situation.

The oral mucosa provides an alternative route for drug delivery as it offers many advantages that could address some of the limitations of conventional drug administration through oral and other routes (e.g. parenteral). The possibility of retentive drug delivery for an extended period of time to the oral mucosa shows favourable opportunities for the application of the new formulation of mucoadhesive bilayer patches containing CP, which is less affected by conditions in the oral cavity as compared to current formulations. Thus, this novel therapeutic approach could increase drug absorption and patient compliance as it accessible and non-invasive, whilst also reducing the frequency of dosing as well as lowering the costs.

7.3 Future work

7.3.1 Factors affecting drug absorption in the oral cavity

The conditions of oral cavity display some significant obstacles where the physiological aspects of the oral cavity such pH, fluid volume and composition (saliva) have become the barriers for drug delivery (Patel et al., 2011). The enzymes that present in the saliva such as aminopeptidase could affect the absorption of the drug (Nielsen and Rassing, 2000). The simulation of oral cavity like-environments in the TEOM could be performed by the addition of enzyme-containing artificial saliva onto the surface of TEOM prior to the application of corticosteroid and this might be a way to assess the effects of enzymes against the absorption corticosteroids.

Permeability of the drug through oral mucosa is also affected by the different lipid composition of the epithelium, even if it is keratinised (e.g. ceramides and acylceramides) or non-keratinised, (e.g. cholesterol sulfate and glucosyl ceramides) (Squier and Wertz, 1996; Consuelo et al., 2005) and also affected by the existence of membrane coating granules (MCG) in the epithelium (Harris and Robinson, 1992; Galey et al., 1976). Thus, a comparative analysis could be performed using the lipophilic (e.g. cyclosporin A) and hydrophilic (e.g. ranitidine) drug that would also validate the composition of the lipids and MCG in the TEOM.

7.3.2 Strategies to improve drug absorption

The emergence of technologies such as permeation enhancers and enzyme inhibitors could be a potential approach to address the obstacles in delivering the drug in the oral cavity (Sudhakar et al., 2006). Therefore, incorporation of permeation enhancers (e.g. bile salts) and enzyme inhibitors (e.g. aminopeptidase inhibitors) (Jani et al., 2012; Ueno et al., 2007) in the formulations could improve the absorption of the corticosteroids across the oral mucosa.

7.3.3 Drug-metabolising cytochrome P450 enzymes expression

The variability in pharmacokinetic and response of corticosteroids may be partly related to the activity of drug-metabolising cytochrome P450 enzymes in the oral epithelium or connective tissue. It has been reported that cytochrome p450 enzymes such as CYP3A4 and CYP3A5 are involved in regulating the level of glucocorticoids (Dvorak and Pavek, 2010; Vondracek et al., 2001). Therefore, understanding of cytochrome p450 enzyme activities in the oral mucosa is likely to be relevant in clinical practice. Understanding drug-drug interactions, different metabolic enzyme activity in different individuals may also help prevent the potential adverse effects (Martin and Fay, 2001).

7.3.4 Oral lichen planus-like model development

The use of primary T cells for OLP-like model construction is necessary as a comparison to the use of immortalised Jurkat T cells. This comparative analysis is needed in order to evaluate any differential response of the cells against stimulants as well as assessing

the sustainability of IL-2 release by the activated T cells. In addition, placing activated T cells in the connective tissue and juxtapose basal keratinocytes would further mimic OLP. More advanced models could use matched keratinocytes, fibroblasts and activated T cells from OLP patients so that the disease model could be replicated in full. It is also possible that OLP models could be generated using induced pluripotent stem cells derived from OLP patients.

The immunosuppressive effects of corticosteroids against OLP are mediated by inhibiting the IL-2 release produced by the activated T cells as well as the signal transduction through IL-2 receptors (De Jong et al., 1999; Paliogianni et al., 1993). Therefore, the analysis of the expression of IL-2 receptors could validate the pathogenesis of the disease and also evaluate the efficiency of the corticosteroids therapy against OLP. In addition, expression analysis of other biomarkers of OLP is required to show robustness of the model.

REFERENCES

Ahluwalia, A. (1998). Topical Glucocorticoids and The Skin-Mechanisms of Action: An Update. *Mediators of Inflammation*, 7(3), pp.183-193.

Aktary, Z. and Pasdar, M. (2012). Plakoglobin: Role In Tumorigenesis And Metastasis. *International Journal of Cell Biology*, 2012, pp.1-14.

Alam, H., Sehgal, L., Kundu, S.T., Dalal, S.N. and Vaidya, M.M. (2011). Novel Function of Keratins 5 And 14 in Proliferation and Differentiation of Stratified Epithelial Cells. *Molecular Biology of the Cell*, 22(21), pp.4068-4078.

Alexandre, G., Philippe, H., Marion, T., Patrice, M., Carole, C.M. and Céline, V. (2015). Effects of Topical Corticosteroids on Cell Proliferation, Cell Cycle Progression and Apoptosis: *In vitro* Comparison on HaCaT. *International journal of pharmaceutics*, 479(2), pp.422-429.

Al-Hashimi, I., Schifter, M., Lockhart, P., Wray, D., Brennan, M., Migliorati, C., Axéll, T., Bruce, A., Carpenter, W., Eisenberg, E., Epstein, J., Holmstrup, P., Jontell, M., Lozada-Nur, F., Nair, R., Silverman, B., Thongprasom, K., Thornhill, M., Warnakulasuriya, S. and van der Waal, I. (2007). Oral Lichen Planus and Oral Lichenoid Lesions: Diagnostic and Therapeutic Considerations. *Oral Surgery, Oral Medicine, Oral Pathology, Oral Radiology, and Endodontology*, 103, pp.S25.e1-S25.e12.

Alikhani, M., Ghalaiani, P., Askariyan, E., Khunsaraki, Z. A., Tavangar, A. and Naderi, A. (2017). Association Between The Clinical Severity Of Oral Lichen Planus And Anti-TPO Level In Thyroid Patients. *Brazilian Oral Research*, *31*(0), pp.10–15.

Allenby, C. and Sparkes, C. (1981). Halogenation And Topical Corticosteroids: A Comparison Between The 17-Butyrate Esters Of Hydrocortisone And Clobetasone In Ointment Bases. *British Journal of Dermatology*, 104(2), pp.179-183.

Allen-Hoffmann, B. and Rheinwald, J. (1984). Polycyclic Aromatic Hydrocarbon Mutagenesis Of Human Epidermal Keratinocytes In Culture. *Proceedings of the National Academy of Sciences*, 81(24), pp.7802-7806.

Almela, T., Brook, I. and Moharamzadeh, K. (2016). Development Of Three-Dimensional Tissue Engineered Bone-Oral Mucosal Composite Models. *Journal of Materials Science: Materials in Medicine*, 27(4), pp.1-8.

Alur, H., Beal, J., Pather, S., Mitra, A. and Johnston, T. (1999). Evaluation Of A Novel, Natural Oligosaccharide Gum As A Sustained-Release And Mucoadhesive Component Of Calcitonin Buccal Tablets. *Journal of Pharmaceutical Sciences*, 88(12), pp.1313-1319.

Amano, S., Akutsu, N., Matsunaga, Y., Kadoya, K., Nishiyama, T., Champliaud, M., Burgeson, R. and Adachi, E. (2001). Importance of Balance between Extracellular Matrix Synthesis and Degradation in Basement Membrane Formation. *Experimental Cell Research*, 271(2), pp.249-262.

Anoop, K.M. (2015). Oral Local Drug Delivery: An Overview. *Pharmacy and Pharmacology Research*, 3 (1), pp. 1-6.

Antoni, D., Burckel, H., Josset, E. and Noel, G. (2015). Three-Dimensional Cell Culture: A Breakthrough in Vivo. *International Journal of Molecular Sciences*, 16(12), pp.5517-5527.

Aoyama, T., Yamano, S., Waxman, D.J., Lapenson, D.P., Meyer, U.A., Fischer, V., Tyndale, R., Inaba, T., Kalow, W., Gelboin, H.V., and Gonzalez, F.J. (1989). Cytochrome P-450 hPCN3, a novel cytochrome P-450 IIIA gene product that is differentially expressed in adult human liver. cDNA and deduced amino acid sequence and distinct specificities of cDNA-expressed hPCN1 and hPCN3 for the metabolism of steroid hormo. *Journal of Biological Chemistry*, 264(18), pp.10388–10395.

Artusi, M., Santi, P., Colombo, P. and Junginger, H. (2003). Buccal Delivery Of Thiocolchicoside: In Vitro And In Vivo Permeation Studies. *International Journal of Pharmaceutics*, 250(1), pp.203-213.

Atkinson, M., Jowett, A. and White, F. (2000). *Principles of Anatomy and Oral Anatomy for Dental Students*. Taddington, U.K.: Cava Cadavers.

Avinash N. (2008). Science And Technology Of Bioadhesive-Based Targeted Oral Delivery Systems. *Pharmaceutical Technology*, 32, pp.100-21.

Ayres, P. and Hooper, G. (1978). Assessment Of The Skin Penetration Properties Of Different Carrier Vehicles For Topically Applied Cortisol. *British Journal of Dermatology*, 99(3), pp.307-317.

Bach, A., Bannasch, H., Galla, T., Bittner, K. and Stark, G. (2001). Fibrin Glue as Matrix for Cultured Autologous Urothelial Cells in Urethral Reconstruction. *Tissue Engineering*, 7(1), pp.45-53.

Bagan, J., Compilato, D., Paderni, C., Campisi, G., Panzarella, V., Picciotti, M., Lorenzini, G. and Di Fede, O. (2012). Topical Therapies for Oral Lichen Planus Management and their Efficacy: A Narrative Review. *Current Pharmaceutical Design*, 18(34), pp.5470-5480.

Bagán-Sebastián, J., Milián-Masanet, M., Peñarrocha-Diago, M. and Jiménez, Y. (1992). A Clinical Study of 205 Patients with Oral Lichen Planus. *Journal of Oral and Maxillofacial Surgery*, 50(2), pp.116-118.

Baid, S. and Nieman, L. (2006). Therapeutic Doses of Glucocorticoids: Implications for Oral Medicine. *Oral Diseases*, 12(5), pp.436-442.

Barange, H. and Asghar, S. (2017). Development Of Analytical Method For Simultaneous Estimation Of Hydroquinone And Monobenzone In Topical Formulation By RP-HPLC. *World Journal of Pharmaceutical Research*, pp.742-753.

Bardag-Gorce, F., Hoft, R., Wood, A., Oliva, J., Niihara, H., Makalinao, A., Thropay, J., Pan, D., Meepe, I., Tiger, K., Garcia, J., Laporte, A., French, S. and Niihara, Y. (2016). The Role of E-Cadherin in Maintaining the Barrier Function of Corneal Epithelium after Treatment with Cultured Autologous Oral Mucosa Epithelial Cell Sheet Grafts for Limbal Stem Deficiency. *Journal of Ophthalmology*, 2016, pp.1-13.

Barnes, P. (1998). Anti-inflammatory Actions of Glucocorticoids: Molecular Mechanisms. *Clinical Science*, 94(6), pp.557-572.

Barnes, P. (2006). How Corticosteroids Control Inflammation: Quintiles Prize Lecture 2005. *British Journal of Pharmacology*, 148(3), pp.245-254.

Barrett, A. and Beynon, A. (1991). A Histochemical Study On The Distribution Of Melanin In Human Oral Epithelium At Six Regional Sites. *Archives of Oral Biology*, 36(10), pp.771-774.

Barrett, A., Cruchley, A. and Williams, D. (1996). Oral Mucosal Langerhans' Cells. *Critical Reviews in Oral Biology & Medicine*, 7(1), pp.36-58.

Basak, N. and Banerjee, S. (2016). Crosstalk between Notch signaling Pathway and Glutamine uptake during Jurkat T cell activation. *Matters (Zürich)*, pp.1–7.

Bastos, L., de Marcondes, P., de-Freitas-Junior, J., Leve, F., Mencalha, A., de Souza, W., de Araujo, W., Tanaka, M., Abdelhay, E. and Morgado-Díaz, J. (2014). Progeny From Irradiated Colorectal Cancer Cells Acquire an EMT-LikePhenotype and Activate Wnt/β-Catenin Pathway. *Journal of Cellular Biochemistry*, 115(12), pp.2175-2187.

Battino, M., Greabu, M., Totan, A., Bullon, P., Bucur, A., Tovaru, S., … Totan, C. (2008). Oxidative Stress Markers in Oral Lichen Planus. *BioFactors (Oxford, England)*, 33(4), pp.301–310.Ergun, S., Troşala, Ş., Warnakulasuriya, S., Özel, S., Önal, A., Ofluoğlu, D., Güven, Y. and Tanyeri, H. (2010). Evaluation of oxidative stress and antioxidant profile in patients with oral lichen planus. *Journal of Oral Pathology & Medicine*, 40(4), pp.286-293.

Bayar, G. R., Aydintuğ, Y. S., Günhan, Ö., Öztürk, K. and Gülses, A. (2012). Ex Vivo Produced Oral Mucosa Equivalent By Using The Direct Explant Cell Culture Technique. *Balkan Medical Journal*, *29*(3), pp.295–300.

Becker, J., Schuppan, D., Hahn, E., Albert, G. and Reichart, P. (1986). The Immunohistochemical Distribution Of Collagens Type IV, V, VI And Of Laminin In The Human Oral Mucosa. *Archives of Oral Biology*, 31(3), pp.179-186.

Belenguer-Guallar, I., Jimenez-Soriano, Y. and Claramunt-Lozano, A. (2014). Treatment Of Recurrent Aphthous Stomatitis. A Literature Review. *Journal of Clinical and Experimental Dentistry*, pp.e168-74.

Benedetti, M., Whomsley, R., Poggesi, I., Cawello, W., Mathy, F., Delporte, M., Papeleu, P. and Watelet, J. (2009). Drug Metabolism And Pharmacokinetics. *Drug Metabolism Reviews*, 41(3), pp.344-390.

Bhargava, S., Chapple, C., Bullock, A., Layton, C. and MacNeil, S. (2004). Tissue-Engineered Buccal Mucosa for Substitution Urethroplasty. *BJU International*, 93(6), pp.807-811.

Bhat, V., Prasad, K., Balaji S, S. and Bhat, A. (2011). Role of Tissue Engineering in Dentistry. *Journal of Acquired Immune Deficiency Syndromes*, 2(1), pp.37-42.

Bhati, R. and K Nagrajan, R. (2012). A Detailed Review on Oral Mucosal Drug Delivery System. *International Journal of Pharmaceutical Sciences and Research*, 3(3), pp.659 -681.

Bianchi, M., Meng, C. and Ivashkiv, L. (2000). Inhibition Of IL-2-Induced Jak-STAT Signaling By Glucocorticoids. *Proceedings of the National Academy of Sciences*, 97(17), pp.9573-9578.

Bircher, A., Pelloni, F., Messmer, S. and Müller, D. (1996). Delayed Hypersensitivity Reactions to Corticosteroids Applied to Mucous Membranes. *British Journal of Dermatology*, 135(2), pp.310-313.

Blumenberg, M. and Tomic-Canic, M. (1997). Human Epidermal Keratinocyte: Keratinization Processes. *EXS.*, 78, pp.1-29.

Boddupalli, B., Mohammed, Z., Nath, R. and Banji, D. (2010). Mucoadhesive Drug Delivery System: An Overview. *Journal of Advanced Pharmaceutical Technology & Research*, 1(4), p.381.

Bodor, N., Harget, A. and Phillips, E. (1983). Structure-Activity Relationships In The Antiinflammatory Steroids: A Pattern-Recognition Approach. *Journal of Medicinal Chemistry*, 26(3), pp.318-328.

Boorghani, M., Gholizadeh, N., Taghavi Zenouz, A., Vatankhah, M. and Mehdipour, M. (2010). Oral Lichen Planus: Clinical Features, Etiology, Treatment and Management; A Review of Literature. *Journal of Dental Research, Dental Clinics, Dental Prospects*, 4(1), pp.3 - 9.

Bornstein, M., Reichart, P., Buser, D. and Bosshardt, D. (2011). Tissue Response and Wound Healing After Placement of Two Types of Bioengineered Grafts Containing Vital Cells in Submucosal Maxillary Pouches: An Experimental Pilot Study in Rabbits. *The International Journal of Oral & Maxillofacial Implants*, 26(4), pp.768–775.

Borradori, L. and Sonnenberg, A. (1999). Structure and Function of Hemidesmosomes: More Than Simple Adhesion Complexes. *Journal of Investigative Dermatology*, 112(4), pp.411-418.

Bos, J. and Meinardi, M. (2000). The 500 Dalton rule for the skin penetration of chemical compounds and drugs. *Experimental Dermatology*, 9(3), pp.165-169.

Brajša, K., Trzun, M., Zlatar, I. and Jelić, D. (2016). Three-Dimensional Cell Cultures As A New Tool In Drug Discovery. *Periodicum Biologorum*, *118*(1), pp.59–65.

Breslin, S. and O'Driscoll, L. (2013). Three-Dimensional Cell Culture: The Missing Link In Drug Discovery. *Drug Discovery Today*, 18(5-6), pp.240-249.

British National Formulary. (2018). *Homepage | BNF Publications*. [online] Bnf.org. Available at: https://www.bnf.org/ [Accessed 2 Aug. 2018].

Broersen, L., Pereira, A., Jørgensen, J. and Dekkers, O. (2015). Adrenal Insufficiency in Corticosteroids Use: Systematic Review and Meta-Analysis. *The Journal of Clinical Endocrinology & Metabolism*, 100(6), pp.2171-2180.

Bruno, B., Miller, G. and Lim, C. (2013). Basics And Recent Advances In Peptide And Protein Drug Delivery. *Therapeutic Delivery*, 4(11), pp.1443-1467.

Bruno, S. and Darzynkiewicz, Z. (1992). Cell Cycle Dependent Expression And Stability Of The Nuclear Protein Detected By Ki-67 Antibody In HL-60 Cells. *Cell Proliferation*, 25(1), pp.31-40.

Bruschi, M. and de Freitas, O. (2005). Oral Bioadhesive Drug Delivery Systems. *Learning and Developmental Disabilities Initiative*, 31(3), pp.293-310.

Buchert, M., Turksen, K. and Hollande, F. (2012). Methods to Examine Tight Junction Physiology in Cancer Stem Cells: TEER, Paracellular Permeability, and Dilution Potential Measurements. *Stem Cell Reviews and Reports*, 8(3), pp.1030-1034.

Buhl, R. (2006). Local Oropharyngeal Side Effects Of Inhaled Corticosteroids In Patients With Asthma. *Allergy*, 61(5), pp.518-526.

Buhse, L., Kolinski, R., Westenberger, B., Wokovich, A., Spencer, J., Chen, C., Turujman, S., Gautam-Basak, M., Kang, G., Kibbe, A., Heintzelman, B. and Wolfgang, E. (2005). Topical Drug Classification. *International Journal of Pharmaceutics*, 295(1-2), pp.101-112.

Burkholder, B. (2000). Topical Corticosteroids: An Update. *Current Problems in Dermatology*, 12(5), pp.222-225.

Buskermolen, J., Reijnders, C., Spiekstra, S., Steinberg, T., Kleverlaan, C., Feilzer, A., Bakker, A. and Gibbs, S. (2016). Development of a Full-Thickness Human Gingiva Equivalent Constructed from Immortalized Keratinocytes and Fibroblasts. *Tissue Engineering Part C: Methods*, 22(8), pp.781-791.

Campisi, G., Giannola, L., Florena, A., De Caro, V., Schumacher, A., Göttsche, T., Paderni, C. and Wolff, A. (2010). Bioavailability *In Vivo* of Naltrexone Following Transbuccal Administration By An Electronically-Controlled Intraoral Device: A Trial on Pigs. *Journal of Controlled Release*, 145(3), pp.214-220.

Carbone, M., Arduino, P., Carrozzo, M., Caiazzo, G., Broccoletti, R., Conrotto, D., Bezzo, C. and Gandolfo, S. (2009). Topical Clobetasol in the Treatment of Atrophic-Erosive Oral Lichen Planus: A Randomized Controlled Trial to Compare Two Preparations with Different Concentrations. *Journal of Oral Pathology & Medicine*, 38(2), pp.227-233.

Carbone, M., Goss, E., Carrozzo, M., Castellano, S., Conrotto, D., Broccoletti, R. and Gandolfo, S. (2003). Systemic and Topical Corticosteroid Treatment of Oral Lichen Planus: A Comparative Study with Long-Term Follow-Up. *Journal of Oral Pathology & Medicine,* 32(6), pp.323-329.

Carrozzo, M. (2014). Understanding the Pathobiology of Oral Lichen Planus. *Current Oral Health Reports*, 1(3), pp.173-179.

Carrozzo, M. and Gandolfo, S. (1999). The Management of Oral Lichen Planus. *Oral Diseases*, (5), pp.196-205.

Carrozzo, M. and Thorpe, R. (2009). Update on oral lichen planus. *Expert Review of Dermatology*, 4(5), pp.483-494.

Çelebi, C.R. and Yörükan, S. (1999). *Physiology of the Oral Cavity. In Oral Diseases*. Springer Berlin Heidelberg, pp. 7-14.

Chai, W., Moharamzadeh, K., Brook, I., Emanuelsson, L., Palmquist, A. and van Noort, R. (2010). Development of a Novel Model for the Investigation of Implant–Soft Tissue Interface. *Journal of Periodontology*, 81(8), pp.1187-1195.

Chang, G. and Kam, P. (1999). The Physiological And Pharmacological Roles Of Cytochrome P450 Isoenzymes. *Anaesthesia*, 54(1), pp.42-50.

Chao, M., Donovan, T., Sotelo, C. and Carstens, M. (2006). *In Situ* Osteogenesis of Hemimandible With rhBMP-2 in a 9-Year-Old Boy. *Journal of Craniofacial Surgery*, 17(3), pp.405-412.

Chatham, W. and Kimberly, R. (2001). Treatment of lupus with corticosteroids. *Lupus*, 10(3), pp.140-147.

Chen, F., Wu, T. and Cheng, X. (2012). Cytotoxic Effects Of Denture Adhesives On Primary Human Oral Keratinocytes, Fibroblasts And Permanent L929 Cell Lines. *Gerodontology*, 31(1), pp.4-10.

Chen, J. and Raymond, K. (2006). Roles Of Rifampicin In Drug-Drug Interactions: Underlying Molecular Mechanisms Involving The Nuclear Pregnane X Receptor. *Annals of Clinical Microbiology and Antimicrobials*, 5, pp.1–11.

Chen, M., Kasahara, N., Keene, D., Chan, L., Hoeffler, W., Finlay, D., Barcova, M., Cannon, P., Mazurek, C. and Woodley, D. (2002). Restoration Of Type VII Collagen Expression And Function In Dystrophic Epidermolysis Bullosa. *Nature Genetics*, 32(4), pp.670-675.

Chen, N., Cui, D., Wang, Q., Wen, Z., Finkelman, R. and Welty, D. (2018). In Vitro Drug–Drug Interactions Of Budesonide: Inhibition And Induction Of Transporters And Cytochrome P450 Enzymes. *Xenobiotica*, 48(6), pp.637-646.

Chen, R., Ho, H. and Sheu, M. (2005). Characterization Of Collagen Matrices Crosslinked Using Microbial Transglutaminase. *Biomaterials*, 26(20), pp.4229-4235.

Chen, Y., Lin, Y., Davis, K., Wang, Q., Rnjak-Kovacina, J., Li, C., Isberg, R., Kumamoto, C., Mecsas, J. and Kaplan, D. (2015). Robust Bioengineered 3D Functional Human Intestinal Epithelium. *Scientific Reports*, 5(1), pp.1-11.

Chillistone, S. and Hardman, J.G. (2017). Factors Affecting Drug Absorption And Distribution. *Anaesthesia and Intensive Care Medicine*, *18*(7), pp.335–339.

Chin, M., Ng, T., Tom, W. and Carstens, M. (2005). Repair of Alveolar Clefts with Recombinant Human Bone Morphogenetic Protein (rhBMP-2) in Patients with Clefts. *Journal of Craniofacial Surgery*, 16(5), pp.778-789.

Chinna Reddy, P., Chaitanya, K. S. C. and Madhusudan Rao, Y. (2011). A Review On Bioadhesive Buccal Drug Delivery Systems: Current Status Of Formulation And Evaluation Methods. DARU *Journal of Pharmaceutical Sciences*, 19(6), pp.385–403.

Chinnathambi, S., Tomanek-Chalkley, A., Ludwig, N., King, E., DeWaard, R., Johnson, G., Wertz, P. and Bickenbach, J. (2003). Recapitulation of Oral Mucosal Tissues in Long-Term Organotypic Culture. *The Anatomical Record Part A: Discoveries in Molecular, Cellular, and Evolutionary Biology*, 270(2), pp.162-174.

Cholerton, S., Daly, A. and Idle, J. (1992). The role of individual human cytochrpmes P450 in drug metabolism and clinical response. *Trends in Pharmacological Sciences*, 13, pp.434-439.

Chrousos, G., Pavlaki, A. N. and Magiakou, M.A. (2000). Glucocorticoid Therapy and Adrenal Suppression. *Endotext*, (2), 1–27.

Chrousos, G.P. (2015). Adrenocorticosteroids and adrenocortical antagonists. In: Katzung BG, Trevor AJ, editors. Basic and clinical pharmacology. 13th ed. New York, NY: McGraw Hill. pp. 680–95.

Colley, H., Hearnden, V., Jones, A., Weinreb, P., Violette, S., MacNeil, S., Thornhill, M. and Murdoch, C. (2011). Development of Tissue-Engineered Models of Oral Dysplasia and Early Invasive Oral Squamous Cell Carcinoma. *British Journal of Cancer*, 105(10), pp.1582-1592.

Colley, H., Said, Z., Santocildes-Romero, M., Baker, S., D'Apice, K., Hansen, J., Madsen, L., Thornhill, M., Hatton, P. and Murdoch, C. (2018). Pre-Clinical Evaluation Of Novel Mucoadhesive Bilayer Patches For Local Delivery Of Clobetasol-17-Propionate To The Oral Mucosa. *Biomaterials*, 178, pp.134-146.

Collins, L. and Dawes, C. (1987). The Surface Area of the Adult Human Mouth and Thickness of the Salivary Film Covering the Teeth and Oral Mucosa. *Journal of Dental Research*, 66(8), pp.1300-1302.

Conrotto, D., Carbone, M., Carrozzo, M., Arduino, P., Broccoletti, R., Pentenero, M. and Gandolfo, S. (2006). Ciclosporin Vs. Clobetasol In The Topical Management Of Atrophic And Erosive Oral Lichen Planus: A Double-Blind, Randomized Controlled Trial. *British Journal of Dermatology*, 154(1), pp.139-145.

Córdova, P., Rubio, A. and Echeverría, P. (2014). Oral Lichen Planus: A Look from Diagnosis to Treatment. *Journal of Oral Research,* 3(1), pp.62-67.

Costea, D. E., Johannessen, A. C. and Vintermyr, O. K. (2005). Fibroblast Control On Epithelial Differentiation Is Gradually Lost During In Vitro Tumor Progression. *Differentiation*, *73*(4),pp.134–141.

Costea, D., Loro, L., Dimba, E., Vintermyr, O. and Johannessen, A. (2003). Crucial Effects of Fibroblasts and Keratinocyte Growth Factor on Morphogenesis of Reconstituted Human Oral Epithelium. *Journal of Investigative Dermatology*, 121(6), pp.1479-1486.

Coutinho, A.E., & Chapman, K.E. (2011). The Anti-Inflammatory And Immunosuppressive Effects Of Glucocorticoids, Recent Developments And Mechanistic Insights. *Molecular and Cellular Endocrinology*, *335*(1), pp.2–13.

Cutroneo, K., Rokowski, R. and Counts, D. (1981). Glucocorticoids and Collagen Synthesis: Comparison of in vivo and Cell Culture Studies. *Collagen and Related Research*, 1(6), pp.557-568.

De Jong, E., Vieira, P., Kalinski, P. and Kapsenberg, M. (1999). Corticosteroids Inhibit The Production Of Inflammatory Mediators In Immature Monocyte-Derived DC And Induce The Development Of Tolerogenic DC3. *Journal of Leukocyte Biology*, 66(2), pp.201-204.

De Vicente, J. C., Fernández-Valle, Á., Vivanco-Allende, B., Rodríguez Santamarta, T., Lequerica-Fernández, P., Hernández-Vallejo, G. and Allonca-Campa, E. (2015). The Prognostic Role Of Claudins -1 And -4 In Oral Squamous Cell Carcinoma. *Anticancer Research*, *35*(5),pp.2949–2959.

Delforno, C., Holt, P. and Marks, R. (1978). Corticosteroid Effect On Epidermal Cell Size. *British Journal of Dermatology*, 98(6), pp.619-623.

Denayer, T., Stöhr, T. and Roy, M. (2014). Animal Models In Translational Medicine: Validation And Prediction. *European Journal of Molecular & Clinical Medicine*, 2(1), p.5.

Deneer, V., Drese, G., Roemelé, P., Verhoef, J., Lie-A-Huen, L., Kingma, J., Brouwers, J. and Junginger, H. (2002). Buccal Transport Of Flecainide And Sotalol: Effect Of A Bile Salt And Ionization State. *International Journal of Pharmaceutics*, 241(1), pp.127-134.

Diaz-del Consuelo, I., Jacques, Y., Pizzolato, G., Guy, R. and Falson, F. (2005). Comparison Of The Lipid Composition Of Porcine Buccal And Esophageal Permeability Barriers. *Archives of Oral Biology*, 50(12), pp.981-987.

Dickson, M.A., Hahn, W.C., Ino, Y., Ronfard, V., Wu, J.Y., Weinberg, R.A., Louis, D.N., Li, F.P. and Rheinwald, J.G. (2000). Human Keratinocytes That Express htert and Also Bypass a P16ink4a-Enforced Mechanism that Limits Life Span Become Immortal Yet Retain Normal Growth and Differentiation Characteristics. *Molecular and Cellular Biology*, 20(4), pp.1436-1447.

DiMasi, J. and Grabowski, H. (2007). Economics of New Oncology Drug Development. *Journal of Clinical Oncology*, 25(2), pp.209-216.

Dodla, S. and Velmurugan, S. (2013). Buccal Penetration Enhancers–An Overview. *Asian Journal of Pharmaceutical and Clinical Research,* 6(3), pp.39-47.

Dominiak, M., Łysiak-Drwal, K., Saczko, J., Kunert-Keil, C. and Gedrange, T. (2012). The Clinical Efficacy of Primary Culture of Human Fibroblasts in Gingival Augmentation Procedures—A Preliminary Report. *Annals of Anatomy - Anatomischer Anzeiger*, 194(6), pp.502-507.

Dongari-Bagtzoglou, A. and Kashleva, H. (2006). Development of a Highly Reproducible Three-Dimensional Organotypic Model of the Oral Mucosa. *Nature Protocols*, 1(4), pp.2012-2018.

Dorrego, M., Correnti, M., Delgado, R. and Tapia, F. (2002). Oral Lichen Planus: Immunohistology of Mucosal Lesions. *Journal of Oral Pathology & Medicine*, 31(7), pp.410-414.

Dott, C., Tyagi, C., Tomar, L., Choonara, Y., Kumar, P., du Toit, L. and Pillay, V. (2013). A Mucoadhesive Electrospun Nanofibrous Matrix for Rapid Oramucosal Drug Delivery. *Journal of Nanomaterials*, 2013, pp.1-19.

Duong, H., Le, A., Zhang, Q. and Messadi, D. (2005). A Novel 3-Dimensional Culture System as an *In Vitro* Model for Studying Oral Cancer Cell Invasion. *International Journal of Experimental Pathology*, 86(6), pp.365-374.

Dvorak, Z. and Pavek, P. (2010). Regulation Of Drug-Metabolizing Cytochrome P450 Enzymes By Glucocorticoids. *Drug Metabolism Reviews*, *42*(4), pp.621–635.

Edmondson, R., Broglie, J.J., Adcock, A.F. and Yang, L. (2014). Three-Dimensional Cell Culture Systems and Their Applications in Drug Discovery and Cell-Based Biosensors. *ASSAY and Drug Development Technologies*, *12*(4), pp.207–218.

Edwards, P. and Kelsch, R. (2002). Oral Lichen Planus: Clinical Presentation and Management. *The Journal of the Canadian Dental Association,* 68(8), pp.494-499.

Eisen, D. (2002). The Clinical Features, Malignant Potential, and Systemic Associations of Oral Lichen Planus: A Study of 723 Patients. *Journal of the American Academy of Dermatology*, 46(2), pp.207-214.

El-Ghannam, A., Starr, L. and Jones, J. (1998). Laminin-5 Coating Enhances Epithelial Cell Attachment, Spreading, and Hemidesmosome Assembly on Ti-6Al-4V Implant Material *In Vitro*. *Journal of Biomedical Materials Research*, 41(1), pp.30-40.

Elias, P. and Friend, D. (1975). The Permeability Barrier In Mammalian Epidermis. *The Journal of Cell Biology*, 65(1), pp.180-191.

El-Sankary, W., Bombail, V., Gibson, G. G. and Plant, N. (2002). Glucocorticoid-Mediated Induction Of CYP3A4 Is Decreased By Disruption Of A Protein: DNA Interaction Distinct From The Pregnane X Receptor Response Element. *Drug Metabolism and Disposition,* 30(9), pp.1029–1034.

Fang, Y., & Eglen, R. M. (2017). Three-Dimensional Cell Cultures in Drug Discovery and Development. *SLAS DISCOVERY: Advancing Life Sciences R&D*, 22(5), pp.456-472.

Farhi, D. and Dupin, N. (2010). Pathophysiology, Etiologic Factors, And Clinical Management Of Oral Lichen Planus, Part I: Facts And Controversies. *Clinics in Dermatology*, 28(1), pp.100-108.

Farthing, P., Matear, P. and Cruchley, A. (1990). The Activation Of Langerhans Cells In Oral Lichen Planus. *Journal of Oral Pathology and Medicine*, 19(2), pp.81-85.

Fathi, E., Mesbah-namin, S.A. and Farahzadi, R. (2014). Biomarkers in Medicine : An Overview. Medicine, 4(8), 1701–1718.

Federman, D.G, Froelich, C.W. and Kirsner, R.S. 1999. Topical Psoriasis Therapy. *American Family Physician*, 59 (4), pp.957-962.

Feinberg, S., Aghaloo, T. and Cunningham, L. (2005). Role of Tissue Engineering in Oral and Maxillofacial Reconstruction: Findings of the 2005 AAOMS Research Summit. *Journal of Oral and Maxillofacial Surgery*, 63(10), pp.1418-1425.

Felton, L. and Porter, S. (2013). An Update on Pharmaceutical Film Coating for Drug Delivery. *Expert Opinion on Drug Delivery*, 10(4), pp.421-435.

Ference, J. And Last, A. (2009). Choosing Topical Corticosteroids. *American Family Physician*, [online] 79(2), pp.135 - 140.

Fernández-Riejos, P., Goberna, R. and Sánchez-Margalet, V. (2008). Leptin Promotes Cell Survival and Activates Jurkat T Lymphocytes By Stimulation of Mitogen-Activated Protein Kinase. *Clinical & Experimental Immunology*, 151(3), pp.505-518.

Fisher, L. and Maibach, H. (1971). The Effect of Corticosteroids on Human Epidermal Mitotic Activity. *Archives of Dermatology*, 103(1), pp.39.

Fontana, M., Rezer, J., Coradini, K., Leal, D. and Beck, R. (2011). Improved Efficacy In The Treatment Of Contact Dermatitis In Rats By A Dermatological Nanomedicine Containing Clobetasol Propionate. *European Journal of Pharmaceutics and Biopharmaceutics*, 79(2), pp.241-249.

Fuchs, E. and Green, H. (1980). Changes In Keratin Gene Expression During Terminal Differentiation Of The Keratinocyte. *Cell*, 19(4), pp.1033-1042.

Fujii, S., Yokoyama, T., Ikegaya, K., Sato, F. and Yokoo, N. (1985). Promoting Effect Of The New Chymotrypsin Inhibitor FK-448 On The Intestinal Absorption Of Insulin In Rats And Dogs. *Journal of Pharmacy and Pharmacology*, 37(8), pp.545-549.

Fulda, S., Gorman, A., Hori, O. and Samali, A. (2010). Cellular Stress Responses: Cell Survival and Cell Death. *International Journal of Cell Biology*, 2010, pp.1-23.

Fusenig, N.E. (1994). Epithelial-Mesenchymal Interactions Regulate Keratinocyte Growth And Differentiation In Vitro. In: The Keratinocyte Handbook. Leigh IM, Lane EB, Watt FM, editors. Cambridge: University Press, pp. 71–94.

Gaballah, K., Costea, D., Hills, A., Gollin, S., Harrison, P. and Partridge, M. (2008). Tissue Engineering Of Oral Dysplasia. *The Journal of Pathology*, 215(3), pp.280-289.

Gaggioli, C., Hooper, S., Hidalgo-Carcedo, C., Grosse, R., Marshall, J., Harrington, K. and Sahai, E. (2007). Fibroblast-Led Collective Invasion Of Carcinoma Cells With Differing Roles For RhoGTPases In Leading And Following Cells. *Nature Cell Biology*, 9(12), pp.1392-1400.

Galey, W., Lonsdale, H. and Nacht, S. (1976). The In Vitro Permeability Of Skin And Buccal Mucosa To Selected Drugs And Tritiated Water. *Journal of Investigative Dermatology*, 67(6), pp.713-717.

Gallico, G. and O'Connor, N. (1995). Engineering a Skin Replacement. *Tissue Engineering*, 1(3), pp.231-240.

Gandhi, R. and Robinson, J. (1994). Oral cavity as a site for bioadhesive drug delivery. *Advanced Drug Delivery Reviews*, 13(1-2), pp.43-74.

Ganem-Quintanar, A., Kalia, Y., Falson-Rieg, F. and Buri, P. (1997). Mechanisms of oral permeation enhancement. *International Journal of Pharmaceutics*, 156(2), pp.127-142.

Garrod, D.R. (1993). Desmosomes And Hemidesmosomes. *Current Opinion in Cell Biology*, 5(1), pp.30–40.

Garzón, I., Sánchez-Quevedo, M., Moreu, G., González-Jaranay, M., González-Andrades, M., Montalvo, A., Campos, A. and Alaminos, M. (2009). *In Vitro* and *In Vivo* Cytokeratin Patterns of Expression in Bioengineered Human Periodontal Mucosa. *Journal of Periodontal Research*, 44(5), pp.588-597.

Gautami, J. (2016). Liquid Dosage Forms. *Nano Science & Nano Technology: An Indian Journal*, 10(3). pp.1-9.

Gazdar, A., Hirsch, F. and Minna, J. (2016). From Mice to Men and Back: An Assessment of Preclinical Model Systems for the Study of Lung Cancers. *Journal of Thoracic Oncology*, 11(3), pp.287-299.

Georgakopoulou, E., Achtari, M., Achtaris, M., Foukas, P. and Kotsinas, A. (2012). Oral Lichen Planus as a Preneoplastic Inflammatory Model. *Journal of Biomedicine and Biotechnology*, 2012, pp.1-8.

Geroski, D. and Hadley, A. (1992). Characterization Of Corneal Endothelium Cell Cultured On Microporous Membrane Filters. *Current Eye Research*, 11(1), pp.61-72.

Gibson, N. and Ferguson, J. (2004). Steroid Cover for Dental Patients on Long-Term Steroid Medication: Proposed Clinical Guidelines Based Upon a Critical Review of The Literature. *British Dental Journal*, 197(11), pp.681-685.

Gilhotra, R. M., Ikram, M., Srivastava, S. And Gilhotra, N. (2014). A Clinical Perspective On Mucoadhesive Buccal Drug Delivery Systems. *Journal of Biomedical Research*, *28*(2), pp.81–97.

Gonzales, F.J. and Tukey, R.H. (2005). Drug Metabolism. In: Brunton, L.L.,Lazo, J.S., Parker, K.L., (Eds.), Goodman and Gilman's the Pharmacological Basis of Therapeutics. McGraw-Hill, New York, United States.

González-Moles, M. Á. (2010). The Use of Topical Corticoids in Oral Pathology. *Medicina Oral, Patologia Oral y Cirugia Bucal*, 15(6), pp.827–831.

Gonzalez-Moles, M. A., Scully, C., and Gil-Montoya, J. A. (2008). Oral Lichen Planus: Controversies Surrounding Malignant Transformation. *Oral Diseases*, 14(3), pp.229–243.

Graham-Evans, B., Tchounwou, P. and Cohly, H. (2003). Cytotoxicity and Proliferation Studies with Arsenic in Established Human Cell Lines: Keratinocytes, Melanocytes, Dendritic Cells, Dermal Fibroblasts, Microvascular Endothelial Cells, Monocytes and T-Cells. *International Journal of Molecular Sciences*, 4(1), pp.13-21.

Griffith, L. and Swartz, M. (2006). Capturing Complex 3D Tissue Physiology *In Vitro*. *Nature Reviews Molecular Cell Biology*, 7(3), pp.211-224.

Gual, A., Paul-Charles, I. and Abeck, D. (2015). Topical Corticosteroids in Dermatology: From Chemical Development to Galenic Innovation and Therapeutic Trends. *Journal of Clinical & Experimental Dermatology Research*, 6(2), pp.1-5.

Gupta, A. and Chow, M. (2004). Prednicarbate (Dermatop®): Profile of a Corticosteroid. *Journal of Cutaneous Medicine and Surgery*, 8(4), pp.244-247.

Gupta, S., Pratibha, P. and Gupta, R. (2015). Mucosal Substitutes for Periodontal Soft Tissue Regeneration. *Dentistry*, 05(09), pp.1-6.

Gursoy, U., Pöllänen, M., Könönen, E. and Uitto, V. (2010). Biofilm Formation Enhances the Oxygen Tolerance and Invasiveness of Fusobacterium nucleatum in an Oral Mucosa Culture Model. *Journal of Periodontology*, 81(7), pp.1084-1091.

Gutsol, A., Sokhonevich, N., Yurova, K., Khaziakhmatova, O., Shupletsova, V. and Litvinova, L. (2015). Dose-dependent effects of dexamethasone on functional activity of T-lymphocytes with different grades of differentiation. *Molecular Biology*, 49(1), pp.130-137.

Habif, T. (1990). *Clinical dermatology*. St. Louis: Mosby.

Hallmon, W. and Rossmann, J. (1999). The role of drugs in the pathogenesis of gingival overgrowth. A collective review of current concepts. *Periodontology*, 21(1), pp.176-196.

Hanania, N., Chapman, K. and Kesten, S. (1995). Adverse Effects Of Inhaled Corticosteroids. *The American Journal of Medicine*, 98(2), pp.196-208.

Hand, A.R. and Frank, M.E. (2014). *Fundamentals of Oral Histology and Physiology*. John Wiley & Sons.

Harmse, J., Carey, F., Baird, A., Craig, S., Christie, K., Hopwood, D. and Lucocq, J. (1999). Merkel Cells In The Human Oesophagus. *The Journal of Pathology*, 189(2), pp.176-179.

Harris, D. and Robinson, J. (1992). Drug Delivery via the Mucous Membranes of the Oral Cavity. *Journal of Pharmaceutical Sciences*, 81(1), pp.1-10.

Hasseus, B., Jontell, M., Brune, M., Johansson, P. and Dahlgren, U. (2001). Langerhans Cells and T Cells in Oral Graft versus Host Disease and Oral Lichen Planus. *Scandinavian Journal of Immunology*, 54(5), pp.516-524.

Hearnden, V., Lomas, H., MacNeil, S., Thornhill, M., Murdoch, C., Lewis, A., Madsen, J., Blanazs, A., Armes, S. and Battaglia, G. (2009). Diffusion Studies of Nanometer Polymersomes across Tissue Engineered Human Oral Mucosa. *Pharmaceutical Research*, 26(7), pp.1718-1728.

Hearnden, V., Sankar, V., Hull, K., Juras, D., Greenberg, M., Kerr, A., Lockhart, P., Patton, L., Porter, S. and Thornhill, M. (2012). New Developments and Opportunities in Oral Mucosal Drug Delivery for Local and Systemic Disease. *Advanced Drug Delivery Reviews*, 64(1), pp.16-28.

Hein, R., Korting, H. and Mehring, T. (1994). Differential Effect of Medium Potent Nonhalogenated Double-Ester-Type and Conventional Glucocorticoids on Proliferation and Chemotaxis of Fibroblasts in vitro. *Skin Pharmacology and Physiology*, 7(5), pp.300-306.

Helander, S. and Rogers, R. (1994). The Sensitivity and Specificity of Direct Immunofluorescence Testing in Disorders of Mucous Membranes. *Journal of the American Academy of Dermatology*, 30(1), pp.65-75.

Hengge, U., Ruzicka, T., Schwartz, R. and Cork, M. (2006). Adverse Effects of Topical Glucocorticosteroids. *Journal of the American Academy of Dermatology*, 54(1), pp.1-15.

Herford, A., Akin, L., Cicciu, M., Maiorana, C. and Boyne, P. (2010). Use of a Porcine Collagen Matrix as an Alternative to Autogenous Tissue for Grafting Oral Soft Tissue Defects. *Journal of Oral and Maxillofacial Surgery*, 68(7), pp.1463-1470.

Hilgendorf, C., Spahn-Langguth, H., Regårdh, C., Lipka, E., Amidon, G. and Langguth, P. (2000). Caco-2 versus Caco-2/HT29-MTX Co-cultured Cell Lines: Permeabilities Via Diffusion, Inside- and Outside-Directed Carrier-Mediated Transport. *Journal of Pharmaceutical Sciences*, 89(1), pp.63-75.

Hilliges, M., Astbäck, J., Wang, L., Arvidson, K. and Johansson, O. (1996). Protein Gene Product 9.5-Immunoreactive Nerves And Cells In Human Oral Mucosa. *The Anatomical Record*, 245(4), pp.621-632.

Hooda, R., Tripathi, M. and Kapoor, K. (2012). A Review on Oral Mucosal Drug Delivery System. *The Pharma Innovation*, [online] 1(1), pp.13-19.

Hoogstraate, A., Cullander, C., Senel, S., Verhoef, J., Boddé, H. and Junqinger, H. (1994). Diffusion Rates And Transport Pathways Of FITC-Labelled Model Compounds Through Buccal Epithelium. *Journal of Controlled Release*, 28(1-3), pp.274.

Hoogstraate, A.J and Boddé, H. E. (1993). Methods For Assessing The Buccal Mucosa As A Route Of Drug Delivery. *Advanced Drug Delivery Reviews*, *12*(1–2), pp.99–125.

Hu, F., Jiang, S., Du, Y., Yuan, H., Ye, Y. and Zeng, S. (2006). Preparation And Characteristics Of Monostearin Nanostructured Lipid Carriers. *International Journal of Pharmaceutics*, 314(1), pp.83-89.

Hughes, J. and Rustin, M. (1997). Corticosteroids. *Clinics in Dermatology*, 15(5), pp.715-721.

Hussan, S. (2012). A Review On Recent Advances Of Enteric Coating. *IOSR Journal of Pharmacy (IOSRPHR)*, 2(6), pp.05-11.

Ichimura, M., Hiratsuka, K., Ogura, N., Utsunomiya, T., Sakamaki, H., Kondoh, T., Abiko, Y., Otake, S. and Yamamoto, M. (2006). Expression Profile Of Chemokines And Chemokine Receptors In Epithelial Cell Layers Of Oral Lichen Planus. *Journal of Oral Pathology and Medicine*, 35(3), pp.167-174.

Iida, T., Takami, Y., Yamaguchi, R., Shimazaki, S. and Harii, K. (2005). Development of a Tissue-Engineered Human Oral Mucosa Equivalent Based on an Acellular Allogeneic Dermal Matrix: A Preliminary Report of Clinical Application to Burn Wounds. *Scandinavian Journal of Plastic and Reconstructive Surgery and Hand Surgery*, 39(3), pp.138-146.

Iijima, W., Ohtani, H., Nakayama, T., Sugawara, Y., Sato, E., Nagura, H., Yoshie, O. and Sasano, T. (2003). Infiltrating CD8+ T Cells in Oral Lichen Planus Predominantly Express CCR5 and CXCR3 and Carry Respective Chemokine Ligands RANTES/CCL5 and IP-10/CXCL10 in Their Cytolytic Granules. *The American Journal of Pathology*, 163(1), pp.261-268.

Imaizumi, F., Asahina, I., Moriyama, T., Ishii, M. and Omura, K. (2004). Cultured Mucosal Cell Sheet with a Double Layer of Keratinocytes and Fibroblasts on a Collagen Membrane. *Tissue Engineering*, 10(5-6), pp.657-664.

Irfan Maqsood, M., Matin, M., Bahrami, A. and Ghasroldasht, M. (2013). Immortality Of Cell Lines: Challenges And Advantages Of Establishment. *Cell Biology International*, 37(10), pp.1038-1045.

Ismail, S., Kumar, S. and Zain, R. (2007). Oral Lichen Planus and Lichenoid Reactions: Etiopathogenesis, Diagnosis, Management and Malignant Transformation. *Journal of Oral Science*, 49(2), pp.89-106.

Itoh, M., Umegaki-Arao, N., Guo, Z., Liu, L., Higgins, C. and Christiano, A. (2013). Generation of 3D Skin Equivalents Fully Reconstituted from Human Induced Pluripotent Stem Cells (iPSCs). *PLoS ONE*, 8(10), pp.e77673.

Izumi K., Takacs, G., Terashi, H., Feinberg, S.E. (1999). *Ex Vivo* Development of a Composite Human Oral Mucosal Equivalent. *Journal of Oral and Maxillofacial Surgery,* 57, pp.571-577.

Izumi, K., Feinberg, S., Iida, A. and Yoshizawa, M. (2003). Intraoral Grafting of an *Ex Vivo* Produced Oral Mucosa Equivalent: A Preliminary Report. *International Journal of Oral and Maxillofacial Surgery*, 32(2), pp.188-197.

Izumi, K., Song, J. and Feinberg, S. (2004). Development of a Tissue-Engineered Human Oral Mucosa: From the Bench to the Bed Side. *Cells Tissues Organs*, 176(1-3), pp.134-152.

Izumi, K., Terashi, H., Marcelo, C. and Feinberg, S. (2000). Development and Characterization of a Tissue-engineered Human Oral Mucosa Equivalent Produced in a Serum-free Culture System. *Journal of Dental Research*, 79(3), pp.798-805.

Jacobsen, J., van Deurs, B., Pedersen, M. and Rassing, M. (1995). TR146 Cells Grown On Filters As A Model For Human Buccal Epithelium: I. Morphology, Growth, Barrier Properties, And Permeability. *International Journal of Pharmaceutics*, 125(2), pp.165-184.

Jacques, C., Pereira, A., Maia, V., Cuzzi, T. and Ramos-e-Silva, M. (2009). Expression Of Cytokeratins 10, 13, 14 And 19 In Oral Lichen Planus. *Journal of Oral Science*, 51(3), pp.355-365.

Jani, P., Manseta, P. and Patel, S. (2012). Pharmaceutical Approaches Related to Systemic Delivery of Protein and Peptide Drugs: An Overview. *International Journal of Pharmaceutical Sciences Review and Research*, 12(1), pp.42 - 52.

Jayatilake, J.A.M.S., Samaranayake, Y.H., Cheung, L.K. and Samaranayake, L.P., 2006. Quantitative Evaluation of Tissue Invasion by Wild Type, Hyphal and SAP Mutants of Candida Albicans, And Non-Albicans Candida Species in Reconstituted Human Oral Epithelium. *Journal of oral pathology & medicine*, 35(8), pp.484-491.

Jennings, L., Colley, H., Ong, J., Panagakos, F., Masters, J., Trivedi, H., Murdoch, C. and Whawell, S. (2016). Development and Characterization of In Vitro Human Oral Mucosal Equivalents Derived from Immortalized Oral Keratinocytes. *Tissue Engineering Part C: Methods*, 22(12), pp.1108-1117.

Jhaveri, H., Chavan, M., Tomar, G., Deshmukh, V., Wani, M. and Miller, P. (2010). Acellular Dermal Matrix Seeded With Autologous Gingival Fibroblasts for the Treatment of Gingival Recession: A Proof-of-Concept Study. *Journal of Periodontology*, 81(4), pp.616-625.

Ji, E., Sun, B., Zhao, T., Shu, S., Chang, C., Messadi, D., Xia, T., Zhu, Y. and Hu, S. (2016). Characterization of Electronic Cigarette Aerosol and Its Induction of Oxidative Stress Response in Oral Keratinocytes. *PLOS ONE*, 11(5), pp.1-13.

John, D., Fort, S., Lewis, M. and Luscombe, D. (1992). Pharmacokinetics and pharmacodynamics of verapamil following sublingual and oral administration to healthy volunteers. *British Journal of Clinical Pharmacology*, 33(6), pp.623-627.

Jones, D., Woolfson, A., Djokic, J. and Coulter, W. (1996). Development and Mechanical Characterization of Bioadhesive Semi-Solid, Polymeric Systems Containing Tetracycline for the Treatment of Periodontal Diseases. *Pharmaceutical Research*, 13(11), pp.1734 - 1738.

Jones, J., Sugiyama, M., Watt, F. and Speight, P. (1993). Integrin Expression In Normal, Hyperplastic, Dysplastic, And Malignant Oral Epithelium. *The Journal of Pathology*, 169(2), pp.235-243.

Kaihara, S. and Vacanti, J.P. (1999). Tissue Engineering: Toward New Solutions For Transplantation And Reconstructive Surgery. *Archives of Surgery*, 134(11), pp.1184-1188.

Kalariya, M., Padhi, B.K., Chougule, M., Misra, A. (2005). Clobetasol Propionate Solid Lipid Nanoparticles Cream For Effective Treatment Of Eczema: Formulation And Clinical Implications. *Indian Journal of Experimental Biology*, 43(3), pp.233-240.

Kameyama, S., Kondo, M., Takeyama, K. and Nagai, A. (2003). Air Exposure Causes Oxidative Stress In Cultured Bovine Tracheal Epithelial Cells And Produces A Change In Cellular Glutathione Systems. *Experimental Lung Research*, 29(8), pp.567-583.

Kansky, A., Podrumac, B. and Godic, A. (2000). Nonfluorinated Corticosteroid Topical Preparations In Children. *Acta Dermatoven APA*, 9(2), pp.67-72.

Kao, J., Fluhr, J., Man, M., Fowler, A., Hachem, J., Crumrine, D., Ahn, S., Brown, B., Elias, P. and Feingold, K. (2003). Short-Term Glucocorticoid Treatment Compromises Both Permeability Barrier Homeostasis and Stratum Corneum Integrity: Inhibition of Epidermal Lipid Synthesis Accounts for Functional Abnormalities. *Journal of Investigative Dermatology*, 120(3), pp.456-464.

Karthikeyan, K., Guhathakarta, S., Rajaram, R. and Korrapati, P. (2012). Electrospun Zein/Eudragit Nanofibers Based Dual Drug Delivery System For The Simultaneous Delivery Of Aceclofenac And Pantoprazole. *International Journal of Pharmaceutics*, 438(1-2), pp.117-122.

Kassem, M., Abdallah, B., Yu, Z., Ditzel, N. and Burns, J. (2004). The Use of hTERT-Immortalized Cells in Tissue Engineering. *Cytotechnology*, 45(1-2), pp.39-46.

Katz, M. and Gans, E. (2008). Topical Corticosteroids, Structure-Activity and the Glucocorticoid Receptor: Discovery and Development—A Process of ‘‘Planned Serendipity’’. *Journal of Pharmaceutical Sciences*, 97(8), pp.2936-2947.

Kerscher, M., Williams, S. and Lehmann, P. (2006). Topical Treatment With Glucocorticoids. *Handbook of Atopic Eczema*, pp.477–490.

Key, S., Hodder, S., Davies, R., Thomas, D. and Thompson, S. (2003). Perioperative Corticosteroid Supplementation and Dento-Alveolar Surgery. *Dental Update.*, 30, pp.316 - 320.

Khan, A., Kingsley, T. and Caroline, P. (2017). Sublingual Tablets and the Benefits of the Sublingual Route of Administration. *Journal of Pharmaceutical Research*, 16(3), pp.257.

Khmaladze, A., Ganguly, A., Kuo, S., Raghavan, M., Kainkaryam, R., Cole, J., Izumi, K., Marcelo, C., Feinberg, S. and Morris, M. (2013). Tissue-Engineered Constructs of Human Oral Mucosa Examined by Raman Spectroscopy. *Tissue Engineering Part C: Methods*, 19(4), pp.299-306.

Kim, J. (2005). Three-Dimensional Tissue Culture Models In Cancer Biology. *Seminars in Cancer Biology*, 15(5), pp.365-377.

Kimura, T., Yamano, H., Tanaka, A., Matsumura, T., Ueda, M., Ogawara, K. and Higaki, K. (2002). Transport Of D-Glucose Across Cultured Stratified Cell Layer Of Human Oral Mucosal Cells. *Journal of Pharmacy and Pharmacology*, 54(2), pp.213-219.

Kinikoglu, B., Auxenfans, C., Pierrillas, P., Justin, V., Breton, P., Burillon, C., Hasirci, V. and Damour, O. (2009). Reconstruction of a Full-Thickness Collagen-Based Human Oral Mucosal Equivalent. *Biomaterials*, 30(32), pp.6418-6425.

Klausner, M., Ayehunie, S., Breyfogle, B., Wertz, P., Bacca, L. and Kubilus, J. (2007). Organotypic Human Oral Tissue Models for Toxicological Studies. *Toxicology In Vitro*, 21(5), pp.938-949.

Knight, M. and Evans, G. (2004). Tissue Engineering: Progress and Challenges. *Plastic and Reconstructive Surgery*, 114(2), pp.26e-37e.

Kolbe, L., Kligman, A., Schreiner, V. and Stoudemayer, T. (2001). Corticosteroid-Induced Atrophy And Barrier Impairment Measured By Non-Invasive Methods In Human Skin. *Skin Research and Technology*, 7(2), pp.73-77.

Köseoğlu, S., Duran, İ., Sağlam, M., Bozkurt, S., Kırtıloğlu, O. and Hakkı, S. (2013). Efficacy of Collagen Membrane Seeded With Autologous Gingival Fibroblasts in Gingival Recession Treatment: A Randomized, Controlled Pilot Study. *Journal of Periodontology*, 84(10), pp.1416-1424.

Kottke, M., Delva, E. and Kowalczyk, A. (2006). The Desmosome: Cell Science Lessons From Human Diseases. *Journal of Cell Science*, 119(5), pp.797-806.

Kowalczyk, A., Hatzfeld, M., Bornslaeger, E., Kopp, D., Borgwardt, J., Corcoran, C., Settler, A. and Green, K. (1999). The Head Domain of Plakophilin-1 Binds to Desmoplakin and Enhances Its Recruitment to Desmosomes. *Journal of Biological Chemistry*, 274(26), pp.18145-18148.

Kriegebaum, U., Mildenberger, M., Mueller-Richter, U., Klammert, U., Kuebler, A. and Reuther, T. (2012). Tissue Engineering Of Human Oral Mucosa on Different Scaffolds: In Vitro Experiments as a Basis for Clinical Applications. *Oral Surgery, Oral Medicine, Oral Pathology and Oral Radiology*, 114(5), pp.S190-S198.

Kulkarni, U., Mahalingam, R., Pather, I., Li, X. and Jasti, B. (2010). Porcine Buccal Mucosa as In Vitro Model: Effect of Biological And Experimental Variables. *Journal of Pharmaceutical Sciences*, 99(3), pp.1265-1277.

Kulkarni, U., Mahalingam, R., Pather, S. I., Li, X. and Jasti, B. (2009). Porcine Buccal Mucosa As An In Vitro Model: Relative Contribution Of Epithelium And Connective Tissue As Permeability Barriers. *Journal of Pharmaceutical Sciences*, *98*(2), pp.471–483.

Kumria, R., Nair, A., Goomber, G. and Gupta, S. (2016). Buccal Films Of Prednisolone With Enhanced Bioavailability. *Drug Delivery*, 23(2), pp.471-478.

Kuo, S., Zhou, Y., Kim, H., Kato, H., Kim, R., Bayar, G., Marcelo, C., Kennedy, R. and Feinberg, S. (2015). Biochemical Indicators of Implantation Success of Tissue-Engineered Oral Mucosa. *Journal of Dental Research*, 94(1), pp.78-84.

Kwatra, G. and Mukhopadhyay, S. (2018). Topical Corticosteroids: Pharmacology. *A Treatise on Topical Corticosteroids in Dermatology*, pp.11-22.

Lange, K., Kleuser, B., Gysler, A., Bader, M., Maia, C., Scheidereit, C., Korting, H. and Schäfer-Korting, M. (2000). Cutaneous Inflammation and Proliferation in vitro: Differential Effects and Mode of Action of Topical Glucocorticoids. *Skin Pharmacology and Physiology*, 13(2), pp.93-103.

Langhans, S. A. (2018). Three-Dimensional In Vitro Cell Culture Models In Drug Discovery And Drug Repositioning. *Frontiers in Pharmacology*, *9*, pp.1–14.

Lavanya, N., Rao, U., Jayanthi, P. and Ranganathan, K. (2011). Oral Lichen Planus: An Update on Pathogenesis and Treatment. *Journal of Oral and Maxillofacial Pathology*, 15(2), pp.127.

Laverdet, B., Micallef, L., Lebreton, C., Mollard, J., Lataillade, J., Coulomb, B. and Desmoulière, A. (2014). Use Of Mesenchymal Stem Cells For Cutaneous Repair And Skin Substitute Elaboration. *Pathologie Biologie*, 62(2), pp.108-117.

Lee, K., Choi, K. and Ouellette, M. (2004). Use of Exogenous hTERT To Immortalize Primary Human Cells. *Cytotechnology*, 45(1-2), pp.33-38.

Leerahawong, A., Tanaka, M., Okazaki, E. and Osako, K. (2012). Stability of the Physical Properties of Plasticized Edible Films from Squid (Todarodes pacificus) Mantle Muscle during Storage. *Journal of Food Science*, 77(6), pp.E159-E165.

Lesch, C., Squier, C., Cruchley, A., Williams, D. and Speight, P. (1989). The Permeability of Human Oral Mucosa and Skin to Water. *Journal of Dental Research*, 68(9), pp.1345-1349.

Liles, W.C., Dale, D. C. and Klebanoff, S. J. (1995). Glucocorticoids Inhibit Apoptosis Of Human Neutrophils. *Blood*, 86(8), pp.3181–3188.

Lippmann, E., Al-Ahmad, A., Azarin, S., Palecek, S. and Shusta, E. (2014). A Retinoic Acid-Enhanced, Multicellular Human Blood-Brain Barrier Model Derived From Stem Cell Sources. *Scientific Reports*, 4(1), pp.4160.

Litjens, S., de Pereda, J. and Sonnenberg, A. (2006). Current Insights Into The Formation And Breakdown Of Hemidesmosomes. *Trends in Cell Biology*, 16(7), pp.376-383.

Liu, J., Mao, J. and Chen, L. (2011). Epithelial–Mesenchymal Interactions as a Working Concept for Oral Mucosa Regeneration. *Tissue Engineering Part B: Reviews*, 17(1), pp.25-31.

Lodi, G., Scully, C., Carrozzo, M., Griffiths, M., Sugerman, P. and Thongprasom, K. (2005). Current Controversies in Oral Lichen Planus: Report of an International Consensus Meeting. Part 2. Clinical Management and Malignant Transformation. *Oral Surgery, Oral Medicine, Oral Pathology, Oral Radiology, and Endodontology*, 100(2), pp.164-178.

López-García, J., Lehocký, M., Humpolíček, P., & Sáha, P. (2014). HaCaT Keratinocytes Response on Antimicrobial Atelocollagen Substrates: Extent of Cytotoxicity, Cell Viability and Proliferation. *Journal of Functional Biomaterials*, 5(2), 43–57.

Lozada-Nur, F., Huang, M. and Zhou, G. (1991). Open Preliminary Clinical Trial of Clobetasol Propionate Ointment in Adhesive Paste For Treatment of Chronic Oral Vesiculoerosive Diseases. *Oral Surgery, Oral Medicine, Oral Pathology*, 71(3), pp.283-287.

Lu, R., Zhang, J., Sun, W., Du, G. and Zhou, G. (2015). Inflammation-related cytokines in oral lichen planus: An overview. *Journal of Oral Pathology and Medicine*, *44*(1), pp.1–14.

Lu, Y. and Low, P. (2002). Folate-Mediated Delivery of Macromolecular Anticancer Therapeutic Agents. *Advanced Drug Delivery Reviews*, 54(5), pp.675-693.

Luitaud, C., Laflamme, C., Semlali, A., Saidi, S., Grenier, G., Zakrzewski, A. and Rouabhia, M. (2007). Development of an Engineering Autologous Palatal Mucosa-Like Tissue for Potential Clinical Applications. *Journal of Biomedical Materials Research Part B: Applied Biomaterials*, 83B(2), pp.554-561.

Luomanen, M., Tiitta, O., Heikinheimo, K., Leimola-Virtanen, R., Heinaro, I. and Happonen, R. (1997). Effect Of Snuff And Smoking On Tenascin Expression In Oral Mucosa. *Journal of Oral Pathology and Medicine*, 26(7), pp.334-338.

Luu-The, V., Duche, D., Ferraris, C., Meunier, J., Leclaire, J. and Labrie, F. (2009). Expression Profiles Of Phases 1 And 2 Metabolizing Enzymes In Human Skin And The Reconstructed Skin Models Episkin™ And Full Thickness Model From Episkin™. *The Journal of Steroid Biochemistry and Molecular Biology*, 116(3-5), pp.178-186.

Lynch, T., and Price, A. (2007). The Effect Of Cytochrome P450 Metabolism On Drug Response, Interactions, And Adverse Effects. *American Family Physician*, 76(3), pp.391–396.

Ma, L., Gao, C., Mao, Z., Zhou, J., Shen, J., Hu, X. and Han, C. (2003). Collagen/Chitosan Porous Scaffolds with Improved Biostability for Skin Tissue Engineering. *Biomaterials*, 24(26), pp.4833-4841.

MacCallum, D. and Lillie, J. (1990). Evidence for Autoregulation of Cell Division and Cell Transit in Keratinocytes Grown on Collagen at an Air-Liquid Interface. *Skin Pharmacology and Physiology* 3(2), pp.86-96.

Mackenzie, I. and Fusenig, N. (1983). Regeneration of Organized Epithelial Structure. *Journal of Investigative Dermatology*, 81(1), pp.189-194.

MacNeil, S. (2007). Progress and Opportunities for Tissue-Engineered Skin. *Nature*, 445(7130), pp.874-880.

Mahato, R., Narang, A., Thoma, L. and Miller, D. (2003). Emerging Trends in Oral Delivery of Peptide and Protein Drugs. *Critical Reviews in Therapeutic Drug Carrier Systems*, 20(2-3), pp.153-214.

Malek, T. (2008). The Biology of Interleukin-2. *Annual Review of Immunology*, 26(1), pp.453-479.

Manganaro, A.M. (1997). Review of transmucosal drug delivery. *Military Medicine*, 162, pp.27–30.

Mao, J.S., Yin, Y.J. and De Yao, K. (2003). The Properties of Chitosan–Gelatin Membranes and Scaffolds Modified with Hyaluronic Acid by Different Methods. *Biomaterials*, 24(9), pp.1621-1629.

Marionnet, C., Pierrard, C., Vioux-Chagnoleau, C., Sok, J., Asselineau, D. and Bernerd, F. (2006). Interactions between Fibroblasts and Keratinocytes in Morphogenesis of Dermal Epidermal Junction in a Model of Reconstructed Skin. *Journal of Investigative Dermatology*, 126(5), pp.971-979.

Marks, R., Barlow, J. and Funder, J. (1982). Steroid-Induced Vasoconstriction: Glucocorticoid Antagonist Studies. *The Journal of Clinical Endocrinology & Metabolism*, 54(5), pp.1075-1077.

Marsh, D., Suchak, K., Moutasim, K., Vallath, S., Hopper, C., Jerjes, W., Upile, T., Kalavrezos, N., Violette, S., Weinreb, P., Chester, K., Chana, J., Marshall, J., Hart, I., Hackshaw, A., Piper, K. and Thomas, G. (2011). Stromal Features are Predictive of Disease Mortality in Oral Cancer Patients. *The Journal of Pathology*, 223(4), pp.470-481.

Martin, J. and Fay, M. (2001). Cytochrome P450 Drug Interactions: Are They Clinically Relevant?. *Australian Prescriber*, 24(1), pp.10-12.

Martin, P. (1997). Wound Healing--Aiming for Perfect Skin Regeneration. *Science*, 276(5309), pp.75-81.

Mason, J., Mason, A. and Cork, M. (2002). Topical Preparations For The Treatment Of Psoriasis: A Systematic Review. *British Journal of Dermatology*, 146(3), pp.351-364.

Masuda, I. (1996). An *In Vitro* Oral Mucosal Model Reconstructed From Human Normal Gingival Cells. *The Journal of the Stomatological Society, Japan*, 63(2), pp.334-353.

Mathias, N., Timoszyk, J., Stetsko, P., Megill, J., Smith, R. and Wall, D. (2002). Permeability Characteristics of Calu-3 Human Bronchial Epithelial Cells: In Vitro - In Vivo Correlation to Predict Lung Absorption in Rats. *Journal of Drug Targeting*, 10(1), pp.31-40.

Matoltsy, A. (1976). Keratinization. *Journal of Investigative Dermatology*, 67(1), pp.20-25.

Matoltsy, A. and Parakkal, P. (1965). Membrane-Coating Granules Of Keratinizing Epithelia. *The Journal of Cell Biology*, 24(2), pp.297-307.

McDonnell, A. and Dang, C. (2013). Basic Review of the Cytochrome P450 System. *Journal of the Advanced Practitioner in Oncology*, 4(4), pp.263–268.

McGregor, F., Muntoni, A., Fleming, J., Brown, J., Felix, D.H., MacDonald, D.G., Parkinson, E.K. and Harrison, P.R. (2002). Molecular Changes Associated with Oral Dysplasia Progression and Acquisition of Immortality Potential for Its Reversal by 5-Azacytidine. *Cancer Research*, 62(16), pp.4757-4766.

McKenzieE, A. and Stoughton, R. (1962). Method for Comparing Percutaneous Absorption of Steroids. *Archives of Dermatology*, 86, pp.608–610.

McLeod, N. M. H., Moutasim, K. A., Brennan, P. A., Thomas, G. and Jenei, V. (2014). In Vitro Effect Of Bisphosphonates On Oral Keratinocytes And Fibroblasts. *Journal of Oral and Maxillofacial Surgery*, *72*(3), pp.503–509.

Mehdipour, M. and Zenouz, A.T. (2012). Role of Corticosteroids in Oral Lesions. INTECH Open Access Publisher.

Mehta, A., Nadkarni, N., Patil, S., Godse, K., Gautam, M. and Agarwal, S. (2016). Topical Corticosteroids In Dermatology. *Indian Journal of Dermatology, Venereology, and Leprology*, *82*(4),pp.371.

Mehta, G., Hsiao, A., Ingram, M., Luker, G. and Takayama, S. (2012). Opportunities and Challenges for Use of Tumor Spheroids as Models to Test Drug Delivery and Efficacy. *Journal of Controlled Release*, 164(2), pp.192-204.

Metcalfe, A. D. and Ferguson, M. W. J. (2007). Tissue Engineering Of Replacement Skin: The Crossroads Of Biomaterials, Wound Healing, Embryonic Development, Stem Cells And Regeneration. *Journal of the Royal Society Interface*, *4*(14), pp.413–417.

Michalets, E. L. (1998). Update: Clinically Significant Cytochrome P-450 Drug Interactions. *Pharmacotherapy*, 18(1), pp.84–112.

Mignogna, M.D., Fedele, S., Lo Russo, L., Lo Muzio, L. and Bucci, E. (2004). Immune Activation And Chronic Inflammation As The Cause Of Malignancy In Oral Lichen Planus: Is There Any Evidence? *Oral Oncology*, 40(2), pp.120–130.

Mills, C. and Marks, R. (1993). Side Effects of Topical Glucocorticoids. *Topical Glucocorticoids with Increased Benefit / Risk Ratio*, 21, pp.122-131.

Minin, A. and Moldaver, M. (2008). Intermediate Vimentin Filaments And Their Role In Intracellular Organelle Distribution. *Biochemistry (Moscow)*, 73(13), pp.1453-1466.

Miret, S., De Groene, E.M. and Klaffke, W. (2006). Comparison of *In Vitro* Assays of Cellular Toxicity in the Human Hepatic Cell Line HepG2. *Journal of Biomolecular Screening*, 11(2), pp.184-193.

Mitchell, J., Belvisi, M., Akarasereenont, P., Robbins, R., Kwon, O., Croxtall, J., Barnes, P. and Vane, J. (1994). Induction Of Cyclo-Oxygenase-2 By Cytokines In Human Pulmonary Epithelial Cells: Regulation By Dexamethasone. *British Journal of Pharmacology*, 113(3), pp.1008-1014.

Miyauchi, S., Moroyama, T., Sakamoto, T., Okamoto, T. and Takada, K. (1985). Establishment Of Human Tumor Cell Line (Ueda-1) Derived From Squamous Cell Carcinoma Of The Floor Of The Mouth. *Japanese Journal of Oral & Maxillofacial Surgery*, 31(6), pp.1347-1351.

Mohammadi, M., Shokrgozar, M. and Mofid, R. (2007). Culture of Human Gingival Fibroblasts on a Biodegradable Scaffold and Evaluation of Its Effect on Attached Gingiva: A Randomized, Controlled Pilot Study. *Journal of Periodontology*, 78(10), pp.1897-1903.

Moharamzadeh, K., Brook, I., Scutt, A., Thornhill, M. and Van Noort, R. (2008a). Mucotoxicity of Dental Composite Resins on A Tissue-Engineered Human Oral Mucosal Model. *Journal of Dentistry*, 36(5), pp.331-336.

Moharamzadeh, K., Brook, I., Van Noort, R., Scutt, A. and Thornhill, M. (2007). Tissue-engineered Oral Mucosa: A Review of the Scientific Literature. *Journal of Dental Research*, 86(2), pp.115-124.

Moharamzadeh, K., Brook, I., Van Noort, R., Scutt, A., Smith, K. and Thornhill, M. (2008b). Development, Optimization and Characterization of a Full-Thickness Tissue Engineered Human Oral Mucosal Model for Biological Assessment of Dental Biomaterials. *Journal of Materials Science: Materials in Medicine*, 19(4), pp.1793-1801.

Moharamzadeh, K., Colley, H., Murdoch, C., Hearnden, V., Chai, W., Brook, I., Thornhill, M. and MacNeil, S. (2012). Tissue-engineered Oral Mucosa. *Journal of Dental Research*, 91(7), pp.642-650.

Moharamzadeh, K., Franklin, K., Brook, I. and van Noort, R. (2009). Biologic Assessment of Antiseptic Mouthwashes Using a Three-Dimensional Human Oral Mucosal Model. *Journal of Periodontology*, 80(5), pp.769-775.

Moharamzadeh, K., Franklin, K.L., Smith, L.E., Brook, I.M. and van Noort, R. (2015). Evaluation of the Effects of Ethanol on Monolayer and 3D Models of Human Oral Mucosa. *Journal of Environmental and Analytical Toxicology*, 5(3), pp. 1 -6.

Mojtahedi, N, Ghalayani, P., Golestannejad, Z., Davari A, and Hy, S. (2017). Comparative Evaluation of Two Forms of Drugs: Patch & Lotion of Clobetasol, on Recovery Indicators of Aphthous Stomatitis. *Annals of Dental Specialty*, *5*(2), pp.27-32.

Moll, R. and Moll, I. (1998). Epidermal Adhesion Molecules And Basement Membrane Components As Target Structures Of Autoimmunity. *Virchows Archiv*, 432(6), pp.487-504.

Moll, R., Divo, M. and Langbein, L. (2008). The Human Keratins: Biology And Pathology. *Histochemistry and Cell Biology*, 129(6), pp.705-733.

Morales, C., Holt, S., Ouellette, M., Kaur, K., Yan, Y., Wilson, K., White, M., Wright, W. and Shay, J. (1999). Absence of cancer–associated changes in human fibroblasts immortalized with telomerase. *Nature Genetics*, 21(1), pp.115-118.

Moriyama, T., Asahina, I., Ishii, M., Oda, M., Ishii, Y. and Enomoto, S. (2001). Development Of Composite Cultured Oral Mucosa Utilizing Collagen Sponge Matrix And Contracted Collagen Gel: A Preliminary Study For Clinical Applications. *Tissue Engineering*, 7, pp.415-427.

Mortimer, K., Harrison, T., Tang, Y., Wu, K., Lewis, S., Sahasranaman, S., Hochhaus, G. and Tattersfield, A. (2006). Plasma Concentrations Of Inhaled Corticosteroids In Relation To Airflow Obstruction In Asthma. *British Journal of Clinical Pharmacology*, 62(4), pp.412-419.

Mosmann, T. (1983). Rapid Colorimetric Assay for Cellular Growth and Survival: Application to Proliferation And Cytotoxicity Assays. *Journal of Immunological Methods*, *65*(1-2), pp.55-63.

Mostefaoui, Y., Claveau, I. and Rouabhia, M. (2004). *In Vitro* Analyses of Tissue Structure and Interleukin-1β Expression and Production by Human Oral Mucosa in Response to *Candida albicans* Infections. *Cytokine*, 25(4), pp.162-171.

Motlekar, N. and Youan, B. (2006). The Quest for Non-Invasive Delivery of Bioactive Macromolecules: A Focus on Heparins. *Journal of Controlled Release*, 113(2), pp.91-101.

Muheem, A., Shakeel, F., Jahangir, M., Anwar, M., Mallick, N., Jain, G., Warsi, M. and Ahmad, F. (2016). A Review On The Strategies For Oral Delivery Of Proteins And Peptides And Their Clinical Perspectives. *Saudi Pharmaceutical Journal*, 24(4), pp.413-428.

Murata, M., Okuda, K., Momose, M., Kubo, K., Kuroyanagi, Y. and Wolff, L. (2008). Root Coverage with Cultured Gingival Dermal Substitute Composed of Gingival Fibroblasts and Matrix: A Case Series. *International Journal of Periodontics & Restorative Dentistry*, 28(5), pp.461–467.

Muschler, G., Nakamoto, C. And Griffith, L. (2004). Engineering Principles of Clinical Cell-Based Tissue Engineering. *The Journal of Bone and Joint Surgery. American Volume,* 86(7), pp.1541-1558.

Nakamura, T., Endo, K.I., Cooper, L.J., Fullwood, N.J., Tanifuji, N., Tsuzuki, M., Koizumi, N., Inatomi, T., Sano, Y. and Kinoshita, S. (2003). The Successful Culture and Autologous Transplantation of Rabbit Oral Mucosal Epithelial Cells on Amniotic Membrane. *Investigative Ophthalmology & Visual Science*, 44(1), pp.106-116.

National Eczema Society. (2018). [online] Eczema.org. Available at: http://eczema.org/documents/578 [Accessed 2 Aug. 2018].

Needleman, I. (1991). Controlled Drug Release in Periodontics: A Review Of New Therapies. *British Dental Journal*, 170(11), pp.405-408.

Nelson, D., Koymans, L., Kamataki, T., Stegeman, J., Feyereisen, R., Waxman, D., Waterman, M., Gotoh, O., Coon, M., Estabrook, R., Gunsalus, I. and Nebert, D. (1996). P450 Superfamily: Update On New Sequences, Gene Mapping, Accession Numbers And Nomenclature. *Pharmacogenetics*, 6(1), pp.1-42.

Ng, K.W., Khor, H.L. and Hutmacher, D.W. (2004). In Vitro Characterization Of Natural And Synthetic Dermal Matrices Cultured With Human Dermal Fibroblasts. *Biomaterials*, 25, pp.2807–2818.

Ng, K.W., Tham, W., Lim, T.C. and Werner Hutmacher, D. (2005). Assimilating Cell Sheets and Hybrid Scaffolds For Dermal Tissue Engineering. *Journal of Biomedical Materials Research Part A*, 75(2), pp.425-438.

Nguyen, S. and Hiorth, M. (2015). Advanced Drug Delivery Systems for Local Treatment of the Oral Cavity. *Therapeutic Delivery*, 6(5), pp.595-608.

Nicolazzo, J., Reed, B. and Finnin, B. (2003). The Effect of Various In Vitro Conditions on the Permeability Characteristics of the Buccal Mucosa. *Journal of Pharmaceutical Sciences*, 92(12), pp.2399-2410.

Nielsen, H. and Rassing, M. (1999). TR146 Cells Grown On Filters As A Model Of Human Buccal Epithelium: III. Permeability Enhancement By Different pH Values, Different Osmolality Values, And Bile Salts. *International Journal of Pharmaceutics*, 185(2), pp.215-225.

Nielsen, H. and Rassing, M. (2002). Nicotine Permeability Across The Buccal TR146 Cell Culture Model And Porcine Buccal Mucosa In Vitro: Effect Of pH And Concentration. *European Journal of Pharmaceutical Sciences*, 16(3), pp.151-157.

Nielsen, H., Verhoef, J., Ponec, M. and Rassing, M. (1999). TR146 Cells Grown On Filters As A Model Of Human Buccal Epithelium: Permeability Of Fluorescein Isothiocyanate-Labelled Dextrans In The Presence Of Sodium Glycocholate. *Journal of Controlled Release*, 60(2-3), pp.223-233.

Nielsen, H.M. and Rassing, M.R. (2000). TR146 Cells Grown On Filters As A Model Of Human Buccal Epithelium: V. Enzyme Activity Of The TR146 Cell Culture Model, Human Buccal Epithelium And Porcine Buccal Epithelium, And Permeability Of Leu-Enkephalin. *International Journal of Pharmaceutics*, 200(2), pp.261-270.

Niessen, C. (2007). Tight Junctions/Adherens Junctions: Basic Structure and Function. *Journal of Investigative Dermatology*, 127(11), pp.2525-2532.

Nishida, K., Yamato, M., Hayashida, Y., Watanabe, K., Yamamoto, K., Adachi, E., Nagai, S., Kikuchi, A., Maeda, N., Watanabe, H., Okano, T. and Tano, Y. (2004). Corneal Reconstruction with Tissue-Engineered Cell Sheets Composed of Autologous Oral Mucosal Epithelium. *New England Journal of Medicine*, 351(12), pp.1187-1196.

Nuutinen, P., Autio, P., Hurskainen, T. and Oikarinen, A. (2001). Glucocorticoid Action On Skin Collagen: Overview On Clinical Significance And Consequences. *Journal of the European Academy of Dermatology and Venereology*, 15(4), pp.361-362.

Nyström, M., Thomas, G., Stone, M., Mackenzie, I., Hart, I. and Marshall, J. (2005). Development Of A Quantitative Method To Analyse Tumour Cell Invasion In Organotypic Culture. *The Journal of Pathology*, 205(4), pp.468-475.

O'Brien, F. (2011). Biomaterials & Scaffolds for Tissue Engineering. *MaterialsToday*, [online] 14(3), pp.88-95.

Odraska, P., Mazurova, E., Dolezalova, L. and Blaha, L. (2011). In Vitro Evaluation Of The Permeation Of Cytotoxic Drugs Through Reconstructed Human Epidermis And Oral Epithelium. *Klinická Onkologie: Casopis Ceské a Slovenské Onkologické Spolecnosti*, *24*(3), pp.195–202.

OECD (2004). Test Guideline 431. OECD Guideline for the Testing of Chemicals. In Vitro Skin Model. Adopted January 20, 2016. Available at: [http://www.oecd.org/env/ehs/testing/43302385.pdf]

OECD. (2015). Test No 439, In Vitro Skin Irritation: Reconstructed Human Epidermis Test Method, 2015 ed., OECD Publishing, Paris.

Ohki, T., Yamato, M., Murakami, D., Takagi, R., Yang, J., Namiki, H., Okano, T. and Takasaki, K. (2006). Treatment of Oesophageal Ulcerations Using Endoscopic Transplantation of Tissue-Engineered Autologous Oral Mucosal Epithelial Cell Sheets in a Canine Model. *Gut*, 55(12), pp.1704-1710.

Oksala, O., Salo, T., Tammi, R., Häkkinen, L., Jalkanen, M., Inki, P. and Larjava, H. (1995). Expression Of Proteoglycans And Hyaluronan During Wound Healing. *Journal of Histochemistry & Cytochemistry*, 43(2), pp.125-135.

Onder, T. and Daley, G. (2012). New Lessons Learned From Disease Modeling With Induced Pluripotent Stem Cells. *Current Opinion in Genetics & Development*, 22(5), pp.500-508.

Ophof, R., Maltha, J., Kuijpers-Jagtman, A. and Von den Hoff, J. (2008). Implantation of Tissue-Engineered Mucosal Substitutes in the Dog Palate. *The European Journal of Orthodontics*, 30(1), pp.1-9.

Orringer, J., Shaw, W., Borud, L., Freymiller, E., Wang, S. and Markowitz, B. (1999). Total Mandibular and Lower Lip Reconstruction with a Prefabricated Osteocutaneous Free Flap. *Plastic and Reconstructive Surgery*, 104(3), pp.793-797.

Owaribe, K., Kartenbeck, J., Stumpp, S., Magin, T., Krieg, T., Diaz, L. and Franke, W. (1990). The hemidesmosomal plaque. *Differentiation*, 45(3), pp.207-220.

Owens, G., Hahn, W. and Cohen, J. (1991). Identification of mRNAs Associated With Programmed Cell Death In Immature Thymocytes. *Molecular and Cellular Biology*, 11(8), pp.4177-4188.

Paderni, C., Compilato, D., Giannola, L. and Campisi, G. (2012). Oral Local Drug Delivery And New Perspectives In Oral Drug Formulation. *Oral Surgery, Oral Medicine, Oral Pathology and Oral Radiology*, 114(3), pp.e25-e34.

Paliogianni, F., Ahuja, S. S., Balow, J. P., Balow, J. E. and Boumpas, D. T. (1993). Novel Mechanism For Inhibition Of Human T Cells By Glucocorticoids. Glucocorticoids Inhibit Signal Transduction Through IL-2 Receptor. *Journal Of Immunology* (Baltimore, Md. : 1950), 151(8), pp.4081–4089.

Palsson, B. and Bhatia, S. (2004). Tissue Engineering. Upper Saddle River, N.J.: Pearson Prentice Hall.

Pang, Y., Schermer, A., Yu, J. and Sun, T. (1993). Suprabasal Change and Subsequent Formation of Disulfide-Stabilized Homo- And Hetero-Dimers of Keratins during Esophageal Epithelial Differentiation. *Journal of Cell Science*, 104, pp.727-740.

Parenteau-Bareil, R., Gauvin, R. and Berthod, F. (2010). Collagen-Based Biomaterials For Tissue Engineering Applications. *Materials*, *3*(3),pp.1863–1887.

Patel, D., Smith, A., Grist, N., Barnett, P. and Smart, J. (1999). An *In Vitro* Mucosal Model Predictive Of Bioadhesive Agents in the Oral Cavity. *Journal of Controlled Release*, 61(1-2), pp.175-183.

Patel, V., Liu, F. and Brown, M. (2011). Advances in Oral Transmucosal Drug Delivery. *Journal of Controlled Release*, 153(2), pp.106-116.

Patel, V., Liu, F. and Brown, M. (2012). Modelling the Oral Cavity: In Vitro And In Vivo Evaluations Of Buccal Drug Delivery Systems. *Journal of Controlled Release*, 161(3), pp.746-756.

Payne, K., Balasundaram, I., Deb, S., Di Silvio, L. and Fan, K. (2014). Tissue Engineering Technology and Its Possible Applications in Oral and Maxillofacial Surgery. *British Journal of Oral and Maxillofacial Surgery*, 52(1), pp.7-15.

Pelkonen, O., Turpeinen, M., Hakkola, J., Honkakoski, P., Hukkanen, J. and Raunio, H. (2008). Inhibition And Induction Of Human Cytochrome P450 Enzymes: Current Status. *Archives of Toxicology*, 82(10), pp.667-715.

Peña, I., Junquera, L., Meana, Á., García, E., Aguilar, C. and Fresno, M. (2011). *In Vivo* Behavior of Complete Human Oral Mucosa Equivalents: Characterization in Athymic Mice. *Journal of Periodontal Research*, 46(2), pp.214-220.

Perioli, L., Ambrogi, V., Angelici, F., Ricci, M., Giovagnoli, S., Capuccella, M. and Rossi, C. (2004). Development Of Mucoadhesive Patches For Buccal Administration Of Ibuprofen. *Journal of Controlled Release*, 99(1), pp.73-82.

Perioli, L., Pagano, C., Mazzitelli, S., Rossi, C. and Nastruzzi, C. (2008). Rheological and Functional Characterization of New Antiinflammatory Delivery Systems Designed for Buccal Administration. *International Journal of Pharmaceutics*, 356(1-2), pp.19-28.

Pershing, L., Corlett, J., Lambert, L. and Poncelet, C. (1994). Circadian Activity of Topical 0.05% Betamethasone Dipropionate in Human Skin In Vivo. *Journal of Investigative Dermatology*, 102(5), pp.734-739.

Piccinni, M.-P., Lombardelli, L., Logiodice, F., Tesi, D., Kullolli, O., Biagiotti, R., … Ficarra, G. (2014). Potential pathogenetic role of Th17, Th0, and Th2 cells in erosive and reticular oral lichen planus. *Oral Diseases*, 20(2), 212–218.

Ponec, M., Kempenaar, J. and De Kloet, E. (1981). Corticoids and Cultured Human Epidermal Keratinocytes: Specific Intracellular Binding and Clinical Efficacy. *Journal of Investigative Dermatology*, 76(3), pp.211-214.

Ponec, M., Kempenaar, J., Shroot, B. and Caron, J. (1986). Glucocorticoids: Binding Affinity and Lipophilicity. *Journal of Pharmaceutical Sciences*, 75(10), pp.973-975.

Poulsen, J., & Rorsman, H. (1980). Ranking Of Glucocorticoid Creams And Ointments. *Acta Dermato-Venereologica*, 60(1), pp.57–62.

Presland, R. and Dale, B. (2000). Epithelial Structural Proteins of the Skin and Oral Cavity: Function in Health and Disease. *Critical Reviews in Oral Biology & Medicine*, 11(4), pp.383-408.

Purdue, G.F. (1997). Dermagraft-TC Pivotal Efficacy And Safety Study. *Journal of Burn Care & Rehabilitation*,18, pp.13-14.

Rainone, A., De Lucia, D., Morelli, C., Valente, D., Catapano, O. and Caraglia, M. (2015). Clinically Relevant Of Cytochrome P450 Family Enzymes For Drug-Drug Interaction In Anticancer Therapy. *World Cancer Research Journal*, 2(2), pp.1-7.

Ramakrishna, S., Fujihara, K., Teo, W., Yong, T., Ma, Z. and Ramaseshan, R. (2006). Electrospun Nanofibers: Solving Global Issues. *Materials Today*, 9(3), pp.40-50.

Rameez, S., Alosta, H. and Palmer, A. (2008). Biocompatible and Biodegradable Polymersome Encapsulated Hemoglobin: A Potential Oxygen Carrier. *Bioconjugate Chemistry*, 19(5), pp.1025-1032.

Ramieri, G., Anselmetti, G., Baracchi, F., Panzica, G., Viglietti-Panzica, C., Modica, R. and Polak, J. (1990). The Innervation Of Human Teeth And Gingival Epithelium As Revealed By Means Of An Antiserum For Protein Gene Product 9.5 (PGP 9.5). *American Journal of Anatomy*, 189(2), pp.146-154.

Ramieri, G., Panzica, G., Viglietti-Panzica, C., Modica, R., Springall, D. and Polak, J. (1992). Non-Innervated Merkel Cells And Merkel-Neurite Complexes In Human Oral Mucosa Revealed Using Antiserum To Protein Gene Product 9.5. *Archives of Oral Biology*, 37(4), pp.263-269.

Rao, G. and Murthy, R.S.R. (2000). Evaluation Of Liposomal Clobetasol Propionate Topical Formulation For Intra-Dermal Delivery. *Indian Journal of Pharmaceutical Science*s, 62, pp.459-462.

Rathbone, M. and Hadgraft, J. (1991). Absorption of Drugs from the Human Oral Cavity. *International Journal of Pharmaceutics*, 74(1), pp.9-24.

Rathbone, M. and Tucker, I. (1993). Mechanisms, Barriers and Pathways of Oral Mucosal Drug Permeation. *Advanced Drug Delivery Reviews*, 12(1-2), pp.41-60.

Rathbone, M., Senel, S. and Pather, I. eds. (2015). Oral Mucosal Drug Delivery and Therapy. Springer.

Rauch, D., Gross, S., Harding, J., Bokhari, S., Niewiesk, S., Lairmore, M., Piwnica-Worms, D. and Ratner, L. (2009). T-Cell Activation Promotes Tumorigenesis In Inflammation-Associated Cancer. *Retrovirology*, 6(1), pp.116.

Ray, A., Zhang, D. H., Siegel, M. D. and Ray, P. (1995). Regulation Of Interleukin-6 Gene Expression By Steroids. *Annals of the New York Academy of Sciences*, *762*, pp.79-87.

Reichl, S. and Müller-Goymann, C. (2003). The Use Of A Porcine Organotypic Cornea Construct For Permeation Studies From Formulations Containing Befunolol Hydrochloride. *International Journal of Pharmaceutics*, 250(1), pp.191-201.

Rendic, S. (2002). Summary Of Information On Human CYP Enzymes: Human P450 Metabolism Data. *Drug Metabolism Reviews*, 34(1-2), pp.83-448.

Rheinwald, J. and Green, H. (1977). Epidermal Growth Factor and the Multiplication of Cultured Human Epidermal Keratinocytes. *Nature*, 265(5593), pp.421-424.

Rheinwatd, J. and Green, H. (1975). Serial Cultivation of Strains of Human Epidemal Keratinocytes: The Formation Keratinizin Colonies from Single Cells. *Cell*, 6(3), pp.331-343.

Rhen, T. and Cidlowski, J. (2005). Antiinflammatory Action of Glucocorticoids — New Mechanisms for Old Drugs. *New England Journal of Medicine*, 353(16), pp.1711-1723.

Richard, N., Anderson, J., Weiss, J. and Binder, P. (1991). Air/Liquid Corneal Organ Culture: A Light Microscopic Study. *Current Eye Research*, 10(8), pp.739-749.

Rodgers, L. S. and Fanning, A. S. (2011). Regulation Of Epithelial Permeability By The Actin Cytoskeleton. *Cytoskeleton (Hoboken, N.J.)*, *68*(12),pp.653–660.

Rossi, S., Sandri, G. and Caramella, C. (2005). Buccal Drug Delivery: A Challenge Already Won?. *Drug Discovery Today: Technologies*, 2(1), pp.59-65.

Rouabhia, M., Mukherjee, P., Lattif, A., Curt, S., Chandra, J. and Ghannoum, M. (2010). Disruption of Sphingolipid Biosynthetic Gene IPT1 Reduces *Candida albicans* Adhesion and Prevents Activation of Human Gingival Epithelial Cell Innate Immune Defense. *Medical Mycology*, pp.1-9.

Roy, R., Boskey, A. and Bonassar, L. (2010). Processing of Type I Collagen Gels Using Nonenzymatic Glycation. *Journal of Biomedical Materials Research Part A*, 93(3), pp.843-851.

Rupniak, H.T., Rowlatt, C., Lane, E.B., Steele, J.G., Trejdosiewicz, L.K., Laskiewicz, B., Povey, S. and Hill, B.T. (1985). Characteristics of Four New Human Cell Lines Derived from Squamous Cell Carcinomas of the Head and Neck. *Journal of the National Cancer Institute*, *75*(4), pp.621-635.

Ruszymah, B.H., 2004. Autologous Human Fibrin as the Biomaterial for Tissue Engineering. *The Medical Journal of Malaysia*, 59, pp.30-31.

Saarni H, and Hopsu-Havu V.K. (1978). The decrease of hyaluronate synthesis by anti-inflammatory steroids in vitro. *British Journal of Dermatology*, 98, pp.445–449.

Saffar, A.S., Ashdown, H. and Gounni, A.S. (2011). The Molecular Mechanisms of Glucocorticoids-Mediated Neutrophil Survival. *Current Drug Targets*, 12(4), pp.556-562.

Sahota, P., Burn, J., Brown, N. and MacNeil, S. (2004). Approaches To Improve Angiogenesis In Tissue-Engineered Skin. *Wound Repair and Regeneration*, 12(6), pp.635-642.

Sahuc, F., Nakazawa, K., Berthod, F., Collombel, C. and Damour, O. (1996). Mesenchymal-Epithelial Interactions Regulate Gene Expression of Type VII Collagen and Kalinin in Keratinocytes and Dermal-Epidermal Junction Formation in a Skin Equivalent Model. *Wound Repair and Regeneration*, 4(1), pp.93-102.

Samprasit, W., Rojanarata, T., Akkaramongkolporn, P., Ngawhirunpat, T., Kaomongkolgit, R. and Opanasopit, P. (2015). Fabrication and In Vitro/In Vivo Performance of Mucoadhesive Electrospun Nanofiber Mats Containing α-Mangostin. *AAPS PharmSciTech*, 16(5), pp.1140-1152.

Sanchez-Quevedo, M., Alaminos, M., Capitan, L., Moreu, G., Garzon, I., Crespo, P. and Campos, A. (2007). Histological and Histochemical Evaluation of Human Oral Mucosa Constructs Developed by Tissue Engineering. *Histology and Histopathology*, [online] 22, pp.631-640.

Sandri, G., Poggi, P., Bonferoni, M. C., Rossi, S., Ferrari, F. and Caramella, C. (2006). Histological Evaluation Of Buccal Penetration Enhancement Properties Of Chitosan And Trimethyl Chitosan. *The Journal of Pharmacy and Pharmacology*, *58*(10),pp.1327–1336.

Sangeetha, S., Nagasamy Venkatesh, D., Krishan, P. and Saraswathi, R. (2010). Mucosa as a Route for Systemic Drug Delivery. *Research Journal of Pharmaceutical, Biological and Chemical Sciences*, 1(3), pp.178.

Sankar, V., Hearnden, V., Hull, K., Juras, D., Greenberg, M., Kerr, A., Lockhart, P., Patton, L., Porter, S. and Thornhill, M. (2011). Local Drug Delivery For Oral Mucosal Diseases: Challenges And Opportunities. *Oral Diseases*, 17, pp.73-84.

Santocildes-Romero, M., Hadley, L., Clitherow, K., Hansen, J., Murdoch, C., Colley, H., Thornhill, M. and Hatton, P. (2017). Fabrication of Electrospun Mucoadhesive Membranes for Therapeutic Applications in Oral Medicine. *ACS Applied Materials & Interfaces*, 9(13), pp.11557-11567.

Santos, C., Jacob, J., Hertzog, B., Freedman, B., Press, D., Harnpicharnchai, P. and Mathiowitz, E. (1999). Correlation of Two Bioadhesion Assays: The Everted Sac Technique and The CAHN Microbalance. *Journal of Controlled Release*, 61(1-2), pp.113-122.

Satheesh Madhav, N., Semwal, R., Semwal, D. and Semwal, R. (2012). Recent Trends in Oral Transmucosal Drug Delivery Systems: An Emphasis on The Soft Palatal Route. *Expert Opinion on Drug Delivery*, 9(6), pp.629-647.

Satheesh Madhav, N., Shakya, A., Shakya, P. and Singh, K. (2009). Orotransmucosal Drug Delivery Systems: A Review. *Journal of Controlled Release*, 140, pp.2–11.

Sathisha, M., Revankar, V. and Pai, K. (2008). Synthesis, Structure, Electrochemistry, and Spectral Characterization of Bis-Isatin Thiocarbohydrazone Metal Complexes and Their Antitumor Activity against Ehrlich Ascites Carcinoma in Swiss Albino Mice. *Metal-Based Drugs*, pp.1-11.

Sato, T., Usui, M., Yoda, T., Enoki, Y. and Kokabu, S. (2015). Possible Neuroimmunomodulation Therapy In T-Cell-Mediated Oral Diseases. *Dental Hypotheses*, 6(2), pp.49.

Sattar, M., Sayed, O. and Lane, M. (2014). Oral Transmucosal Drug Delivery – Current Status and Future Prospects. *International Journal of Pharmaceutics*, 471(1-2), pp.498-506.

Schäcke, H, Döcke, W.D. Asadullah K. (2002). Mechanisms Involved In The Side Effects Of Glucocorticoids. *Pharmacology & Therapeutics*, 96(1), pp.23-43.

Schalkwijk, C., Vervoordeldonk, M., Pfeilschifter, J., Märki, F. and van den Bosch, H. (1991). Cytokine-And Forskolin-Induced Synthesis Of Group II Phospholipase A2 And Prostaglandin E2 in Rat Mesangial Cells Is Prevented By Dexamethasone. *Biochemical and Biophysical Research Communications*, 180(1), pp.46-52.

Schaller, M., Zakikhany, K., Naglik, J., Weindl, G. and Hube, B. (2006). Models Of Oral And Vaginal Candidiasis Based On In Vitro Reconstituted Human Epithelia. *Nature Protocols*, 1(6), pp.2767-2773.

Schlosser, B. (2010). Lichen Planus and Lichenoid Reactions of the Oral Mucosa. *Dermatologic Therapy*, 23(3), pp.251-267.

Schmidt, C. (2012). GINTUIT Cell Therapy Approval Signals Shift at US Regulator. *Nature Biotechnology*, 30(6), pp.479-479.

Schneider, U., Schwenk, H. and Bornkamm, G. (1977). Characterization of EBV-Genome Negative “Null” And “T” Cell Lines Derived From Children With Acute Lymphoblastic Leukemia And Leukemic Transformed Non-Hodgkin Lymphoma. *International Journal of Cancer*, 19(5), pp.621-626.

Schoepe, S., Schacke, H., May, E. and Asadullah, K. (2006). Glucocorticoid Therapy-Induced Skin Atrophy. *Experimental Dermatology*, 15(6), pp.406-420.

Scholz, O., Wolff, A., Schumacher, A., Giannola, L., Campisi, G., Ciach, T. and Velten, T. (2008). Drug Delivery From The Oral Cavity: Focus on a Novel Mechatronic Delivery Device. *Drug Discovery Today*, 13(5-6), pp.247-253.

Schoop, V., Mirancea, N. and Fusenig, N. (1999). Epidermal Organization and Differentiation of HaCaT Keratinocytes in Organotypic Coculture with Human Dermal Fibroblasts. *Journal of Investigative Dermatology,* 112(3), pp.343-353.

Schroeder, H. (1981). *Differentiation of human oral stratified epithelia*. Basel: Karger.

Schroeder, H. (1991). *Oral structural biology*. Thieme.

Schultz, G., Davidson, J., Kirsner, R., Bornstein, P. and Herman, I. (2011). Dynamic Reciprocity In The Wound Microenvironment. *Wound Repair and Regeneration*, 19(2), pp.134-148.

Scully, C. and Carrozzo, M. (2008). Oral Mucosal Disease: Lichen Planus. *British Journal of Oral and Maxillofacial Surgery*, 46(1), pp.15-21.

Scully, C. and Porter, S. (2008). Oral Mucosal Disease: Recurrent Aphthous Stomatitis. *British Journal of Oral and Maxillofacial Surgery*, 46(3), pp.198-206.

Scully, C., Eisen, D. and Carrozzo, M. (2000). Management of Oral Lichen Planus. *American Journal of Clinical Dermatology*, 1(5), pp.287-306.

Seggewiss, R., Loré, K., Greiner, E., Magnusson, M. K., Price, D. A., Douek, D. C., Dunbar, C. E. and Wiestner, A. (2005). Imatinib Inhibits T-Cell Receptor–Mediated T-Cell Proliferation And Activation In A Dose-Dependent Manner. *Blood*, 105(6), pp.2473-2479.

Şenyiğit, T., Sonvico, F., Barbieri, S., Özer, Ö., Santi, P. and Colombo, P. (2010). Lecithin/Chitosan Nanoparticles Of Clobetasol-17-Propionate Capable Of Accumulation In Pig Skin. *Journal of Controlled Release*, 142(3), pp.368-373.

Senyigit, T.and Ozer, O. (2012). Corticosteroids for Skin Delivery: Challenges and New Formulation Opportunities. *Glucocorticoids - New Recognition of Our Familiar Friend*, pp.595–612.

Shakya, P., Madhav, N., Shakya, A. and Singh, K. (2011). Palatal Mucosa as a Route for Systemic Drug Delivery: A Review. *Journal of Controlled Release*, 151(1), pp.2-9.

Sheu, H., Lee, J., Chai, C. and Kuo, K. (1997). Depletion Of Stratum Corneum Intercellular Lipid Lamellae And Barrier Function Abnormalities After Long-Term Topical Corticosteroids. *British Journal of Dermatology*, 136(6), pp.884-890.

Shinkar, D., Dhake, A. and Setty, C. (2012). Drug Delivery from the Oral Cavity: A Focus on Mucoadhesive Buccal Drug Delivery Systems. *PDA Journal of Pharmaceutical Science and Technology*, 66(5), pp.466-500.

Shirasuna, K. (2014). Oral Lichen Planus: Malignant Potential And Diagnosis. *Oral Science International,* 11, pp.1–7.

Shojaei AH, Li X. In Vitro Permeation Of Acyclovir Through Porcine Buccal Mucosa (1996). *Proc Int Symp Control Release Bioact Mater*,23, pp.507-508.

Shoulders, M. and Raines, R. (2009). Collagen Structure and Stability. *Annual Review of Biochemistry*, 78(1), pp.929-958.

Silva, L., Taveira, S., Lima, E. and Marreto, R. (2012). In Vitro Skin Penetration Of Clobetasol From Lipid Nanoparticles: Drug Extraction And Quantitation In Different Skin Layers. *Brazilian Journal of Pharmaceutical Sciences*, 48(4), pp.811-817.

Singh, S., Singh, R., Gupta, S., Kalyanwat, R. and Yadav, S. (2011). Buccal Mucosa as A Route for Drug Delivery: Mechanism, Design and Evaluation. *Research Journal of Pharmaceutical, Biological and Chemical Sciences*, 2(3), pp.358 -372.

Sivaraman, A., Leach, J., Townsend, S., Iida, T., Hogan, B., Stolz, D., Fry, R., Samson, L., Tannenbaum, S. and Griffith, L. (2005). A Microscale In Vitro Physiological Model of the Liver: Predictive Screens for Drug Metabolism and Enzyme Induction. *Current Drug Metabolism*, 6(6), pp.569-591.

Smart, J. (2004). Lectin-Mediated Drug Delivery in The Oral Cavity. *Advanced Drug Delivery Reviews*, 56(4), pp.481-489.

Smart, J. (2005). The Basics And Underlying Mechanisms Of Mucoadhesion. *Advanced Drug Delivery Reviews*, 57(11), pp.1556-1568.

Smith, G., Ibbotson, S., Comrie, M., Dawe, R., Bryden, A., Ferguson, J. and Wolf, C. (2006). Regulation Of Cutaneous Drug-Metabolizing Enzymes And Cytoprotective Gene Expression By Topical Drugs In Human Skin In Vivo. *British Journal of Dermatology*, 155(2), pp.275-281.

Smith, S., Colley, H., Sharma, P., Slowik, K., Sison-Young, R., Sneddon, A., Webb, S. and Murdoch, C. (2018). Expression And Enzyme Activity Of Cytochrome P450 Enzymes CYP3A4 And CYP3A5 In Human Skin And Tissue-Engineered Skin Equivalents. *Experimental Dermatology*, 27(5), pp.473-475.

Smola, H., Stark, H., Thiekötter, G., Mirancea, N., Krieg, T. and Fusenig, N. (1998). Dynamics of Basement Membrane Formation by Keratinocyte–Fibroblast Interactions in Organotypic Skin Culture. *Experimental Cell Research*, 239(2), pp.399-410.

Sohi, H., Ahuja, A., Ahmad, F. and Khar, R. (2010). Critical evaluation of permeation enhancers for oral mucosal drug delivery. *Drug Development and Industrial Pharmacy*, 36(3), pp.254-282.

Sonthalia, S. and Singal, A. (2012). Comparative Efficacy of Tacrolimus 0.1% Ointment and Clobetasol Propionate 0.05% Ointment in Oral Lichen Planus: A Randomized Double-Blind Trial. *International Journal of Dermatology*, 51(11), pp.1371-1378.

Southgate, J., Williams, H. K., Trejdosiewicz, L. K. and Hodges, G. M. (1987). Primary Culture Of Human Oral Epithelial Cells. Growth Requirements And Expression Of Differentiated Characteristics. Laboratory Investigation. *Journal of Technical Methods and Pathology*, 56(2), pp.211–223.

Squier, C. (1977). Membrane Coating Granules In Nonkeratinizing Oral Epithelium. *Journal of Ultrastructure Research*, 60(2), pp.212-220.

Squier, C. (1991). The Permeability of Oral Mucosa. *Critical Reviews in Oral Biology & Medicine*, 2, pp.13–32.

Squier, C. and Brogden, K. (2011). Human Oral Mucosa. https://doi.org/10.1002/9781118710470

Squier, C. and Kremer, M. (2001). Biology of Oral Mucosa and Esophagus. *Journal of the National Cancer Institute (JNCI) Monographs*, 2001(29), pp.7-15.

Squier, C. and Wertz, P. (1993). Permeability and the Pathophysiology of Oral Mucosa. *Advanced Drug Delivery Reviews*, 12(1-2), pp.13-24.

Squier, C.A. and Finkelstein, M.W. (1998). Oral mucosa. In: Oral histology, development, structure and function. St. Louis (MO): CV Mosby, pp. 345–85.

Squier, C.A., Johnson, N.W., Hackemann, M. (1975). Structure And Function Of Normal Human Oral Mucosa. In: Dolby A.E., editor. Oral mucosa in health and disease. Oxford: Blackwell Scientific Publications, pp.1-112.

Sriram, G., Bigliardi, P. L. and Bigliardi-Qi, M. (2015). Fibroblast Heterogeneity And Its Implications For Engineering Organotypic Skin Models In Vitro. *European Journal of Cell Biology*, *94*(11), pp.483–512.

Sriram, G., Bigliardi, P. L. and Bigliardi-Qi, M. (2018). Full-Thickness Human Skin Equivalent Models of Atopic Dermatitis*. In Methods in molecular biology (Clifton, N.J.).* pp.1-17.

Stanbury, R. and Graham, E. (1998). Systemic Corticosteroid Therapy---Side Effects And Their Management. *British Journal of Ophthalmology*, 82(6), pp.704-708.

Stephens, P. and Genever, P. (2007). Non-Epithelial Oral Mucosal Progenitor Cell Populations. *Oral Diseases*, 13(1), pp.1-10.

Stoughton, R. (1987). Are Generic Formulations Equivalent to Trade Name Topical Glucocorticoids?. *Archives of Dermatology*, 123(10), p.1312.

Subramani, T., Rathnavelu, V., Yeap, S. and Alitheen, N. (2013). Influence of Mast Cells in Drug-Induced Gingival Overgrowth. *Mediators of Inflammation*, pp.1-8.

Sudhakar, Y., Kuotsu, K. and Bandyopadhyay, A. (2006). Buccal Bioadhesive Drug Delivery — a Promising Option for Orally Less Efficient Drugs. *Journal of Controlled Release*, 114(1), pp.15-40.

Sugerman, P. and Savage, N. (2002). Oral Lichen Planus: Causes, Diagnosis and Management. *Australian Dental Journal*, 47(4), pp.290-297.

Sugerman, P., Savage, N., Walsh, L., Zhao, Z., Zhou, X., Khan, A., Seymour, G. and Bigby, M. (2002). The Pathogenesis of Oral Lichen Planus. *Critical Reviews in Oral Biology & Medicine*, 13(4), pp.350-365.

Sun, T., Jackson, S., Haycock, J.W. and MacNeil, S. (2006). Culture of skin cells in 3D rather than 2D improves their ability to survive exposure to cytotoxic agents. *Journal of Biotechnology*, *122*(3), pp.372–381.

Szefler, S. (1999). Pharmacodynamics and pharmacokinetics of budesonide: A new nebulized corticosteroid. *Journal of Allergy and Clinical Immunology*, 104(4), pp.S175-S183.

Takagi, R., Yamato, M., Kanai, N., Murakami, D., Kondo, M., Ishii, T., Ohki, T., Namiki, H., Yamamoto, M. and Okano, T. (2012). Cell Sheet Technology for Regeneration of Esophageal Mucosa. *World Journal of Gastroenterology*, 18(37), pp.5145-5150.

Tammi, R. and Jansén, C. (1980). Effect Of Serum And Oxygen Tension On Human Skin Organ Culture: A Histometric Analysis. *Acta Dermato-Venereologica*, 60(3), pp.223–228.

Terris, B. and Potet, F. (1995). Structure and Role of Langerhans' Cells in the Human Oesophageal Epithelium. *Digestion*, 56(1), pp.9-14.

Thomason, J., Seymour, R. and Rice, N. (1993). The Prevalence And Severity Of Cyclosporin And Nifedipine-Induced Gingival Overgrowth. *Journal of Clinical Periodontology*, 20(1), pp.37-40.

Thompson, D.F. and Skaehill, P.A. (1994). Drug-Induced Lichen Planus. *Pharmacotherapy*, 14(5), 561–571.

Thongprasom, K. and Dhanuthai, K. (2008). Steroids in the Treatment of Lichen Planus: A Review. *Journal of Oral Science*, 50(4), pp.377-385.

Thorburn, D.N. and Ferguson, M.M. (1994). Topical Corticosteroids and Lesions of the Oral-Mucosa. *Advanced Drug Delivery Reviews*, *13*, pp.135–149.

Tiwari, G., Tiwari, R., Bannerjee, S., Bhati, L., Pandey, S., Pandey, P. and Sriwastawa, B. (2012). Drug Delivery Systems: An Updated Review. *International Journal of Pharmaceutical Investigation*, 2(1), p.2.

Truong-Le, V., Lovalenti, P. and Abdul-Fattah, A. (2015). Stabilization Challenges and Formulation Strategies Associated with Oral Biologic Drug Delivery Systems. *Advanced Drug Delivery Reviews*, 93, pp.95-108.

Tunggal, L., Ravaux, J., Pesch, M., Smola, H., Krieg, T., Gaill, F., Sasaki, T., Timpl, R., Mauch, C. and Aumailley, M. (2002). Defective Laminin 5 Processing in Cylindroma Cells. *The American Journal of Pathology*, 160(2), pp.459-468.

Ueno, Y., Ohmi, T., Yamamoto, M., Kato, N., Moriguchi, Y., Kojima, M., Shimozono, R., Suzuki, S., Matsuura, T. and Eda, H. (2007). Orally-Administered Caspase Inhibitor PF-03491390 Is Retained in the Liver for Prolonged Periods with Low Systemic Exposure, Exerting a Hepatoprotective Effect Against α-Fas-Induced Liver Injury in a Mouse Model. *Journal of Pharmaceutical Sciences*, 105(2), pp.201-205.

Ulukaya, E., Ozdikicioglu, F., Oral, A. and Demirci, M. (2008). The MTT Assay Yields a Relatively Lower Result of Growth Inhibition than the ATP Assay Depending on the Chemotherapeutic Drugs Tested. *Toxicology In Vitro*, 22(1), pp.232-239.

US Food and Drug Administration. (2009). EntocortEC (budesonide) capsules product label. Available from: http://www.accessdata.fda.gov/drugsatfda_docs/label/2009/021324s008lbl.pdf [last accessed 7 Mar 2017].

Uva, L., Miguel, D., Pinheiro, C., Antunes, J., Cruz, D., Ferreira, J. and Filipe, P. (2012). Mechanisms of Action of Topical Corticosteroids in Psoriasis. *International Journal of Endocrinology*, 2012, pp.1-16.

Vacanti, N., Cheng, H., Hill, P., Guerreiro, J., Dang, T., Ma, M., Watson, S., Hwang, N., Langer, R. and Anderson, D. (2012). Localized Delivery of Dexamethasone from Electrospun Fibers Reduces the Foreign Body Response. *Biomacromolecules*, 13(10), pp.3031-3038.

Vaidya, M. M., Sawant, S. S., Borges, A. M., Naresh, N. K., Purandare, M. C. and Bhisey, A. N. (2000). Cytokeratin expression in human fetal tongue and buccal mucosa. *Journal of Biosciences*, *25*(3),pp.235–242.

Van Boven, J., de Jong-van den Berg, L. and Vegter, S. (2013). Inhaled Corticosteroids and the Occurrence of Oral Candidiasis: A Prescription Sequence Symmetry Analysis. *Drug Safety*, 36(4), pp.231-236.

Van Der Velden, V. (1998). Glucocorticoids: Mechanisms Of Action And Anti-Inflammatory Potential In Asthma. *Mediators of Inflammation*, 7(4), pp.229-237.

Van Der Worp, H., Howells, D., Sena, E., Porritt, M., Rewell, S., O'Collins, V. and Macleod, M. (2010). Can Animal Models of Disease Reliably Inform Human Studies?. *PLoS Medicine*, 7(3), pp.1-8.

Van Rossum, J. (1962). The Relation Between Chemical Structure and Biological Activity. *Journal of Pharmacy and Pharmacology*, 15(1), pp.285-316.

Varoni, E., Molteni, A., Sardella, A., Carrassi, A., Di Candia, D., Gigli, F., Lodi, F. and Lodi, G. (2012). Pharmacokinetics Study About Topical Clobetasol On Oral Mucosa. *Journal of Oral Pathology & Medicine*, 41(3), pp.255-260.

Verma, N. and Chattopadhay, P. (2011). Polymeric Platform for Mucoadhesive Buccal Drug Delivery System: A Review. *International Journal of Current Pharmaceutical Research*, 3(3), pp.3-8.

Veuillez, F., Kalia, Y., Jacques, Y., Deshusses, J. and Buri, P. (2001). Factors And Strategies For Improving Buccal Absorption Of Peptides. *European Journal of Pharmaceutics and Biopharmaceutics*, 51(2), pp.93-109.

Vllasaliu, D., Falcone, F. H., Stolnik, S. and Garnett, M. (2014). Basement Membrane Influences Intestinal Epithelial Cell Growth And Presents A Barrier To The Movement Of Macromolecules. *Experimental Cell Research*, *323*(1), pp.218–231.

Vondracek, M., Xi, Z., Larsson, P., Baker, V., Mace, K., Pfeifer, A., Tja¨lve, H., Donato, M.T., Gomez-Lechon, M.J. and Grafström, R. C. (2001). Cytochrome P450 expression and related metabolism in human buccal mucosa. *Carcinogenesis*, *22*(3), pp. 481–488.

Voss, P., Sauerbier, S., Wiedmann-Al-Ahmad, M., Zizelmann, C., Stricker, A., Schmelzeisen, R. and Gutwald, R. (2010). Bone Regeneration in Sinus Lifts: Comparing Tissue-Engineered Bone and Iliac Bone. *British Journal of Oral and Maxillofacial Surgery*, 48(2), pp.121-126.

Walker, G., Langoth, N. and Bernkop-Schnürch, A. (2002). Peptidase Activity On The Surface Of The Porcine Buccal Mucosa. *International Journal of Pharmaceutics*, 233(1-2), pp.141-147.

Walko, G., Castañón, M. and Wiche, G. (2015). Molecular Architecture And Function Of The Hemidesmosome. *Cell and Tissue Research*, 360(3), pp.529-544.

Wang, Y., Zuo, Z. and Chow, M. (2009). HO-1-u-1 model for screening sublingual drug delivery—Influence of pH, osmolarity and permeation enhancer. *International Journal of Pharmaceutics*, 370(1-2), pp.68-74.

Wang, Y., Zuo, Z., Lee, K. and Chow, M. (2007). Evaluation of HO-1-u-1 Cell Line As An In Vitro Model For Sublingual Drug Delivery Involving Passive Diffusion—Initial Validation Studies. *International Journal of Pharmaceutics*, 334(1-2), pp.27-34.

Warnakulasuriya, S., Johnson, N. and Van Der Waal, I. (2007). Nomenclature and Classification of Potentially Malignant Disorders of the Oral Mucosa. *Journal of Oral Pathology & Medicine*, 36(10), pp.575-580.

Warnke, P., Springer, I., Wiltfang, J., Acil, Y., Eufinger, H., Wehmöller, M., Russo, P., Bolte, H., Sherry, E., Behrens, E. and Terheyden, H. (2004). Growth and Transplantation of a Custom Vascularised Bone Graft in a Man. *The Lancet*, 364(9436), pp.766-770.

Wiedersberg, S., Leopold, C. and Guy, R. (2008). Bioavailability and Bioequivalence of Topical Glucocorticoids. *European Journal of Pharmaceutics and Biopharmaceutics*, 68(3), pp.453-466.

Wiegand, C., Hewitt, N., Merk, H. and Reisinger, K. (2014). Dermal Xenobiotic Metabolism: A Comparison between Native Human Skin, Four in vitro Skin Test Systems and a Liver System. *Skin Pharmacology and Physiology*, 27(5), pp.263-275.

Wilk-Zasadna, I., Bernasconi, C., Pelkonen, O. and Coecke, S. (2015). Biotransformation In Vitro: An Essential Consideration In The Quantitative In Vitro-To-In Vivo Extrapolation (QIVIVE) of Toxicity Data. *Toxicology*, 332, pp.8-19.

Will, J., Melcher, R., Treul, C., Travitzky, N., Kneser, U., Polykandriotis, E., Horch, R. and Greil, P. (2008). Porous Ceramic Bone Scaffolds for Vascularized Bone Tissue Regeneration. *Journal of Materials Science: Materials in Medicine*, 19(8), pp.2781-2790.

Winning, T. and Townsend, G. (2000). Oral Mucosal Embryology And Histology. *Clinics in Dermatology*, 18(5), pp.499-511.

Wojtowicz, A., Oliveira, S., Carlson, M., Zawadzka, A., Rousseau, C. and Baksh, D. (2014). The Importance Of Both Fibroblasts And Keratinocytes In A Bilayered Living Cellular Construct Used In Wound Healing. *Wound Repair and Regeneration*, 22(2), pp.246-255.

World Health Organisation. (2018). *WHO Model Prescribing Information: Drugs Used in Skin Diseases: Annex: Classification of topical corticosteroids*. [online] Apps.who.int. Available at: http://apps.who.int/medicinedocs/en/d/Jh2918e/32.html#Jh2918e.32.1 [Accessed 2 Aug. 2018].

Xu, H., Huang, K., Zhu, Y., Gao, Q., Wu, Q., Tian, W., Sheng, X., Chen, Z. and Gao, Z. (2002). Hypoglycaemic Effect of a Novel Insulin Buccal Formulation on Rabbits. *Pharmacological Research*, 46(5), pp.459-467.

Yadev, N., Murdoch, C., Saville, S. and Thornhill, M. (2011). Evaluation of Tissue Engineered Models of The Oral Mucosa to Investigate Oral Candidiasis. *Microbial Pathogenesis*, 50(6), pp.278-285.

Yamada, K. and Cukierman, E. (2007). Modeling Tissue Morphogenesis and Cancer in 3D. *Cell*, 130(4), pp.601-610.

Yamamoto, A. (2001). Improvement of Transmucosal Absorption of Biologically Active Peptide Drugs. *Yakugaku Zasshi*, 121(12), pp.929-948.

Yamazaki, K., Ohmori, T., Kumagai, Y., Makuuchi, H. and Eyden, B. (1991). Ultrastructure of Oesophageal Melanocytosis. *Virchows Archiv A Pathological Anatomy and Histopathology*, 418(6), pp.515-522.

Ye, P., Chapple, C., Kumar, R. and Hunter, N. (2000). Expression Patterns Of E-Cadherin, Involucrin, And Connexin Gap Junction Proteins In The Lining Epithelia Of Inflamed Gingiva. *The Journal of Pathology*, 192(1), pp.58-66.

Yehia, S., El-Gazayerly, O. and Basalious, E. (2009). Fluconazole Mucoadhesive Buccal Films: In Vitro/In Vivo Performance. *Current Drug Delivery*, 6(1), pp.17-27.

Yiemwattana, I., Ngoenkam, J., Paensuwan, P., Kriangkrai, R., Chuenjitkuntaworn, B. and Pongcharoen, S. (2012). Essential Role Of The Adaptor Protein Nck1 in Jurkat T Cell Activation And Function. *Clinical & Experimental Immunology*, 167(1), pp.99–107.

Yin, T., and Green, K.J. (2004). Regulation Of Desmosome Assembly And Adhesion. *Seminars in Cell & Developmental Biology,* 15(6), pp.665–677.

Yoshizawa, M., Feinberg, S., Marcelo, C. and Elner, V. (2004). *Ex Vivo* Produced Human Conjunctiva and Oral Mucosa Equivalents Grown in a Serum-Free Culture System. *Journal of Oral and Maxillofacial Surgery*, 62(8), pp.980-988.

Yoshizawa, M., Koyama, T., Kojima, T., Kato, H., Ono, Y. and Saito, C. (2012). Keratinocytes of Tissue-Engineered Human Oral Mucosa Promote Re-Epithelialization After Intraoral Grafting in Athymic Mice. *Journal of Oral and Maxillofacial Surgery*, 70(5), pp.1199-1214.

Younes, A. and Younes, N. (2017). Recovery of steroid induced adrenal insufficiency. *Translational Pediatrics*, 6(4), pp.269-273.

Yuspa, S., Kilkenny, A., Cheng, C., Roop, D., Hennings, H., Kruszewski, F., Lee, E., Strickland, J. and Greenhalgh, D. (1991). Alterations in Epidermal Biochemistry As a Consequence of Stage-Specific Genetic Changes in Skin Carcinogenesis. *Environmental Health Perspectives*, 93, pp.3-10.

Zafar, M., Najeeb, S., Khurshid, Z., Vazirzadeh, M., Zohaib, S., Najeeb, B. and Sefat, F. (2016). Potential of Electrospun Nanofibers for Biomedical and Dental Applications. *Materials*, 9(2), pp. 1-21.

Zampetti, A., Feliciani, C., Tulli, A. and Amerio, P. (2010). Pharmacotherapy of Inflammatory and Pruritic Manifestations of Corticosteroid-Responsive Dermatoses Focus on Clobetasol Propionate. *Clinical Medicine Insights: Therapeutics*, 2, pp.532-537.

Zanger, U. and Schwab, M. (2013). Cytochrome P450 Enzymes In Drug Metabolism: Regulation Of Gene Expression, Enzyme Activities, And Impact Of Genetic Variation. *Pharmacology & Therapeutics*, 138(1), pp.103-141.

Zendegui, J., Inman, W. and Carpenter, G. (1988). Modulation Of The Mitogenic Response Of An Epidermal Growth Factor-Dependent Keratinocyte Cell Line By Dexamethasone, Insulin, And Transforming Growth Factor-?. *Journal of Cellular Physiology*, 136(2), pp.257-265.

Zhang, H. and Robinson, J.R. (1996). Routes of Drug Transport across Oral Mucosa. In: Rathbone, M.J. (Ed.), Oral Mucosal Drug Delivery. Marcel Dekker Inc., New York, pp. 51–63.

Zhang, H., Zhang, J. and Streisand, J. (2002). Oral Mucosal Drug Delivery. *Clinical Pharmacokinetics*, 41(9), pp.661-680.

Zhao, Z., Sugerman, P., Zhou, X., Walsh, L. and Savage, N. (2001). Mast Cell Degranulation And The Role of T Cell RANTES in Oral Lichen Planus. *Oral Diseases*, 7(4), pp.246-251.

Zhou, X., Sugerman, P., Savage, N. and Walsh, L. (2001). Matrix Metalloproteinases And Their Inhibitors In Oral Lichen Planus. *Journal of Cutaneous Pathology*, 28(2), pp.72-82.Boobis, A. R. (1998). Comparative physicochemical and pharmacokinetic profiles of inhaled beclomethasone dipropionate and budesonide. *Respiratory Medicine*, 92 Suppl B, pp. 2–6.

APPENDICES

APPENDIX I

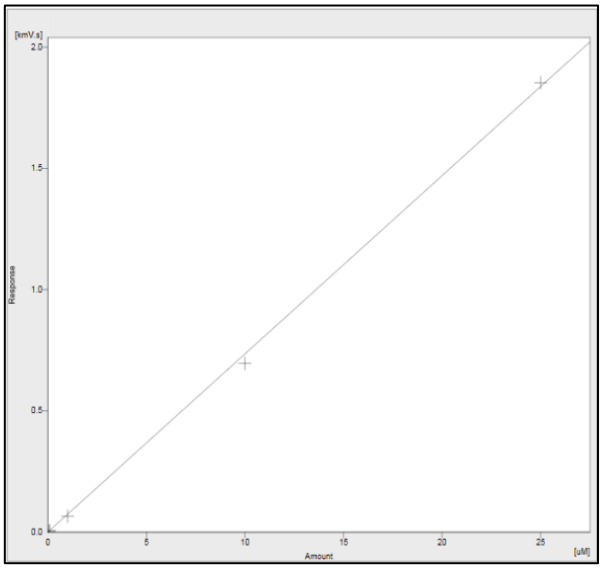

A

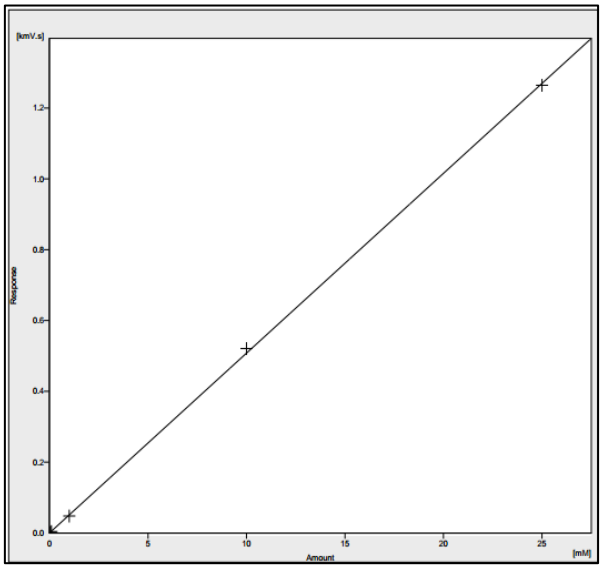

B

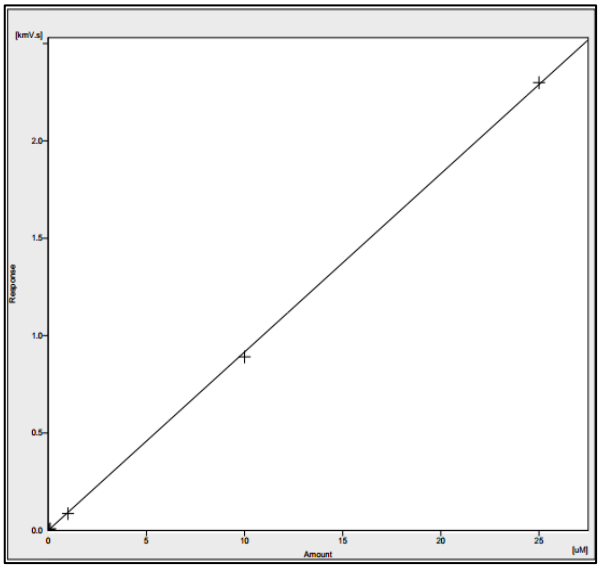

C

HPLC calibration standard for (A) clobetasol-17-propionate, (B) betamethasone-17-valerate and (C) hydrocortisone-17-valerate.

APPENDIX 2

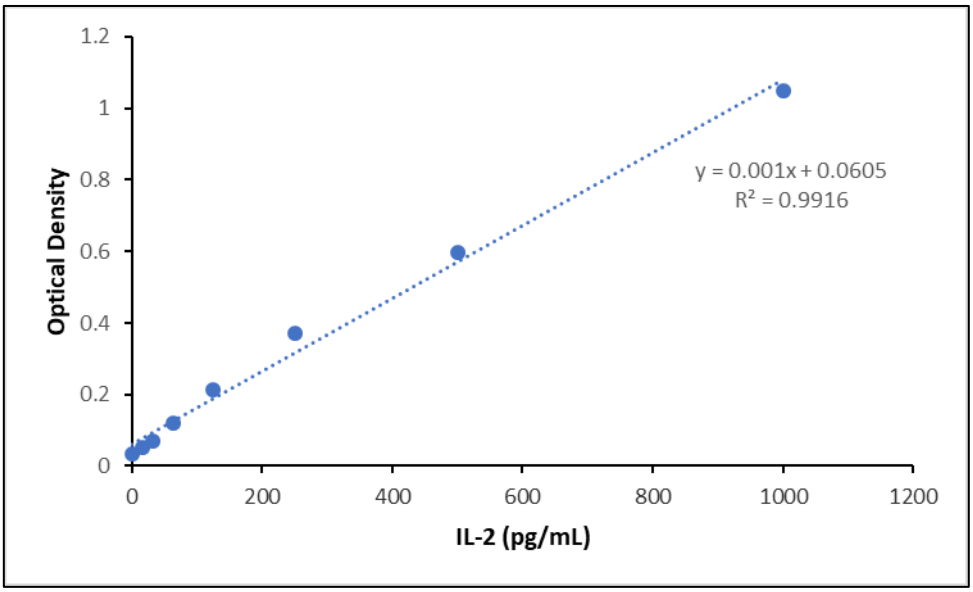

Standard curve of interleukin-2 (IL_2)